



Trinity
College
Dublin

The University of Dublin

Investigation of Objective Neurophysiological Measures of Auditory Temporal Processing Abilities and Their Applicability in Cochlear Implant Rehabilitation

Saskia M. Waechter, B. Sc., M. Sc.

Under the supervision of Prof. Richard B. Reilly

A dissertation submitted to the

University of Dublin, Trinity College

In fulfilment of the requirements for the degree of

Doctor of Philosophy

June, 2019



Department of Electronic and Electrical Engineering

University of Dublin, Trinity College

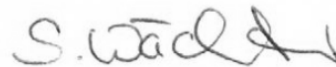
Declaration

I declare that this thesis has not been submitted as an exercise for a degree at this or any other university and it is entirely my own work.

I agree to deposit this thesis in the University's open access institutional repository or allow the Library to do so on my behalf, subject to Irish Copyright Legislation and Trinity College Library conditions of use and acknowledgement.

I consent / do not consent to the examiner retaining a copy of the thesis beyond the examining period, should they so wish (EU GDPR May 2018).

Signed,



Saskia M. Waechter

June 20th, 2019

Summary

Speech is the most important form of human communication. For people affected by disabling hearing loss, speech information may become unavailable causing social isolation and cognitive decline. People with mild to profound sensorineural hearing loss may benefit from cochlear implantation which can bypass the impaired auditory pathway and may restore functional hearing through direct electrical stimulation. The fitting process, which refers to the continuous adjustment of software parameters of the cochlear implant (CI) after implantation, is an important part of the success of clinical rehabilitation procedures. Current fitting approaches are strongly reliant on subjective feedback, which can be unreliable, e.g. in individuals with test anxiety, or missing in cohorts such as infants and people with cognitive impairments. For children who are born profoundly deaf, it is imperative that they receive a CI as early as possible in life to achieve optimal rehabilitation outcomes, which has led to a large increase of cochlear implantation at a young age. Therefore, there is an urgent clinical need for objective methods to assess auditory processing abilities after implantation. Such objective metrics can not only guide the clinical fitting procedures, but also provide additional information to aid expectation management particularly for parents of infants who receive a CI.

In the literature, potential objective metrics have been evaluated for spectral as well as temporal auditory processing. Both, temporal and spectral acoustic cues, contribute to the intelligibility and recognisability of sounds and particularly of speech. A multitude of research studies has assessed objective metrics of spectral resolution, however, fewer research studies have investigated objective metrics of temporal auditory processing, which is of particular importance for speech perception. In this thesis, objective neurophysiological measures representative of auditory discrimination abilities were explored for two different aspects of temporal auditory processing, and their applicability in a clinical cohort was investigated. The temporal features under

investigation were amplitude modulation (AM) detection abilities (**Chapter 3 – Chapter 5**) and discrimination abilities based on temporal fine structure (TFS) cues (**Chapter 6**), both of which play an important role in speech recognition.

The first study focused on the methodology of how to derive individual neural thresholds of auditory discrimination abilities from electroencephalography (EEG) data. Consecutively, the relationship between these neural thresholds and corresponding behavioural thresholds was analysed by means of correlation analysis to assess the informational value of the neural threshold estimates. Successful neural threshold estimation and significant correlations with behavioural thresholds provided support for the expansion to a clinical cohort in Study 2. This study addressed another important research question regarding the applicability of the novel approach in a clinical CI user cohort. Moreover, signal processing methods were proposed to automatically (Case Study) or manually (Study 2) reduce the electrical artefact in EEG data which arises from CI stimulation. Significant correlations between behavioural and neural thresholds obtained in Study 2 corroborate findings from Study 1 and provide evidence for the feasibility of employing such an objective metric in a clinical CI user cohort.

The third study as well as multiple accompanying pilot studies have explored tone discrimination based on two types of TFS cues and whether cortical neural change detection measures reflect behavioural discrimination abilities. Findings showed that change detection based on TFS cues is encoded in cortical neural measures, if tones can be confidently distinguished. However, measured amplitudes were low in comparison to studies which employ acoustic change features based on spectral or intensity cues. Moreover, for one of the two types of assessed TFS cues, precise stimulus replication based on information in the literature was unsuccessful despite further correspondence with authors, highlighting the need for more thorough descriptions of employed methods in Journal publications.

In conclusion, the original contribution of this thesis to the literature has multiple facets and includes the novel application of widely researched neurophysiological measures of auditory change detection to acoustic features that have previously not been assessed with this approach, such as TFS processing and AM detection for varying AM depths. Furthermore, novel signal processing methodologies have been proposed to enhance neural signal analysis on an individual level. This included the development of a new methodology to quantify neurophysiological change responses, to aid the estimation of individual neural discrimination thresholds. These thresholds showed

significant correlations with behavioural discrimination thresholds in a normal-hearing cohort as well as in a clinical CI cohort, and thus, may enhance the objective assessment of auditory processing abilities in clinical environments in the future.

Acknowledgments

I would like to take this opportunity to thank everybody who supported me over the last four years. It has been a great journey, an emotional roller coaster with many ups and downs.

In particular, I would like to thank Professor Richard Reilly, for his never-ending optimism, motivation, professional guidance, and overall mentoring.

Alejandro Lopez Valdes, for *always* responding to my questions, for his tireless efforts in helping me shape publications, for his constant emotional support, and for believing in me.

Cristina Simoes-Franklin, for her helping hand on all clinical aspects, her input on manuscripts and our conversations about postdoc positions and life after the PhD.

The National Cochlear Implant Team in Beaumont Hospital, especially Jaclyn Smith for sharing her clinical expertise and her input on manuscripts, Deborah Peyton and Susan Gray for their support with patient recruitment, and Dr. Laura Viani for the fantastic opportunity to collaborate on the CI Research and for including me in her team at Christmas Parties and other events.

Surbhi Hablani, for being a fantastic student to work with, for the endless discussions on temporal fine structure literature, and for her assistance on the temporal fine structure studies.

Denis Drennan and Terence Taylor, for many late nights staying in the office to have chats about our work and the occasional pint to go with it.

Clodagh O’Keeffe, for work-related and work-unrelated chats over many coffees and her outstanding creativity and thoughtfulness which caused me to smile even in the darkest phase of this PhD.

Celine DeLooze, Shruti Narasimham, Joyce Hoogendorn, and Michael Broderick for the engaging lunch conversations which provided the daily breaks from work.

Rebecca Beck, for sending the loveliest and most encouraging occasional text messages, which were so appreciated.

Everybody else of the Reilly and Lalor labs who have all played their own role in my life over the last four years.

Professor Brian Moore, for his remarkable response times, for his continued input on our temporal fine structure work as well as for his detailed comments as the Section Editor on my first publication.

Pauric Dooley, for his constant love and support, his patience and never-ending optimism.

And last, but not least, my family, most importantly my parents, who played a major role in the writing of this thesis by offering the “All-inclusive Hotel Mum” for weeks on end, which enabled me to fully concentrate on the work, and for the tireless proof-reading at the very end of this four-year journey. Additionally, without their financial support I would not have been able to achieve any of the educational milestones and it gave me the freedom to concentrate on studying.

Everybody who engaged with me over the last four years had a real impact on my PhD, either by keeping me sane or direct discussions about my work, and without all this help I would not have achieved what I did! So thank you, also to all the unnamed people from various sports teams.

SASKIA M. WAECHTER

Trinity College Dublin
June 2019

Publications arising from this research

International journal publications

- **Waechter, S. M.**, Lopez Valdes, A., Simoes-Franklin, C., Viani, L. & Reilly, R. B. (2018) Depth matters – Towards finding an objective neurophysiological measure of behavioral amplitude modulation detection based on neural threshold determination. *Hearing research*, **359**, 13-22.

Conference Papers

- **Waechter, S. M.**, Simoes-Franklin, C., Smith, J., Viani, L., and Reilly, R. B.; Cochlear implant artefact reduction in electroencephalography data obtained with the auditory oddball paradigm and stimuli with differing envelopes; 9th IEEE EMBS, San Francisco, USA, March 2019

International conference abstracts

- **Waechter, S. M.**, Lopez Valdes, A., Simoes-Franklin, C., Viani, L., Reilly, R. B., “Do speech-in-noise scores in normal-hearing humans correlate with amplitude modulation depth detection abilities?”, Proceedings of the *Speech in Noise Workshop*, Groningen, The Netherlands, January 2016
- **Waechter, S. M.**, Lopez Valdes, A., Simoes-Franklin, C., Viani, L., Reilly, R. B., “Evaluation of the mismatch waveform elicited by amplitude modulated auditory stimuli as an objective measure for temporal discrimination abilities to aid future Cochlear Implant fitting”, Proceedings of the *39th Annual MidWinter Meeting*, Association for Research in Otolaryngology, San Diego, February 2016

- **Waechter, S. M.**, Lopez Valdes, A., Simoes-Franklin, C., Viani, L., Reilly, R. B. “Investigating the relationship between evoked potentials, amplitude modulation detection and speech-in-noise recognition in CI users- a study design proposal and pilot data”, Proceedings of the *Speech in Noise Workshop*, Oldenburg, Germany, January 2017
- **Waechter, S. M.**, Lopez Valdes, A., Simoes-Franklin, C., Smyth, J., Viani, L., Reilly, R. B. “Preliminary results and challenges of artefact reduction in analysis of mismatch responses elicited by amplitude modulation detection in cochlear implant users”, Proceedings of the *International Evoked Response Audiometry Study Group (IERASG) Biennial Symposium*, Warsaw, Poland, May 2017
- Hablani, S., **Waechter, S. M.**, Reilly, R. B. “Mismatch response versus acoustic change complex: Assessment of auditory temporal fine structure processing – finding an objective paradigm”, Proceedings of the *International Evoked Response Audiometry Study Group (IERASG) Biennial Symposium*, Warsaw, Poland, May 2017
- **Waechter, S. M.**, Lopez Valdes, A., Simoes-Franklin, C., Smith, J., Viani, L., Reilly, R. B. “Investigation of the identity-MMN as a measure of amplitude modulation detection in cochlear implant users”, Proceedings of the *Auditory EEG Signal Processing (AESoP) symposium*, Leuven, Belgium, May 2018
- **Waechter, S. M.**, Hablani, S., Reilly, R. B. “Is auditory temporal fine structure processing encoded in the MMN?”, Proceedings of *MMN2018: The 8th Mismatch Negativity Conference*, Helsinki, Finland, June 2018
- **Waechter, S. M.**, Lopez Valdes, A., Simoes-Franklin, C., Smith, J., Viani, L., Reilly, R. B. “Investigation of the identity-MMN as a measure of amplitude modulation detection in cochlear implant users”, Proceedings of *MMN2018: The 8th Mismatch Negativity Conference*, Helsinki, Finland, June 2018

Table of Contents

- Declaration ii
- Summary iii
- Acknowledgmentsvi
- Publications arising from this research viii
- Table of Contentsx
- List of figuresxv
- List of tablesxix
- List of acronyms.....xx
- Chapter 1 Introduction 1
 - 1.1 Motivation 1
 - 1.2 Research goals and collaborations.....4
 - 1.3 Thesis outline.....4
- Chapter 2 Fundamentals.....6
 - 2.1 The auditory system.....6
 - 2.1.1 The healthy auditory pathway6
 - 2.1.2 Types of hearing loss 15
 - 2.2 Cochlear implants 15
 - 2.2.1 Engineering principles 15
 - 2.2.2 Rehabilitation procedure 18
 - 2.3 Electrophysiology in auditory processing21
 - 2.3.1 Auditory evoked potentials21
 - 2.3.2 Late cortical auditory evoked potentials23

2.3.3 CAEPs in CI users	27
2.4 Envelope processing and amplitude modulation detection	29
2.4.1 Objective measures of AM detection	31
2.5 Temporal fine structure processing	33
2.5.1 Assessment of TFS sensitivity.....	34
2.5.2 Objective measures of TFS sensitivity	34
2.6 Research questions	37
2.6.1 Study 1	38
2.6.2 CI Case Study (CS).....	39
2.6.3 Study 2	39
2.6.4 Study 3	39
Chapter 3 Depth matters – towards finding an objective neurophysiological measure of behavioural amplitude modulation detection.....	40
3.1 Methods.....	42
3.1.1 Participants	42
3.1.2 AM Stimuli.....	42
3.1.3 Psychoacoustics	43
3.1.4 Speech-in-noise test.....	45
3.1.5 Electrophysiology.....	45
3.2 Results	50
3.2.1 Psychoacoustics	50
3.2.2 Speech-in-noise test.....	51
3.2.3 Correlations speech vs. psychoacoustics	51
3.2.4 Electrophysiology.....	52
3.2.5 Correlations between BTs vs. NTs	54
3.3 Discussion	56
3.3.1 Objective measure	56

3.3.2	Psychoacoustics	60
3.3.3	Speech-in-noise recognition vs. AM detection	61
3.3.4	Clinical applications.....	62
Chapter 4	Case study: Exploring CI artefact reduction for the acoustic change complex paradigm.....	64
4.1	Materials and Methods	65
4.1.1	Participant information	65
4.1.2	Experimental design.....	65
4.1.3	Post-processing of EEG data.....	68
4.2	Results	70
4.3	Discussion.....	75
Chapter 5	Investigation of the MMW as an objective measure of low-rate AM detection in CI users	78
5.1	Materials and methods.....	79
5.1.1	Clinical recruitment process.....	79
5.1.2	Participants.....	81
5.1.3	Study design.....	81
5.1.4	EEG post-processing CI users.....	87
5.1.5	EEG post-processing NH cohort.....	89
5.1.6	Quantification of the MMW	90
5.2	Results	91
5.2.1	Behavioural results.....	91
5.2.2	EEG acquired from CI cohort	93
5.2.3	Quantification of individual EEG data from CI users.....	99
5.2.4	Correlations between BTs and NTs in CI users	101
5.2.5	EEG acquired from NH cohort	101
5.3	Discussion.....	104
5.3.1	Behavioural tests	104

5.3.2 Findings from CI users	105
5.3.3 Findings from NH data	107
5.3.4 Limitations.....	108
Chapter 6 Objective measure of auditory temporal fine structure processing	110
6.1 Phase 1 – Explorative pilot experiments.....	112
6.1.1 Methods	112
6.1.2 Results and discussion.....	114
6.2 Phase 2 – Feasibility case study	116
6.2.1 Methods	117
6.2.2 Results and discussion.....	120
6.3 Phase 3 – A study on the feasibility of neural change detection measures for TFS processing.....	122
6.3.1 Methods	123
6.3.2 Results and Discussion	126
6.4 Phase 4 – Addressing limitations of Phase 3 with psychoacoustic experiments.....	129
6.4.1 Methods	130
6.4.2 Results and discussion.....	133
6.5 Summary	135
Chapter 7 General discussion	138
7.1 Thesis summary	138
7.2 Discussion of the main findings.....	139
7.3 Challenges of the research	142
7.4 Clinical impact of the research.....	143
7.4.1 Cochlear implant rehabilitation	143
7.4.2 Auditory neuropathy spectrum disorder	144
7.5 Future research directions	145
7.6 Final conclusions.....	146

References	148
Appendices	175
Appendix A: Supplementary Material for Chapter 6	175
A.1 Validation of recording equipment	175
Appendix B: The influence of experimental parameters on the neural response – Insights from NH pilot studies	177
B.1 Observations ACC experiments	178
Appendix C: Measurement set-ups	184
C.1 Single-channel set-ups	184
C.2 Dual-channel set-up for normal-hearing participants	185

List of figures

Figure 2.1: Overview of the peripheral auditory system and its components.	7
Figure 2.2: Simplified schematic of the ascending central auditory pathway.	9
Figure 2.3: Schematic of auditory processing of a complex harmonic tone.	12
Figure 2.4: Power spectra of a harmonic and inharmonic complex tone with unresolved components and threshold-equalizing noise (TEN).	13
Figure 2.5: Simulated waveforms of harmonic and inharmonic stimuli after passing through an auditory filter.	13
Figure 2.6: Components and position of a cochlear implant.	16
Figure 2.7: Overview of an envelope based speech processing strategy.	17
Figure 2.8: Overview of auditory evoked potential (AEP) classifications (A) and latencies (B).	22
Figure 2.9: Waveforms of transient and following auditory evoked potentials (AEP). .	22
Figure 2.10: P1-N1-P2 complex followed by the acoustic change complex (ACC).	24
Figure 2.11: Example of the mismatch negativity (MMN).	25
Figure 2.12: Example of the electrical artefact elicited by cochlear implant (CI) stimulation and its reduction with independent component analysis (ICA).	28
Figure 2.13: Temporal envelope and temporal fine structure of a complex signal.	30
Figure 2.14: Example measurements of auditory steady state (ASSR) signals and measurement noise at different amplitude modulation (AM) rates.	31
Figure 2.15: Grand average (black) and individual (grey) inter-aural phase modulation (IPM) following responses.	35
Figure 2.16: Grand average envelope following response (EFR) and stimulus Hilbert transforms of the acoustic stimuli.	36
Figure 2.17: Grand average N1-P2 and acoustic change complex (ACC) waveforms. .	37
Figure 3.1: Examples of amplitude modulated (AM) noise stimuli.	43

Figure 3.2: Graphical User Interface (GUI) to obtain amplitude modulation (AM) detection thresholds and visualisation of the presented stimuli.	44
Figure 3.3: Pseudocode of data processing steps to obtain morphology weighted area-under-the curve (AUC) values of mismatch waveforms (MMWs).....	47
Figure 3.4: Mismatch waveform (MMW) alignment for example participant.	48
Figure 3.5: Visualisation of data processing steps involved in neural threshold (NT) estimation.	49
Figure 3.6: Behavioural results and their correlation analysis results.....	50
Figure 3.7: Individual and grand average cortical auditory evoked potentials (CAEPs).	53
Figure 3.8: Grand average mismatch waveforms and area-under-the-curve data.....	53
Figure 3.9: Examples of the correlation analysis between behavioural thresholds (BTs) and neural thresholds (NTs).	53
Figure 3.10: Permutation distributions of correlation analysed with randomised sets of standard epochs.	55
Figure 3.11: Comparison of neural and behavioural AM detection for varying AMDs.	57
Figure 4.1: Placement of a cochlear implant (CI) in an Otocube® (Otoconsult NV, Belgium).....	66
Figure 4.2: Data processing pipeline for the acoustic change complex paradigm in cochlear implant (CI) users.	69
Figure 4.3: Examples of the correlation-based bad channel rejection to reduce cochlear implant (CI) artefact prior to independent component analysis.	71
Figure 4.4: Topographical, butterfly and global field power (GFP) plots of the four ACC conditions.	72
Figure 4.5: Overview of the electrode clusters and neural responses.	73
Figure 4.6: Re-referenced cortical auditory evoked potentials (CAEPs) and their global field power (GFP).....	74
Figure 5.1: Clinical recruitment process for the research study.....	80
Figure 5.2: Custom-designed graphical user interface (GUI) of the speech-reception-threshold test.	82
Figure 5.3: Visualization of acoustic and electrical amplitude modulated stimuli.	83
Figure 5.4: Graphical User Interface (GUI) to execute subjective loudness balancing.	85
Figure 5.5: Stimulus overview of the new mismatch waveform paradigm.	86

Figure 5.6: Data processing pipelines for Electroencephalography (EEG) data recorded from the cochlear implant (CI) user cohort.	87
Figure 5.7: Behavioural results for cochlear implant (CI) users and normal-hearing (NH) participants.	92
Figure 5.8: Relationship between speech reception thresholds (SRTs) and behavioural thresholds (BTs) of amplitude modulation (AM) detection.	93
Figure 5.9: Examples of cortical auditory evoked potentials (CAEPs) and mismatch waveforms (MMWs) after subtraction-based artefact reduction.	94
Figure 5.10: Examples of independent components (ICs) associated with cochlear implant (CI) artefact.	95
Figure 5.11: Topographical overview of individual and grand average mismatch waveforms (MMW) for the CI group.	96
Figure 5.12: Overview of the electrode clusters in the regions of interest (ROI) and their mismatch waveforms (MMWs).	96
Figure 5.13: Group mean difference waveforms obtained with the subtraction-based processing pipeline.	97
Figure 5.14: Comparison of mismatch waveforms (MMWs) for MMW1s and MMW2s for each amplitude modulation depth (AMD).	98
Figure 5.15: Comparison of mismatch waveforms (MMWs) across amplitude modulation depths (AMDs).	98
Figure 5.16: Butterfly plots and topographical plots of the mismatch waveforms (MMWs).	99
Figure 5.17: Example mismatch waveforms (MMWs) for individual participant CI8.	100
Figure 5.18: Neural threshold estimates from the individual area-under-the-curve (AUC) values.	100
Figure 5.19: Overview of correlation results between behavioural thresholds (BTs) and neural thresholds (NTs) of amplitude modulation (AM) detection.	101
Figure 5.20: Overview of difference waves from the normal-hearing cohort across the four tested amplitude modulation depths.	102
Figure 5.21: Individual absolute and normalised area-under-the-curve (AUC) values for the normal-hearing (NH) cohort.	103
Figure 5.22: Overview of difference waves with and without subjective loudness balancing (LB).	103
Figure 6.1: Schematic with a condensed overview of the four phases in Chapter 6. ...	111

Figure 6.2: Behavioural thresholds of temporal fine structure (TFS) discrimination...	114
Figure 6.3: Cortical auditory evoked potentials (CAEPs) elicited by temporal fine structure stimuli.....	115
Figure 6.4: Difference waveforms elicited by temporal fine structure stimulus pairs..	115
Figure 6.5: Bandpass filter to create HCU-ICU stimuli.....	118
Figure 6.6: Positive and negative Schroeder-phase harmonic complex tones.	119
Figure 6.7: Cortical auditory evoked potentials (CAEPs) elicited by five different stimulus pairs for a pilot participant.....	121
Figure 6.8: Behavioural tone discrimination results.	126
Figure 6.9: Questionnaire responses on temporal fine structure tone discrimination...	127
Figure 6.10: Comparison of grand average cortical auditory evoked potentials (CAEPs) and their respective difference waveforms.....	127
Figure 6.11: Overview of grand average mismatch waveforms (MMWs).	128
Figure 6.12: Detailed processing steps of the statistical analysis of the difference waveform with false discovery rate (FDR) adjustment.	128
Figure 6.13: Peak timing of harmonic and inharmonic complex stimuli with a fundamental frequency F0 of 200 Hz.....	129
Figure 6.14: Example of signal distortions due to non-linear phase effects.	130
Figure 6.15: Harmonic and inharmonic stimuli with threshold-equalizing noise (TEN).	131
Figure 6.16: Psychoacoustic results for discrimination performance between harmonic (H) and inharmonic (I) stimuli.	134
Figure 6.17: Comparison of discrimination performance between harmonic and inharmonic tones for two presentation modes.....	135
Figure 7.1: Mindmap illustrating the complexity of auditory research.....	142

List of tables

Table 2.1: Overview of the main studies.	38
Table 3.1: Group mean and standard deviation (SD) data of the psychometric function for different amplitude modulation depths (AMD).	50
Table 3.2: Speech-in-noise recognition group mean data and their standard deviations (SDs) for native speakers for the three tested signal-to-noise ratios (SNRs).	51
Table 3.3: Overview of correlation results with data based on all standard epochs.	54
Table 4.1: Acoustic change complex (ACC) amplitudes.	74
Table 4.2: Signal-to-noise ratios (SNRs) for two time windows of interest.	74
Table 5.1: Demographics and CI-related characteristics.	80
Table 5.2: Overview of the employed paradigms in the individual normal-hearing participants.	102
Table 6.1: Overview of stimulus assignment in the neurophysiological paradigm.	125

List of acronyms

3AFC	Three-Alternative Forced Choice
ABR	Auditory Brainstem Response
ACC	Acoustic Change Complex
ACE	Advanced Combination Encoder
AEP	Auditory Evoked Potential
AM	Amplitude Modulation
AMD	Amplitude Modulation Depth
AM-STD	Amplitude Modulated Standard (stimulus or CAEP)
ANSD	Auditory Neuropathy Spectrum Disorder
ASSR	Auditory Steady-State Response
AUC	Area-Under-the-Curve
BKB	Bamford-Kowal-Bench
BT	Behavioural Threshold
CAEP	Cortical Auditory Evoked Potentials
CI	Cochlear Implant
CIS	Continuous Interleaved Sampling
CS	Case Study
DEV	Deviant (stimulus or CAEP)
EABR	Electrical Auditory Brainstem Response
EASSR	Electrical Auditory Steady-State Response
ECAP	Electrically Evoked Compound Action Potential
EEG	Electroencephalography
EFR	Envelope Following Response
ERB	Equivalent Rectangular Bandwidth
F0	Fundamental Frequency

FDR	False Discovery Rate
FFR	Frequency Following Response
FFT	Fast-Fourier Transform
FIR	Finite Impulse Response
fMRI	Functional Magnetic Resonance Imaging
fNIRS	Functional Near-Infrared Spectroscopy
HCU	Harmonic Complex with Unresolved components
IC	Independent Component
ICA	Independent Component Analysis
ICU	Inharmonic Complex with Unresolved components
IIR	Infinite-Impulse Response
IPM	Inter-aural Phase Modulation
ISI	Inter-Stimulus Interval
IV	Intersection Value
LTASS	Long-Term Average Speech Spectrum
MEG	Magnetoencephalography
MMN	Mismatch Negativity
MMW	Mismatch Waveform
NH	Normal-Hearing
NT	Neural Threshold
PET	Positron Emission Tomography
r_p	Pearson's Correlation Coefficient
r_s	Spearman's Rank Correlation Coefficient
RMS	Root Mean Square
ROI	Region Of Interest
SD	Standard Deviation
SNR	Signal-to-Noise Ratio
SPEAK	Spectral Peak
SPL	Sound Pressure Level
SRT	Speech Reception Threshold
STD	Standard (Stimulus or CAEP)
TEN	Threshold-Equalizing Noise
TFS	Temporal Fine Structure

TFS_{BM}	TFS of the waveform on the basilar membrane at a specific place
TFS_n	Neural Representation of TFS _{BM}
TFS_P	TFS of the Physical Stimulus
TRF	Temporal Response Function
TOI	Time (Window) of Interest

Chapter 1 Introduction

1.1 Motivation

Speech is the most important form of human communication. However, speech recognition and functional hearing may be severely impacted by disabling hearing loss. Disabling hearing loss is associated with social isolation, depression, loss of independence, cognitive decline and overall decreased quality of life (Ciorba *et al.*, 2012; Davis *et al.*, 2016; Tseng *et al.*, 2016). In 2015, almost seven percent of the global population suffered from a disabling hearing loss and this trend is increasing (Wilson *et al.*, 2017). In Ireland, one in six adults suffers from some degree of hearing loss and every second person over the age of 75 years has a disabling hearing loss (HSE, 2011). In today's ageing demographic this constitutes an important social, medical and economical challenge that needs to be addressed.

Hearing loss is mostly seen as sensory deprivation. However, hearing loss has a far greater reach and can lead to re-organization of brain connectivity, and thus, alterations of brain processes (Kral & O'Donoghue, 2010; Peelle *et al.*, 2011; Sharma & Glick, 2016; Glick & Sharma, 2017). Young children below the age of three years are particularly affected (Kral & O'Donoghue, 2010). Disabling hearing loss in infants may lead to developmental delays and limited communication and educational attainments (Schroeder *et al.*, 2006; Marschark *et al.*, 2015). Hearing aids can amplify sounds and restore functional hearing for mild to moderate hearing losses. However, for severe to profound hearing losses, sound amplification may not be sufficient. Such a diagnosis may qualify a patient for cochlear implantation if the underlying cause is sensorineural hearing loss.

Cochlear implants (CIs) are the current gold-standard rehabilitation approach to partially restore hearing in deaf individuals. However, treatment outcomes vary widely

and many challenges remain. The CI enables sound transmission from the environment through the ear to the brain and takes over the conversion from environmental acoustic to neural electric information, and thus, repairs the gate-way for sound to reach the brain. In people suffering from sensorineural hearing loss, this transformation process is impaired due to dead hair cells in the cochlea, disrupting the pathway of sound to the brain. However, to successfully restore hearing, the brain needs to integrate the auditory input it receives, which is a learning process enabled by the brain's plasticity. In particular, speech is a complex signal and speech recognition is a very cognitively demanding task for the brain. After device activation in the so-called switch-on appointment, patients' performance in speech recognition tests reportedly improves throughout the first year of implant use (Oh *et al.*, 2003; Ruffin *et al.*, 2007; Drennan *et al.*, 2015), emphasizing the fact that the brain has to adapt to the new input it receives from the CI. After the implantation, CI users attend numerous clinical fitting appointments in which the device parameters are adjusted to the individual to maximize device performance, and in turn to optimize speech recognition performance. This process is very time consuming and, to date, it heavily relies on patient feedback. The new-born hearing screening programme (HSE, 2013), which was rolled-out nationwide in Ireland in 2013, enables early intervention to improve auditory abilities as the child's brain is more adaptive to sounds. CIs are implanted in infants from the age of one year or in the time-sensitive case of meningitis as young as six months. However, behavioural feedback for the clinical fitting process may be lacking or highly unreliable in infants. This can also be an issue in people with cognitive impairments. Thus, there is a need for objective measures of auditory discrimination abilities to aid clinical rehabilitation procedures (Hall & Swanepoel, 2010).

Neuroimaging offers such objective assessment tools for neural function to clinicians and researchers that range from invasive to non-invasive methods. The different functional neuroimaging methods have trade-offs between temporal and spatial resolution, availability and cost-efficiency. Non-invasive methods comprise of functional Magnetic Resonance Imaging (fMRI), Magnetoencephalography (MEG), functional Near-Infrared Spectroscopy (fNIRS), Positron Emission Tomography (PET), and Electroencephalography (EEG). When good spatial resolution is required, fMRI is the

most popular neuroimaging method¹. However, the temporal resolution is poor in the order of seconds, as the measured neural response is based on the haemodynamic response. Also based on the haemodynamic response is fNIRS, which provides a more cost-efficient and portable alternative to fMRI. Compared to fMRI, fNIRS offers poorer spatial resolution and the low penetration depth of the light emitter limits the measurement depth to outer cortical areas. MEG offers good spatial and temporal resolution, but this technology is not readily available in most clinics and research facilities. PET scans provide very poor temporal resolution and require radioactively labelled chemical agents, but offer a very useful tool to study specific neurotransmitters and neuroreceptors. EEG provides a readily-available, cost-efficient tool with very good temporal resolution in the order of milliseconds, thus, making it the ideal tool to investigate the rapid neural processes underlying auditory perception.

The perception of a sound relies on its acoustic features as well as the sound environment. The acoustic features can be divided into the spectral properties (e.g. the fundamental frequency) and the temporal properties. Temporal properties include the temporal fine structure (TFS), which refers to the faster oscillations of the sound's waveform, and the sound's envelope. Envelope fluctuations may be simplified as low-rate amplitude modulation (AM) of a carrier signal. Therefore, envelope processing may be assessed by means of AM detection tasks with a low AM rate.

Speech recognition constitutes the ultimate goal of CI rehabilitation. Given the importance of these temporal features for speech recognition, it is of interest to develop objective metrics of sound discrimination for each of these acoustic features to be able to assess the individual aspects of auditory processing required for functional hearing. Section 2.4 and Section 2.5 provide a more detailed description of the role of envelope and TFS cues for speech recognition, respectively, and summarise the recent literature with a particular focus on potential objective assessment approaches. The importance of these temporal features in electric hearing is discussed in Section 2.2.

¹ It should be noted that CI users are commonly not eligible for MRI scans due to the magnetic restrictions of the implanted device. An Australian team of researchers has engineered the first MEG system that is compatible with CIs Johnson, B.W., Tesan, G., Meng, D. & Crain, S. (2013) A custom-engineered MEG system for use with cochlear implant recipients. *Front. Hum. Neurosci. Conference Abstract: ACNS-2013 Australasian Cognitive Neuroscience Society Conference*. PET, EEG and fNIRS are also compatible with CIs.

1.2 Research goals and collaborations

The principal goal of this research is to determine neurophysiological measures to objectively assess temporal auditory processing abilities. In order to improve hearing rehabilitation, it is necessary to understand how sounds are processed neurally when the auditory pathway is intact, and how neural activity in people with hearing impairments may be altered. Experimental paradigms were therefore evaluated for a NH cohort prior to expanding to a clinical cohort. The present research involved several studies investigating two different aspects of temporal auditory processing: temporal envelope processing and TFS processing. These studies complement research which has focused on finding objective measures of spectral discrimination abilities. This research combined theoretical basic auditory research with clinical applicability of potential objective measures. Expertise was drawn from a multi-professional network of researchers and clinicians from Trinity Centre for Bioengineering and the National Cochlear Implant Programme in Beaumont Hospital.

1.3 Thesis outline

This thesis is divided into multiple studies. **Chapter 2** provides background information and a review of the relevant literature. In this chapter the neural anatomy of auditory processing is described with a focus on sensorineural hearing impairment. Furthermore, this chapter discusses hearing restoration with CIs and their engineering principles. This is followed by an overview of neurophysiological measures employed in the assessment of auditory processing. The role of temporal acoustic features for functional hearing is discussed and the literature on objective neurophysiological measures of temporal auditory processing is reviewed. This chapter concludes with the research questions that are addressed in the subsequent research studies.

In **Chapter 3**, the first study investigated an EEG-based neurophysiological measure as an objective assessment tool for temporal envelope processing. This study was conducted in a NH cohort. As part of the study, a novel signal processing procedure is proposed to improve quantification of individual neurophysiological data. Neural thresholds of auditory discrimination abilities are estimated from quantified neurophysiological data, and their relationship with corresponding behavioural thresholds is investigated.

Chapter 4 describes a case study with a CI user, which explores the challenge of minimising the electrical artefact in EEG data, which is introduced from CI stimulation. An automated EEG post-processing pipeline for CI artefact reduction is proposed. Its efficacy and the influence of the physical stimulus envelope and the presentation mode on the recorded CI artefact is discussed.

The study presented in **Chapter 5** builds on the gained insights from studies presented in **Chapter 3** and **Chapter 4**. This study investigates the clinical applicability of the neurophysiological measure introduced in **Chapter 3** by employing the experiments in a CI user cohort. Two alternative EEG post-processing pipelines are discussed with regards to CI artefact rejection. Neural thresholds of discrimination performance are estimated and their relationship with behavioural AM detection thresholds is assessed.

Chapter 6 aims to complement the work on objective measures of envelope fluctuations outlined in **Chapters 3 – 5**, by investigating the acoustic temporal feature relating to the TFS of sounds. Behavioural and neurophysiological data of acoustic change detection are presented for two different types of TFS tone pairs.

Finally, **Chapter 7** discusses the main findings of this research and proposes future studies.

Chapter 2 Fundamentals

This chapter provides an overview of the relevant literature and is divided into six sections. The first section provides an introduction to both the healthy and impaired auditory system and is divided into the peripheral and central auditory system. Furthermore, this section elaborates on the potential mechanisms involved in pitch perception, which are of importance for TFS processing. The second section describes the engineering principles of a CI and discusses the clinical rehabilitation procedures in cochlear implantation. The third section provides an overview of EEG-based methodologies to assess auditory processing with a focus on CAEPs in the larger framework of auditory evoked potentials. The fourth section provides an overview of the literature concerning the relationship between temporal envelope processing, as indicated by AM detection abilities, and speech perception abilities in NH and CI user cohorts, as well as potential neurophysiological measures of AM detection. The fifth section transfers from envelope processing to the other important temporal feature in auditory processing, namely TFS processing, and its role in auditory perception. The last section presents the research questions and their hypotheses.

2.1 The auditory system

2.1.1 The healthy auditory pathway

The peripheral auditory system

Sound refers to mechanical vibrations travelling as pressure waves through a medium such as air. When pressure waves reach a listener's ear, the sound energy travels through the outer ear to the eardrum, from where it is transmitted along the bones of the ossicular chain of the middle ear to the cochlea of the inner ear (see Figure 2.1, top). In

the cochlea, the mechanical signal is converted into the electrical signal, also referred to as action potential, which ascends the neural auditory pathway via the auditory nerve. The healthy human auditory system is sensitive to frequencies between 20 Hz and 20 kHz and pressure levels between 0 dB and 140 dB sound pressure level (SPL), making the cochlea's task to faithfully transduce rapid changes of a wide range of amplitudes and frequencies very complex.

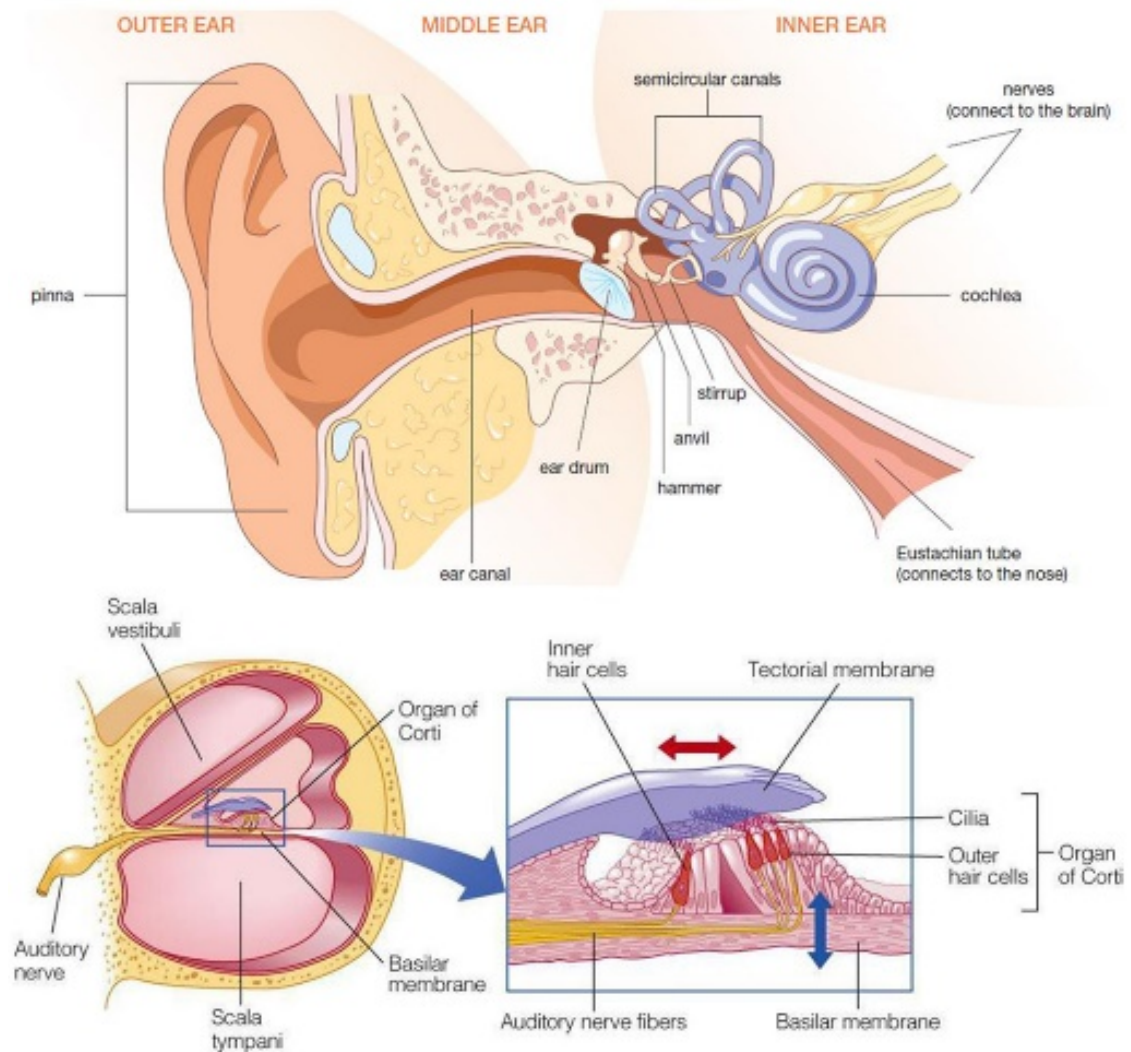


Figure 2.1: Overview of the peripheral auditory system and its components. *Anatomic drawings of the outer, middle, and inner ear (top), cross-section through the cochlea (bottom-left), and close-up of the organ of Corti (bottom-right). Courtesy of the American Academy of Audiology.*

Along the length of the spiral-shaped cochlea runs the organ of Corti with its basilar membrane, which acts as a spectral analyser due to its geometry (Figure 2.1, bottom). High frequency sounds are transduced at the narrow and stiff basal end whereas the wider and more flexible apical end responds to lower frequencies. Sound that reaches the cochlea proceeds as a travelling wave via the basilar membrane, resulting in tonotopic

displacement of the basilar membrane, which is connected to the inner hair cells of the organ of Corti. This displacement creates sheer forces, causing displacement of the stereocilia at the tips of the inner hair cells which act as mechanoreceptors, resulting in the opening of ion channels in the spiral ganglion neuron's membrane. The following depolarization of the membrane potential may create action potentials once a threshold level is reached. These action potentials carry neural information along the auditory nerve ascending the neural auditory pathway towards the central auditory system.

The central auditory system

Auditory information as extracted in and transmitted by the peripheral auditory system is relayed to the brainstem via the auditory nerve and the cochlear nucleus. The following summary of the core structures of the central auditory system focuses on the afferent (ascending) pathways as depicted in Figure 2.2. The efferent (descending) pathways from the auditory cortex to the hair cells are disregarded, but have important influence on the adaptability of the hearing system and attentional selection in dynamic environments (Clark, 2003).

The central auditory system is a highly complex system, which extracts information patterns of growing complexity when ascending the neural pathway from brainstem to primary auditory cortex. The auditory fibres of the central auditory pathway are frequency selective and have a characteristic frequency. In this manner, frequency information as extracted by the cochlea with its tonotopic nature is passed on through all stages of the central auditory system. Neurons' firing profiles become more specialized when ascending the central auditory pathway, i.e. neurons may fire in response to inter-aural level differences, frequency modulation or AM (Fastl & Zwicker, 2007). For spatial sound localisation it is necessary that information from both ears is exchanged, even at low-level neural structures where temporal information is more accurately presented, to extract and compare patterns, latencies and intensities between ears. The first bilateral sound presentation takes place in the superior olivary nuclei, where inter-aural level differences and time delays are determined (Clark, 2003). Afferent connections of the superior olivary nuclei lead to the inferior colliculi, which form a spatial representation of sounds (Purves *et al.*, 2004). From the inferior colliculi, information is relayed to the primary auditory cortex via the medial geniculate nuclei. Higher-order processing of complex sounds takes place in the auditory cortex, which is located in Heschl's gyrus in the temporal lobes and consists of the core (primary) and belt areas (secondary). The

primary auditory cortex (A1) receives frequency mapped input from the tonotopically organized medial geniculate nuclei, whereas the belt areas receive more diffuse input from the medial geniculate nuclei (Purves *et al.*, 2004). The auditory cortex projects across hemispheres, which is of particular importance for lateralized processing such as speech in the dominant and music in the non-dominant hemisphere (Clark, 2003), as well as to association cortices.

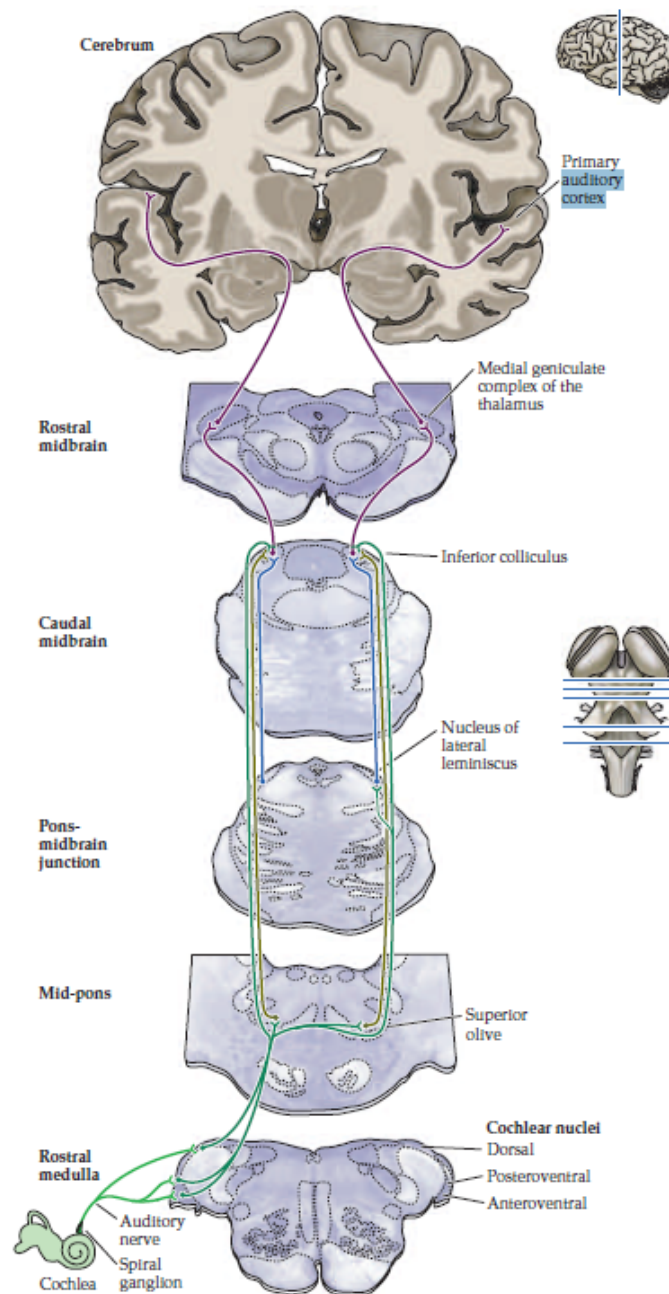


Figure 2.2: Simplified schematic of the ascending central auditory pathway.

*This schematic shows a very basic diagram of the ascending neural connections from the hair cell in the Cochlea to the primary auditory cortex. Connections are shown originating from one ear for simplification purposes. Adapted from Purves *et al.* (2004).*

Pitch perception

In the following, a brief history of the underlying theories of pitch perception is provided with a particular focus on the pitch of harmonic complex tones with unresolved harmonics. This background information will facilitate a better understanding of the challenges encountered when investigating TFS processing, which is briefly introduced in Section 2.5 and later investigated in studies presented in **Chapter 6**.

Pitch refers to the rather vague “attribute of auditory sensation in terms of which sounds may be ordered on a scale extending from low to high” (ANSI, 1994). Pitch is a percept, and not a physical property of a sound, and thus, is dependent on an individual’s perception. Pitch perception is the key factor for melody perception in music. Furthermore, it is used to convey meaning in speech by changing melody, to segregate a voice in a cocktail-party environment, and to discriminate male from female voices and adult voices from children’s voices. The key predictor of pitch is a sound’s periodicity, which for a pure tone equates to its frequency and for a harmonic complex tone it relates to the fundamental frequency $F0$. The precise mechanisms underlying pitch perception, however, are still widely debated among researchers (Walker *et al.*, 2011; Oxenham, 2012), but heavily rely on the spectral composition of the presented sound. For an in-depth review of the current knowledge on the neural mechanisms underlying pitch perception the reader is referred to Schnupp *et al.* (2011) and Plack and Oxenham (2005).

Three main theories have been proposed as an explanation for pitch perception: Helmholtz’s place theory, Schouten’s timing theory and Goldstein’s pattern recognition theory which are briefly outlined in the following:

- A. *Place theory (Von Helmholtz, 1895)*: The location of maximum excitation along the basilar membrane determines a tone’s pitch. This may hold true for the perception of pure tones, however, the place theory is unable to account for the “missing fundamental” effect, which explains the phenomenon of a complex tone without spectral content at $F0$ being perceived as pitch at $F0$ (Schouten, 1938; Licklider, 1956).
- B. *Timing theory (Schouten, 1940)*: According to the timing theory, the pitch of a sound depends on the timing of neuronal activity based on phase locking of neurons to the frequency of the incoming sound stimulus. Thus, frequency perception is believed to originate from differences in time intervals of neuronal activity. However, neuronal phase locking is only possible for sound frequencies below approximately 4 kHz.

C. *Pattern theory (Goldstein, 1973)*: Goldstein's pattern theory suggests that perceived pitch is determined by the harmonic series that best fits the pattern of frequencies in a sound.

None of these theories can fully explain all phenomena of pitch perception. However, a combination may be possible and modern theories propose the integration of place and timing models (de Cheveigne, 2005), where timing mechanisms refer to the temporal pattern of phase locking in the auditory nerve.

A common assumption states that pitch perception of pure tones mainly relies on neural timing cues for low and medium frequencies, but with increasing frequencies the phase locking ability of neurons weakens (Rose *et al.*, 1967). Therefore, it is believed that the place mechanism dominates pitch perception for high frequencies. The value of the approximate transition frequency is not yet determined. Musical pitch perception suggests a transition around 5 kHz, which is the area where musical pitch "breaks down" (Plack & Oxenham, 2005), but frequency discrimination results suggest a higher transition frequency around 8 kHz (Ernst & Moore, 2013).

Pitch of harmonic complex tones and the role of unresolved harmonics

The underlying mechanisms for pitch perception of a complex tone are still debated and models vary with the harmonic rank of its components. Generally speaking, the pitch of a harmonic complex tone, also commonly referred to as periodicity pitch, is determined according to the greatest-common-divisor model: A harmonic complex tone with components from 200 Hz to 600 Hz in steps of 100 Hz has a pitch of 100 Hz, whereas a tone with a sub-set of only the even components (e.g. 200, 400 and 600 Hz) has a pitch of 200 Hz. This is a simple rule of thumb and there are exceptions to the rule. One exception concerns high-order harmonics ($> 15^{\text{th}}$), for which a combination tone with components at 2100, 2200 and 2300 Hz would have a pitch of roughly 2200 Hz. This is in line with the theory that pitch perception relies on place cues for harmonic complex tones with a small number of high-order ($> 15^{\text{th}}$) harmonics (Schnupp *et al.*, 2011). Harmonic complex tones with components below the fifth harmonic are considered as resolved and harmonic complex tones with components above the 10th harmonic are considered as unresolved, with a grey area in between where resolvability transitions depend on the F_0 . For low numbered harmonics ($\approx 2^{\text{nd}}$ to 8^{th}) it is believed that pitch is extracted based on a combination of timing and place cues: Individual harmonics are (partially) resolved, meaning harmonics fall into different auditory filters creating ripples

in the excitation pattern of the basilar membrane (see Figure 2.3). This effect provides place cues and similar to pure tone pitch perception, pitch may then be extracted from a combination of place cues and cues originating from the neural representation of TFS on the basilar membrane, which are subsequently labelled TFS_n cues. Note that precise neural mechanisms underlying pitch perception are still a topic of debate. For harmonic complex tones with unresolved components ($> 8^{th}$), no place cues (also referred to as excitation pattern cues) of the individual components are available and components interact on the basilar membrane (Moore & Sek, 2011; Jackson & Moore, 2014). Pitch percepts of harmonic complex tones with unresolved components are less salient than for resolved components (Shackleton & Carlyon, 1994), which may be attributed to the dominance region of pitch perception, which lies below the sixth harmonic, but differs with F_0 .

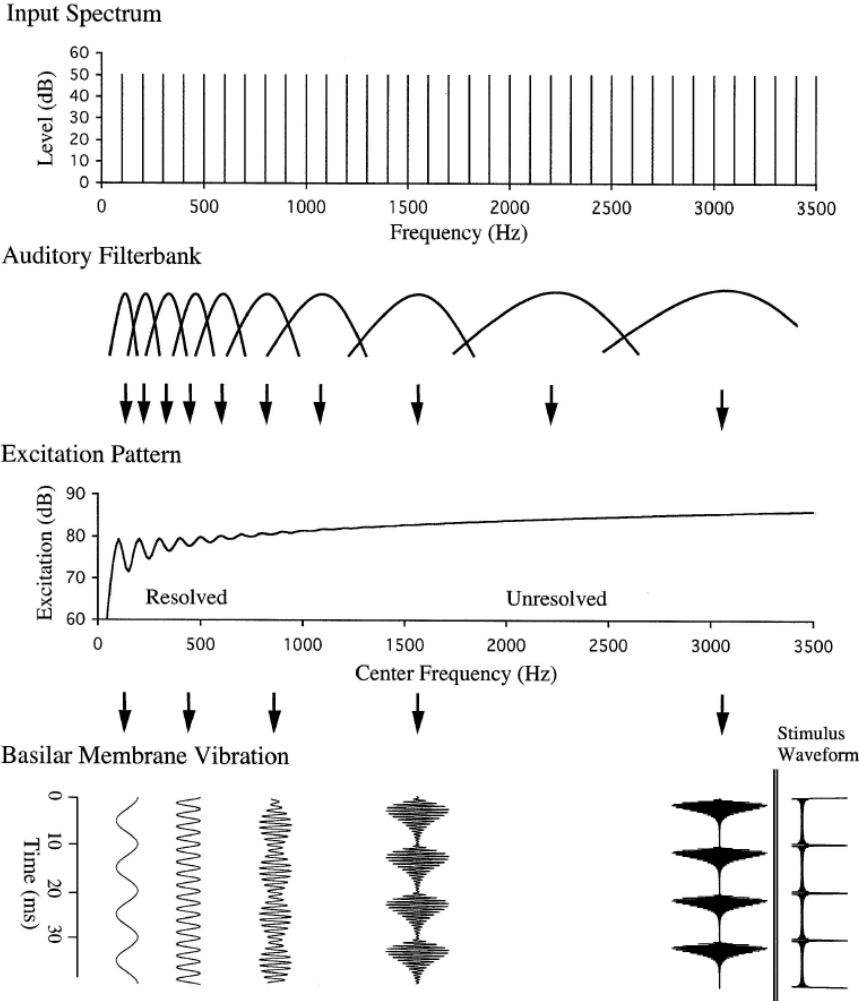


Figure 2.3: Schematic of auditory processing of a complex harmonic tone. An equal-amplitude harmonic complex tone with a fundamental frequency of 100 Hz is passed through the auditory filter bank and the resulting basilar membrane excitation pattern is depicted with its resolved and unresolved parts. Examples of basilar membrane vibration for different auditory filters are shown below. Adapted from Plack and Oxenham (2005).

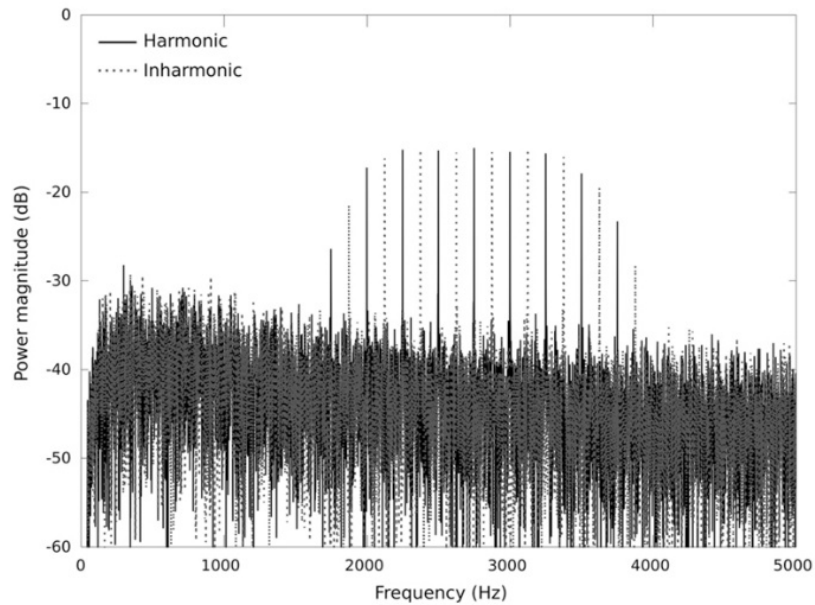


Figure 2.4: Power spectra of a harmonic and inharmonic complex tone with unresolved components and threshold-equalizing noise (TEN).

Both, harmonic and inharmonic complex tone have a fundamental frequency F_0 of 250 Hz. The bandpass filter has a width of $5 \cdot F_0$ and is centred at the 11th component with a roll-off of approximately 30 dB/octave. The TEN level in dB/ERBN is approximately 16.6 dB below the level of the harmonic/inharmonic sound. Adapted from Marmel et al. (2015).

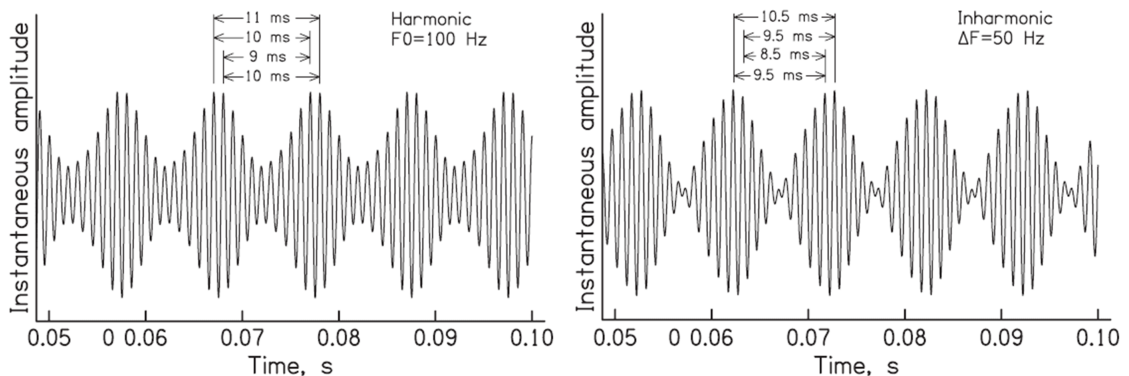


Figure 2.5: Simulated waveforms of harmonic and inharmonic stimuli after passing through an auditory filter.

The auditory filter was centred at 1 kHz, the fundamental frequency was 100 Hz and the bandpass filter was centred at 1.1 kHz. The left panel shows the harmonic tone and the right panel shows the inharmonic tone, shifted by 50 Hz. The envelope varies due to randomised starting phases of the components, but envelope cues are not used for discrimination performance. The repetition rate of the envelopes is equal, but the time between envelope maxima differs as indicated. Adapted from Moore and Sek (2009).

To assess the mechanisms involved in pitch perception for harmonic complex tones with unresolved harmonics, Moore and colleagues have carried out numerous behavioural studies (Moore & Moore, 2003; Hopkins & Moore, 2007; Moore, 2008; Moore et al., 2009; Moore & Sek, 2009; Hopkins & Moore, 2011; Moore & Sek, 2011; Moore et al., 2012; Sek & Moore, 2012). Variations of the same task, which is usually

referred to as the TFS1 test, have been employed in these studies. Tone pairs were generated to contain a harmonic complex tone with unresolved components and an inharmonic complex tone with unresolved components, subsequently labelled HCU and ICU, respectively. Each component of the ICU tone was frequency-shifted upwards compared to the HCU tone by a frequency shift Δf (see Figure 2.4). This frequency shift resulted in small variations of the TFS without affecting the repetition rate of the envelope (Figure 2.5), which relates to the unchanged $F0$. Threshold-equalizing noise (TEN) was added to the tones to mask unwanted cues. Successful pitch discrimination between HCU and ICU tones provides evidence for the use of TFS_n cues for pitch perception in contrast to solely envelope cues. The test can be adapted to employ different fundamental frequencies and to include different harmonic ranks of the components.

Early studies by Moore and colleagues suggested lacking discrimination abilities if the harmonic complex tone only contains components above the 14th harmonic, suggesting the use of envelope cues rather than TFS_n cues for higher order harmonics (Moore & Moore, 2003; Hopkins & Moore, 2007). Although Moore *et al.* (2009) reported above-chance performance when components were centred on the 15th harmonic. For harmonics in a range of the 9th to the 14th component approximately, NH participants are generally able to discriminate HCU and ICU tones for a range of fundamental frequencies (Hopkins & Moore, 2011; Moore *et al.*, 2012; Füllgrabe *et al.*, 2014; Jackson & Moore, 2014; Marmel *et al.*, 2015; Innes-Brown *et al.*, 2016; Mathew *et al.*, 2016). These findings suggest that pitch is extracted from timing cues derived from the TFS_n, and not from envelope cues, even for very high frequencies up to 8 kHz with an $F0$ of 800 Hz (Moore & Sek, 2011). This supports evidence by Ernst and Moore (2013) for the use of phase locking cues beyond 5 kHz. A cause of concern is the potential use of excitation pattern cues to discriminate HCU and ICU tones in the TFS1 test. Moore and Sek (2011) addressed this concern by varying the presentation level. If excitation pattern cues were used, discrimination performance would deteriorate at higher presentation levels caused by the widening of auditory filters with increasing level (Oxenham & Simonson, 2006). This was not reported to be the case (Moore & Sek, 2011). While most NH individuals are able to perform the TFS1 test, most individuals with hearing loss are unable to discriminate harmonic and inharmonic tones based on TFS cues (Hopkins & Moore, 2011). The next section provides an overview of the different types of hearing loss.

2.1.2 Types of hearing loss

Hearing loss is characterised by its laterality (unilateral or bilateral), its severity (i.e. mild to profound) and its type (dependent on the anatomical location of the impairment in the auditory pathway). Hearing loss can be caused by issues at any stage in the auditory pathway. When the source of the hearing loss is located in the outer or middle ear, it is referred to as conductive hearing loss, which may often be reversible (Schnupp *et al.*, 2011). Possible causes are ear wax build-up in the ear canal, a burst ear drum, trauma to the ossicles, fluid in the middle ear due to inflammation and many more. If the source of the hearing loss stems from the inner ear it is referred to as sensorineural hearing loss. A typical case of sensorineural hearing loss is the degeneration or loss of hair cells. In mammals, the hair cells in the organ of Corti are not regenerated, resulting in irreversible loss of acoustic hearing (Groves, 2010). A less prevalent type of hearing loss is neural hearing loss, which derives from absence or damage to the auditory nerve, which mostly results in profound and irreversible hearing loss.

2.2 Cochlear implants

As mentioned in **Chapter 1**, the gold-standard treatment to restore hearing in the case of sensorineural hearing loss is cochlear implantation. In the following, the engineering principles of a CI are outlined and the clinical rehabilitation procedures are briefly discussed.

2.2.1 Engineering principles

CI devices can be divided into the internal and external parts (see Figure 2.6). The internal parts consist of an electrode array, which is inserted into the cochlea, and the receiver-stimulator. The external part comprises of the microphone, the speech processor, which is usually worn behind the ear, the transmitter coil and the battery. The microphone picks up sounds such as speech, which the speech processor converts into stimulation patterns containing temporal and spatial information. The information stored in the stimulation patterns are transmitted to the internal receiver-stimulator via magnetic induction from the transmitter coil. In addition to the stimulation patterns, the receiver-stimulator also receives power to send electrical pulses to the electrode array according to the stimulation patterns, inducing action potentials in the auditory nerve.

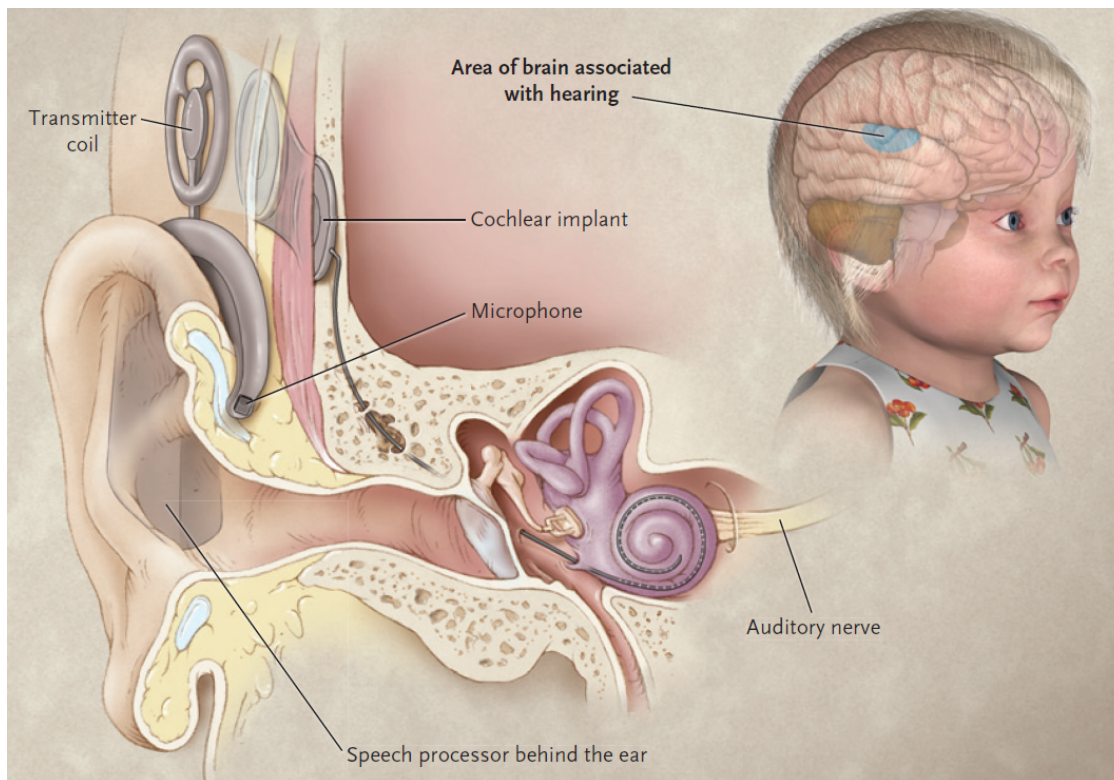


Figure 2.6: Components and position of a cochlear implant.

The speech processor with the microphone and battery is worn behind the ear, the transmitter coil is held in place by a magnet to ensure a stable connection with the internal receiver-stimulator, which is placed subcutaneously. From there signals are passed to the electrode array, which is inserted into the Scala tympani of the cochlea. Adapted from Kral and O'Donoghue (2010).

The design of the speech processing strategy varies between manufacturers and versions. Most current speech processing strategies are based on envelope processing such as the continuous interleaved sampling (CIS), the advanced combination encoder (ACE), the spectral peak (SPEAK), and the “n-of-m” strategies (Wilson & Dorman, 2009). The SPEAK strategy is shown as an example in Figure 2.7. The sound signal is passed through a filter bank similar in design to the auditory filters to extract frequency bands according to the number of available electrode channels. The envelope is extracted from each channel, which usually involves rectification and low-pass filtering of the signal. Subsequently, the signal is compressed to map the wide range of envelope amplitudes to the small dynamic range in electric hearing. Biphasic pulse trains are modulated with the extracted envelopes to stimulate the electrodes. This highlights the central role of the sound envelope for sound perception in CI users, motivating the investigation of objective measures of temporal auditory processing with a particular focus on slow modulation sensitivity in this research.

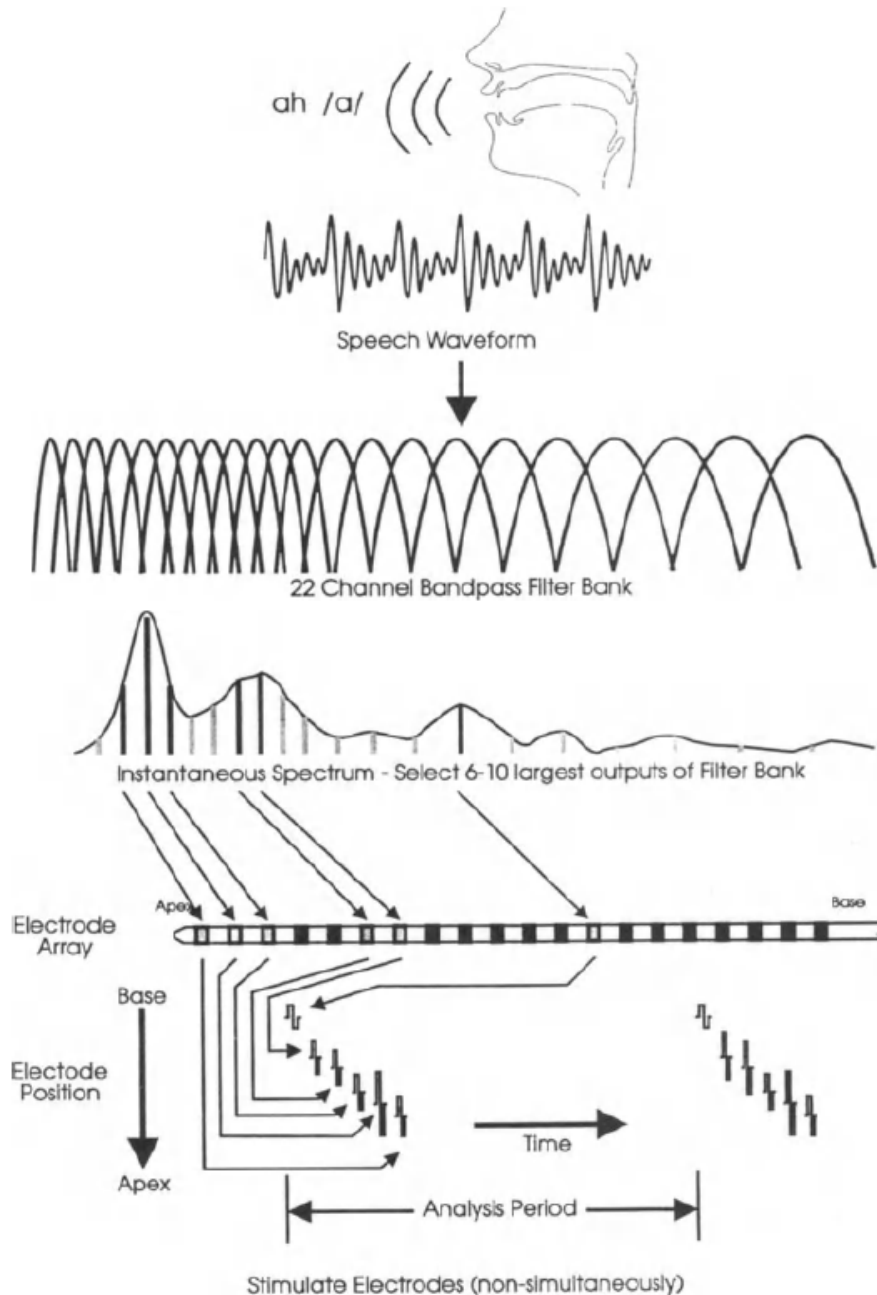


Figure 2.7: Overview of an envelope based speech processing strategy.

Main aspects of the spectral peak (SPEAK) processing strategy. Sound is bandpass filtered with a filter bank, and the envelope is detected in each channel. Prior to electrode stimulation, between one and ten channels are selected based on their amplitude and spectral composition. The selected channels are stimulated in the order from base to apex. Adapted from Patrick et al. (1997).

Most envelope-based processing strategies disregard the acoustic cues conveyed in the TFS of the sounds and stimulation timing carries no additional acoustic information. This is in spite of the fact that TFS information is of critical importance for speech-in-noise recognition and music appreciation. The technological hurdles to improve spectral and TFS cues in CI users include the limitation of current spread and improving the conveyed phase-locked information in the neural spiking pattern by means

of new stimulation approaches (Shamma & Lorenzi, 2013). New approaches address this challenge with current-steering methods and adaptations of the filter-bank (i.e. bell-shaped bandpass filters). Other approaches attempt to convey more TFS information by using higher stimulation pulse rates or by new speech processing strategies such as the fine structure processing strategy (Müller *et al.*, 2012). For a detailed review of speech processing strategies and their development refer to Wilson and Dorman (2009). The efforts by researchers and manufacturers towards improving TFS processing in CI users motivated the investigation of potential objective measures of TFS discrimination abilities presented in **Chapter 6**. It should be noted that current state-of-the-art CI technology is unable to accurately convey the subtle TFS cues on which stimulus discrimination is based in the carried out tests. However, it was of interest to carry out these investigations in a normal-hearing cohort as a primary feasibility study with an eye toward the future.

2.2.2 Rehabilitation procedure

CIs are the most implanted neuroprosthesis worldwide (Ziat & Bensmaia, 2015). Despite its success story, rehabilitation outcomes vary widely and cannot be reliably predicted prior to implantation (Cooper, 2006). This prevents adequate expectation management of patients and family members. Speech perception performance with a CI can span from 0% to 100% recognition with the same device type (Wilson & Dorman, 2009).

With increasing duration of hearing loss, the structures of the central auditory pathway deteriorate as evidenced by neuron degeneration (Moore *et al.*, 1994; Moore *et al.*, 1997). Severe degeneration of the central auditory system is believed to limit rehabilitation success through cochlear implantation (Geier *et al.*, 1999; Leake & Rebscher, 2013). Therefore, it is recommended to minimise the time window between onset of deafness and cochlear implantation. Of course there are numerous other influencing factors such as the condition of the cochlea, the electrode-neural interface, age at implantation (mostly relevant for young children), use of hearing aids, and aetiology among others (Wilson, 2004; Cooper, 2006).

New-borns with a severe to profound hearing loss may receive a CI as early as six months (Graham, 2006). The cochlea is fully grown at birth making replacements of the implanted part of a CI in adolescence unnecessary. Since the introduction of the

nationwide new-born hearing screening in Ireland in 2013, new-borns who fail the hearing screening are referred to specialists to initiate appropriate intervention procedures as early as possible. Since the introduction of the National Cochlear Implant Programme in 1995 in Beaumont Hospital, cochlear implantation is one of the options available to infants from the age of one year or even earlier should time urgency arise from potential ossification of the cochlea due to meningitis (Axon *et al.*, 1998).

In children, the age at implantation has a great influence on later speech performance outcomes. Studies have shown that children who are implanted before the age of two have superior language development compared with children who are implanted after the age of two. Children who are implanted in the first 16 months of their life are more likely to achieve language development similar to NH peers (Manrique *et al.*, 2004; McConkey Robbins *et al.*, 2004; Nicholas & Geers, 2007; Houston & Miyamoto, 2010). Although overall language development is highly affected by the age at implantation, speech perception outcomes are not as closely linked to the age at implantation (Houston & Miyamoto, 2010).

Cochlear implantation is followed by a life-long rehabilitation procedure. Regular fitting appointments are necessary to tune the parameters of the speech processor to continuously adapt parameters and improve performance. This optimization process heavily relies on patient feedback, which can be unreliable or lacking for certain patient cohorts. Current gold-standards for the assessment of rehabilitation performance are consonant, vowel, word and speech recognition tests. Test results can be skewed by subjective factors such as test anxiety, concentration level, mood and fatigue among others. Therefore, objective neurophysiological performance measures are of particular interest in order to clinically assess patients' rehabilitation success (Ponton & Don, 1995; Visram *et al.*, 2015; Hoppe *et al.*, 2016). The development of such objective measures can help clinical teams with rehabilitation procedures and patients' expectation management (Hughes, 2012). For a detailed explanation of the fitting process refer to Cooper (2006).

Objective measures in CI rehabilitation

Neural measures of auditory processing in CI users have been widely investigated over the last three decades. Findings from the neural measures have greatly improved the understanding of the central auditory system and its plasticity in CI users. Unfortunately, the application of neural measures in clinical procedures is limited. To date, neural

measures are mainly implemented pre-implantation to assess the integrity of the auditory nerve and post-implantation to set loudness levels in infants (Abbas & Miller, 2004; Abbas & Brown, 2006) with low-level brain responses such as the electrically evoked auditory brainstem response (EABR) and the electrically evoked compound action potential (ECAP).

Although the EABR has certain advantages over the ECAP, such as better artefact reduction and measurement of AEPs higher up in the auditory pathway, ECAPs are preferred in clinical settings. This is due to their time-efficient acquisition with reverse telemetry from intra-cochlear electrodes. ECAPs are measured for each electrode, and speech processor maps' threshold and comfort levels (T and C-levels, respectively) may be scaled according to the measured profiles (Botros & Psarros, 2010). ECAPs provide an objective fitting approach for cohorts where feedback is lacking, however, ECAP profiles are only moderately correlated with behavioural profiles obtained in adults and large inter-subject variability limits their applicability (Brown *et al.*, 2000; Potts *et al.*, 2007; Miller *et al.*, 2008). Most importantly, these measures have not shown correlations with speech performance (Firszt *et al.*, 2002). To assess hearing ability rather than audibility, higher-level auditory processing, as is required in speech recognition, should be assessed. Low-level neural markers are elicited with simplistic sounds such as individual pulses or pulse trains. Cortical auditory evoked potentials (CAEPs) may also be elicited by more complex and naturalistic sounds as encountered in every-day life. For a detailed review of electrically evoked auditory potentials and their applications in clinical practice refer to Abbas and Brown (2006).

Research studies have investigated change-related CAEPs, such as the acoustic change complex (ACC) and the mismatch negativity (MMN) in CI users with regards to spectral resolution (Stoody *et al.*, 2011; Lonka *et al.*, 2013; Lopez Valdes *et al.*, 2015), pitch perception (Zhang *et al.*, 2013b; Liang *et al.*, 2014; Wagner *et al.*, 2017), intensity perception (Brown *et al.*, 2008; Dinces *et al.*, 2009; Kim *et al.*, 2009; Sandmann *et al.*, 2010), electrode discrimination (Wable *et al.*, 2000; Hoppe *et al.*, 2010; He *et al.*, 2014; Mathew *et al.*, 2017), TFS perception (Leijsen *et al.*, 2015), musical feature perception (Rahne *et al.*, 2011; Zhang *et al.*, 2013a; Timm *et al.*, 2014; Petersen *et al.*, 2015) and speech sound discrimination (Kraus *et al.*, 1993b; Lonka *et al.*, 2004; Friesen & Tremblay, 2006; Rahne *et al.*, 2010; Ortmann *et al.*, 2013; Turgeon *et al.*, 2014; Moberly *et al.*, 2015), and their correlations with behavioural measures as well as their relationship to speech recognition (Hoppe *et al.*, 2010; Won *et al.*, 2011a; He *et al.*, 2014; Leijsen *et*

al., 2015; Lopez Valdes *et al.*, 2015). The successful measurement of CAEPs in electrical hearing requires the consideration of the artefact from electrical stimulation in the experimental design. Additional artefact reduction methods are required to reduce the artefact during post-processing. For an overview of post-processing methods refer to the introduction of **Chapter 5**.

Additionally to CAEPs, the electrically evoked auditory steady-state response (EASSR) has been evaluated as a measure of temporal modulation sensitivity and stimulation thresholds (Hofmann & Wouters, 2010; 2012; Deprez *et al.*, 2014; Luke *et al.*, 2015; Gransier *et al.*, 2016; Luke *et al.*, 2016).

2.3 Electrophysiology in auditory processing

This section introduces objective measures of auditory processing, referred to as auditory evoked potentials (AEPs), with a particular focus on the late occurring CAEPs and their applicability as a change detection measure in neural responses.

2.3.1 Auditory evoked potentials

EEG recordings provide a non-invasive and readily available tool to obtain AEPs. As shown in Figure 2.8, human AEPs may be classified as transient, sustained or following responses (Picton, 2013). Transient responses are evoked by sudden stimulus changes (e.g. silence to sound or sound A to sound B), whereas sustained responses are elicited continuously throughout the stimulus duration. Following responses share characteristics with both, transient and sustained responses: They track stimulus properties in a continuous stimulus and respond to changes such as amplitude variations (envelope following response, EFR) or frequency variations (frequency following response, FFR). The auditory steady-state response (ASSR) constitutes a special case of the following responses, which is evoked if the changes within the stimulus are periodic, e.g. amplitude fluctuations with a constant AM rate (Dimitrijevic *et al.*, 2016). Neural responses elicited by varying AM rates have different neural generators, i.e. AM rates below 70 Hz originate predominantly from the cortex, whereas AM rates above 70 Hz are associated with generators in the brainstem (Dimitrijevic & Ross, 2008).

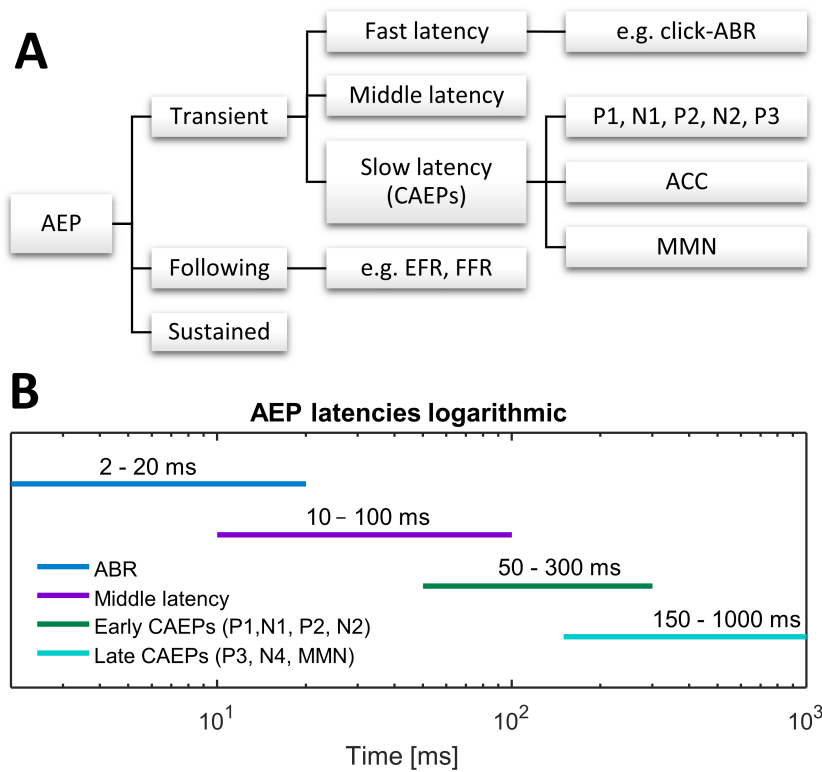


Figure 2.8: Overview of auditory evoked potential (AEP) classifications (A) and latencies (B).

(A) Indicated by the box are the late cortical auditory evoked potentials (CAEPs), which are the focus of this thesis. (B) Latencies of AEPs are shown on a logarithmic scale to capture the wide range. Abbreviations and acronyms: CAEPs – Cortical auditory evoked potentials, EFR – Envelope following response, FFR – Frequency following response, ABR – Auditory brainstem response, ACC – Acoustic change complex, MMN – Mismatch negativity.

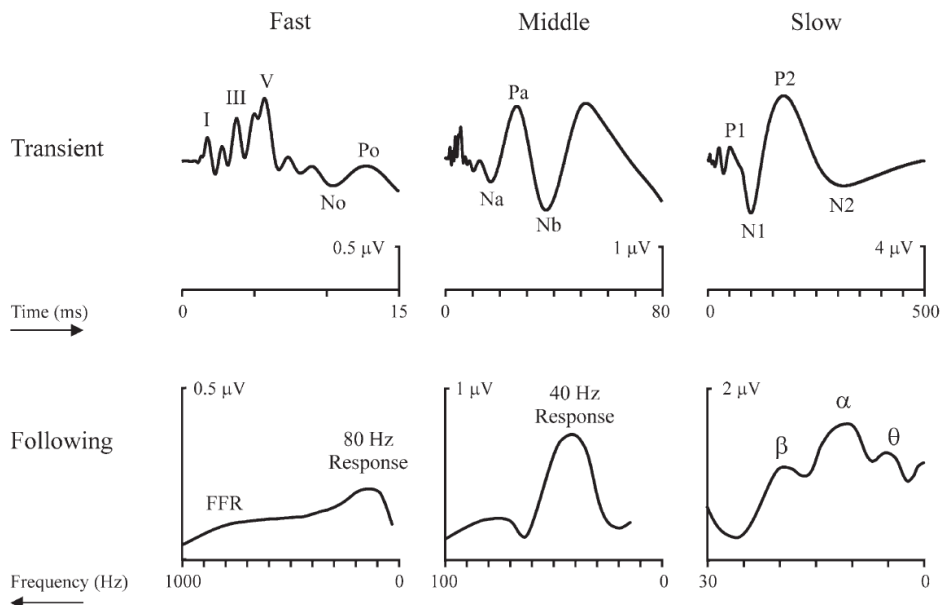


Figure 2.9: Waveforms of transient and following auditory evoked potentials (AEP).

Depicted transient responses (top) were elicited by audible clicks with a repetition rate of one click per second. The following responses (bottom) were elicited by amplitude modulated noise stimuli with low amplitude modulation (AM) rates on the right and increasing AM rates towards the left. Adapted from Picton (2013).

Transient AEPs are commonly distinguished by their latency with fast/early, middle and slow/late latency AEPs. Examples are depicted in Figure 2.9. Early AEPs, i.e. the auditory brainstem response (ABR) towards click-stimuli, originate from the cochlea and brainstem; middle latency responses are recorded from early activation of the auditory cortex; late AEPs derive from auditory cortex and association cortices (Picton, 2013), and thus, are labelled CAEPs.

2.3.2 Late cortical auditory evoked potentials

Slow transient CAEPs refer to AEPs elicited later than 50 ms post-stimulus onset (Pryse-Phillips, 2009). Numerous studies have provided evidence for the scope of cortical auditory evoked potentials (CAEPs) to objectively assess the perception of acoustic features including low-level features such as gap detection (Bertoli *et al.*, 2001; Todd *et al.*, 2011; He *et al.*, 2013), intensity discrimination (Martin & Boothroyd, 2000; Näätänen *et al.*, 2004; Dimitrijevic *et al.*, 2009) and spectral discrimination (Martin & Boothroyd, 2000; Dimitrijevic *et al.*, 2008), as well as based on complex higher-order features such as regularity (Tervaniemi *et al.*, 1994; Vuust *et al.*, 2005) and spatial localisation (Paavilainen *et al.*, 1989; Deouell *et al.*, 2006).

CAEPs elicited by sound onset/offset mainly comprise the P1, N1, and P2 components (Figure 2.9, top right). The amplitude and latency of these components depends on stimulus characteristics, and thus, they are considered to be exogenous responses (Näätänen *et al.*, 2007). Sound onset/offset can be regarded as the change from silence to sound and vice versa. Other change responses classified as slow CAEPs, which rely on changes in stimulus properties, are the P3 component, the ACC and the MMN. Stimulus changes in the auditory domain may arise from spectral, temporal, intensity, durational or spatial stimulus properties among others (Näätänen *et al.*, 2007; Bartha-Doering *et al.*, 2015; Kim, 2015). Cortical measures of change detection are briefly outlined in the following and for more in-depth information refer to Picton (2011).

Acoustic Change Complex

The ACC is an unattended secondary P1-N1-P2 complex elicited by an acoustic change in an on-going sound indicating change detection on the auditory cortex level. Examples for low-level acoustic changes are intensity or pitch differences without a change in a different acoustic domain (e.g. onset responses always include intensity

variations in addition to the acoustic features of the tone) or higher-level changes such as timbre or speech sounds (e.g. /ui/). The ACC can be recorded in a continuous paradigm, where stimuli repeatedly change between tones without silent intervals, or in an intermittent paradigm. In the continuous paradigm, the stimulus can change between two tones (A to B and B to A) or the stimulus can change between multiple tones (e.g. A to B to C to D). In the intermittent paradigm, concatenated tone pairs are interleaved with silent periods, providing primary and secondary (ACC) N1-P2 complexes (Figure 2.10).

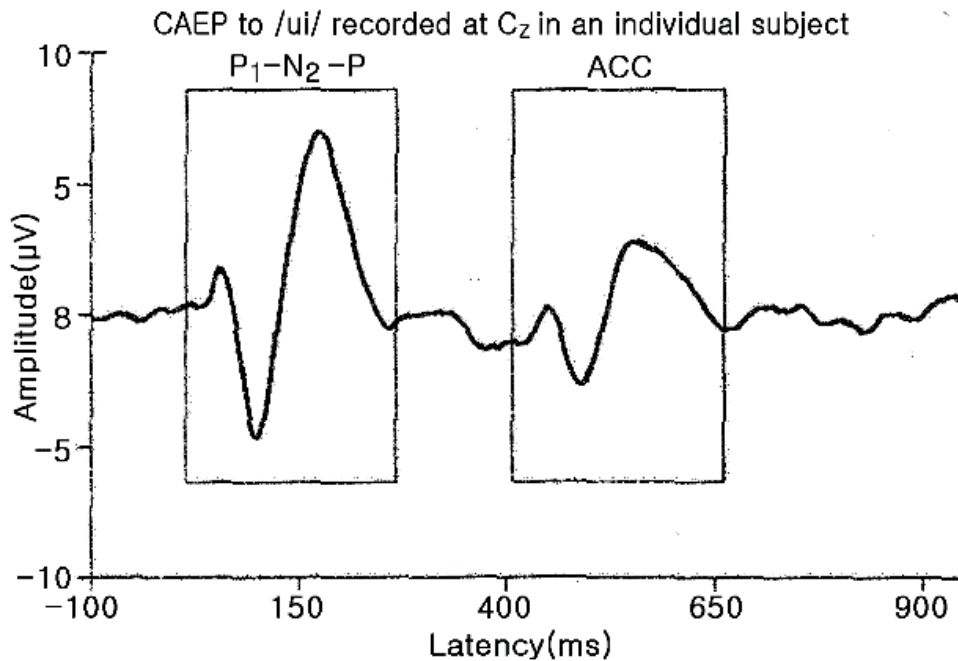


Figure 2.10: P1-N1-P2 complex followed by the acoustic change complex (ACC).
The primary P1-N1-P2 complex was elicited at sound onset of the vowel-vowel stimulus /ui/ and the secondary P1-N1-P2 complex, referred to as ACC, was elicited following the acoustic change at 400 ms. Adapted from Burkard et al. (2007).

Auditory mismatch negativity

The MMN is commonly obtained from neurophysiological data acquired with an oddball paradigm. It may also be acquired with multiple-deviant paradigms. The MMN may be elicited in various sensory modalities, however, for continuing with the theme of research here the MMN refers to the auditory MMN. CAEPs elicited by a frequent standard stimulus (e.g. occurrence probability 90%) are subtracted from the CAEPs towards an infrequent deviant stimulus (e.g. occurrence probability 10%). The difference waveform as shown in Figure 2.11 demonstrates a late negative component usually observed with peak latencies between 100 ms and 250 ms (Garrido *et al.*, 2009b), namely the MMN. The MMN is elicited independent of the participant's arousal or attentional

state (Näätänen *et al.*, 1978; Näätänen, 1990). Its amplitude increases, whereas its latency decreases with increasing acoustic change saliency (Näätänen *et al.*, 1989; Tiitinen *et al.*, 1994). The MMN can be elicited across all age groups (Cheour *et al.*, 1998; Kushnerenko *et al.*, 2002; Morr *et al.*, 2002) and even new-borns and infants have a reliable mismatch response, albeit sometimes with a different morphology (Kushnerenko *et al.*, 2002; He *et al.*, 2007; Cheng *et al.*, 2015). Source localization studies have revealed a mix of generators in the temporal lobes consistent with the auditory cortex (Lappe *et al.*, 2013) and inferior frontal lobes, which is likely associated with attention switching following deviant presentation (Alho, 1995).

The physiological processes underlying the MMN are unknown and different models have been proposed to explain the generation of the change-related negativity. The two most popular MMN-mechanism models are the memory-trace model, which suggests that the MMN is the result of perceptual change detection in stimulus sequences based on stimulus deviations from sensory memory traces (Näätänen, 1990; Näätänen *et al.*, 2007; Fishman, 2014); and the more recent regularity-violation or prediction model, which claims that the MMN is elicited due to a mismatch between the incoming auditory information of the deviant and predictions formed based on patterns of recent incoming information (Winkler, 2007; Näätänen *et al.*, 2011; Paavilainen, 2013).

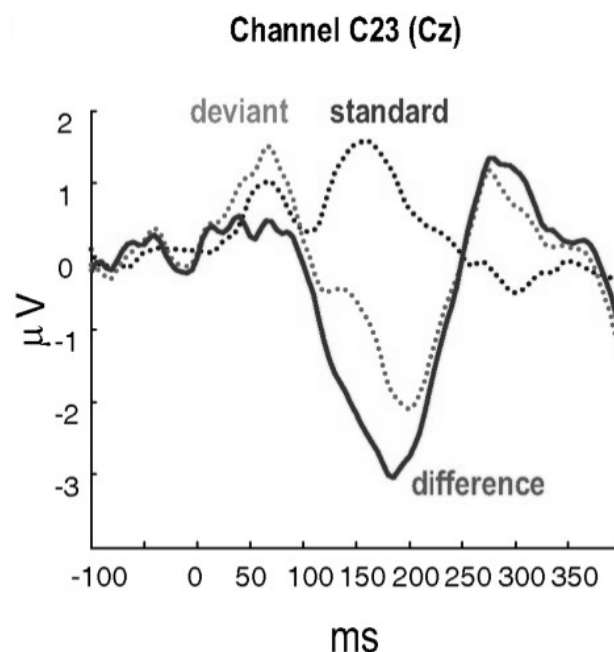


Figure 2.11: Example of the mismatch negativity (MMN). Cortical auditory evoked potentials (CAEPs) are shown for a central electrode location (Cz) in response to the standard and deviant stimulus. Their respective difference waveform shows the mismatch negativity (MMN) with the characteristic negative deflection at around 170 ms (generally seen between 100 ms and 250 ms). Adapted from Garrido *et al.* (2009a).

Similar to the ACC, the acoustic change feature can be a low-level (e.g. frequency, intensity or location difference) or a higher-level change such as timbre or in speech sounds (e.g. /ui/). Furthermore, the MMN can be elicited by temporal pattern violations, e.g. varying inter-stimulus intervals (Kujala *et al.*, 2001; Brannon *et al.*, 2008), varying stimulus duration (Baldeweg *et al.*, 2004), directional changes in pitch sweeps (Saarinen *et al.*, 1992; Tervaniemi *et al.*, 1994; Haigh Sarah *et al.*, 2017), musical rhythm irregularities (Vuust *et al.*, 2005) or omission of stimuli (Salisbury, 2012). One limitation of the MMN is the long acquisition time with oddball paradigms, as deviants are only presented with a low probability (e.g. 10%) and sufficient stimulus repetitions are required to obtain robust CAEPs for the deviant. Picton (2011) claims that 200 – 1000 deviant repetitions are required per condition, however, most published MMN studies average between 50 and 200 deviants due to time constraints. The number of required deviants is highly reliant on the stimulus type and saliency of the acoustic change as well as on the subject.

The MMN can be elicited with the classical single-deviant (oddball) paradigm, where only one type of deviant, e.g. one acoustic change type, is presented in a block, but also with multi-deviant paradigms (Näätänen *et al.*, 2004; Petermann *et al.*, 2009; Sandmann *et al.*, 2010; Fisher *et al.*, 2011; Hay *et al.*, 2015). Multi-deviant paradigms have included up to six different deviants (Näätänen *et al.*, 2004; Fisher *et al.*, 2011; Petersen *et al.*, 2015), where each standard *S* is followed by a different deviant *D* (e.g. *S*, *D1*, *S*, *D2*, *S*, *D3*, *S*, *D4*, [...]) resulting in greatly improved efficiency with regards to data acquisition time. This is of high importance for clinical settings and addressing one major drawback of the MMN. Each standard presentation enforces its memory trace with an overall occurrence probability around 50%, and deviants elicit the MMN despite the predictability of a deviant occurrence with individual deviant probabilities of about 10%. However, one important limitation of this multi-deviant paradigm is the fact that deviant types also have to differ in an acoustic feature from each other, not solely from the deviant, as otherwise their occurrence probability would not be perceived as 10% for each, but as 50%. As a result, the multi-deviant MMN cannot be used to determine neural thresholds for a specified acoustic property. An example for a multi-deviant paradigm would be a standard pure tone of 500 Hz, and deviant changes based on pitch (e.g. a 1000 Hz pure tone), presentation level, duration, spectral complexity/timbre or location.

P3a/P3b/P300

In an active oddball paradigm, the participant has to respond to the deviant sound presentation (the target) by means of a button click or by counting the number of presented deviants. Target detection results in a CAEP referred to as the P3b/P300 component, visible as a positive deflection in the target CAEPs with a broad latency range of 250 ms to 500 ms depending on the modality and task details (Polich, 2007). The P3b is related to decision making, and thus, is considered to be an endogenous response. The introduction of another infrequent, but task-unrelated, distractor stimulus to the active oddball paradigm may evoke a novelty response referred to as the P3a component (Polich, 2007). The active auditory oddball paradigm may defeat the purpose of finding a non-feedback based assessment tool, but nonetheless, it may prove valuable in the process of understanding neural processes underlying change detection and decision making.

2.3.3 CAEPs in CI users

Given the applicability of CAEPs to investigate central auditory function, CAEPs have been implemented to assess auditory function throughout CI rehabilitation procedures, as well as to monitor brain maturation in paediatric cohorts (Ponton *et al.*, 1996b; Eggermont *et al.*, 1997; Ponton *et al.*, 2000; Sharma *et al.*, 2005), and to identify neural plasticity as indicated by cortical re-organization due to altered sensory input (Ponton *et al.*, 1996a; Sharma *et al.*, 2007).

However, measuring CAEPs in CI users is hindered by the artefact which is induced by the electrical stimulation. This artefact is time-locked to the stimulus presentation like the neural response that is associated with the CAEP, and the artefact is commonly an order of magnitude higher than the neural response of interest (Gilley *et al.*, 2006; Sandmann *et al.*, 2009; Friesen & Picton, 2010; Mc Laughlin *et al.*, 2013).

An example of a CI artefact in CAEP measurements is presented in Figure 2.12. The artefact shows the typical “pedestal effect” at sound onset and offset, as well as the continuous artefact for the duration of the stimulus, which resembles the stimulus envelope for recording electrodes near the stimulation electrodes of the CI. The CI artefact is highly variable across and within participants (Gilley *et al.*, 2006). Within-participant variation is mostly related to stimulus properties such as presentation level and stimulus envelope. Across-participant variability arises from differences in the position of the stimulation electrodes, the electrode neuron interface, as well as from

stimulation parameters and speech processing strategies (Sandmann *et al.*, 2009). The CI artefact is substantially larger when stimulation is applied in monopolar mode compared to bipolar stimulation (Gilley *et al.*, 2006; Li *et al.*, 2010) and most current commercial CI devices employ monopolar stimulation. Furthermore, the artefact severity increases with the pulse width duration and stimulation levels (Li *et al.*, 2010; Wagner *et al.*, 2018). Wagner *et al.* (2018) proposed an artificial brain setup to evaluate the influence of stimulation parameters such as patient map and stimulation current magnitude on the electrical CI artefact, which may provide a valuable tool to assess the artefact for novel complex stimuli prior to the experiments for future studies.

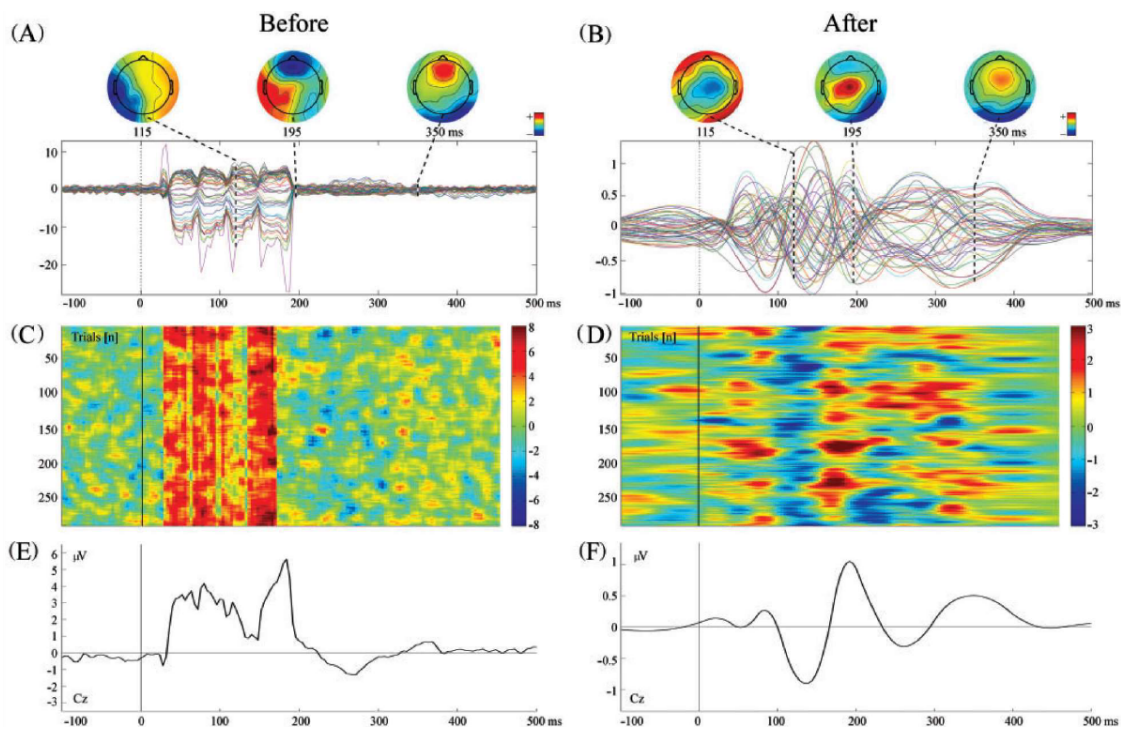


Figure 2.12: Example of the electrical artefact elicited by cochlear implant (CI) stimulation and its reduction with independent component analysis (ICA).

*Topographical plots, butterfly plots, and single-trial imaging of cortical auditory evoked potentials (CAEPs) before (left) and after (right) ICA-based artefact reduction. Depicted CAEPs were elicited by target stimuli in a P3b-paradigm. Images (E) & (F) show the CAEP for electrode Cz located at the vertex. Note the different scaling of CAEP amplitudes across images. Adapted from Sandmann *et al.* (2009).*

With specially designed research platforms (e.g. the NIC from Cochlear Ltd.), the stimulation settings can be closely controlled, however, a different research platform is required for each manufacturer, and in most clinical settings these platforms are unavailable. In the research presented here, CI user research studies utilize the clinical processors for sound presentation, which limits the opportunities with regards to control over stimulation settings, but makes the research more clinically friendly, and thus, more applicable.

Studies investigating EEG responses in CI users proposed artefact rejection algorithms based on beam formers (Wong & Gordon, 2009), polynomial fitting (Mc Laughlin *et al.*, 2013), “blanking” (Hofmann & Wouters, 2010; 2012) and independent component analysis (ICA) (Gilley *et al.*, 2006; Viola *et al.*, 2012; Miller & Zhang, 2014) among others. Each of these approaches has its own limitations: ICA is often subjective, time-consuming and computationally expensive. “Blanking”, which is a popular method for EASSR recordings, requires stimulation of a single electrode via a research interface, high sampling rates, low to intermediate stimulation rates (≤ 500 pulses per second for monopolar stimulation mode), and it can only reliably reduce the CI artefact at contralateral electrodes with respect to the implanted ear (Gransier *et al.*, 2016). Polynomial fitting requires a sampling rate which is sufficient to resolve the individual pulses, similar to the blanking method, and relies on flat envelopes of the acoustic signal to fit the polynomial to the CI artefact².

2.4 Envelope processing and amplitude modulation detection

Speech processing in humans is a complex process based on the integration of spectral and temporal information, where temporal information can be divided into the slow amplitude fluctuations in the envelope and the faster temporal changes conveyed in the TFS (Figure 2.13).

The temporal envelope is considered as one of the most important features for speech intelligibility (Drullman, 1995; Shannon *et al.*, 1995). Specifically, envelope fluctuations with rates below 16 Hz are crucial for phoneme recognition (Drullman *et al.*, 1994; Xu *et al.*, 2005). Simplified, speech envelope fluctuations can be regarded as low-rate AM of a carrier signal. The significance of slow envelope fluctuations for speech recognition has prompted wide-spread investigations of brain activity in response to sounds with low-rate AM in the last decade (Edwards & Chang, 2013). In this context, low-rate AM refers to AM rates in the fluctuation range, in which the human ear can follow the modulations ($\sim 1 - 20$ Hz). In contrast, the human ear cannot follow the

² Flat envelopes of the acoustic stimulus are necessary to constrain the fit of the polynomial to the artefact and not to the neural response. For detailed information refer to Mc Laughlin, M., Lopez Valdes, A., Reilly, R.B. & Zeng, F.G. (2013) Cochlear implant artifact attenuation in late auditory evoked potentials: a single channel approach. *Hearing research*, **302**, 84-95.

amplitude variation of sounds with higher AM rates. AM sounds with rates above the fluctuation range may be perceived as roughness or periodicity pitch, depending on the AM rate and the carrier frequency (Fastl & Zwicker, 2007).

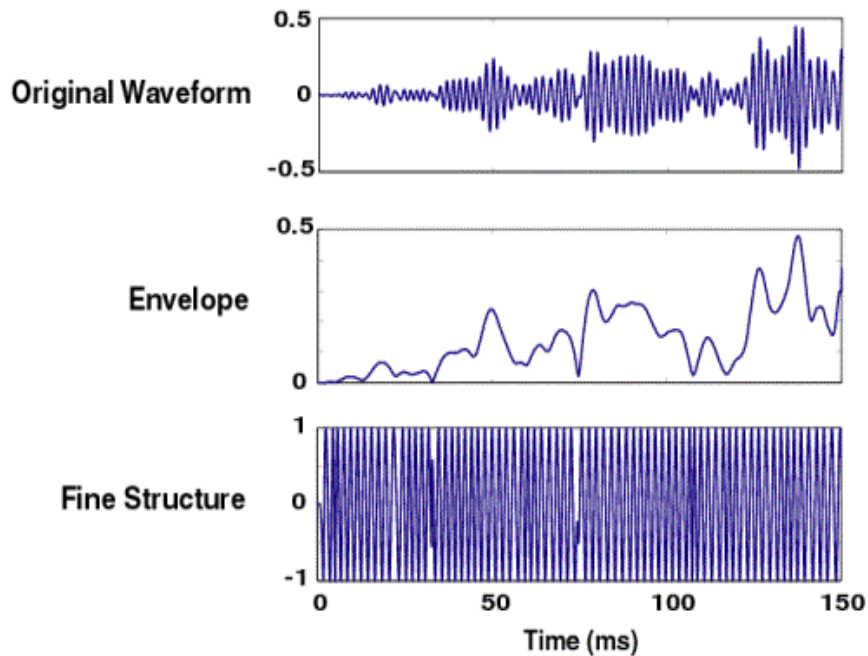


Figure 2.13: Temporal envelope and temporal fine structure of a complex signal.
 (<http://research.meei.harvard.edu/chimera/motivation.html>, last accessed on 09.08.2018)

A literature review by Edwards and Chang (2013) highlighted the tuning of the human auditory system to fluctuations between 1 Hz and 10 Hz and its implications for speech processing. Behavioural research studies in CI users have reported positive correlations between speech measures (i.e. vowel, consonant, phoneme, syllable, and sentence detection) and low-rate ($f_m < 20$ Hz) AM detection abilities (Gnansia *et al.*, 2014; De Ruiter *et al.*, 2015) as well as high-rate ($f_m \geq 20$ Hz) AM detection abilities (Cazals *et al.*, 1994; Fu, 2002; Luo *et al.*, 2008; Won *et al.*, 2011b; De Ruiter *et al.*, 2015), emphasizing the particular importance of AM sensitivity for electrical hearing. Across groups of younger and older NH and CI participants, Jin *et al.* (2014) found significant correlations between AM detection thresholds (2 Hz & 4 Hz) and speech-in-noise recognition with a modulated noise masker, but not for 8 Hz AM detection. However, no within-group correlations were reported.

Due to its significance for speech recognition, recent research efforts have focused on the underlying mechanisms of slow AM processing in the brain. Neuroimaging studies have explored the brain's source activity towards AM sounds and underlined its relevance for speech recognition. Giraud *et al.* (2000) found that AM sounds are processed

according to their AM rate, with slow fluctuations (< 32 Hz) in the cortex, medium AM rates (32 Hz to 64 Hz) in the inferior colliculus and fast AM rates (> 64 Hz) in the cochlear nucleus (brainstem). Furthermore, Giraud *et al.* (2000) found that the brain regions Heschl's gyrus, superior temporal gyrus (STG), superior temporal sulcus (STS) and supramarginal gyrus are more activated for AM stimuli compared to unmodulated stimuli. This finding is supported by Scott *et al.* (2006), who showed that the superior temporal sulcus and superior temporal gyrus activity increases from silence to noise, from noise to AM noise, and from AM noise to speech. The overlap in involved brain regions for AM processing and speech processing, particularly for the slow AM rates, is further evidence for the importance of AM for speech processing (Giraud *et al.*, 2000; Scott *et al.*, 2006).

2.4.1 Objective measures of AM detection

Previous attempts in determining an objective, neural measure of AM detection abilities have investigated transient CAEPs in form of the ACC (Han & Dimitrijevic, 2015) as well as following neural responses such as the ASSR (Manju *et al.*, 2014; Luke *et al.*, 2015) and the EFR (Purcell *et al.*, 2004). The reader is referred to Picton (2013) for an in-depth review on evoked potentials representing temporal processing abilities.

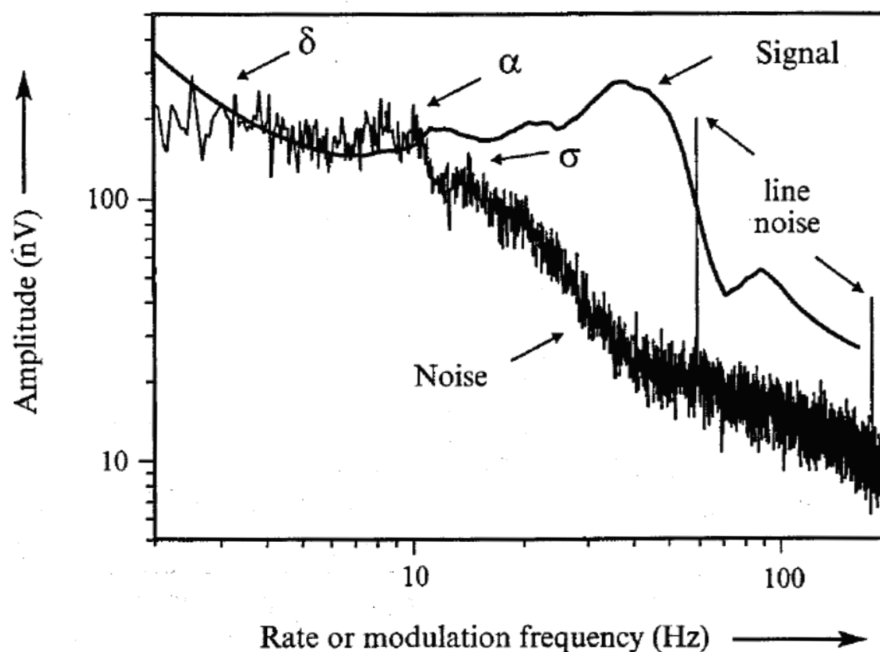


Figure 2.14: Example measurements of auditory steady state (ASSR) signals and measurement noise at different amplitude modulation (AM) rates.

*Due to increased neural activity in lower frequency bands (< 10 Hz), the signal-to-noise ratio of ASSRs is considerably poorer at those AM rates compared to the ASSRs elicited by AM rates of i.e. 40 Hz. Adapted from Picton *et al.* (2003).*

Investigation of the EFR and the ASSR in NH cohorts for differing AM rates above 20 Hz and with constant AMDs showed significant correlations between neural response amplitudes and behavioural AM detection thresholds (Purcell *et al.*, 2004; Manju *et al.*, 2014). A similar study by Luke *et al.* (2015) explored the EASSR in CI users for AM rates of 4 Hz and 40 Hz and found significant correlations between EASSRs at 40 Hz and behavioural AM detection thresholds at 20 Hz. Although the EFR and (e)ASSR are commonly employed to assess neural sensitivity towards AM stimuli, there are also clear disadvantages associated with these methods: ASSRs have low amplitudes in the 50 – 200 nV range (Picton *et al.*, 2003) compared to late cortical potentials which are commonly in the range of several μV ; ASSRs can be readily measured for higher AM rates such as 40 Hz, however, for AM rates below 10 Hz the neural ‘background noise’ is greatly increased (Picton *et al.*, 2003; Goossens *et al.*, 2016) as depicted in Figure 2.14, resulting in poor signal-to-noise ratios (SNRs); last but not least, EASSRs have not been successfully obtained from CI users with clinical device settings (monopolar stimulation mode and stimulation rate of equal to or above 900 pulses per second) as the artefact cannot be reliably reduced.

To date, artefact reduction of EASSRs relies on stimulus presentation through research interfaces, in contrast to every-day speech processors, in bipolar stimulation mode (Hofmann & Wouters, 2010; 2012) or monopolar stimulation mode with stimulation rates below 500 pulses per second (Gransier *et al.*, 2016). Dimitrijevic *et al.* (2016) presented the first study comparing neural thresholds derived from EFRs towards AMD sweeps with behavioural AM detection thresholds for 41 Hz AM and reported significant correlations. However, no studies are known to the author investigating the relationship between AM detection abilities and EFRs elicited for differing AMDs for low AM rates.

Han and Dimitrijevic (2015) have investigated the influence of AMDs on AM detection as measured with ACCs for differing AM rates including low-rate AM of 4 Hz. They showed a fast decline in ACC amplitude for decreasing AMDs above behavioural AM detection thresholds. No studies are known to the author that investigate the MMN as an objective measure of AM detection.

The temporal response function (TRF) (Lalor *et al.*, 2009; O'Sullivan *et al.*, 2015; Crosse *et al.*, 2016; Wong *et al.*, 2018) offers an alternative approach to assess cortical processing of the sound envelope. Rather than measuring the neural response to repetitions of a discrete stimulus, the TRF is also able to calculate the auditory system's

response to ongoing stimuli, such as natural speech. Based on this approach, one can investigate how stimulus features are encoded in the measured neural response.

2.5 Temporal fine structure processing

As mentioned in Section 2.4, temporal acoustic features can be divided into the slow temporal envelope and more rapid oscillations (Figure 2.13) which are referred to as the TFS (Moore, 2014). TFS processing is of particular importance for the perception of pitch, music appreciation and spatial localisation (Moore, 2008) as well as speech perception (Xu *et al.*, 2017). Furthermore, there is evidence that TFS cues can enhance speech recognition in adverse listening conditions due to dip listening (Hopkins & Moore, 2009; 2010b). TFS processing and its role in auditory perception has been the topic of great interest over the last decade and is still hotly debated among linguists, psychoacousticians and neurophysiologists. People suffering from hearing impairments show poor use of TFS cues (Moore, 2008), which may be an important detrimental factor in the difficulty with speech-in-noise perception (Lorenzi *et al.*, 2006; Hopkins *et al.*, 2008; Hopkins & Moore, 2011). Similarly, CI users show poorer performance compared to NH controls in tasks reliant on TFS processing (Drennan *et al.*, 2008; Zirn *et al.*, 2016; Dincer D'Alessandro *et al.*, 2017). This can partly be attributed to the fact that the most common CI speech processing strategies concentrate on conveying temporal envelope information, and often neglect TFS processing (Wilson, 2000; Heng *et al.*, 2011). However, research efforts have been addressing this shortcoming particularly with the aim of improving speech-in-noise recognition, spatial localisation and musical perception in CI users (Wilson, 2000; Hochmair *et al.*, 2006; Arnoldner *et al.*, 2007; Müller *et al.*, 2012; Li *et al.*, 2013; Churchill *et al.*, 2014; Apoux *et al.*, 2015). Future advancements in speech processing algorithms may improve TFS cues in electric hearing, further increasing the clinical need for objective measures of TFS processing. It has to be noted that the term TFS is used inconsistently throughout literature. Moore (2014) suggested to distinguish the terms TFS_p , TFS_{BM} and TFS_n , referring to the TFS of the physical stimulus, the basilar membrane excitation at a specified auditory filter and the neural firing, respectively.

2.5.1 Assessment of TFS sensitivity

The TFS of a sound is closely linked to its spectral content. For example, the TFS of a 500 Hz pure tone is different to a pure tone of 1000 Hz. However, their discrimination would be based on a combination of place and timing codes. In order to assess “pure” TFS processing, tone pairs void of identifiable spectral cues have to be designed, which poses challenges in the experimental design.

Different tests have been proposed to assess TFS sensitivity which can be divided into monaural and binaural tests. Binaural tests commonly assess inter-aural phase difference (IPD) discrimination, such as the TFS-LF test (Hopkins & Moore, 2010a; Sek & Moore, 2012) and the TFS-AF test (Füllgrabe *et al.*, 2017).

The research carried out within the framework of this thesis concentrated on monaural TFS processing abilities. This decision was motivated by the idea that potential objective measures of TFS processing should be applicable in CI users once technology has advanced sufficiently to provide high-quality TFS information, and to date a large proportion of CI users have received only unilateral CIs. Monaural TFS discrimination abilities may be assessed with the TFS1 test (Moore & Sek, 2009) which was introduced on pp. 13-14, and further details on stimulus creation are provided in **Chapter 6**. A drawback of the TFS1 test is that it can only be reliably administered for fundamental frequencies above 75 Hz, which relates to harmonics above 750 Hz (Moore & Sek, 2009; Jackson & Moore, 2014). In contrast, the binaural tests can also be employed at low frequencies (Hopkins & Moore, 2010a; Füllgrabe *et al.*, 2017).

An alternative approach to assessing monaural TFS processing abilities is based on the discrimination of Schroeder-phase harmonic complex tone pairs, which were first described by Schroeder (1970). Schroeder-phase complex tone pairs consist of the so called positive and negative Schroeder-phase harmonic complex tone, which have equal frequency spectra and envelopes, but the two stimuli differ in their fine temporal dynamics resulting from phase effects. More in-depth details of the stimulus creation are provided in Section 6.2.1.

2.5.2 Objective measures of TFS sensitivity

Studies exploring potential objective measures of TFS processing have investigated cortical and brainstem responses for monaural and binaural TFS processing in NH cohorts (Innes-Brown *et al.*, 2016; Mathew *et al.*, 2016; McAlpine *et al.*, 2016),

participants with sensorineural hearing loss (Mathew *et al.*, 2016) and CI users (Leijssen *et al.*, 2015) and they are discussed in the following.

McAlpine *et al.* (2016) have successfully elicited neural following responses corresponding to the detection of inter-aural phase modulation (IPM) changes for low-frequency tones in a NH cohort. A cleverly laid out experimental design showed that neural responses exhibited a spectral peak in the FFT at the rate of IPM changes. IPM was changed several times a second by switching the ear with the leading phase without changing the overall magnitude of the inter-aural phase difference, each time resulting in a neural response. It should be mentioned, that significant responses have been recorded on a group mean level, however, it remains to be seen whether IPM detection can be reliably distinguished on an individual level (Figure 2.15).

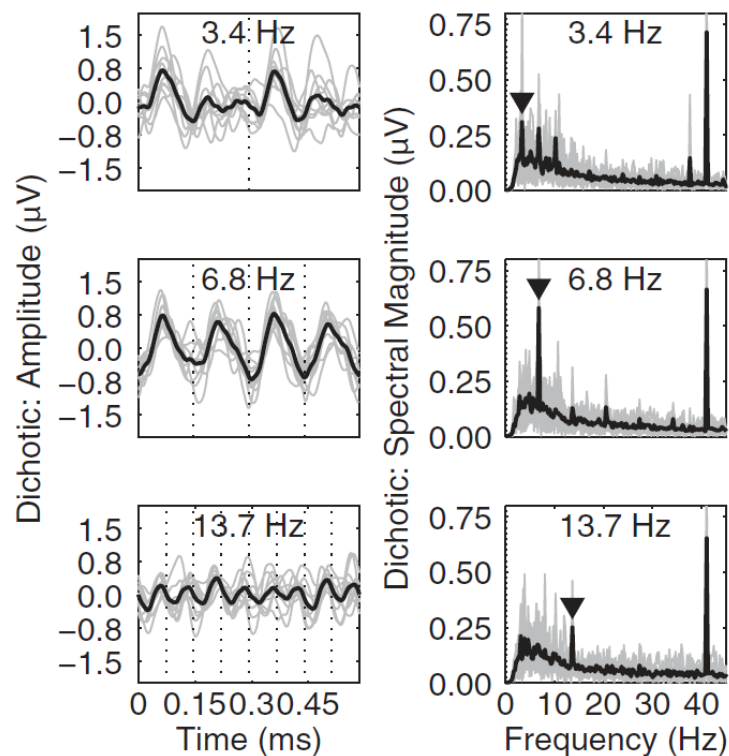


Figure 2.15: Grand average (black) and individual (grey) inter-aural phase modulation (IPM) following responses.

*The left column shows the temporal representation of the neural response and the right column shows its FFT. The three rows relate to the IPM rate, e.g. 3.4 IPM changes per second. Adapted from McAlpine *et al.* (2016).*

Innes-Brown *et al.* (2016) have explored the relationships between speech-in-noise recognition, behavioural TFS1 scores and EFRs elicited by a resolved harmonic complex tone and an AM tone modulated at 110 Hz. However, the use of the term TFS sensitivity in relationship to the neural EFR is somewhat misleading, as the neural response is most likely elicited by envelope cues related to the periodicity. I believe the

authors refer to TFS sensitivity because the periodicity of the stimuli has a rate above 100 Hz, which according to some definitions relates to the TFS of the physical stimulus, not its envelope. However, on a neural level, the EFR is a measure of envelope cues on the basilar membrane and the reader should be aware of this discrimination. EFRs were successfully measured on a group mean level (Figure 2.16), and individual correlations between EFR and stimulus envelope provided a measure of encoding accuracy. TFS1 scores were correlated with neural encoding accuracy for the harmonic complex tone ($p = 0.04$). However, the lack of correction for multiple comparisons has to be considered when interpreting the results.

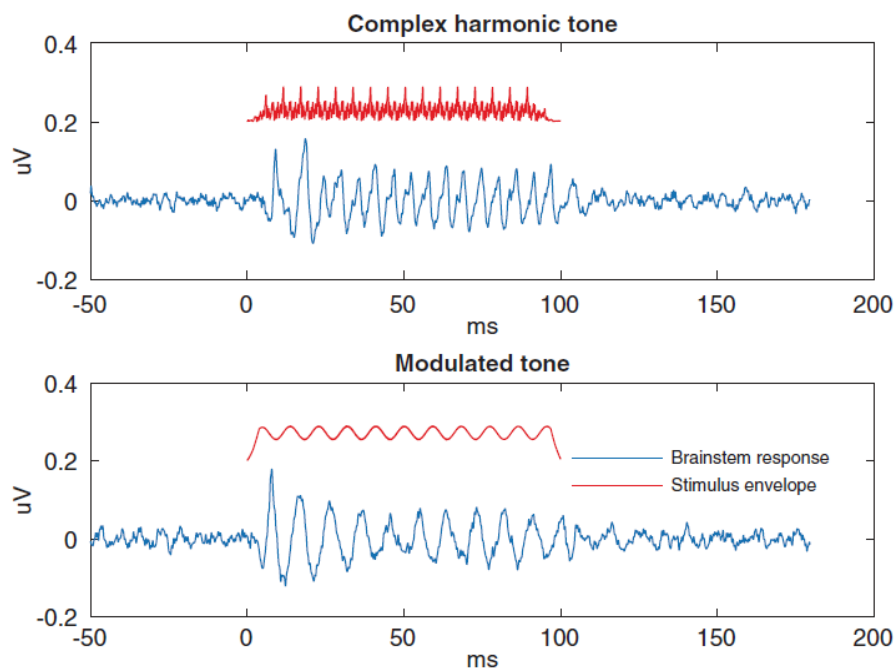


Figure 2.16: Grand average envelope following response (EFR) and stimulus Hilbert transforms of the acoustic stimuli.

The complex harmonic tone with resolved components had a fundamental frequency of 180 Hz and the modulated tone had a pure tone carrier of 4 kHz and a modulation rate of 110 Hz. Adapted from Innes-Brown et al. (2016).

The ACC was assessed as an objective version of the TFS1 test by measuring neural change detection in response to the acoustic change between HCU and ICU tones when presented monaurally (Mathew *et al.*, 2016). ACCs were recorded in response to harmonic-inharmonic tone combinations for resolved and unresolved components, and for NH and sensorineural hearing loss cohorts. As expected, ACCs had larger amplitudes in the presence of place cues, i.e. resolved harmonics, which provide greater pitch change saliency (Figure 2.17). However, results have to be regarded with caution as (1) the grand average ACC was very small in amplitude relative to the surrounding neural activity; (2) no individual ACC traces are provided to judge SNRs; (3) the ACC in the control

condition with 0 Hz shift did not look different in morphology to the 30 Hz and 50 Hz shift.

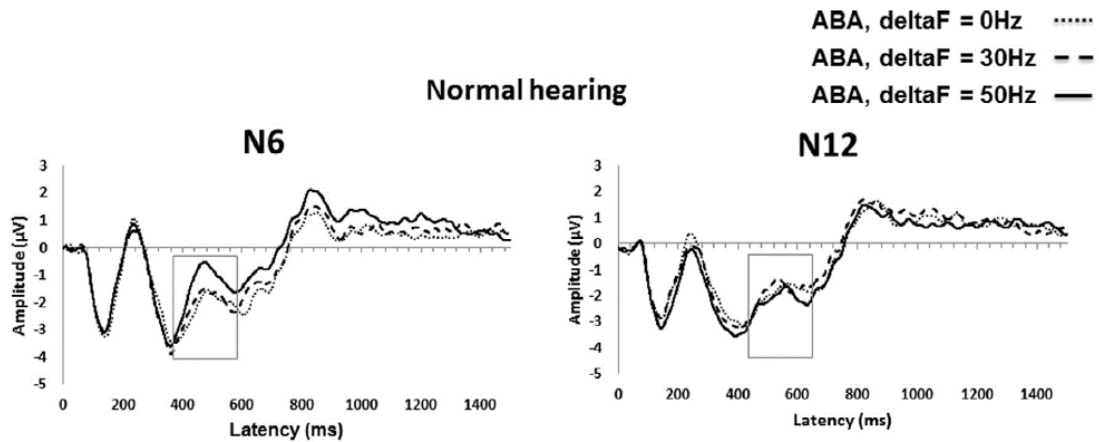


Figure 2.17: Grand average N1-P2 and acoustic change complex (ACC) waveforms. Stimuli are time-locked to the stimulus onset at 0 ms. Stimuli had an “ABA”-pattern, with the acoustic changes occurring at 200 ms and 400 ms, and sound offset was at 600 ms. Boxes indicate the expected time range of ACCs. The N6 condition refers to the condition with resolved harmonics and N12 refers to the condition where harmonics are considered to be unresolved. Adapted from Mathew *et al.* (2016).

A study by Leijssen *et al.* (2015) investigated the mismatch waveform (MMW), which consists of the MMN followed by a positive component associated with the P3a component, as a potential objective measure of TFS processing based on Schroeder-phase harmonic complex pairs in a cohort of six CI users. The electrical artefact was successfully reduced and clear standard and deviant CAEPs were elicited by stimulus pairs. Different fundamental frequencies $F0$ were assessed, where task difficulty increased with higher $F0$ s. The grand average MMW showed no significant MMW, which was defined as area-under-the-curve (AUC) exceeding a bootstrapped noise floor at any of the tested $F0$ s, despite of evident behavioural discrimination abilities at lower $F0$ s. However, the number of deviant repetitions per condition was small ($n = 54$). A follow-up study in NH participants with increased repetition numbers of the deviant may address, whether an MMW can be elicited with Schroeder-phase harmonic complex tones.

2.6 Research questions

The research aims to complement findings from the literature by investigating CAEPs as a potential objective measure of temporal auditory processing abilities with regards to two different temporal features: low-rate AM detection and TFS processing.

Studies in NH cohorts will determine whether sound discrimination of the acoustic feature of interest is encoded in the CAEP-based change detection metrics. The chosen CAEP-based neural metrics of interest are the MMW and the ACC. Findings may increase our understanding of the neural mechanisms underlying auditory processing in the healthy auditory system. Studies with CI users address the applicability of such neural measures in electrical hearing, and their potential impact on clinical procedures will be discussed.

Outlined in the following are the research questions which have not yet been answered in the literature. The studies presented in Chapter 3 – Chapter 6 aimed to address these research questions to increase our understanding of neurophysiological measures of temporal auditory processing. Table 2.1 provides a brief overview of the main study characteristics.

Table 2.1: Overview of the main studies. *Abbreviations and acronyms: ACC – Acoustic change complex, AM – Amplitude modulation, AMD – Amplitude modulation depth, CI – Cochlear implant, MMW – Mismatch waveform, NH – Normal-hearing, TFS – Temporal fine structure.*

Chapter	Study	Cohort	EEG system	Neural measure	Acoustic change feature
Chapter 3	Study 1	NH	1-channel	MMW	AM (AMD)
Chapter 4	Case Study	CI	128-channel	ACC	AM (AMD)
Chapter 5	Study 2	CI+NH	128-channel	MMW	AM (AMD)
Chapter 6	Study 3 + pilot studies	NH	1-channel or 2-channel	MMW (+ACC)	TFS

2.6.1 Study 1

- Q1.1: Can the neurophysiological MMW be obtained when the acoustic change constitutes AM of a noise sound with a low AM rate?
- Q1.2: Do MMWs change when parametrically manipulating the deviant stimuli with regards to the AMD?
- Q1.3: Can “meaningful” neural thresholds be estimated from MMWs elicited by different AMDs?
- Q1.4: Are neural thresholds significantly correlated with behavioural thresholds of AM detection?
- Q1.5: Are behavioural AM detection abilities correlated with speech-in-noise recognition in a NH cohort?

2.6.2 CI Case Study (CS)

- Q-CS.2: Can the ACC be elicited in CI users when the acoustic change constitutes AM with a low AM rate?
- Q-CS.1: Can the electrical artefact from CI stimulation be sufficiently reduced in a discrete and/or continuous paradigm when stimuli have fluctuating envelopes and how does the presentation mode influence artefacts?

2.6.3 Study 2

- Q2.1: Can individual MMWs be obtained that are visually identifiable/have the distinct MMW morphology for the different AMDs?
- Q2.2: Can the electrical artefact, which is introduced from CI stimulation, be sufficiently reduced to obtain the MMW when stimulus envelopes differ between standard and deviant stimuli?
- Q2.3: Can the introduction of an “AM-standard” stimulus aid the artefact reduction procedure? Here, the “AM-standard” means presentation of the deviant sound (with AM) additionally presented as the standard sound, and thus, the neural response has the characteristics of a standard response with the artefact of the deviants.
- Q2.4: Can individual neural thresholds be estimated from MMW data at varying AMDs?
- Q2.5: Are neural thresholds correlated with behavioural AM detection thresholds?
- Q2.6: Does speech performance correlate with AM detection thresholds in CI users?
- Q2.7: Are MMWs elicited when potential loudness cues are removed by subjective loudness balancing?

2.6.4 Study 3

- Q3.1: Can neurophysiological MMWs and/or ACCs be recorded when the stimulus change characteristics relate to subtle TFS properties as conveyed in the stimuli of the TFS1 test or the Schroeder-phase stimuli?

Chapter 3 Depth matters – towards finding an objective neurophysiological measure of behavioural amplitude modulation detection

Given the importance of slow envelope fluctuations for sound perception and particularly for speech processing, this study explored human auditory brain responses to modulated sounds with a low AM rate and examined their applicability as an objective measure. Such an objective measure may provide a valuable tool for clinical hearing assessment without relying on subjective feedback (Hall & Swanepoel, 2010), addressing the clinical demand for objective measures of auditory processing due to increasing numbers undergoing intervention against hearing impairment at a young age (Rajan *et al.*, 2017). Experiments were conducted for a NH cohort to verify the feasibility of a neurophysiological approach based on neural change detection. Paradigms were designed in a way that allows future replication of the same test battery in a CI user cohort.

As detailed by Picton (2013), neural responses elicited by temporal auditory features can be employed to assess various aspects of temporal auditory processing. Previous studies have assessed the relationship between behavioural AM detection abilities and corresponding neural measures (Purcell *et al.*, 2004; Manju *et al.*, 2014; Han & Dimitrijevic, 2015; Luke *et al.*, 2015; Dimitrijevic *et al.*, 2016). The main objective of this study was to build on this research by estimating individual neural thresholds (NTs) from CAEPs for low-rate AM detection. These NTs were derived from CAEP data elicited by various AMDs, and compared to behavioural AM detection thresholds for an AM rate of 8 Hz. It was hypothesized that NTs would be significantly correlated with behavioural AM detection thresholds of the same AM rate.

This study explored a transient neurophysiological response referred to as the MMW (Lopez Valdes *et al.*, 2014). The MMW was obtained using an auditory oddball

paradigm by subtracting the standard CAEP from the deviant CAEP. This difference waveform showed two distinct components: a negative component corresponding to the widely studied MMN, which is the result of perceptual change detection in stimulus sequences (Näätänen *et al.*, 2007; Fishman, 2014), followed by a positive component which is associated with cognitive processes and may be a result of involuntary attention directed towards the deviant stimulus, similar to the P3a response (He *et al.*, 2009). Previous studies have shown that both components are positively correlated with the magnitude of stimulus change (Katayama & Polich, 1998; He *et al.*, 2009). Thus, both components were investigated as part of the MMW, similar to work by Lopez Valdes *et al.* (2014), who have demonstrated positive correlations between MMW-based neurophysiological thresholds and psychoacoustic thresholds for spectral ripple discrimination. This study aimed to expand on those findings, transitioning from spectral processing to temporal processing with the overall goal of designing a combined test battery to assess spectro-temporal auditory processing abilities.

While not the main focus of this study, the relationship between the ability to detect low-rate AM with AMDs near threshold and speech recognition scores was also addressed. Although the literature suggests a lack of correlations between psychoacoustic measures (e.g. pitch discrimination, intensity discrimination and modulation detection) and speech recognition measures within NH cohorts (Strouse *et al.*, 1998; Watson & Kidd, 2002; Goldsworthy *et al.*, 2013), the calculation of correlations was implemented in order to have a fully translatable experimental battery for replication in CI users. Across groups of younger and older NH and CI participants, Jin *et al.* (2014) found significant correlations between AM detection thresholds (at 2 Hz and 4 Hz AM rates) and speech-in-noise recognition with a modulated noise masker, but no within-group correlations were reported. Experiments with CI user cohorts have shown significant correlations between speech measures (i.e. vowel, consonant, phoneme, syllable, and sentence recognition) and low-rate (AM rate $f_m < 20$ Hz) (Gnansia *et al.*, 2014; De Ruiter *et al.*, 2015) as well as high-rate ($f_m \geq 20$ Hz) AM detection abilities (Cazals *et al.*, 1994; Fu, 2002; Luo *et al.*, 2008; Won *et al.*, 2011b; De Ruiter *et al.*, 2015). These reported correlations in CI user cohorts provide support for the importance of AM sensitivity in electrical hearing and encourage the investigation of an objective measure of AM sensitivity. Results from this research were published in the journal *Hearing Research*.

3.1 Methods

3.1.1 Participants

15 young adults (9 female, 6 male; 19 – 28 years, mean: 23.2 ± 2.5 years) with no known hearing impairment participated in this study. Three participants were not native English speakers and their data were excluded from analysis relating to the speech test, but their results from electrophysiological and AM detection paradigms were included. Informed written consent was obtained from all participants prior to participation and all experimental procedures were approved by the Ethics (Medical Research) Committee at Beaumont Hospital, Beaumont, Dublin and the Research Ethics Committee at Trinity College Dublin.

Participants were seated in a quiet room and auditory stimuli were presented monaurally to the left ear via headphones (Sennheiser HD 205) for all experimental paradigms. The presentation level of 70 dB SPL was verified with a KEMAR mannequin (45 BC) with pinna simulator (KB 0091), pre-amplifier (26CS) and pre-polarized pressure microphone (40A0) (all from G.R.A.S. Sound & Vibration). All stimuli were energy matched by adjusting the root mean square (RMS) amplitude.

3.1.2 AM Stimuli

Stimuli were created in MATLAB (Release 2013b, The MathWorks, Inc., Natick, Massachusetts, United States) with a sampling rate of 44100 Hz. A low modulation rate of 8 Hz was chosen for several reasons: from a motivational aspect it was chosen due to its importance for speech intelligibility (Drullman, 1995; Edwards & Chang, 2013; Gnansia *et al.*, 2014) and from a practical aspect it provides four full AM cycles for the chosen stimulus duration of 500 ms³ (Figure 3.1). An alternative popular AM rate for behavioural AM detection studies is 4 Hz, however, this would only result in two AM cycles for a 500 ms stimulus duration. The noise carrier was created by filtering a 500 ms white Gaussian noise stimulus with a long-term average speech spectrum (LTASS) filter (Byrne *et al.*, 1994). The AM signal, $s(t)$, was created by multiplying the noise carrier, $c(t)$, with a sinusoidal signal according to Equation 3.1:

³ The stimulus duration of 500 ms was chosen based on the desire to replicate the study in a clinical CI user cohort. The electrical CI artefact related to the stimulus offset should not fall into the time range of interest of the mismatch waveform (100 ms to 450 ms) to avoid unnecessary contamination of the measured neural response.

$$s(t) = [1 + m \cdot \sin(2 \cdot \pi \cdot f_m \cdot t + \Phi)] \cdot c(t),$$

Equation 3.1

where t denotes time, f_m is the AM rate (8 Hz), Φ is the starting phase ($-\pi/2$) and m is the AMD with values between zero and one. The psychoacoustics literature commonly reports the AMD in dB expressed as $20\log_{10}(m)$, but m may also be reported in percentage, in line with the literature investigating neurophysiological measures of AM processing (Purcell *et al.*, 2004; Han & Dimitrijevic, 2015; Dimitrijevic *et al.*, 2016). For the neurophysiological paradigm, AMDs were chosen on a linear scale with a constant step size of 25% (100%, 75%, 50% and 25%). Thus, the AMD m in this study is reported in percentage, unless noted otherwise. The chosen starting phase Φ resulted in a minimum amplitude of the noise signal at stimulus onset. To avoid loudness cues resulting from changes in AMD, the unmodulated and modulated stimuli were energy matched by adjusting the RMS amplitude to a constant value. Additionally, level roving was applied in the psychoacoustic paradigm with a range of ± 3 dB to reduce the usefulness of any potentially remaining loudness cues.

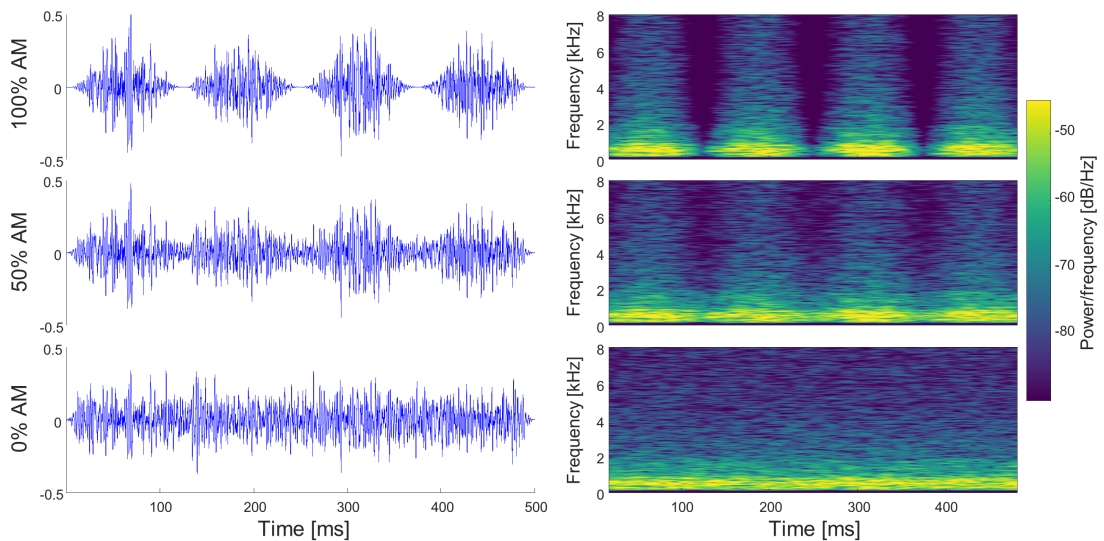


Figure 3.1: Examples of amplitude modulated (AM) noise stimuli.

Visualisations of the instantaneous amplitude (left) and spectro-temporal stimulus characteristics of stimuli with differing AM depths (AMD); 0% AMD equates to unmodulated noise.

3.1.3 Psychoacoustics

Behavioural AM detection was evaluated with two paradigms: One paradigm estimated the behavioural threshold (BT) for AM detection with an adaptive procedure,

and the second paradigm yielded the percentage of correct discrimination for a set of specific AMDs, providing an estimate of the overall psychometric function.

BTs were determined with a three-alternative forced choice (3AFC), two-down/one-up paradigm yielding an estimate of the 70.7% correct point on the psychometric function (Levitt, 1971). The inter-stimulus interval (ISI) for each trial of three consecutive stimuli was set to 100 ms. Participants were provided with visual feedback, with the selected button lighting up green or red for a correct or incorrect response, respectively (Figure 3.2). The starting AMD was 0 dB, expressed as $20\log_{10}(m)$. The step size was 4 dB for the first four reversals and 2 dB thereafter. A run was completed after 12 reversals and the BT was taken as the arithmetic mean of the $20\log_{10}(m)$ values at the last eight reversals. Data were acquired for four runs and the final BTs were calculated as the mean across runs. The AMD m representing the BTs are reported, both in percentage and in dB ($20\log_{10}(m)$), to facilitate easy comparison with neural thresholds (NTs) and BTs reported in the literature, respectively.

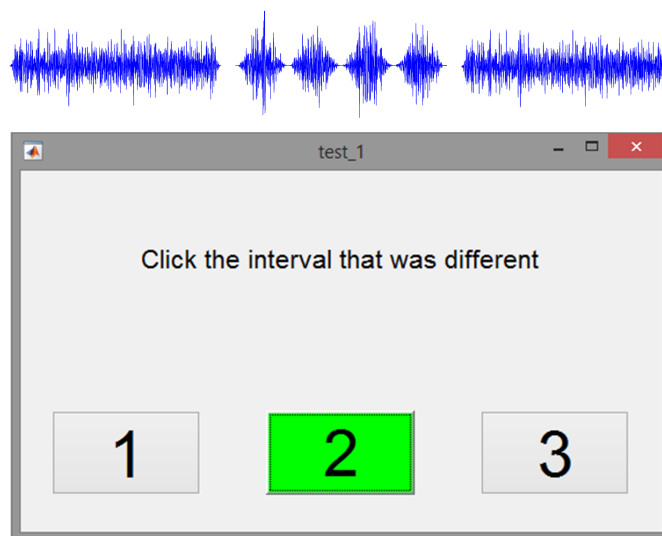


Figure 3.2: Graphical User Interface (GUI) to obtain amplitude modulation (AM) detection thresholds and visualisation of the presented stimuli.

Three stimuli were presented, with two stimuli being unmodulated noise and one randomly chosen stimulus consisted of modulated noise. The AM depth varied according to the adaptive two-down/one-up procedure.

To obtain an estimate of the psychometric function, unmodulated and modulated stimuli with a duration of 500 ms were presented in a single interval yes/no task with blocked AMDs (i.e. 10%, 12.5%, 25%, 50%, 75%, and 100%). The participant had a 2 s time window following stimulus presentation to decide whether the stimulus was modulated or unmodulated by clicking the corresponding button. No feedback was provided. Modulated and unmodulated stimuli had equal probability of presentation.

Stimulus presentations were divided into three runs for each AMD with a total of 120 stimulus presentations for each AMD. To avoid fatigue, data for this paradigm were acquired in a separate session to the other tests. The percentage of correct responses was calculated for each AMD as the sum of hits and correct rejections divided by the total number of trials, where hits refers to the number of trials in which modulated stimuli were correctly identified as modulated and correct rejections refers to the number of trials in which unmodulated stimuli were correctly identified as unmodulated. Additionally, the sensitivity index, d' (d-prime), is reported. In the case of extreme values of zero and one for the hit rate or false alarm rate, a correction was applied by adjusting zero to $0.5N$ and one to $(1 - 0.5N)$, where N is the number of possible hits or false alarms, respectively (Macmillan & Kaplan, 1985).

3.1.4 Speech-in-noise test

The AzBio speech test (Spahr *et al.*, 2012) was employed. Recorded sentences were presented with male and female speakers with an American English accent and masked with a ten-talker babble noise. Three SNRs (10 dB, 5 dB and 0 dB) were used for one sentence list each. Speech recognition scores for a NH cohort were expected to show ceiling effects for SNRs of 10 dB and 5 dB, but were included in the test battery to facilitate study replication in a CI user cohort, in which speech-in-noise recognition is known to be poorer (Oxenham & Kreft, 2014). Every sentence list included 20 sentences with four to seven words per sentence. The number of correctly identified words was counted and the speech recognition score was calculated as the percentage of correctly identified words. All presented words were considered for each sentence's recognition score. The speech signal was presented at a constant level and the noise signal was adjusted according to the SNR.

3.1.5 Electrophysiology

Data acquisition

Single-channel EEG data were acquired through a custom-built, single-channel, high sampling rate EEG setup, previously designed and validated to acquire EEG data from CI recipients and which includes an electrical artefact reduction algorithm (Mc Laughlin *et al.*, 2013). In this setup, the recording electrode is positioned at the vertex and referenced to the right mastoid; the right collar bone is used as the system ground. As the

long term goal is to use the protocol with CI users, data were sampled at a high rate of 125 kHz for artefact reduction purposes (Mc Laughlin *et al.*, 2013). Such a high sampling rate is unnecessary for EEG signals from NH participants and uneconomical for further post-processing. Hence, data were down-sampled offline by a factor of 100. The amplifier's high-pass filter was set to 0.03 Hz and the low-pass filter was set to 100 Hz and data were amplified with a gain of 2000. Electrode impedances were measured before, during and after the electrophysiological recordings. Impedances were kept below 5 k Ω for all electrode combinations.

Cortical responses were elicited using an unattended, auditory oddball paradigm in which modulated (deviant) and unmodulated (standard) noise sounds were presented for deviants with AMDs of 100%, 75%, 50%, and 25%. Each stimulus had a duration of 500 ms and an ISI of 1 s. Each condition was presented in separate blocks of 160 stimulus repetitions each with a total of four blocks per condition. Each block contained 20 initial presentations of the standard, followed by 140 mixed presentations of the standard (90% occurrence probability) and deviant (10% occurrence probability), resulting in 56 deviant and 584 standard presentations in total for each AMD. The order of AMD blocks was pseudo-randomized for each participant.

Participants were seated in a quiet room, watching a silent, captioned movie of their choice and were instructed to keep body movements to a minimum. As a measure of signal quality, an additional brief block of pure tone stimuli was added at the start and end of the EEG recording to elicit the robust N1-P2 complex (500 Hz, 500 ms duration, 1 s ISI). All participants exhibited visible N1-P2 complexes, so no participant's data were excluded from further analysis.

Data processing

Offline post-processing of the down-sampled data included zero-phase bandpass filtering between 1 Hz and 15 Hz with a 4th order Butterworth filter, gain removal, epoching (-300 ms pre-stimulus to 700 ms post-stimulus), linear de-trending, baseline correction, and separation into standard and deviant epochs. Epochs were marked for rejection if their activity exceeded a threshold value, which was very conservatively calculated by multiplying each epochs' standard deviation by five and averaging across epochs. Standard and deviant epochs were averaged to form the respective CAEPs and the MMW was obtained by subtracting the standard from the deviant CAEP.

Morphology weighting: The MMW was evaluated in terms of AUC in the region of 110 ms to 310 ms post-stimulus onset (Figure 3.5A). Random non-task related fluctuations in the EEG data may result in spurious AUC measurements. For this reason, a morphology weighting approach was developed (Figure 3.3). Morphology weighting was achieved by assessing the Pearson’s correlation between MMWs at differing AMDs and a participant-specific template. These correlation coefficients were associated with weights according to a weighting function (binary or exponential weighting, Figure 3.5C). Multiplication of the AUC values with the assigned weights for each AMD and each participant provided the morphology weighted AUC curves. The application of weights to AUC values based on similarity of the MMW with the participant-specific template reduced the influence of random fluctuations on AUC values.

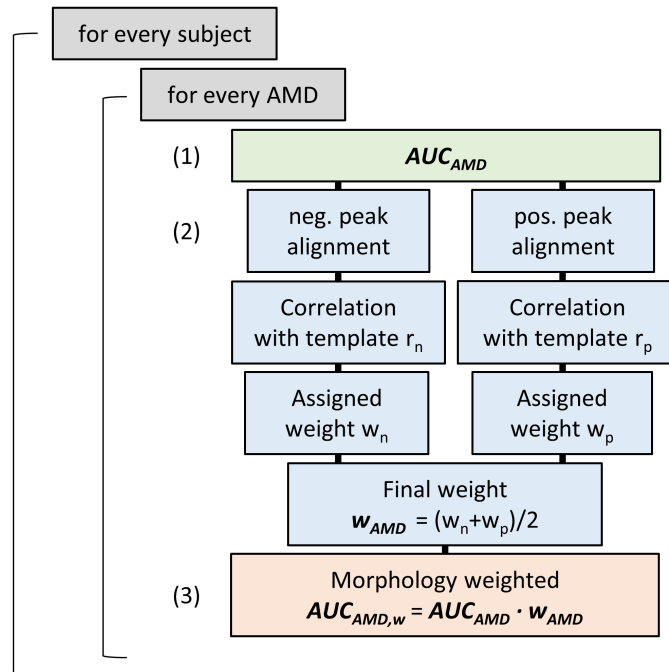


Figure 3.3: Pseudocode of data processing steps to obtain morphology weighted area-under-the curve (AUC) values of mismatch waveforms (MMWs).

For each participant and each amplitude modulation depth (AMD), (1) the AUC is calculated between 110 ms and 310 ms post-stimulus onset. (2) Separately for the negative and the positive peaks, the MMWs were aligned (Figure 3.2) by shifting the waveforms. The correlation coefficients between the template (MMW100) and MMWs for lower AMDs are calculated. Based on the correlation coefficient, a weight is assigned (binary or exponential weighting function). The overall weight is the average of the obtained values for negative and positive peak alignment. (3) The morphology weighted AUC values are obtained by multiplying the determined weights with their respective AUC values.

Morphology weights calculation: Each participant showed a clear MMW for the 100% AMD, i.e. a negative component followed by a positive component in the time region of interest. Thus, the individual MMW at 100% AMD served as a participant-specific template for the morphology weighting approach and is referred to as the

‘template’ in the following. Subsequently, correlation coefficients between the individual MMWs at lower AMDs (MMW_{75} , MMW_{50} and MMW_{25}) and this template were calculated.

It has been reported that increasing task difficulty may result in increased MMW latencies (Tiitinen *et al.*, 1994; Kimura & Takeda, 2013). MMW latency shifts may lead to lower correlation coefficients despite overall similar morphology. To compensate for such latency shifts, MMW_{75} , MMW_{50} and MMW_{25} were aligned with the template prior to the correlation calculation (Figure 3.4). To determine the latency shift required for the alignment, the peaks of the template were determined in the corresponding time range of interest and a time window of -5 ms to +40 ms around these peak latencies served as the search window for peak detection of the remaining MMWs. The search window was chosen to be asymmetrical, as latencies were not expected to decrease for lower AMDs. MMWs were aligned separately, by positive peak and by negative peak, providing two sets of correlation coefficients. Correlation coefficients were calculated after the MMWs were aligned. Each correlation coefficient was assigned a weight and to obtain the final weight for each AUC value, the weights derived from negative and positive peak alignments were averaged. The morphology weighted AUC values (Figure 3.5D) were obtained by multiplying the unweighted AUC values (Figure 3.5B) with the obtained weights.

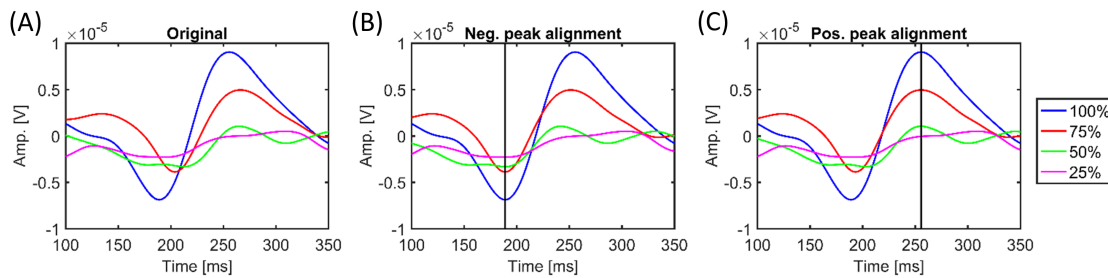


Figure 3.4: Mismatch waveform (MMW) alignment for example participant.

Alignment prior to correlation coefficient calculation allows for MMW latency shifts between differing amplitude modulation depths (AMDs); MMWs for 75%, 50% and 25% AMD were aligned with the template (100% AMD) with regard to the negative peak (B) and the positive peak (C) of the MMW.

Weighting functions: Weight assignment was based on two weighting approaches, binary and exponential weighting. The binary weighting represents an “all-or-nothing” approach in which a weight of one was assigned to all MMWs with correlation coefficients of 0.85 or above and a weight of zero was assigned otherwise (Figure 3.5C). The threshold of 0.85 was determined empirically and preserves MMWs that show the characteristic waveform with little variation, but suppresses MMWs that do not show high

similarity to the template. For the less stringent exponential weighting, correlation coefficients were assigned into bins of 0.1 width. The first bin with correlation coefficients between one and 0.9 was assigned a weight of one, and with each bin the weight was halved (i.e. 0.5, 0.25, 0.12) (Figure 3.5C). All correlation coefficients below 0.6 were assigned a weight of zero. Each weighting type was applied individually throughout the data analysis to obtain morphology weighted AUC curves (Figure 3.5D) and final correlations between BTs and NTs were compared to assess the influence of the weighting approach.

Neural threshold calculation: The NT was taken as the interpolated AMD at which the individual's weighted AUC curve dropped below a derived intersection value (IV, Figure 3.5E). A range of different IVs was investigated.

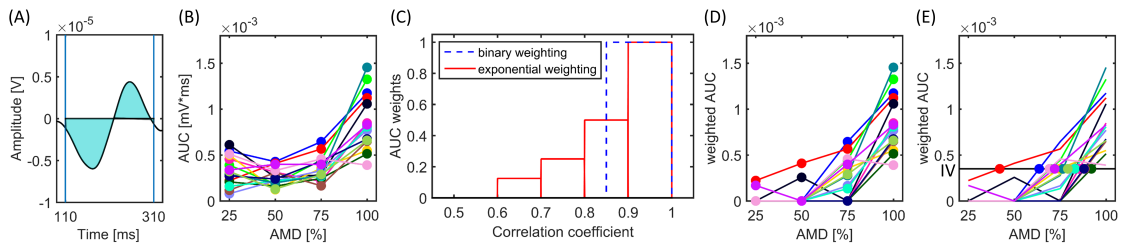


Figure 3.5: Visualisation of data processing steps involved in neural threshold (NT) estimation.

(A) Example area-under-the-curve (AUC) between 110 ms and 310 ms for an individual participant's mismatch waveform (MMW) for the 100% amplitude modulation depth (AMD); (B) unprocessed AUC curves derived from individual MMWs for all participants; (C) exponential and binary weighting function assigning weights to AUC scores depending on correlation coefficients between the associated MMW and the participant's template; (D) weighted AUC curves obtained by multiplying assigned weights with unweighted AUC values for all participants' weighted AUC curves; results displayed for binary weighting function; (E) neural thresholds determined as the intersection point between weighted AUC curves and the chosen intersection value (IV); the NT represents the highest, interpolated AMD at which the AUC curve drops below the IV.

Correlation analysis between BTs and NTs: The relationship between BTs and NTs was assessed with Pearson's linear correlation coefficient as well as Spearman's rank-order correlation coefficient r_s , which is equivalent to Pearson's linear correlation coefficient, but applied to ranked data. Pearson's correlation coefficient assesses the linear relationship between two variables, whereas Spearman's correlation coefficient assesses their monotonic relationship. Correlation analysis was carried out for a range of potential IVs with both weighting functions. For this analysis, all standard epochs were averaged for each AMD. To verify the validity of the novel methodology, the entire analysis was carried out for 300 permutations of different sub-sets of 56 standards for an example IV of 0.35 and both weighting functions.

3.2 Results

3.2.1 Psychoacoustics

The individual mean BTs were between 8.1% (-21.8 dB) and 16.7% (-15.5 dB) AMD. The group mean threshold was 12.1% (-18.3 dB) with a standard deviation of 2.4% (1.74 dB). Behavioural AM detection scores in the psychometric function showed expected ceiling effects at the group level for AMDs of 25% and above, while detection accuracy decreased significantly below 25% AMD (Figure 3.6A).

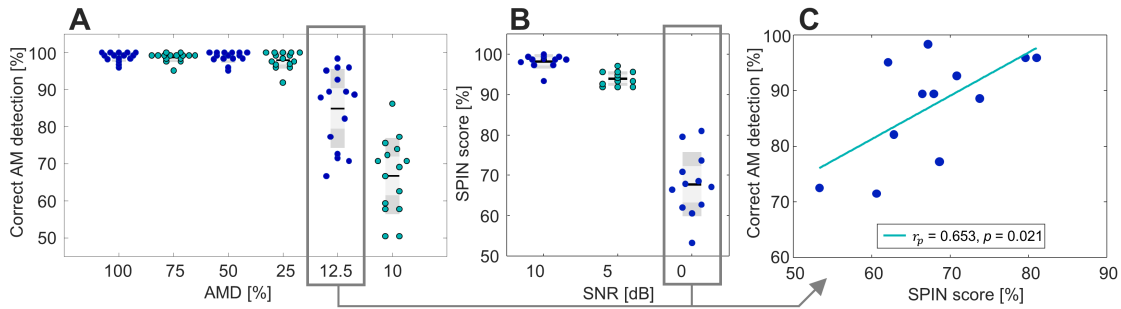


Figure 3.6: Behavioural results and their correlation analysis results.

Individual scores, arithmetic means (black line) and standard deviations (shaded grey boxes) for (A) the psychometric function of amplitude modulation (AM) detection at varying AM depths (AMD) for all participants ($n = 15$), and (B) the speech-in-noise scores for three signal-to-noise ratios (SNRs) for the native speakers ($n = 12$). Indicated by the two grey boxes are the conditions underlying the correlation analysis shown in (C). Both levels represent the tested level at which participants showed poorer task performance and increased performance variability.

Table 3.1: Group mean and standard deviation (SD) data of the psychometric function for different amplitude modulation depths (AMD).

Group mean results of the psychometric function reporting the total percentage of correct responses (hits and correct rejections), the corresponding SD, hit rates, false alarm rates and the sensitivity index d' (d -prime) for six AMDs m which are reported in percentage, or in dB, expressed as $20\log_{10}(m)$.

AMD [%]	AMD [dB]	Total correct [%]	SD	Hit rate	False alarm rate	d'
100	0	98.8	1.2	0.985	0.016	4.44
75	-2.5	98.7	1.2	0.983	0.018	4.41
50	-6.0	98.8	1.4	0.990	0.024	4.46
25	-12.0	97.9	2.2	0.973	0.024	4.20
12.5	-18.0	84.9	10.3	0.831	0.131	2.41
10	-20	66.7	9.8	0.494	0.170	1.01

Table 3.1 summarizes the group mean percentage of correct responses and their standard deviations for the various AMDs. Additionally, the group mean hit rates, false alarm rates and the sensitivity index d' are reported. A non-parametric Friedman test

revealed a statistically significant difference in task performance between differing AMDs ($X^2(5) = 55.03, p < 0.001$). Post-hoc analysis with Wilcoxon signed-rank tests was conducted with Bonferroni correction to adjust for multiple comparisons with an adjusted significance level of 0.003 for 15 comparisons. There were significant differences between 12.5% and all other AMDs ($Z \leq -3.24, p \leq 0.001$) and between 10% and all other AMDs ($Z \leq -3.24, p \leq 0.001$).

3.2.2 Speech-in-noise test

Speech-in-noise recognition scores for the native English speakers revealed ceiling effects at the 10 dB SNR and close to ceiling effects at the 5 dB SNR, but for 0 dB SNR a decline in speech recognition and increased variation among participants occurred (Figure 3.6B, Table 3.2). A non-parametric Friedman test revealed significant differences between SNRs ($X^2(2) = 24.00, p < 0.001$). Post-hoc analysis with Wilcoxon signed-rank tests was conducted with Bonferroni correction to adjust for multiple comparisons with an adjusted significance level of 0.017 for three comparisons. Significant differences were observed between all three conditions (10 dB vs. 5 dB: $Z = -3.06, p = 0.002$; 10 dB vs. 0 dB: $Z = -5.06, p = 0.002$; 5 dB vs. 0 dB: $Z = -3.06, p = 0.002$). Non-native speakers showed large variations in their performance as well as overall poorer performance for lower SNRs and were therefore excluded from data analysis relating to speech recognition scores.

Table 3.2: Speech-in-noise recognition group mean data and their standard deviations (SDs) for native speakers for the three tested signal-to-noise ratios (SNRs).

SNR	Mean	SD
10 dB	98.2	1.65
5 dB	94.0	1.67
0 dB	67.8	7.54

3.2.3 Correlations speech vs. psychoacoustics

Only conditions without evident floor or ceiling effects in the group mean scores were included in the correlation analysis, namely the 0 dB condition of the speech test which was compared to the AM detection scores of the psychometric function at 10% and 12.5% AMD, and the BTs. Potential linear relationships between experimental measures were investigated with Pearson's correlation coefficients. No significant correlations were found between speech scores at 0 dB SNR and BTs ($r_p = -0.15, p = 0.638$) and AM

detection at 10% AMD ($r_p = 0.24$, $p = 0.461$). Comparison of the speech scores at 0 dB SNR and the behavioural AM detection scores for the 12.5% AMD (Figure 3.6C) suggested a moderately strong linear relationship between the two measures ($r_p = 0.65$, $p = 0.021$), but the correlation did not remain significant after adjusting the significance level to 0.017 with the conservative Bonferroni correction for multiple comparisons.

3.2.4 Electrophysiology

The group mean MMWs revealed a clear morphology for 100% and 75% AMD, whereas the waveforms for 50% and 25% AMD only showed random fluctuations (Figure 3.7 and Figure 3.8A). A strong decline in the individual morphology weighted AUC values was noted from 100% to 75% and from 75% to 50% AMD, but then the AUC values remained constant at a low (mostly zero) level for 50% and 25% AMD (Figure 3.5D and Figure 3.8B). Statistical analysis by means of a non-parametric Friedman test revealed a significant effect of AMD for the binary weighted MMW AUC values ($\chi^2(3) = 37.08$, $p < 0.001$). Post-hoc analysis was carried out with Wilcoxon signed-rank tests, and Bonferroni correction provided an adjusted significance level of 0.008 for six comparisons. Weighted MMW AUC values for 100% AMD differed significantly from those for all other AMDs (100% vs. 25%: $Z = -3.41$, $p = 0.001$, 100% vs. 50%: $Z = -3.41$, $p = 0.001$, 100% vs. 75%: $Z = -3.35$, $p = 0.001$) and 75% AMD scores differed significantly from those for 25% AMD ($Z = -2.80$, p -value = 0.005), but not 50% AMD ($Z = -2.58$, $p = 0.010$). No significant difference was found between scores for 25% and 50% AMD ($Z = -0.54$, $p = 0.593$).

For binary weighting, five out of the 15 MMW₇₅ values were assigned a weight of zero, suggesting that five participants only exhibited a clear MMW response for the MMW₁₀₀. For the MMW₅₀ and MMW₂₅ only two non-zero weights were observed for each set of 15 MMWs (Figure 3.8B). Closer analysis of the MMWs associated with non-zero weights at 25% and 50% AMD showed that participant ‘NH2’ demonstrated clearer MMWs than other participants and AUC values different from zero for all AMDs. Further inspection of the data suggested that non-zero AUC values for participant ‘NH4’ at 50% AMD and for ‘NH16’ at 25% AMD were unexpected based on the observed waveform since the MMW did not resemble the template. However, minimal random fluctuations with the shape of the template in the region of interest led to high correlation values, therefore, assigning greater weights to these AUC values.

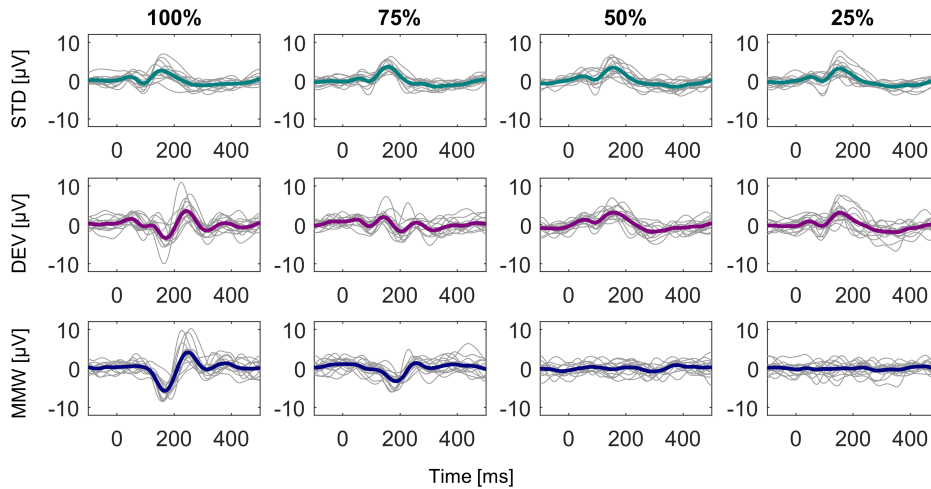


Figure 3.7: Individual and grand average cortical auditory evoked potentials (CAEPs). CAEPs are shown for the four amplitude modulation depth conditions (left to right) and for standard (STD, first row) and deviant (DEV, second row) CAEPs as well as their respective difference waveform with the expected mismatch waveform (MMW, bottom row).

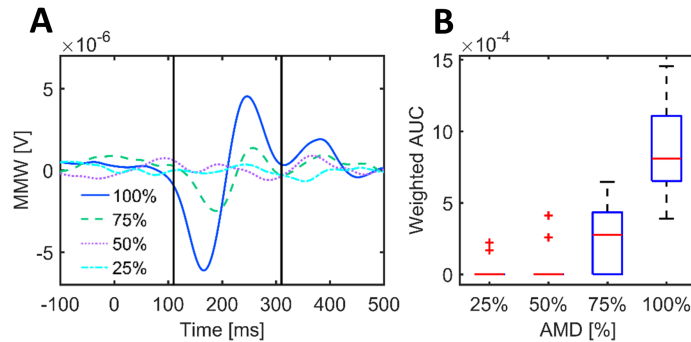


Figure 3.8: Grand average mismatch waveforms and area-under-the-curve data. (A) Group mean mismatch waveform (MMW) data for the four tested amplitude modulation depths (AMDs) with the indicated region of interest (110 ms – 310 ms); (B) Boxplots visualizing variation in group data for weighted area-under-the-curve (AUC) values (shown for binary weighting) across AMDs with outliers indicated by the red plus signs.

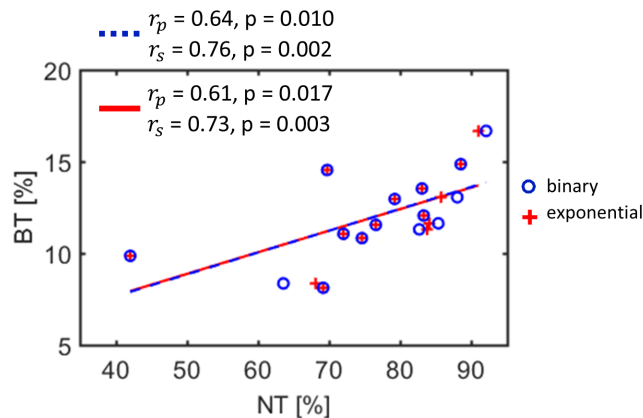


Figure 3.9: Examples of the correlation analysis between behavioural thresholds (BTs) and neural thresholds (NTs).

Correlation results are presented for data obtained with binary weighting ('o', blue) and with exponential weighting ('+', red). NTs were calculated with an intersection value of 0.35 and all standard epochs were averaged to obtain the difference wave. Correlation results are pictured for Pearson's correlation coefficient r_p as well as for Spearman's correlation coefficient r_s for data from both, binary and exponential, weighting approaches.

3.2.5 Correlations between BTs vs. NTs

Analysis based on all standard epochs

Individuals' BTs and NTs for AM detection showed statistically significant correlations for a range of tested IVs when all standard epochs were included in the analysis (Table 3.3). For IVs of 0.25 or below and 0.5 and above, NT calculation failed for one or more participants. Results for a chosen IV of 0.35 are also illustrated in Figure 3.9.

Table 3.3: Overview of correlation results with data based on all standard epochs.

Correlation results are reported for Pearson's and Spearman's correlation coefficients for correlations between neural thresholds (NTs) and behavioural thresholds for binary and exponential morphology weighting. The NTs included in this analysis were estimated based on the reported intersection values (IVs). For high (≥ 0.5) and low (≤ 0.2) IVs, NT calculation failed for some participants. The IV 0.35 (bold) indicates the IV for which the correlation analysis was additionally carried out for 300 permutations of randomly chosen subsets of standard epochs (see Figure 3.10).

Spearman's correlation analysis							
Binary				Exponential			
IV	r_s	p	no NT	IV	r_s	p	no NT
0.10	0.716	0.006	1	0.10	0.63	0.018	1
0.15	0.71	0.006	1	0.15	0.66	0.013	1
0.20	0.71	0.006	1	0.20	0.66	0.013	1
0.25	0.75	0.002	0	0.25	0.73	0.003	0
0.30	0.76	0.002	0	0.30	0.74	0.002	0
0.325	0.76	0.002	0	0.325	0.73	0.003	0
0.35	0.76	0.002	0	0.35	0.73	0.003	0
0.40	0.39	0.157	0	0.40	0.36	0.192	0
0.45	0.61	0.017	0	0.45	0.61	0.017	0
0.50	0.54	0.048	1	0.50	0.53	0.057	1
Pearson's correlation analysis							
Binary				Exponential			
IV	r_p	p	no NT	IV	r_p	p	no NT
0.10	0.59	0.026	1	0.10	0.56	0.037	1
0.15	0.62	0.019	1	0.15	0.58	0.030	1
0.20	0.64	0.015	1	0.20	0.61	0.021	1
0.25	0.59	0.021	0	0.25	0.56	0.031	0
0.30	0.61	0.015	0	0.30	0.58	0.024	0
0.325	0.63	0.013	0	0.325	0.59	0.020	0
0.35	0.64	0.010	0	0.35	0.61	0.017	0
0.40	0.39	0.156	0	0.40	0.34	0.216	0
0.45	0.65	0.009	0	0.45	0.61	0.016	0
0.50	0.65	0.012	1	0.50	0.60	0.023	1

Permutation analysis based on sub-sets of the standard epochs

To validate the applied procedure, the correlation analysis was carried out for 300 permutations of different sub-sets of 56 standards and for an example IV of 0.35. The distributions of correlation coefficients and their respective p-values across 300 permutations are shown in Figure 3.10.

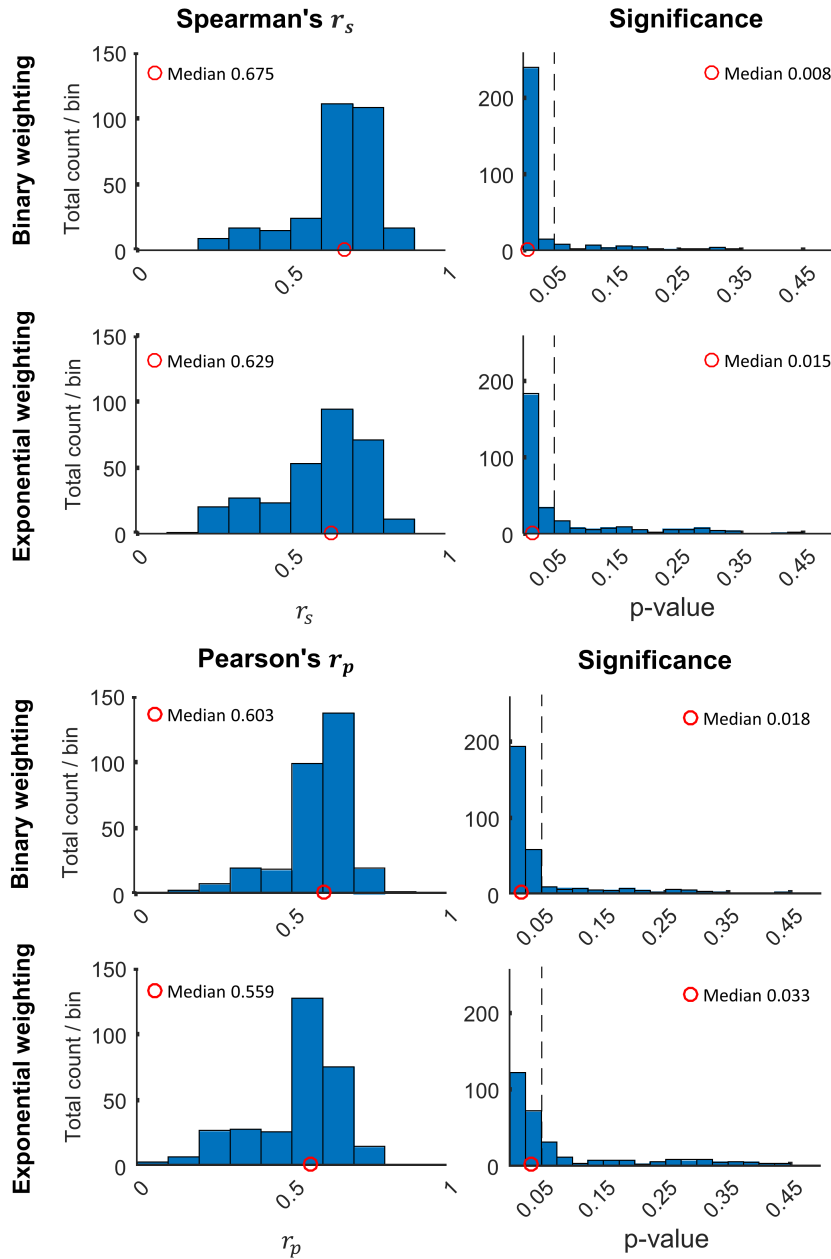


Figure 3.10: Permutation distributions of correlation analysed with randomised sets of standard epochs.

Depicted are the distributions of Spearman's linear correlation coefficient r_p (top) and Pearson's linear rank correlation coefficient r_s (bottom) between behavioural and neural thresholds of amplitude modulation detection and their respective p-values based on binary and exponential weighting functions for the morphology weighting. NTs were estimated based on an intersection value of 0.35. Distributions were based on 300 permutations of randomly chosen sub-sets of 56 standard epochs for the calculation of the mismatch waveform. The median of each distribution is indicated by the circle.

The central tendency of the skewed distributions of the correlation coefficients and p-values obtained with the permutation analysis can be expressed by the median. For the specified IV of 0.35 and based on *Spearman's* linear rank correlation coefficients, median correlation coefficients of $r_s = 0.675$ ($p = 0.008$) and $r_s = 0.629$ ($p = 0.015$) were obtained for the linear relationship between BTs and NTs based on binary and exponential weighting, respectively (Figure 3.10). For the specified IV of 0.35 and based on *Pearson's* correlation analysis, median correlation coefficients of $r_p = 0.603$ ($p = 0.018$) and $r_p = 0.559$ ($p = 0.033$) were obtained for the linear relationship between BTs and NTs based on binary and exponential weighting, respectively (Figure 3.10). The non-parametric Mann-Whitney test showed that the distributions of Pearson's as well as Spearman's correlation coefficients between BTs and NTs across 300 permutations were statistically significantly different for the binary and exponential morphology weighting with $p < 0.001$ for both tests.

3.3 Discussion

There were five main findings: (1) MMWs can be elicited by change detection from unmodulated to modulated noises. (2) The MMW amplitude decreases with decreasing AMD. (3) Morphology weighting of MMWs allows the objective estimation of NTs. (4) NTs are significantly correlated with BTs. (5) No significant correlations were observed between AM detection and speech scores at 0 dB SNR.

3.3.1 Objective measure

Mismatch waveforms

To my knowledge, this is the first application of the MMW to evaluate the perception of acoustic changes related to AM detection. Previous studies have assessed the MMW as a measure of auditory temporal resolution via gap detection (Desjardins *et al.*, 1999; Trainor *et al.*, 2001; Uther *et al.*, 2003). Overall, the successful elicitation of neural responses provides evidence for the feasibility of the application of the MMW for this type of acoustic change.

The morphology weighting approach reduced AUC values for the lower AMDs (Figure 3.5B and Figure 3.5D), showing that MMWs at lower AMDs do not strongly resemble the template, which is in line with observations of random fluctuations of the

individual MMWs at 25% and 50% AMD. Figure 3.11 shows a comparison of the psychometric function of behavioural AM detection and the weighted AUCs of neural responses at the corresponding AMDs, highlighting the difference in response development with decreasing AMD. AUC values declined at much higher AMDs compared to behavioural responses. The psychometric function showed ceiling effects for AMDs of 25% and above, and deteriorating performance for AMDs below 25%, which agrees with the literature concerning 4 Hz AM detection (Han & Dimitrijevic, 2015). In contrast, the MMW amplitudes decreased from 100% to 75% AMD, and for an AMD of 50% no clear MMW was detectable in the group mean data. Similarly, Han and Dimitrijevic (2015) reported declines in ACC amplitudes between 100% and 50% AMD, and only a weakly discernible ACC for 25% AMD for an AM rate of 4 Hz.

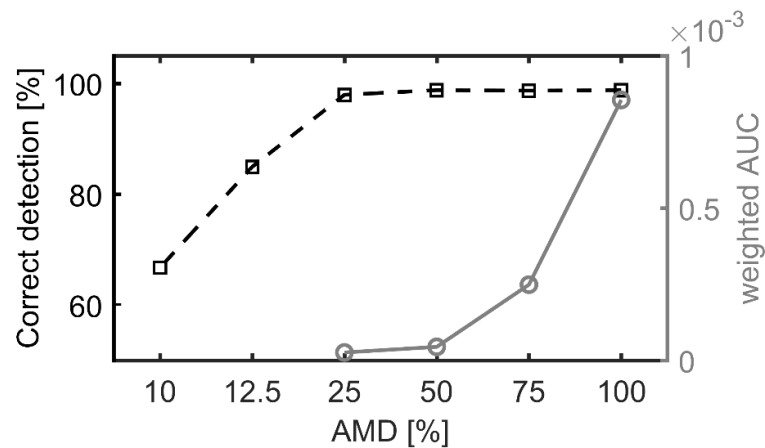


Figure 3.11: Comparison of neural and behavioural AM detection for varying AMDs. Group mean scores of the psychometric function (dashed line, left y-axis) contrasted with group mean weighted area-under-the-curve (AUC) values obtained from the neurophysiological data (solid line, right axis) at different amplitude modulation depths (AMDs).

MMWs have been elicited when acoustic changes were only just perceptible (Kraus *et al.*, 1993a) or even consciously imperceptible (Allen *et al.*, 2000). In light of this, the disappearance of the MMW for AMDs at which behavioural performance showed ceiling effects raises questions about the underlying mechanisms that result in MMW elicitation for this acoustic change type. Auditory information may have to be accumulated for a longer time period to result in AM detection for low AMDs than for high AMDs. Increasing reaction times with decreasing AMD support this interpretation (Han & Dimitrijevic, 2015). In the case of the MMW, prolonged temporal integration of stimulus information for low AMDs may result in temporally jittered neural change detection, preventing a clear MMW.

Neural thresholds

The morphology weighting approach reduced AUC values at low AMDs based on dissimilarities with the individual MMW template. This allowed objective NT calculation, where the NT was determined as the AMD at which the weighted AUC curve dropped below a specified IV. Correlation analyses revealed significant correlations between BTs and NTs for both types of correlation analysis (Spearman's and Pearson's), for both weighting methods (binary and exponential weighting), and for a range of IVs (Table 3.3). The IV of 0.4 constituted an exception with non-significant correlation results. Closer inspection of the data revealed that this is due to an outlier with a very low NT (participant 'NH2'). In an alternative implementation of the analysis procedure with stricter epoch rejection criteria, the IV of 0.4 achieved comparable results to the other IVs. However the stricter epoch rejection resulted in very low deviant epoch numbers for some participants and a more liberal epoch rejection procedure was preferred. The 'best' IV of 0.35 was selected to further validate the analysis procedure by repeating the analysis with 300 permutations of randomly chosen sub-sets of 56 standards. The resulting distributions of correlation coefficients and p-values showed that results were repeatable and did not strongly rely on the choice of standard epochs. Spearman's linear rank correlation coefficients were greater than Pearson's correlation coefficients for most IVs, which may be due to the superior robustness against outliers of the Spearman's algorithm (de Winter *et al.*, 2016) or it may indicate that the relationship between BTs and NTs is monotonous, but not strictly linear. Based on the skewed BT and NT data, non-parametric correlation analysis with Spearman's linear rank correlation coefficient is preferable, but both analysis methods were presented to present a more detailed analysis in this exploratory study.

Non-parametric statistical analysis of the distributions showed that the distributions of correlation results were significantly different for binary and exponential weighting procedures, with binary weighting yielding higher correlations than exponential weighting, which is likely a result of the more stringent rejection of MMWs with poor resemblance to the template.

Intersection value

As stated in Section 3.2.5, the statistical significance of the correlation between BTs and NTs was not strongly dependent on the IV. To objectively determine a specific IV for data analysis, different approaches may be applied. Unless a thresholding paradigm

is employed, task difficulty levels in psychoacoustic paradigms are commonly selected with the goal of deriving a measure of performance between floor and ceiling. Such difficulty levels provide a means of comparing task performance across participants and a means for performing correlation analysis across paradigms. The 75% AMD fulfils these requirements for NTs: Some participants exhibited clear waveforms for the 75% AMD condition while in others MMW morphologies were poorer. At the 50% AMD level, no clear MMWs were recognizable. Given the suitability of the 75% AMD level for correlation analysis, one could determine the IV as the group mean AUC value at this level. This would provide a value of 0.325 (binary weighting) or 0.323 (exponential weighting), which lies in the range of the IVs with the highest correlations (see Table 3.3).

AM loudness cues

The challenge of loudness balancing AM stimuli is usually overcome by energy adjustment and/or level roving for behavioural testing (Viemeister, 1979; Bacon & Viemeister, 1985; Shen & Richards, 2013; Shen, 2014). Unfortunately, level roving cannot be employed in MMW paradigms as it may result in MMWs being elicited purely through intensity change detection (von Wedel, 1982; Martin & Boothroyd, 2000; Harris *et al.*, 2007). The loudness may change with the overall presentation level, the AM rate (Zhang & Zeng, 1997; Moore *et al.*, 1999) and the AMD (Moore *et al.*, 1999). Despite energy adjustment of AM stimuli, subjective perception of loudness differences cannot be prevented without individual behavioural loudness balancing, which would be required for each tested AMD.

Moore *et al.* (1999) reported an average difference of approximately 1.5 dB in the RMS level required to achieve equal loudness for unmodulated and modulated speech-shaped noise at an AM rate of 8 Hz and with 100% AMD. For 50% AMD, the RMS-level difference decreased to less than 0.5 dB. Neurophysiological studies have reported ACC responses elicited by intensity changes of 2 dB in a vowel change stimulus (Martin & Boothroyd, 2000) and for pure tone intensity increments (Harris *et al.*, 2007). These findings do not support the interpretation that unwanted overall loudness cues between modulated and unmodulated stimuli had a strong influence on the MMW, but some influence cannot be ruled out.

Limitations

Some limitations of this study should be acknowledged. The use of only 56 deviant presentations for each condition may be a confounding factor in NT estimation. Kraus *et al.* (1993a) averaged neural responses for 200 deviant presentations to show neural change detection near the perception threshold. Increasing the number of deviant trials would likely have a positive impact on the SNR of the acquired neural responses. However, this study included four acoustic change conditions (four AMDs), which required a fine balance between the number of deviant presentations and participant fatigue. In comparison, Kraus *et al.* (1993a) only employed one acoustic change type when they recorded MMNs near perception threshold which enabled more deviant repetitions.

The low number of recording channels can be an advantage or a limitation. The chosen single-channel setup is clinically friendly, which is important for future extension to clinical cohorts. However, it also introduces the possibility of slight misplacement of the recording electrode, resulting in altered MMW amplitudes across participants, but not influencing recordings within participants.

The discrepancy between the magnitudes of BTs and NTs, despite significant correlations, needs to be explained and may be due to several factors: (1) the difference in the experimental paradigm may in part account for a threshold difference as 3AFC-discrimination is easier than single-interval discrimination. (2) MMW amplitudes are known to decrease with increasing task difficulty, and therefore, for the 50% and 25% AMD conditions the MMW may exist but is not distinguishable from the noise floor. The SNR of the EEG data can be improved by increasing the number of deviant repetitions, potentially resulting in distinguishable MMWs at low AMDs, which would in turn lead to lower NTs and decrease the gap between BTs and NTs. Future research has to identify where the large discrepancy between BTs and NTs originates from.

3.3.2 Psychoacoustics

The AM detection thresholds found in this study were higher than those commonly reported in the literature, although similar AM detection thresholds were presented for 4 Hz AM, with an average threshold of 13% for a stimulus duration of 1 s (Han & Dimitrijevic, 2015), equating to 4 AM cycles, as in this study. AM rates below 10 Hz yield constant AM thresholds, provided that the stimulus duration is chosen

sufficiently long with regard to the number of AM cycles at a given AM rate (Viemeister, 1979; Bacon & Viemeister, 1985; Sheft & Yost, 1990). Previous studies investigating AM detection thresholds for an 8 Hz AM rate and broadband noise carriers for young NH cohorts reported mean thresholds of approximately 8% (Jin *et al.*, 2014) and 5% – 6% (Viemeister, 1979; Bacon & Viemeister, 1985; Takahashi & Bacon, 1992). In all reported studies broadband noise stimuli, with and without AM, and with a duration of 500 ms were presented monaurally via headphones and reported thresholds provide an estimate of the AMD required for 70.7% correct identification. Presentation levels differed across studies, but do not significantly affect AM detection thresholds unless presentation levels are very low (Viemeister, 1979). A potential cause for the higher thresholds reported here, is the carrier bandwidth. A reduced carrier bandwidth is associated with poorer AM detection thresholds (Bacon & Viemeister, 1985; Bacon & Gleitman, 1992; Strickland & Viemeister, 1997). The speech-shaped noise carrier in this study emphasized frequencies below 1 kHz while higher frequency content was lower in level. Similar to band-limited carriers, this speech-shaped noise carrier may result in poorer AM detection thresholds than for broadband noise carriers. Higher average AM detection thresholds may also be caused by the level roving (± 3 dB), as the loudness changes may distract from the task at hand, particularly at low AMDs (Chatterjee & Oberzut, 2011).

3.3.3 Speech-in-noise recognition vs. AM detection

The lack of significant correlations between speech-in-noise recognition and behavioural AM detection abilities is not surprising and in line with the literature. Previous studies in NH cohorts have already demonstrated the difficulty in teasing out relationships between speech measures and various psychoacoustic measures (Strouse *et al.*, 1998; Watson & Kidd, 2002; Goldsworthy *et al.*, 2013). Watson and Kidd (2002) proposed that speech-in-noise recognition in NH cohorts largely depends on a combination of pattern recognition abilities and the ability to infer the meaning of degraded speech from splinters of information. In contrast to this, deficits in spectral and temporal auditory processing caused by hearing impairment may negatively impact speech processing, which is supported by significant correlations between psychoacoustic and speech measures (Dreschler & Plomp, 1980; Festen & Plomp, 1983; Dreschler & Plomp, 1985; Glasberg & Moore, 1989). Moreover, various studies for CI cohorts have shown significant correlations between speech measures and AM detection (Cazals *et al.*,

1994; Fu, 2002; Luo *et al.*, 2008; Won *et al.*, 2011b; Gnansia *et al.*, 2014; De Ruiter *et al.*, 2015), upholding the hypothesis that AM detection may play a role in speech processing in the case of electric hearing. As stated previously, the aim of the test battery design presented in this study was its future implementation in a CI user cohort, thus, the inclusion of the speech measure was deemed justified.

3.3.4 Clinical applications

In this study, data was acquired from NH participants. However, all data acquisition was planned in a manner that allows future study replication with CI users. These additional considerations mainly impacted the sampling rate and additional lower difficulty levels in behavioural testing.

The findings support the hypothesis that NTs obtained from MMWs towards differing AMDs correlate with behavioural AM detection thresholds. This supports the MMW as a potential objective measure of temporal processing. Although correlations between behavioural AM detection thresholds and speech-in-noise recognition did not reach significance after (conservatively) adjusting for multiple comparisons, a relationship should not be ruled out. Correlation results may have been impeded by commonly small observed differences in performance for NH cohorts. Larger performance variability in CI users may strengthen the correlation results. The applicability of neural measures of AM detection for auditory performance assessment should be further investigated as they may provide “speech-relevant non-speech measures”, which would be beneficial in pre-lingual cohorts in order to estimate the benefit of aided hearing.

Based on the presented findings it seems feasible to extend this study to clinical cohorts to explore whether relationships persist. However, challenges have to be anticipated. In order to apply the presented data processing method based on morphology weighting to EEG data, it is crucial to obtain a clear MMW template for the 100% AMD condition. EEG data acquired from CI users is contaminated by the stimulation artefact and even with efficient artefact removal techniques, the data quality is often poorer than for NH participants. Without a clear template, the morphology weighting procedure may not be feasible. Regarding the psychometric function, it may be challenging to determine a specific AMD level which provides responses above chance level and below ceiling effect for all participants in hearing impaired cohorts due to large variations in

performance. For NH participants, these conditions were met by the 12.5% AMD level. If these conditions are not met, correlation analysis with other metrics is not feasible. Threshold paradigms should be considered for speech-in-noise recognition and AM detection assessment.

Key Points

- The study presented in this chapter addressed the research questions Q1.1 – Q1.5.
- MMWs were successfully elicited by AM stimulus pairs (Q1.1) and their area-under-the-curve values changed in line with acoustic change saliency (Q1.2).
- Findings support the estimation of NTs from MMW data (Q1.3), and showed significant correlations with BTs (Q1.4), which encourage further research into the application of the MMW as an objective measure of low-rate AM detection.
- The morphology weighting procedure had a positive impact on AUC values at lower AMDs, and may provide a useful analysis tool in CAEP research at the individual level.
- Correlations were observed between speech-in-noise scores and BTs of AM detection, however, they did not reach significance after adjusting the significance level for multiple comparisons (Q1.5).
- Future work should address the discrepancy between the magnitudes of BTs and NTs.
- These findings, or parts thereof, were presented at the Speech in Noise Workshop, Groningen 2016; the ARO MidWinter Meeting, San Diego 2016.
- The study presented in this chapter was published as “Depth matters – Towards finding an objective neurophysiological measure of behavioral amplitude modulation detection based on neural threshold determination” *Hearing Research*, 359, 13-22.

Chapter 4 Case study: Exploring CI artefact reduction for the acoustic change complex paradigm

Following Study 1, which was outlined in the previous chapter, and numerous pilot studies which are summarised in Appendix B, this chapter presents a case study carried out with a CI user, to address the challenge of CI artefact reduction in multi-channel EEG data elicited by stimuli with fluctuation envelopes.

Despite the promising correlations between BTs and NTs in Study 1, this case study investigated the ACC instead of the MMW as a potential objective measure of AM detection in CI users. For future clinical studies it was of interest to determine whether the ACC could be a suitable paradigm to assess neural change detection towards low-rate AM stimuli as it would be preferable to an auditory oddball paradigm due to its improved time efficiency with regards to data acquisition (Martin & Boothroyd, 1999). Furthermore, the ACC paradigm offered the opportunity to assess the influence of stimulus presentation mode on the electrical artefact, specifically how the artefact differs between continuous stimulus presentation and intermittent stimulus presentation.

The ACC pilot studies summarised in Appendix B were carried out with NH participants following the completion of Study 1 to determine if the choice of any one stimulus parameter had a noticeable effect on the amplitude of the neural measure especially for the conditions with low AMDs. These pilot studies investigated the influence of stimulus duration, of different AM rates (e.g. 0 Hz vs. 4 Hz, 8 Hz and 40 Hz), of the AM onset phase (0.5π , π , 1.5π and 2π), of AM rate discrimination (6 Hz vs. 15 Hz), of stimulus carrier type (pure tone, noise), of acoustic change type (AM, intensity decrement), of stimulus presentation mode (monaural, binaural, continuous, intermittent)

and of attentional state (passive, active) on the measured ACC. The experience gained from those pilot studies aided in the experimental design of the subsequent studies.

To date, no study investigating CAEPs as a potential objective measure of AM detection in CI users has been reported in the literature. The main question to be addressed was whether the CI artefact could be reliably minimised to assess the neural response of interest, and how CI artefact reduction is influenced by the stimulus presentation mode (intermittent or continuous stimulation), and the stimulus envelope (flat or fluctuating). For AM stimuli with the desired low AM rates, which are important for speech, the continuous artefact falls into the same frequency region as the CAEPs, and thus, cannot be filtered out. Furthermore, an active condition was included to assess whether the SNR of the measured response is greatly influenced by the attentional state of the participant.

4.1 Materials and Methods

4.1.1 Participant information

One male CI user, aged 44 years, participated in this case study. The participant had five years of device experience with a Cochlear Nucleus CP810 (N5 speech processor) implanted in the right ear. The device employed the ACE speech processing strategy with a stimulation rate of 1800 pulses per second in MP1+2 stimulation mode. With a clinical British Bamford-Kowal-Bench (BKB) test score in quiet of 55.7% correct at nine months post-implantation⁴, this CI user was considered to be a “moderately good performer”. Behavioural AM detection thresholds measured in line with the procedures outlined in Section 3.1.3 provided relatively poor thresholds of 47% AMD (4 Hz AM rate) and 48% (40 Hz AM rate).

4.1.2 Experimental design

The participant was seated in a dark, quiet room. Stimuli were presented monaurally through an Otocube® (Otoconsult NV, Belgium), which is a portable sound-attenuated suitcase in which the participant’s CI can be placed to approximate free-field conditions in a controlled environment. The speech processor is placed inside the Otocube

⁴ No updated clinical BKB scores were available, but the participant was able to communicate with the CI only and BKB scores in quiet are assumed to be improved.

(see Figure 4.1). Stimuli were presented with the in-built loudspeakers inside the Otocube, picked up by the CI's microphone and processed in line with every-day settings. The CI sound processor is connected to the CI coil via a long CI cable which was specially purchased for the different compatible CI devices. The participants' own speech processors were used with their most commonly used map. The Otocube contains a built-in monitor and calibration tool, which utilises the in-built microphone to enable efficient stimulus calibration.

The participant in this case study was implanted in the right ear. Therefore, the EEG recording cap was modified. EEG electrodes and holders D24, D25 and D26 of the 128-channel Biosemi Active Two system (Biosemi B. V., Amsterdam, Netherlands) were located in close proximity of this participant's CI coil, and thus, were removed to ensure participant comfort during the EEG recording.



Figure 4.1: Placement of a cochlear implant (CI) in an Otocube® (Otoconsult NV, Belgium).

The pictures show the placement of a CI in front of the in-built loudspeaker. The Otocube contains its own soundcard which is controlled from a PC via USB. The sound is picked up by the CI microphone in free-field conditions with everyday speech processor settings and the stimulation information is transmitted to the CI coil via a long CI cable.

Four experimental conditions were tested: (1) one control condition which assessed a pure tone change, and three AM conditions with the differing presentation modes (2) passive intermittent, (3) passive continuous and (4) active continuous. AM

stimuli were created according to the procedure outlined in Section 3.1.2, but with an AM rate of 4 Hz and a constant AMD of 80% for the modulated noise segment.

The intermittent (2) and continuous (3 + 4) presentation modes were included to analyse the effects of the presentation mode on the recorded CI artefact. In the passive intermittent presentation mode, the acoustic stimulus varied from unmodulated noise (0% AMD) to modulated noise (80% AMD) to silence, whereas in the continuous presentation modes, the stimulus varied continuously between unmodulated noise and modulated noise without silent periods. In the continuous modes, the duration of the unmodulated noise was randomised between 1.5 s and 2.5 s to allow for the behavioural response following AM onset in the active condition. For the continuous modes, 210 repetitions were recorded for the acoustic change from unmodulated to modulated noise, and for the intermittent mode 300 repetitions were recorded. Data acquisition was divided into three recording blocks for each condition. Ideally, epoch numbers should be similar between conditions, however, for the active condition data acquisition time had to be limited to allow sustained attention throughout the recording blocks and it was decided to increase the number of epochs for the intermittent paradigm to potentially improve the SNR. While disparities are strongly discouraged between conditions, it was deemed acceptable for the purposes of this exploratory case study.

The pure tone control condition was included, as pure tone changes or in the case of electric hearing also changes in the stimulation electrode, are known to elicit a clear ACC of large magnitude (Brown *et al.*, 2008; He *et al.*, 2014; Mathew *et al.*, 2017), and the stimulus envelope is flat for both segments of the acoustic change stimulus. The condition alternated from a 500 Hz pure tone, to a 1000 Hz pure tone, to a silent inter-stimulus interval with each segment having a duration of 1 s. CI artefacts were expected particularly at sound onset and offset, but no strong DC artefact was expected at the acoustic change from 500 Hz to 1000 Hz.

To enable the recording of neural responses towards changes in on-going stimuli such as the ACC, alterations had to be made to the EEG measurement software and hardware. Multi-channel data was acquired with a 128-channel Active Two BioSemi acquisition system in combination with ActiView software (both BioSemi B. V., Amsterdam, Netherlands). Stimuli were presented with Presentation® software (Version 18.1, Neurobehavioural Systems, Inc., Berkeley, CA), and triggers sent by Presentation® indicate the latencies of stimulus onset in the EEG. However, in the case of stimulus changes in an on-going sound with randomized durations, Presentation® software's in-

built triggers at sound onset were not inefficient. The measurement system was augmented with an Arduino Uno microcontroller, which sent a trigger when a threshold was exceeded in the trigger channel. This trigger signal was conveyed in an otherwise unused audio channel of the Otocube sound card. This arrangement required some hardware adjustments to the sound card. The trigger signal consisted of a 4 kHz pure tone for the duration of each AM stimulus segment. The Arduino accurately detected the onset of this trigger signal and sent a compatible trigger code, which was fed into the existing pathway for Presentation® software triggers via a parallel port. A schematic with the overview of the hardware connections in this set-up is pictured in Figure C.6 in Appendix C.

4.1.3 Post-processing of EEG data

Data post-processing was carried out with custom-written scripts (Figure 4.2) based on EEGLAB functions in MATLAB (Release 2016a, The MathWorks, Inc., Natick, Massachusetts, United States). Continuous data of the individual recordings were merged for each condition (`pop_mergeset.m`) and down-sampled to 512 Hz (`pop_resample.m`) to reduce processing time. Continuous data was bandpass-filtered between 1 and 15 Hz (`pop_eegfiltnew.m`). The low cut-off frequency of 1 Hz was necessary as slow signal drifts can negatively affect the success of ICA. Data was epoched (`pop_epoch.m`) with -200 ms pre-stimulus presentation and 1400 ms (ACC) post-stimulus presentation. EEG artefact rejection included bad channel interpolation in the channel-space and ICA component rejection in the component space. Bad channels were determined based on high correlation coefficients ($|r_p| \geq 0.6$) with an individual CI artefact template for each condition (Figure 4.3). Cut-off values for correlation coefficient thresholds were determined iteratively and may vary for a larger cohort. The CI artefact is greatly dependent on the stimulus envelope and the presentation method. Intermittent stimulus presentation introduced onset and offset artefacts to the CAEPs and fluctuating stimulus envelopes such as for the AM stimuli added additional CI artefact fluctuations. “Bad” recording channels and channels which were disconnected due to the CI coil location were removed from analysis, temporarily reducing the number of available channels. Data was average referenced (`pop_reref.m`) and the baseline was corrected for a 200 ms pre-stimulus window (`pop_rmbase.m`). Independent components (ICs) were calculated with ICA (`pop_runica.m`) and the number of available ICs depended on the number of

remaining good channels in each condition. Interpolation of bad channels prior to ICA should be avoided. Typical EEG artefacts such as eye movement, eye blinks and generic discontinuities were removed with the fully automated ADJUST algorithm (Mognon *et al.*, 2011), which screens ICs for pre-determined spatial and temporal features that are associated with such artefacts. ADJUST is a plug-in of the MATLAB based EEGLAB software (Delorme & Makeig, 2004). A limitation of the ADJUST algorithm is the lack of heart beat detection within ICs. Furthermore, bad ICs originating from CI artefacts were identified with a correlation approach: For the AM conditions, the temporal activation of each independent component (IC) within the time window corresponding to the presentation of the AM sound was correlated with a 4 Hz sinusoid. ICs with correlation coefficients exceeding $|r_p| \geq 0.6$ were marked as bad components and rejected.

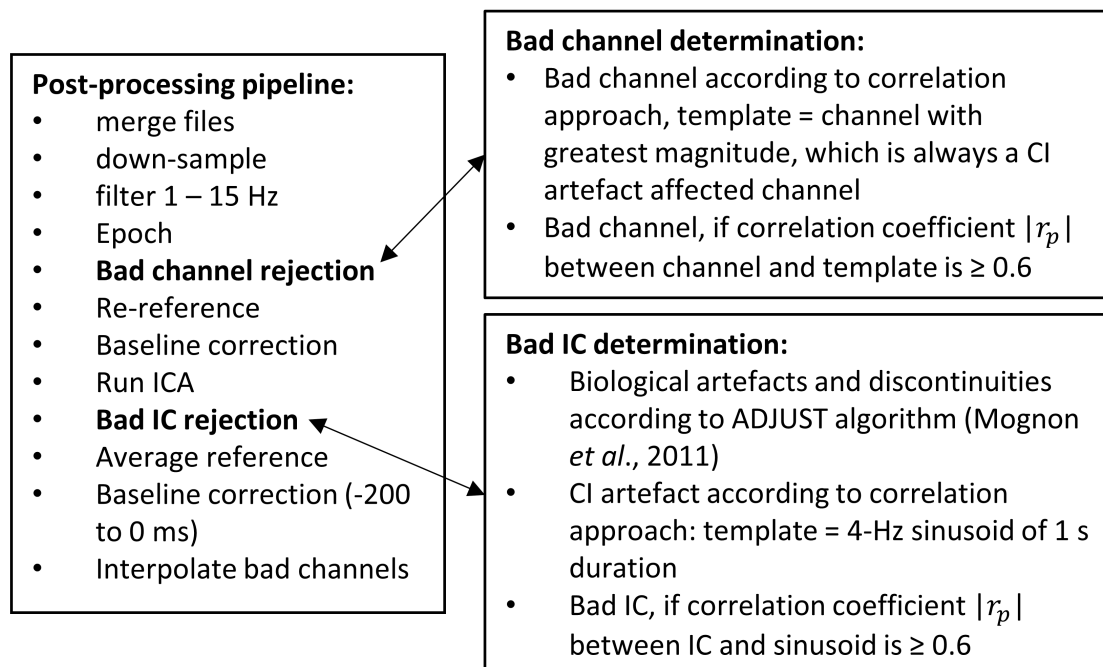


Figure 4.2: Data processing pipeline for the acoustic change complex paradigm in cochlear implant (CI) users.

The processing pipeline includes automatic bad channel detection and bad independent component (IC) detection arising from CI stimulation. Abbreviations and acronyms: IC – Independent component, ICA – Independent component analysis.

CAEPs were extracted and visually assessed for two electrode clusters in a fronto-central ROI and an occipital ROI (see Figure 4.5 for exact electrodes), where the ACC was maximal, albeit with reversed polarities. Furthermore, topographical plots of the potential distribution across the entire scalp were generated for the time points where activation was maximal in the ROIs (Figure 4.4). Global field power (GFP) was calculated as the standard deviation of activity across all channels and presents a channel-independent measure of overall activation across time (Figure 4.4 and Figure 4.6). As a

final step, data was re-referenced to the occipital ROI to maximise the ACC amplitudes for a fronto-central ROI (Figure 4.6). The SNRs were calculated for a time window that surrounded the ACC (90 ms – 350 ms) and for an equal-length time window after the ACC potentials (600 ms – 860 ms). The SNRs were calculated as

$$SNR = 20 \cdot \log_{10} \left(\frac{A_{signal}}{A_{baseline}} \right),$$

Equation 4.1

where A_{signal} refers to the RMS-potentials of the desired time window (ACC or post-ACC) and $A_{baseline}$ refers to the RMS-potential of the baseline window (-200 ms – 0 ms).

4.2 Results

As indicated by Figure 4.3, the different conditions produced very distinct CI artefacts in the recorded CAEPs, which reflected the stimuli's envelopes and the presentation mode, i.e. whether there were any transitions from sound to silence. Filtering of CAEPs caused temporally smeared artefacts, in particular for the artefact elicited by CI power-up and power-down. The continuous AM condition (Figure 4.3, middle) produced a CI artefact that closely resembled a 4 Hz sinusoid, whereas the intermittent AM condition (Figure 4.3, left) created the typical pedestal artefact at sound offset at 1000 ms and a distorted 4 Hz sinusoid throughout the duration of the AM noise (0 ms to 1000 ms). The intermittent pure tone condition resulted in strong pedestal artefacts at the acoustic change (0 ms) and sound offset (1000 ms). When comparing the first row with the last row of Figure 4.3 it is evident that channels which were severely affected by CI artefact were successfully removed. Additional IC rejection followed by re-referencing to average reference provided the CAEPs shown in Figure 4.4 and Figure 4.5.

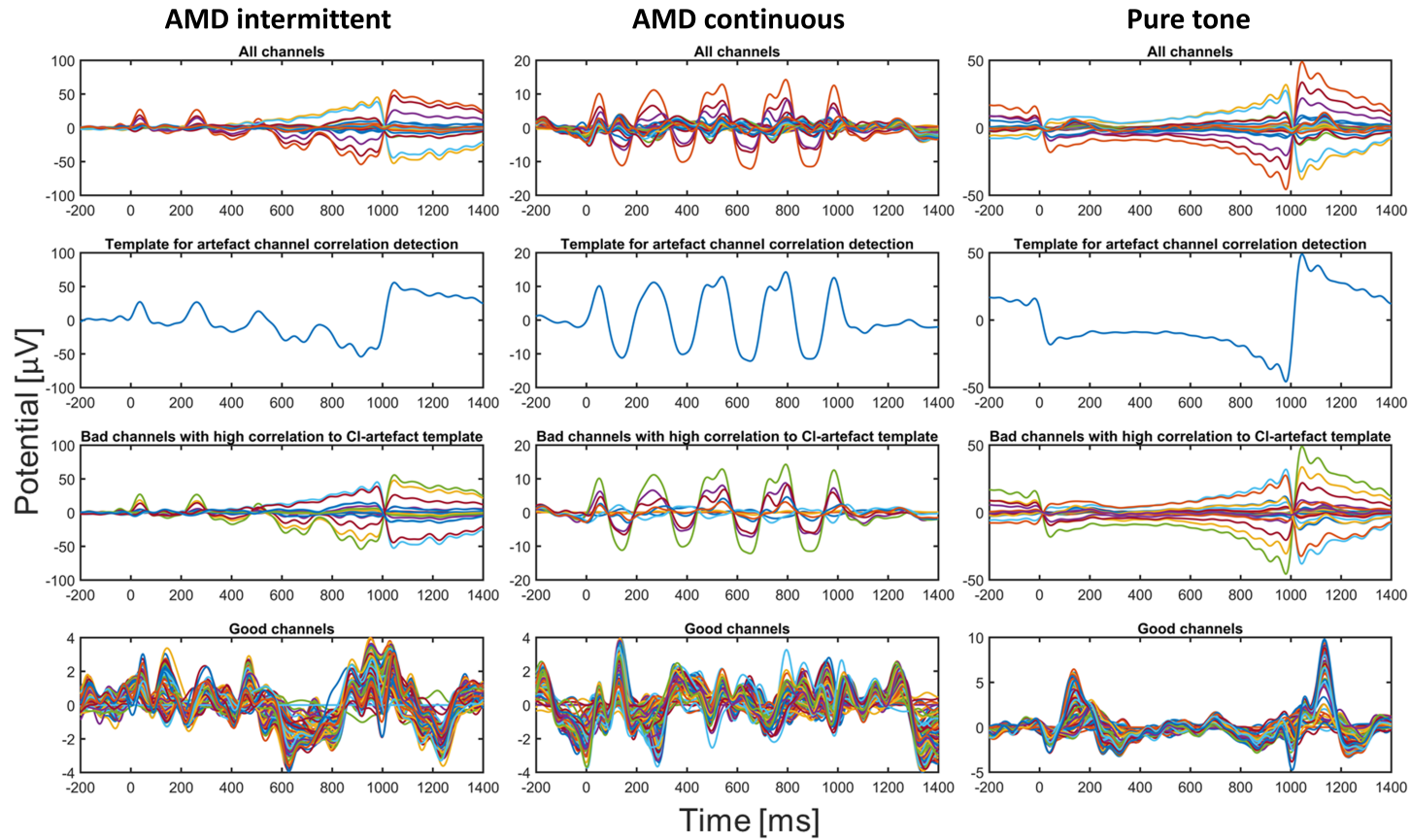


Figure 4.3: Examples of the correlation-based bad channel rejection to reduce cochlear implant (CI) artefact prior to independent component analysis. Pictured are cortical auditory evoked potentials with the differing CI artefacts for three example conditions: amplitude modulation depth (AMD) change intermittent (left), AMD change continuous (middle) and pure tone change intermittent (right). Note that channels are not re-referenced to average reference and scales differ between plots.

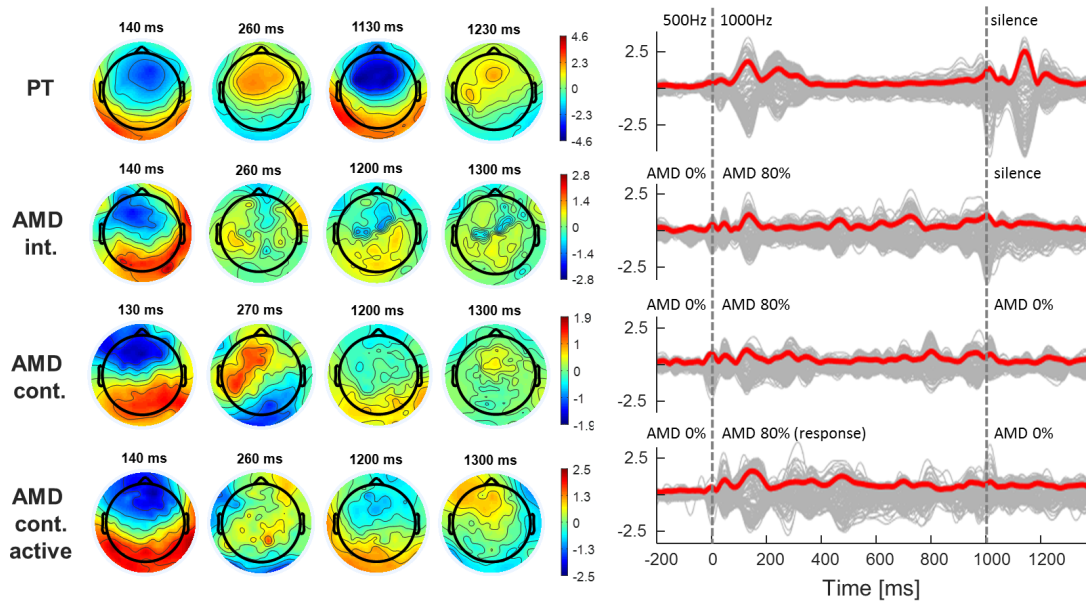


Figure 4.4: Topographical, butterfly and global field power (GFP) plots of the four ACC conditions.

Topographical plots (left) show the scalp potentials' distribution for chosen time points. Butterfly plots (right, grey) provide an overview of the cortical auditory evoked potentials at all channel locations and their global field power (GFP) is plotted in red. Note the different colour scales on the topographical plots for each condition (row). Abbreviations and acronyms: PT – Pure tone, AMD – Amplitude modulation depth, int. – Intermittent, cont. – Continuous.

Small CI artefacts at the acoustic changes (0 ms and 1000 ms) were still noticeable in the bottom row of Figure 4.3, however, topographical plots, butterfly plots and global field power (GFP) plots in Figure 4.4 suggest that the ACC, occurring between 100 ms and 350 ms post-stimulus, was not notably influenced by the remaining artefact. If this were the case, topographical plots would show strong local activation at the site of the implant. All three AM conditions showed the distinct N1 topography following the acoustic change at 0 ms, but only the (passive) continuous AM condition showed the P2 topography in addition (Figure 4.4, left). It should be noted that contrary to the pure tone condition, the CAEPs following the acoustic change at 1000 ms were greatly diminished or not identifiable at all in the AM conditions (Figure 4.4, left).

Figure 4.5 provides an overview of the CAEPs for the two ROIs as well as the detailed electrodes contained in each ROI. Overall, CAEPs showed the anticipated reversed polarities for the two ROIs. For the pure tone control condition, a clearly distinguishable ACC was observed following the acoustic change at 0 ms, followed by a very prominent offset response after 1000 ms, despite minimal CI artefact rejection procedures for this condition. All three AM conditions displayed distinguishable ACCs, although the intermittent AM condition showed additional peaks in rhythmic intervals

with peaks at 460 ms and 730 ms, which may either reflect remaining CI artefact or CAEPs elicited by the troughs of the AM noise. The artefact template channel from Figure 4.3 (second row) contained peaks at 505 ms and 750 ms for the AMD intermittent condition, which were not coinciding with the peaks observed in the CAEPs in the ROI. Therefore, it seemed reasonable to assume that these peaks arose from neural activity in response to the trough of the AM noise, but it cannot be proven. However, the artefact reduction procedure has optimisation potential for the intermittent AM condition, as the correlation template for bad IC determination was a pure 4 Hz sinusoid, which seemed appropriate for the continuous AM condition according to Figure 4.3, while for the intermittent AM condition a different template should be chosen for correlation analysis with ICs in future studies.

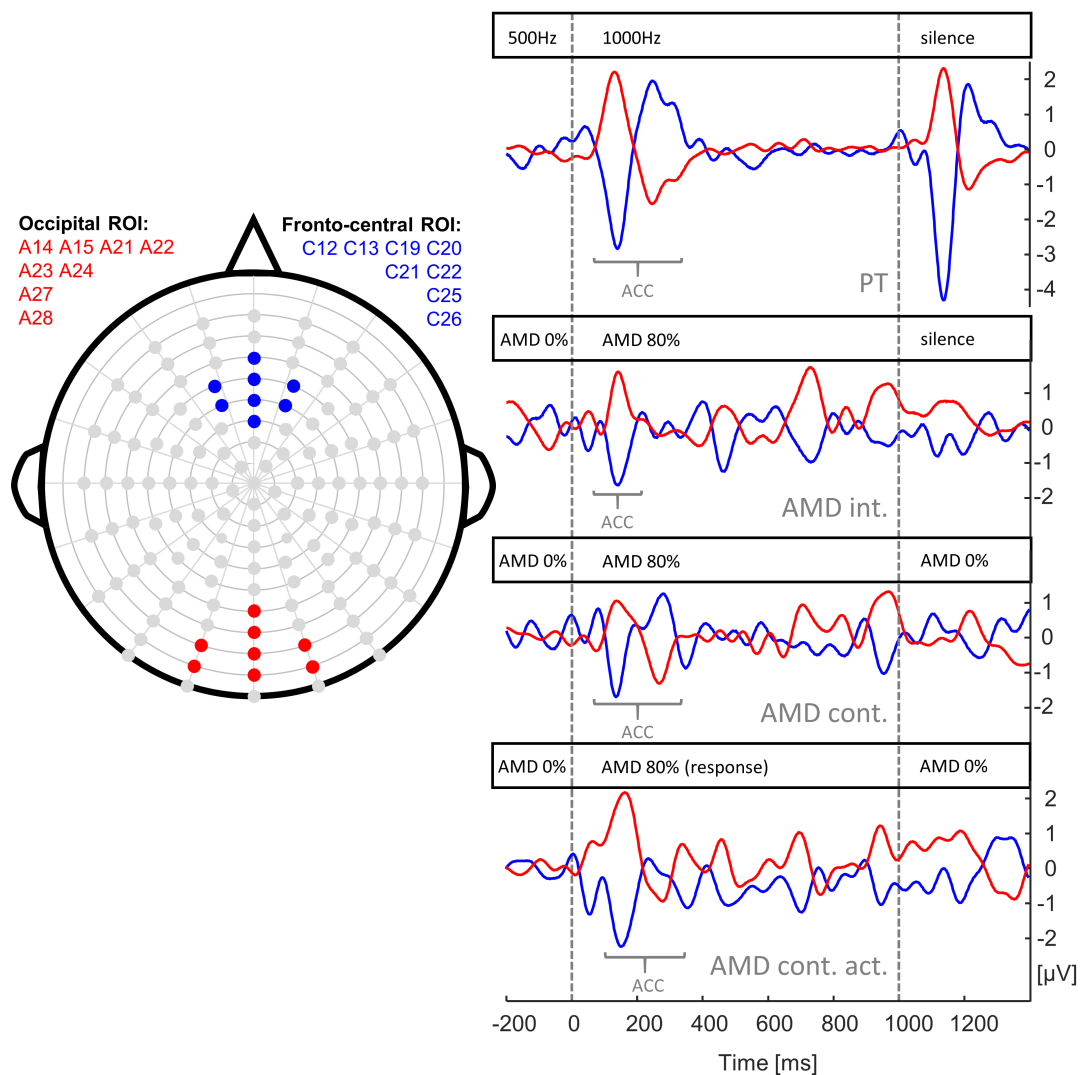


Figure 4.5: Overview of the electrode clusters and neural responses.

The electrodes included in each region of interest (ROI) are indicated on the left, and the neural responses for each ROI are indicated on the right for the three conditions. Pictured above the neural responses are the corresponding acoustic stimuli. An amplitude modulation depth (AMD) of 0% represents unmodulated noise.

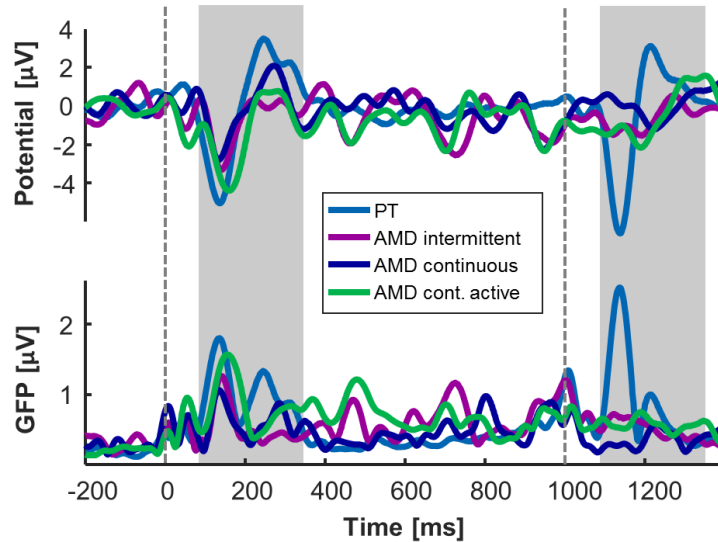


Figure 4.6: Re-referenced cortical auditory evoked potentials (CAEPs) and their global field power (GFP).

At 0 ms each condition contained the acoustic change from tone A to tone B, eliciting the acoustic change complex. At 1000 ms tone B changed to silence (PT & AMD intermittent conditions) or to tone A (AMD continuous & AMD cont. active conditions). The time ranges of the change responses/offset responses are highlighted in grey. CAEPs (top) are shown for the fronto-central electrode cluster, re-referenced to the occipital electrode cluster (Figure 4.5). The GFP (bottom) was calculated as the standard deviation of all electrodes across time. Abbreviations and acronyms: PT – Pure tone, AMD – Amplitude modulation depth, cont. – Continuous.

Table 4.1: Acoustic change complex (ACC) amplitudes.

Peak amplitudes were measured for the fronto-central electrode cluster pictured in Figure 4.6 (top). Peak amplitudes were measured separately for the negative and positive and additionally the peak-to-peak amplitude is provided.

Condition	ACC _n [µV]	ACC _p [µV]	ACC _{p-p} [µV]
Pure tone	-5.1	3.5	8.6
AMD int.	-3.3	0.3	3.6
AMD cont.	-2.8	2.1	4.9
AMD cont. active	-4.4	0.8	5.2

Table 4.2: Signal-to-noise ratios (SNRs) for two time windows of interest.

SNR_{ACC} represents the SNR of the ACC window (90 ms – 350 ms) with respect to baseline (-200 ms – 0 ms) and SNR_{post-ACC} represents a control condition, for which the SNR was calculated for an equal-length time window beyond ACC activity (600 ms – 860 ms).

Condition	SNR _{ACC} [dB]	SNR _{post-ACC} [dB]
Pure tone	15.7	-9.9
AMD int.	6.6	4.5
AMD cont.	8.6	1.9
AMD cont. active	14.1	9.7

In order to maximise the SNR of the ACCs, data was re-referenced to the occipital ROI and averaged across the fronto-central ROI as depicted in Figure 4.6 (top). Figure 4.6 provides a direct comparison of CAEPs across conditions, as well as a channel-independent visualisation by means of the global field power (GFP), which represents the standard deviation of scalp potentials across all channels (bottom plot). Peak amplitudes as well as peak-to-peak amplitudes were measured for CAEPs depicted in Figure 4.6 (top) and are displayed in Table 4.1. Overall, the SNR of the pure tone and active AM conditions (Table 4.2) were similar despite differing peak-to-peak amplitudes. The intermittent AM condition had the lowest peak-to-peak amplitude and the lowest SNR_{ACC} , which was similar to the magnitude of the $SNR_{post-ACC}$ of the control window (Table 4.2). The pure tone control condition had the largest peak-to-peak amplitude and SNR, as well as the lowest $SNR_{post-ACC}$, indicating very low on-going stimulus-locked neural activity throughout the duration of the change-pure-tone beyond the ACC. No statistical analysis was carried out, as this was an exploratory case study.

4.3 Discussion

This case study explored the feasibility of measuring ACCs in response to AM stimuli in a CI user. ACCs were successfully extracted based on an automatic processing pipeline, which provided an objective and less time-expensive alternative approach to the common visual assessment of channels and ICs for artefact rejection purposes. It should be noted that the CI artefact can vary greatly across participants as the artefact is dependent on a number of factors such as the stimulation rate, stimulation mode and pulse width (Hofmann & Wouters, 2010; Li *et al.*, 2010). The efficacy of this proposed processing pipeline should be validated with further datasets. As was shown in this case study, the CI artefact can vary in its morphology even within a participant, depending on the presentation mode (continuous or intermittent), and the stimulus envelope.

The preferred AM condition for future CI studies would be the passive continuous AM condition, as the continuous presentation mode eliminates the onset and offset pedestal artefacts associated with the power-up and power-down of the device. In this study, a clear ACC was recorded for this condition, which exceeded the intermittent AM condition, but fell below the active AMD continuous condition in terms of its ACC peak-to-peak amplitude. The active continuous condition does however not present a viable

alternative to the passive conditions, as active participant engagement defeats the purpose of developing an objective measure that is independent of participant feedback.

In ACC studies the existence of the ACC often relies on visual determination (Mathew *et al.*, 2016; Brown *et al.*, 2017; Small *et al.*, 2017). This is highly subjective. ACC quantification is commonly limited to the peak amplitude and peak latencies (Han & Dimitrijevic, 2015; Kirby & Brown, 2015; Mathew *et al.*, 2016; Brown *et al.*, 2017) or the RMS amplitude (He *et al.*, 2015). For MMW studies, however, more complex objective statistical methods can be employed such as permutation analysis (Files *et al.*, 2013; Lappe *et al.*, 2013; Stothart & Kazanina, 2013). Furthermore, the MMW may not only be quantified in terms of peak measures, but quantification may also be achieved by calculating a bootstrapped noise floor and the AUC exceeding the noise floor (Lopez Valdes *et al.*, 2014) which reduces the influence of noise on quantification measures.

A major limitation of employing the ACC paradigm in a CI user cohort is posed by the lack of control over stimulation parameters. Unless stimuli are presented with specialized research processors, unwanted cues at the acoustic change such as gaps and electrode changes may be introduced. In the following **Chapter 5**, a study is presented investigating the MMW rather than the ACC as an objective measure of AM detection in a clinical CI user cohort. The choice of the MMW paradigm has some advantages, including better control over artefact rejection procedures and determination of the existence of neural change detection responses in the MMW paradigm. CAEPs elicited by the AM stimulus in this case study suggested the potential existence of not only the ACC components, but elicitation of N1-P2-complex-like CAEPs with each trough of the AM cycle (in some conditions). In an ACC paradigm it is difficult to disentangle neural responses from random noise, and only increasing the number of stimulus repetitions would allow differentiation of fluctuations as due to noise or synchronized neural activity. This issue can be avoided with the MMW paradigm, by calculating the difference waveform between the standard and deviant CAEPs elicited by the same physical stimulus. Presentation of the same physical stimulus as the deviant and separately in a deviant-alone condition eliminates stimulus specific neural processing and extracts components related to the neural change detection when calculating the difference waveform. Furthermore, in an ACC paradigm the acoustic difference is sudden and rather limited to the time point of the acoustic change. However, in an MMW paradigm the change response can be elicited by higher order acoustic changes such as pattern differences (for detailed examples and references refer to Section 2.3.2), which may

indicate that a wider temporal portion of the deviant sound contributes to the acoustic change.

Key Points

- The study presented in this chapter addressed the research questions Q-CS.1 and Q-CS.2.
- The CI artefact depends on the stimulus presentation mode with cleaner artefact responses for continuous presentation of stimuli due to the elimination of the onset and offset pedestals.
- The ACC was elicited in all stimulus conditions, but with reduced amplitudes and SNRs in the AM change conditions compared to the pure tone change condition.
- The CI artefact was successfully reduced, if not fully eliminated, with the proposed automated processing script.
- For the pure tone change condition, neural activity returned to baseline after the ACC, whereas for AM stimuli, on-going CAEPs were observed, making data difficult to interpret due to noise.

Chapter 5 Investigation of the MMW as an objective measure of low-rate AM detection in CI users

This study is built on the foundations of Study 1 (**Chapter 3**), expanding it from a NH cohort to a clinical CI user cohort. Positive, statistically significant correlations between behavioural and neural thresholds in Study 1 provided evidence for the feasibility of exploring the MMW as a potential objective measure of AM-detection. However, data acquisition from a CI user cohort introduced new challenges. Listening performance varies greatly in CI users (Zeng *et al.*, 2013) and behavioural paradigms had to be adjusted to allow for large variability in the data. The speech-in-noise test from Study 1 (**Chapter 3**) was altered to an adaptive speech reception threshold (SRT) test allow for large variation in performance without resulting in ceiling or floor effects. The adaptive SRT test may also improve comparability to behavioural AM detection thresholds. Furthermore, electrical artefacts resulting from the electrical stimulation of the CI commonly exceed the neural activity of interest. As with CAEPs, CI artefacts are time-locked to the presentation of the stimulus. Therefore, it is important to address the need for CI artefact reduction in the experimental design to minimise the confounding influence of the artefact on the neurophysiological response. In addition, post-processing protocols must be defined to further reduce the CI artefact.

In the study described in this chapter, the widely employed auditory oddball paradigm was extended with the goal of simplifying CI artefact reduction to investigate the MMW in CI users. Given the envelope difference between the standard (flat envelope) and deviant (fluctuating envelope) stimuli, subtraction of the corresponding CAEPs would not result in reliable artefact reduction as in other MMW studies with flat stimulus

envelopes (Wable *et al.*, 2000; Kelly *et al.*, 2005; Lopez Valdes *et al.*, 2014; Leijsen *et al.*, 2015).

By presenting the same physical tone as the standard *and* deviant stimulus in separate segments, subtracting their respective CAEPs can be argued to result in a difference wave free of stimulus-related differences (Picton *et al.*, 2000). This approach has been successfully implemented for CI artefact reduction purposes (Friesen & Picton, 2010; Ortmann *et al.*, 2013; Ortmann *et al.*, 2017). Additionally, it is critical to design the experiment in such a way, that the neurophysiological response of interest does not overlap with the CI artefact (Presacco *et al.*, 2017). In the case of the MMW paradigm this implies that the stimulus duration should exceed the time window of interest for the MMW (\approx 100 ms until 400 ms). For the purpose of this study a stimulus duration of 500 ms was chosen.

5.1 Materials and methods

5.1.1 Clinical recruitment process

In line with the recruitment process outlined in Figure 5.1, the database of the Irish National Cochlear Implant Programme was searched for CI users with ages between 20 and 65 years with more than one year of experience with their CI. A clinical audiologist screened the list of participants meeting the age criterion and excluded non-native English speakers as well as any individuals with neurological conditions, serious health impairments, speech perception in quiet below 40%, or a home address that was not in commuting distance from Dublin. Furthermore, CI users who have previously participated in the longitudinal study carried out by our research group were excluded, as well as any participants that did not have a speech processor that is compatible with the Otocube®⁵. Following this pre-screening process, recruitment letters were sent out to 82 individuals in four recruitment phases with information leaflets, consent forms and stamped return envelopes. As a result of the recruitment process, 14 CI users participated

⁵ For compatibility with the Otocube, a long additional coil cable is required, which is only available for Cochlear's Nucleus Freedom, Nucleus CP9 and CP8 series (N5 and N6) processors, AB's Naida and Harmony processors, MED-EL's Opus 2 processor, and Oticon Medical's (Neurelec) Digisonic processor.

in the experiments. The first two participants were pilot participants and assisted in tuning the paradigm.

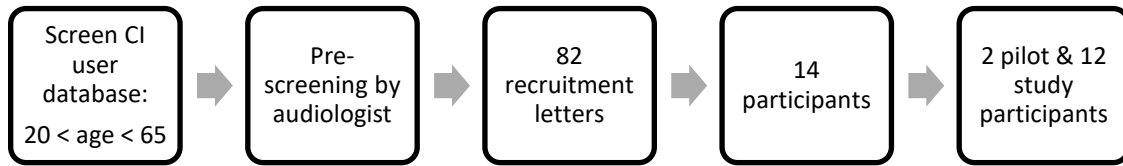


Figure 5.1: Clinical recruitment process for the research study.

From 14 recruited participants, 12 participated in the final study. Two CI users generously offered their time for a pilot study which provided guidance for the final study design, but their data is not further mentioned in this study.

Table 5.1: Demographics and CI-related characteristics.

Speech scores represent the most recent Bamford-Kowal-Bench (BKB) test scores in quiet. Abbreviations and acronyms: CI – Cochlear implant, n. a. – Not available.

ID	Age	Sex	Implant side	Duration CI use	Duration of hearing loss pre-CI	Manufacturer	Implant model	Speech processor model	Coding strategy	Stimulation rate	Mode	BKB scores CI	BKB scores CI + hearing aid
CI3	42	f	L	10y 1mo	18 y	Cochlear	Freedom Contour Advanced	CP910	ACE	900	MP1+2	45	n. a.
CI4	47	f	R	5y 5mo	4 y	Cochlear	Freedom Straight CI24RE	CP810	ACE	900	MP1+2	83	94
CI5	52	f	L	1y 9mo	18 y	Cochlear	Profile Series N512	CP910	ACE	900	MP1+2	98	98
CI6	52	m	R	9y 10mo	35 y	Cochlear	Freedom Contour Advanced	CP910	ACE	1200	MP1+2	98	n. a.
CI7	58	f	R	2 y 0mo	18 y	AB	Clarion HiRes 90K	Naida CIQ70	HiRes Optima-S	3712	Monopolar current steering	70	68
CI8	50	f	L	2y 8mo	44 y	Cochlear	Freedom Contour Advanced	CP910	ACE	900	MP1+2	54	53
CI9	47	m	L	4y 2mo	4 y	Cochlear	Freedom Contour Advanced	CP910	MP3000	500	MP1+2	80	100
CI10	25	f	R	4y 7mo	22 y	AB	Clarion HiRes 90K	Neptune	HiRes Optima-S	2250	Monopolar current steering	91	97
CI11	54	f	L	9y 6mo	54 y	Cochlear	Freedom Contour Advanced	CP910	ACE	900	MP1+2	100	n. a.
CI12	57	m	R	9y 1mo	33 y	Cochlear	Freedom Contour Advanced	CP910	ACE	1200	MP1+2	97	n. a.
CI13	42	f	R	1y 5mo	40 y	Cochlear	Profile Series N512	CP910	ACE	900	MP1+2	51	94
CI14	63	f	L	8y 5mo	44 y	Cochlear	Freedom Contour Advanced	CP910	ACE	1200	MP1+2	100	100

5.1.2 Participants

Twelve post-lingually deafened CI users and ten controls without reported hearing impairment participated in this study⁶. Participants were native English speakers between the ages of 20 and 65 years old. CI users were recruited through the National Cochlear Implant Programme in Beaumont Hospital, Dublin. Detailed information on duration of hearing loss, device experience, device types, and stimulation settings are displayed in Table 5.1. This study focused on the CI user cohort and unless explicitly stated, study descriptions and results refer to the CI user cohort. NH participants were recruited to obtain EEG data without CI artefacts for visual comparison. Furthermore, the influence of loudness balancing was investigated for a sub-set of NH participants. No statistical comparisons were made between cohorts, and thus, groups were not matched.

Informed written consent was obtained from all participants prior to study participation and all experimental procedures were approved by the Ethics (Medical Research) Committee at Beaumont Hospital, Dublin, and the Ethical Review Board at Trinity College Dublin. Participants were asked to spend a maximum of four hours in the research facilities at Trinity College Dublin.

5.1.3 Study design

The experimental protocol consisted of active behavioural tests (≈ 45 minutes) and passive neurophysiological tests (≈ 50 minutes set-up, ≈ 80 minutes data acquisition). Behavioural tests comprised of an adaptive speech-in-noise recognition test, an AM detection threshold test and a loudness matching task. The neurophysiological paradigm consisted of an auditory oddball paradigm to elicit the MMW.

Participants were seated in a quiet room and auditory stimuli were presented monaurally for all experimental paradigms. For CI users, sounds were presented through the Otocube® (Otoconsult NV, Belgium). Stimuli were presented through the participant's speech processor with their most commonly used map. The presentation level was calibrated using the Monitor Tool of the AŞE® software (Otoconsult NV, Belgium) with the unmodulated noise stimulus to yield 60 dB SPL. The presentation level was decreased compared to Study 1 (**Chapter 3**) to avoid potential clipping effects of the stimuli in CI users, which can occur for higher presentation levels. Clipping refers to the

⁶ Two CI users (CI1 & CI2) and two NH participants (NH1 & NH2) assisted in tuning the experimental paradigms. Their data was excluded from final analysis due to parameter changes.

distortion of the signal envelope when the acoustic signal's envelope does not lie within the dynamic range of the individual CI user (Zeng *et al.*, 2013). NH participants were presented with the sounds to the left ear via headphones (Sennheiser HD 205). All stimuli were energy matched by adjusting the RMS amplitude.

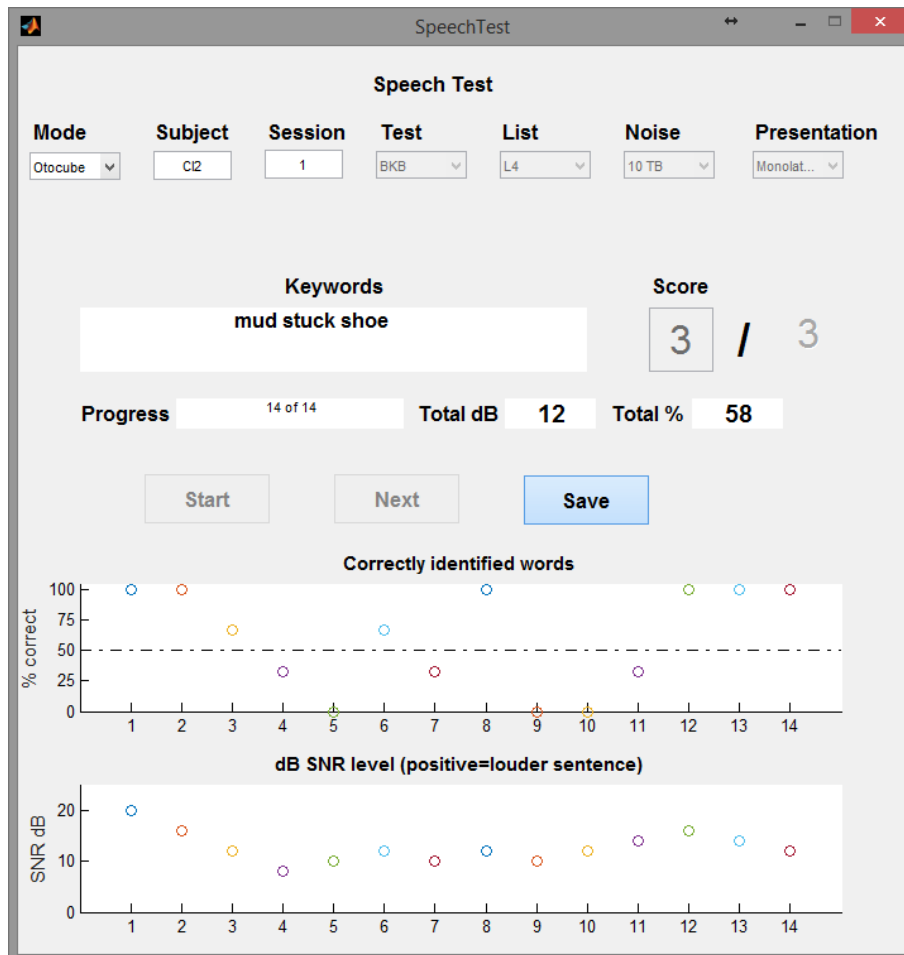


Figure 5.2: Custom-designed graphical user interface (GUI) of the speech-reception-threshold test.

The GUI tracks the performance and provides feedback to the researcher during data acquisition; the GUI is custom written in MATLAB (Release 2016a, The MathWorks, Inc., Natick, Massachusetts, United States).

Speech recognition

Speech recognition in background noise was tested with an adaptive procedure which estimated the SNR at which participants correctly identified 50% of the keywords (Schoof *et al.*, 2013; Schoof & Rosen, 2015). This provided an estimate of the SRT. The test was custom-designed and inspired by the commercially available BKB-SINTM test (Niquette *et al.*, 2003; Etymotic Research, 2005). Sentence lists were taken from the BKB sentence corpus (Bench *et al.*, 1979). Each sentence list contained 16 sentences with three

or four keywords. Only two sentences contained four keywords, which were removed, decreasing the number of sentences per list to 14. Each sentence was spoken by the same male speaker with a standard Southern British accent and the background noise consisted of random samples of ten-talker babble noise. The presentation level of the target sentence was fixed, the noise presentation level was adjusted as specified by the adaptive SNR, and thus, the overall presentation level may have varied. If at least two out of the three keywords were identified correctly, the SNR was decreased, but if only one or no keyword was correctly identified, the SNR was increased (see bottom plot in Figure 5.2).

The initial SNRs were 20 dB and 5 dB for CI users and NH participants, respectively, and the step size was 4 dB until the first reversal and 2 dB in the subsequent stimulus presentations. The SRT for each sentence list was calculated as the arithmetic mean of the SNRs at each reversal point from the second reversal onwards. The overall SRT was calculated as the average of the SRTs of the three sentence lists.

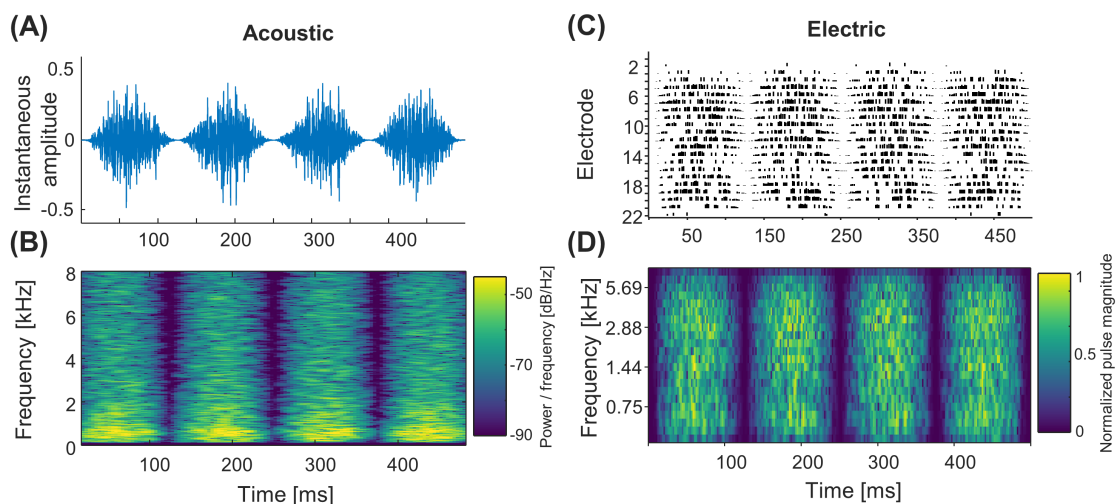


Figure 5.3: Visualization of acoustic and electrical amplitude modulated stimuli. (A) Acoustic noise stimuli with 100% AMD (left) and 50% AMD (right); (B) Spectrogram showing the spectro-temporal distribution of the acoustic stimuli with linear axes; (C) & (D) show alternative visualisations of the electrodegram, which were both created with Cochlear’s “Nucleus MATLAB® Toolbox” based on the ACE speech processing strategy. (C) shows the pulse intensities height-scaled for each electrode over time, whereas (D) shows the pulse intensity colour-coded and the y-axis represents each electrodes’ centre frequency.

Behavioural AM detection threshold

The experimental procedure for the AM detection threshold aligns with the procedure described in Section 3.1.3, but in a slightly abbreviated form as the test was terminated after eight reversals and the threshold was calculated as the geometric mean of the last six reversals. The AM stimuli were created as described in Section 3.1.2 with an AM rate of 8 Hz and 500 ms duration. The electrodegram in Figure 5.3 visualizes the

100% AM stimulus after it was processed by a Cochlear Nucleus® speech processor as simulated in the Nucleus MATLAB toolbox with the ACE strategy. An electrodiagram shows a representation of the pulse intensity per electrode over time for a given stimulus. The electrodiagram shown in Figure 5.3 is based on the n-of-m principle, which means only n of the available m active electrodes are stimulated, where m is 22 and n is nine for the given example.

Behavioural loudness balancing

The perceived loudness of modulated and unmodulated stimuli may vary between participants despite objective RMS-matching of the stimuli. To investigate the extent of potential loudness cues and to assess whether loudness cues may elicit the MMW in the auditory oddball paradigm, an additional behavioural loudness balancing test was included. The perceived difference between modulated and unmodulated stimuli would be maximal for an AMD of 100%, and therefore, loudness balancing was carried out for this AMD. Participants were presented with the unmodulated stimulus, fixed at a specified presentation level, followed by the modulated stimulus. The participants were required to adjust the loudness of the modulated stimulus with a slider in a graphical user interface (GUI, Figure 5.4) so as to match the perceived loudness of the unmodulated stimulus. The slider represented a dB scale, where the position of the slider indicated the value of the desired change value f_{dB} in dB, which in turn determined the factor by which the RMS-balanced AM-noise s_{rms} was adjusted to yield the adjusted AM-noise s_{adj} :

$$s_{adj} = s_{rms} \cdot \left(10^{\frac{f_{dB}}{20}}\right).$$

Equation 5.1

The middle of the slider in the GUI (Figure 5.4) represented the RMS-balanced condition with $f_{dB} = 0$. The 0 dB ratio (middle position of slider) represented the level at which sounds were RMS-balanced. Negative outcome-SNRs indicate that the AM stimulus had to be decreased in level and positive outcome-SNRs indicate that the AM stimulus had to be increased to satisfy the participant's perception of equal loudness. Participants were encouraged to explore the entire range available with the slider and to approach their final position from both sides. Once participants were satisfied that both stimuli were loudness matched, the SNR was saved. This procedure was repeated three times in total and the final SNR was the arithmetic mean of the three SNRs.

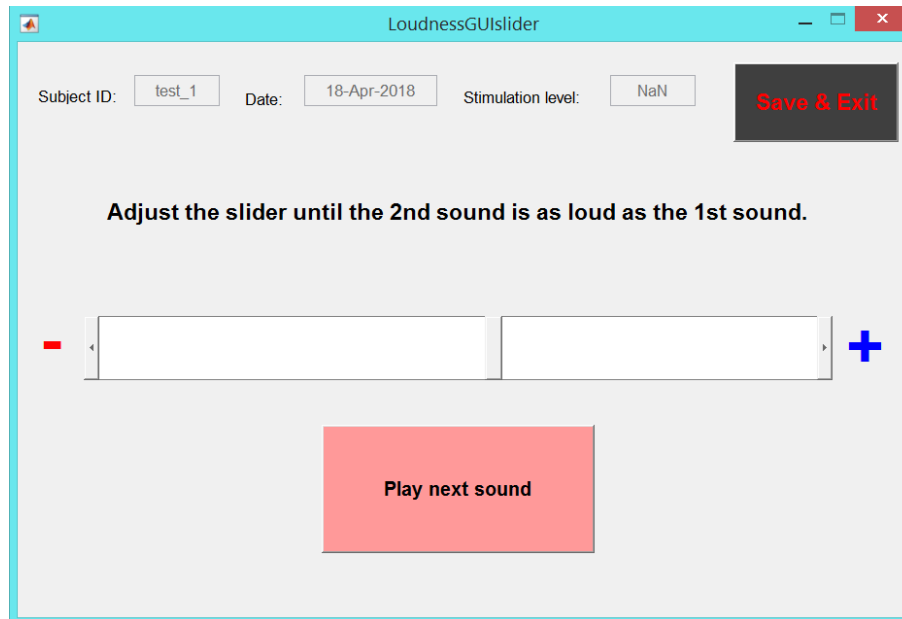


Figure 5.4: Graphical User Interface (GUI) to execute subjective loudness balancing. The unmodulated noise was presented at a fixed presentation level followed by the presentation of the amplitude modulated noise, of which the presentation level was adjusted with the slider.

Neurophysiological paradigm

To enable CI artefact rejection based on ICA, EEG data was acquired with a 128-channel Biosemi ActiveTwo System (BioSemi B. V., Amsterdam, Netherlands), in contrast to the single-channel set-up employed in the study presented in **Chapter 3**. The electrode holders above the participants' CI coils were removed from the EEG cap to avoid uncomfortable pressure. The commonly employed auditory oddball paradigm was enhanced to allow artefact reduction stemming from the electrical stimulation in CI users: the auditory oddball paradigm generally contains a number of repetitions of the standard stimulus (unmodulated stimuli) to create a strong neural representation of the standard stimulus. This was followed by the oddball part in which deviants (here AM noise) are presented with e.g. 10% probability and standards otherwise. The new paradigm introduced a block of 20 repetitions of the AM stimulus, referred to as the “AM-standard”, prior to the common oddball paradigm (see Figure 5.5). This had a two-fold implication for the study: (1) Neural standard and deviant responses were obtained from the same acoustic stimulus, and thus, deflections in the difference waveform should therefore represent change detection and not differing neural processing of acoustic features (Allen *et al.*, 2000; Picton *et al.*, 2000; Sharma *et al.*, 2004; Alexandrov *et al.*, 2011; Robson *et al.*, 2014); (2) The presentation of the AM stimulus at the beginning of

each block resulted in neurophysiological data with the characteristics of a standard response, but with the electrical artefact of the deviant. In theory, subtraction of the AM-standard from the deviant responses should provide the MMW devoid of electrical CI artefact. The additional presentation of AM-standards at the start of each block added acquisition time to an already lengthy paradigm, but the potential benefit of objective CI artefact reduction outweighed this challenge.

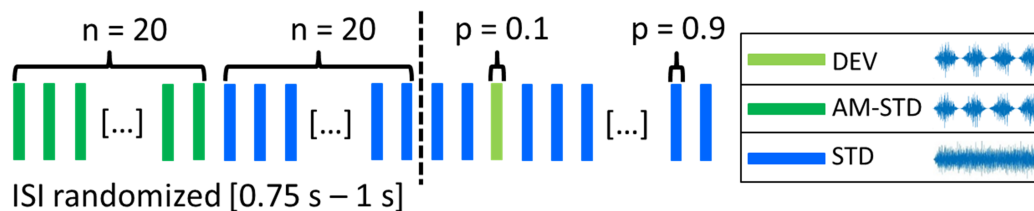


Figure 5.5: Stimulus overview of the new mismatch waveform paradigm.

Each condition was split into four blocks with 20 initial presentations of the amplitude modulated (AM) deviant (DEV) noise as a “standard”, which is labelled the AM-standard (AM-STD) stimulus. This was followed by 20 repetitions of the unmodulated noise standard stimulus to prime the brain and then the AM deviant was presented with a probability of 10%, totalling 14 deviant presentations per block.

Stimulus conditions were in line with those described in **Chapter 3**, namely four deviant conditions with varying AMDs of 100%, 75%, 50% and 25% (0 dB, 2.5 dB, 6 dB, and 12 dB, respectively) and standard stimuli were unmodulated (0% AMD) speech-shaped noise. For each condition 68 deviant stimuli, and 760 standard stimuli (680 in oddball segments, 80 in initial “priming” segments) were presented, divided into four blocks. Stimuli had a duration of 500 ms and the ISI was randomised between 0.75 s and 1 s. This jitter resulted in noticeable differences in the ISI. The ISI was jittered for all stimulus types, and thus, not affecting the calculation of the MMW. Quantitatively, the jitter was less than in previous studies by Ortmann *et al.* (2013) and Ortmann *et al.* (2017) who presented stimuli with ISIs that were jittered by ± 200 ms.

For two NH participants, an additional subjectively loudness balanced condition was added with 100% AMD, totalling five deviant conditions for the EEG paradigm, and for a further two NH participants, the 25% AMD condition was replaced with the subjectively loudness balanced version of the 100% AMD condition. This provided four datasets to evaluate the influence of any remaining loudness cues on the MMW by comparing MMWs elicited with objectively and subjectively loudness matched stimulus pairs.

5.1.4 EEG post-processing CI users

Two alternative artefact reduction processing pipelines were employed. Both are outlined below. Figure 5.6 provides an overview of the processing steps. The first pipeline relied on ICA for artefact reduction purposes, which made it computationally costly, and therefore, not very time-efficient. Furthermore, ICs associated with artefacts were rejected after visual inspection which introduced a subjective bias, and rejection of components may remove neural activity related to the stimulus presentation. The second pipeline was subtraction-based and relied on artefact reduction by means of subtraction of standard and deviant CAEPs, and thus, required the newly introduced AM-standard (Figure 5.5), which had the same artefact characteristics as the standard stimulus.

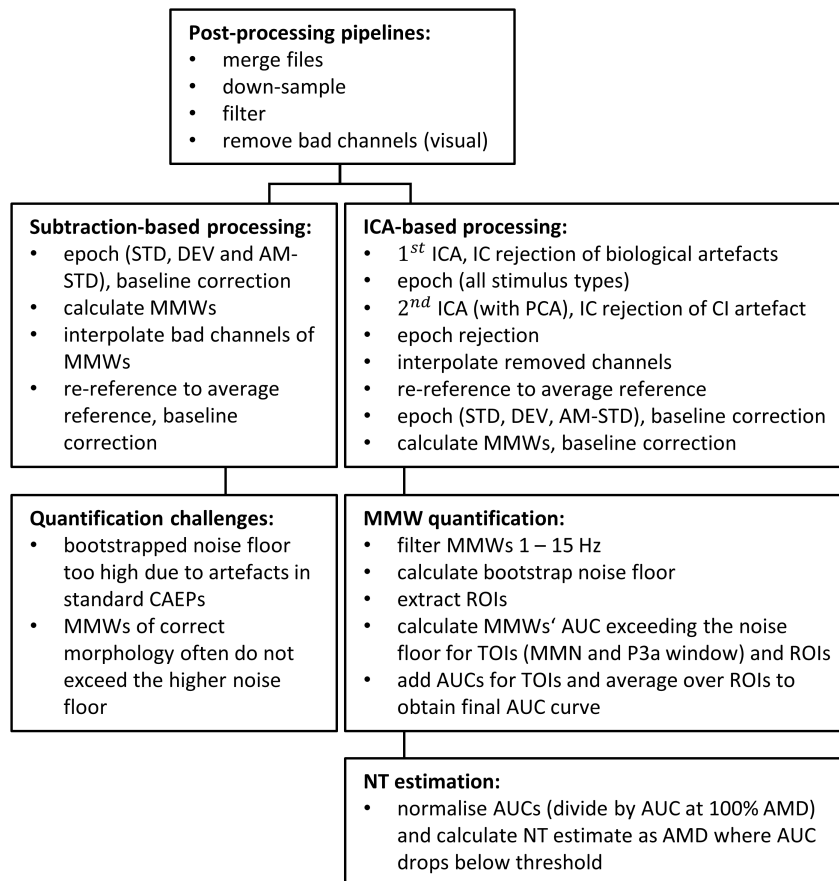


Figure 5.6: Data processing pipelines for Electroencephalography (EEG) data recorded from the cochlear implant (CI) user cohort.

Overview of post-processing pipelines for EEG data with two different artefact reduction approaches (subtraction-based and ICA-based). Quantification of mismatch waveform (MMW) data was negatively impacted by remaining CI artefacts in the standard cortical auditory evoked potentials (CAEPs) for the subtraction-based artefact reduction, which resulted in high bootstrapped noise floors. Therefore, MMW quantification and neural threshold estimation were reported based on MMWs from the ICA-based processing pipeline. Abbreviations and acronyms: STD – Standard, DEV – Deviant, AM-STD – Amplitude-modulated standard, ICA – Independent component analysis, PCA – Principal component analysis, IC – Independent component, ROI – Region of interest, AUC – Area-under-the-curve, TOI – Time window of interest, AMD – Amplitude modulation depth.

ICA-based processing pipeline

Post-processing of EEG data was carried out with custom-written scripts based on the MATLAB EEGLAB toolbox (Delorme & Makeig, 2004). The order of processing steps was inspired by procedures reported in (Viola *et al.*, 2012) and (Sandmann *et al.*, 2014). Continuous EEG data files were merged (pop_mergeset.m) for all conditions and trials, to create one combined EEG data set for each participant to decrease processing time. Processing time was further reduced by down-sampling data to 256 Hz (pop_resample.m). Data was bandpass filtered with a windowed sinc finite impulse response (FIR) filter with cut-off frequencies of 1 Hz to 30 Hz (pop_firws.m). Channels with detached electrodes due to the position of the CI coil as well as channels with signals exceeding the activity probability limit of five standard deviations were rejected (pop_rejchan.m). Additional ‘bad channel’ rejection was implemented based on visual inspection. ICA was carried out on the continuous data (pop_runica.m) based on the Infomax algorithm. ICs associated with eye-blinks, horizontal eye movement and heart beat were rejected after visual inspection of topographic plots (pop_selectcomps.m) and component activity (pop_eegplot.m). Data was epoched to a time window of -500 ms pre-stimulus and 1000 ms post-stimulus presentation. Prior removal of ICs related to biological artefacts reduced the dimensionality of the data. In order to run ICA a second time on the epoched data for CI artefact rejection purposes, as was suggested by Sandmann *et al.* (2014) and Schierholz *et al.* (2017), the dimensionality had to be reduced to the number of remaining components by implementing principal component analysis (PCA)⁷. Component activity was again visually assessed with topographic plots and average component activity (pop_plotdata.m). ICs were removed (pop_subcomp.m) if they resembled typical CI artefact activity, such as (1) peaks at the time of sound onset and offset, (2) topographical plots that presented a centroid of activity at the site of the implant, or (3) continuous activity for the duration of the stimulus (Gilley *et al.*, 2006). The next processing step further assessed epoch quality, and ‘bad epochs’ were determined based on a thresholding approach (pop_eegthresh.m), in which epochs were removed if activity exceeded $\pm 100 \mu\text{V}$, and based on a joint-probability approach (pop_jointprob.m) with a five standard deviations criterion. Finally, removed channels were interpolated (pop_interp.m) and data was re-referenced to the average reference of

⁷ The second implementation of ICA with reduced dimensionality was achieved with the command ‘EEG = pop_runica(EEG, 'icatype', 'runica', 'pca', number_of_components)’ from the MATLAB EEGLAB toolbox.

all electrode channels (pop_reref.m). From the cleaned data the standard, deviant, and AM-standard epochs were extracted for time windows of -200 ms to 700 ms post-stimulus presentation followed by baseline correction. CAEPs were generated by averaging across all epochs for each stimulus type and condition. The ‘classic’ MMW was generated by subtracting the standard CAEP from the deviant CAEP and is labelled MMW1 in the following, whereas the “new” MMW was calculated as the difference waveform between AM-standard CAEP and deviant CAEP and is labelled MMW2 in the following.

Subtraction-based processing pipeline

Similar to the ICA-based processing pipeline, data was merged across conditions and blocks, down sampled to 512 Hz, and filtered between 1 and 30 Hz. Missing channels due to the CI coil placement and bad channels as determined by visual inspection were removed. Continuous data was epoched separately for each condition and stimulus type, and data was corrected for a pre-stimulus baseline of -100 ms to 0 ms. CAEPs were calculated by averaging across epochs for each stimulus type. Finally, MMWs were calculated by subtracting the average CAEPs. Previously removed channels were interpolated. MMWs were subsequently re-referenced to average reference followed by baseline correction.

5.1.5 EEG post-processing NH cohort

EEG data from the NH cohort was processed with a semi-automated ICA-based processing pipeline, which is summarised in the following. EEG files were merged for all blocks and conditions and down-sampled to 256 Hz to speed up ICA. The continuous merged data was bandpass filtered with a windowed sinc FIR-filter (cutoff: 1 – 30 Hz, Hann window). Bad channels were determined and rejected based on visual inspection, and based on a joint probability criterion (pop_rejchan.m) with a threshold of three standard deviations. ICA was carried out on the continuous data of the remaining electrodes. Components associated with eye movement, eye blinks and generic discontinuities were removed with the ADJUST algorithm (Mognon *et al.*, 2011), which was introduced in **Chapter 4**. A shortcoming of this automated IC removal is the lack of ECG identification. Data was epoched (-200 ms until 700 ms) according to stimulus type and deviant condition. For each stimulus type and deviant condition, bad epochs were determined based on a conservative thresholding approach (pop_eegthresh.m) with

thresholds of $\pm 100 \mu\text{V}$ and the joint probability algorithm (`pop_jointprob.m`) with a threshold criterion of five standard deviations. This very conservative approach was chosen to preserve as many epochs as possible, due to the already low number of deviant repetitions of 68. Following epoch rejection, previously removed channels were interpolated (`pop_interp.m`). Epochs were re-referenced to average reference. Baseline correction was applied and CAEPs were calculated by averaging across epochs. Finally, the difference waveforms MMW1 and MMW2 were calculated.

5.1.6 Quantification of the MMW

The correlation analysis between behavioural and neural AM detection thresholds required a quantification of neural change detection responses which also takes into account the influence of noise inherent in CAEP recordings. In theory, the subtraction of the standard and deviant CAEPs should result in a flat difference wave if no acoustic change was detected. However, in practice CAEP recordings are very susceptible to noise, and random fluctuations in the CAEPs result in deviations of the difference waveform. Therefore, it is necessary to quantify the noise as well as the change related neural response. Based on the quantified MMW data, an objective procedure was developed to estimate neural thresholds from the MMWs at varying AMDs.

Noise floor calculation

Inherent noise was quantified for each participant by calculating a noise floor with a bootstrap procedure (Lopez Valdes *et al.*, 2014). Standard CAEPs were randomly divided into bootstrap-standards (90%) and bootstrap-deviants (10%). Following this step, their respective difference waves were calculated and this procedure was repeated 100 times. The noise floor was determined as ± 1 standard deviation of these difference waves. Due to the required artefact-free standard CAEPs for noise floor calculation, this quantification approach was not employed for the subtraction-based processing pipeline. For this reason, quantification of MMWs and consequently NT estimation and correlation analysis with BTs was only carried out for the ICA-based processing pipeline.

Area-under-the-curve calculation

The objective quantification of MMWs required minimisation of any noise influence, and thus, MMWs were filtered from 1 – 15 Hz to remove any higher-frequency

noise. The MMW was quantified as the AUC exceeding the noise floor in the time windows of interest and for two electrode ROIs. The AUC was calculated for a fronto-central cluster of electrodes in which the change-related negativity of the MMN is commonly observed to be maximal (Sams *et al.*, 1985), as well as for an occipital-parietal cluster of electrodes, in which the polarities of the MMN and P3a are commonly reversed (Trainor *et al.*, 2014). The MMN was assessed for a time range of 190 ms to 300 ms and the P3a component was assessed for a time window of 300 ms to 410 ms for the 100% AMD condition. For each 25%-step decrement of the AMD, the time windows were shifted by +5 ms to allow for latency increases of the responses with increasing task difficulty. AUC values were added for the two time regions of interest and averaged over the two ROIs.

Neural threshold estimation

Despite having employed the bootstrapped noise floor procedure, some difference waves may randomly exceed the noise floor. Thus, the AMD at which an individual's AUC values reach zero would not provide a reliable NT estimate. Alternatively, in order to disregard small AUCs arising from random fluctuations, a NT of AM detection can be estimated as the interpolated AMD at which the AUC first drops below a pre-determined threshold level as indicated by the intersection value. Sets of NTs were estimated from normalised AUCs, where AUCs were normalised to individual AUC values of the 100% AMD condition, and for a range of intersection values to assess the dependence of findings on the specified intersection value. These NTs were then correlated with BTs to investigate their linear relationship based on Pearson's correlation coefficient.

5.2 Results

5.2.1 Behavioural results

Behavioural results comprising of SRTs, AM detection thresholds, and loudness matching results are presented in Figure 5.7 and results are described in the following paragraphs. Descriptive statistics include the median and the standard deviation of group data. Additionally, Figure 5.7 provides the arithmetic mean of the group data indicated by the black horizontal lines. Note that the arithmetic mean is biased by outlier data points

and the median provides a more accurate representation especially in the case of skewed distributions.

Speech reception thresholds

SRTs showed an even distribution between 4 dB and 22 dB for the CI user cohort (Figure 5.7, left) with a median SRT of 10.0 dB (standard deviation = ± 5.7 dB). All NH participants outperformed the CI users, and variation in performance was smaller with a standard deviation of ± 1.2 dB and a median score of -1.4 dB.

AM detection thresholds

Median behavioural thresholds lay at -17.8 dB (standard deviation = ± 5.3 dB) for CI users and -22.1 dB (standard deviation = ± 2.0 dB) for NH participants. Five CI users had behavioural AM detection thresholds in line with the poorer performing NH peers, but others showed poorer performance indicated by the higher thresholds (Figure 5.7, middle). One CI user showed no AM detection abilities. The task was repeatedly explained and the participant seemingly understood the task. This participant was excluded from further analysis that included behavioural AM detection, as it is assumed that the participant used loudness cues arising from the level roving, despite clear instructions to ignore any loudness cues.

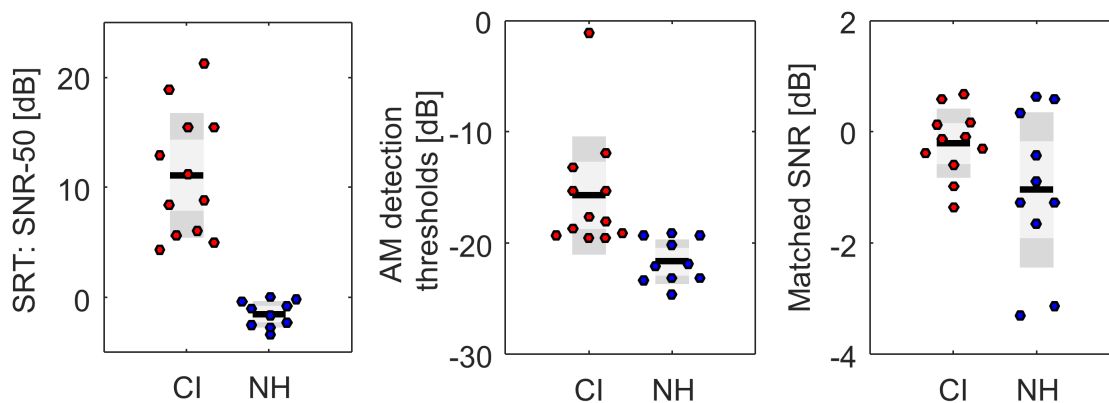


Figure 5.7: Behavioural results for cochlear implant (CI) users and normal-hearing (NH) participants.

Individual results and group statistics are shown for speech reception thresholds (SRTs, left), amplitude modulation (AM) detection thresholds (middle) and loudness matching results (right). SRTs vary greatly between cohorts, whereas AM detection thresholds and loudness matching results show smaller differences between cohorts. Descriptive statistics include the arithmetic means (black line) and standard deviations (shaded grey boxes). Note that loudness matching data of participant CI3 is missing due to time constraints. Abbreviations and acronyms: SNR – signal-to-noise ratio.

Loudness matching results

Loudness matching results were comparable between the two cohorts except for two outliers in the NH data (Figure 5.7, right). The median SRTs were calculated to be -0.1 dB (standard deviation = ± 0.6 dB) and -1.3 dB (standard deviation = ± 1.5 dB) for CI users and NH participants, respectively. Two NH participants matched the unmodulated stimulus with the AM noise stimulus for an SNR around -3 dB. This means the objectively energy-matched AM noise was decreased in level by 3 dB to match the perceived level of the unmodulated noise.

Correlations between BTs and SRTs

The relationship between behavioural AM detection thresholds and speech-in-noise recognition as measured with SRTs was assessed by means of Pearson's correlation coefficient r_p and Spearman's linear rank correlation coefficient r_s . SRTs showed no significant correlations with BTs of AM detection for neither the CI cohort, nor the NH cohort independent of the correlation measure (Figure 5.8).

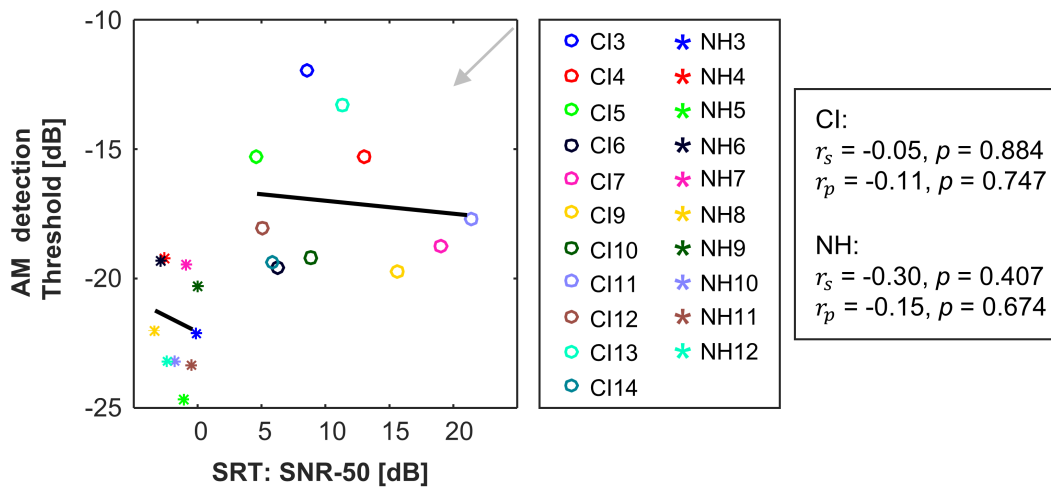


Figure 5.8: Relationship between speech reception thresholds (SRTs) and behavioural thresholds (BTs) of amplitude modulation (AM) detection.

Correlations results for Pearson's linear correlation coefficient r_p and Spearman's rank correlation coefficient r_s are shown on the right. The grey arrow indicates the combined direction of good performance for x - and y -axis. Note: CI1, CI2, NH1 and NH2 participated in a pilot study, but were not included in this final study due to experimental changes.

5.2.2 EEG acquired from CI cohort

CI artefact in the subtraction-based processing pipeline

CI artefacts varied greatly between participants. Figure 5.9 illustrates two examples of artefacts for users of a Cochlear device (CI13) and an Advanced Bionics device (CI17): Data from participant CI13 (Figure 5.9, left) shows CI artefacts that are

quite similar for the two stimulus types (unmodulated and AM noise), except at the sound onset. Therefore, subtraction of standard and deviant CAEPs to calculate MMW1 reduced the artefact considerably except at the sound onset. The calculation of MMW2 provided better artefact reduction at sound onset due to greater similarity of the artefact in deviant and AM-standard CAEPs.

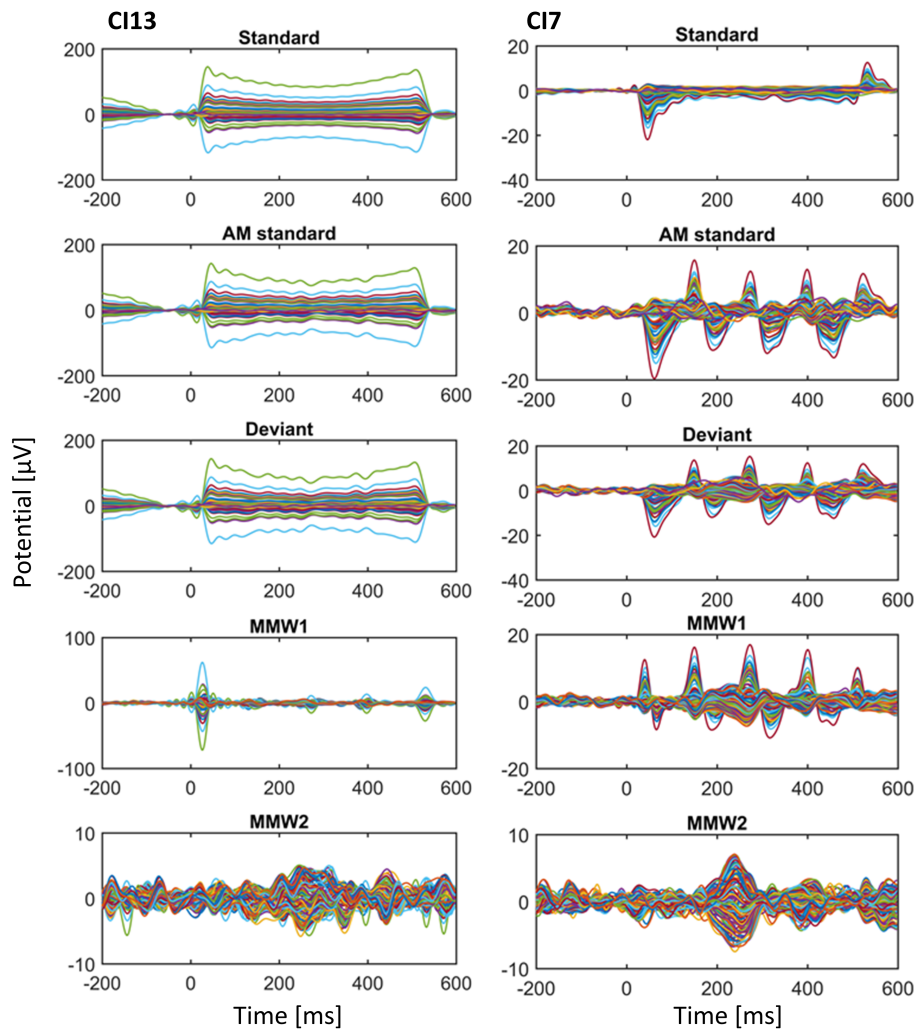


Figure 5.9: Examples of cortical auditory evoked potentials (CAEPs) and mismatch waveforms (MMWs) after subtraction-based artefact reduction.

Individual examples are depicted for participants CI13 (left, Cochlear device) and CI7 (right, Advanced Bionics device). The standard, deviant and AM-standard CAEPs are depicted before and the mismatch waveforms (MMW) after the removal of bad channels and epochs. MMW data is average referenced.

Data from participant CI7 showed a different artefact type, clearly demonstrating the AM of the modulated noise stimuli. Due to the difference between the artefacts of the two physical stimulus types, subtraction of standard and deviant CAEPs did not reduce the artefact sufficiently (Figure 5.9, right). However, subtraction of the deviant and AM-standard CAEPs generated successful CI artefact reduction for MMW2s (Figure 5.9, bottom right).

CI artefact in the ICA-based processing pipeline

Many of the ICs calculated by means of ICA were dominated by CI artefact. Every participant showed ICs where the spatial distribution and temporal activation resembled the typical CI artefact activation patterns as pictured in the two examples in Figure 5.10. However, not all ICs that were affected by CI artefact were as easily identified. Some showed a peak at sound onset or offset, but the spatial distribution did not suggest a main source at the site of the implant. Particularly for participants for whom the artefact was widespread across a number of electrodes that were not close to the site of the implant, the spatial distribution of the ICs was not a reliable indicator. Each IC was visually investigated and a judgment call had to be made whether it should be removed or kept for further analysis, introducing a subjective bias to the procedure.

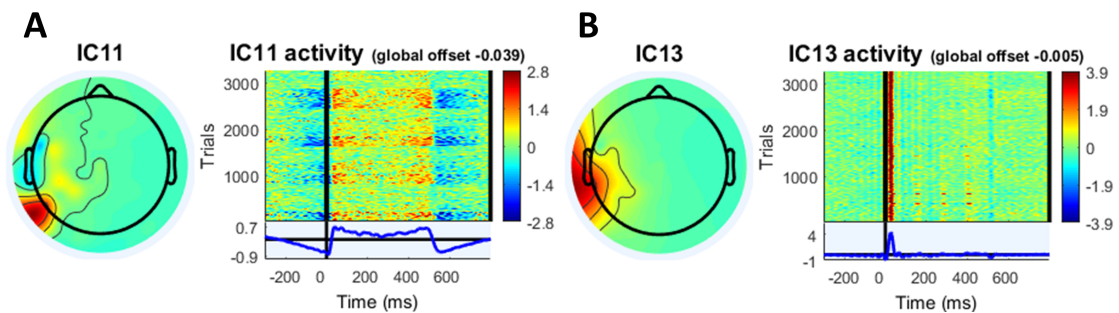


Figure 5.10: Examples of independent components (ICs) associated with cochlear implant (CI) artefact.

(A) and (B) show examples of two typical ICs associated with the electrical artefact from CI stimulation. For each IC, plots include the spatial distribution of activity across the scalp (left), trial-by-trial activity (top right), and the average activation across time and trials (bottom right).

Determination of the electrode clusters in the regions of interest

The choice of the two electrode ROIs was based on literature, and the electrodes within each cluster were determined with a data-driven approach. Figure 5.11 shows the difference waveforms for specified electrodes according to the 10-20-system (note: Modified Combinatorial Nomenclature). In Figure 5.11, the individual data as indicated by grey lines represents single-channel CAEPs, and therefore, data looks noisier than for electrode cluster averages. In line with the literature, MMWs were found to be maximal for the area around Fz and Cz, and reversed in polarity for the temporal-occipital electrodes (Figure 5.11). Figure 5.12A shows the chosen individual electrodes contained in each ROI. Figure 5.12B depicts the individual and grand average MMW1s for the two ROIs for the maximum AMD of 100%.

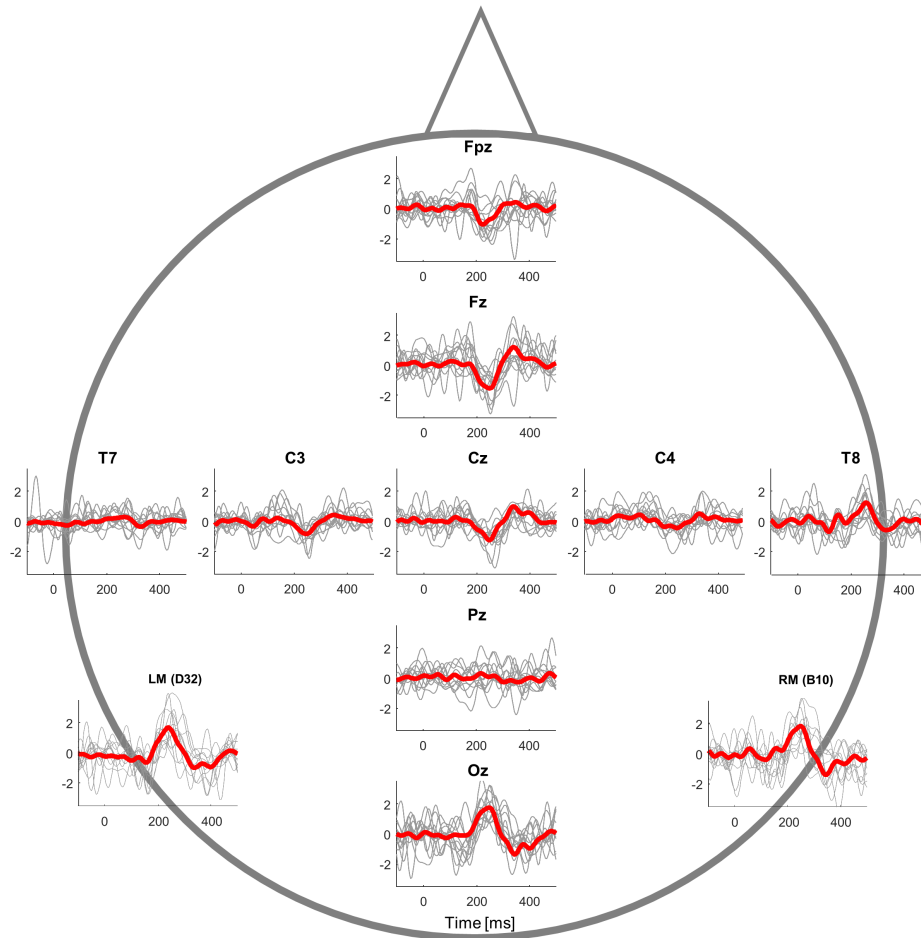


Figure 5.11: Topographical overview of individual and grand average mismatch waveforms (MMW) for the CI group.

The depicted MMWs were derived from the deviant condition with 100% amplitude modulation depth. Individual MMWs are depicted as thin grey lines and the grand average MMWs are overlaid in bold. Data is filtered from 1 – 30 Hz.

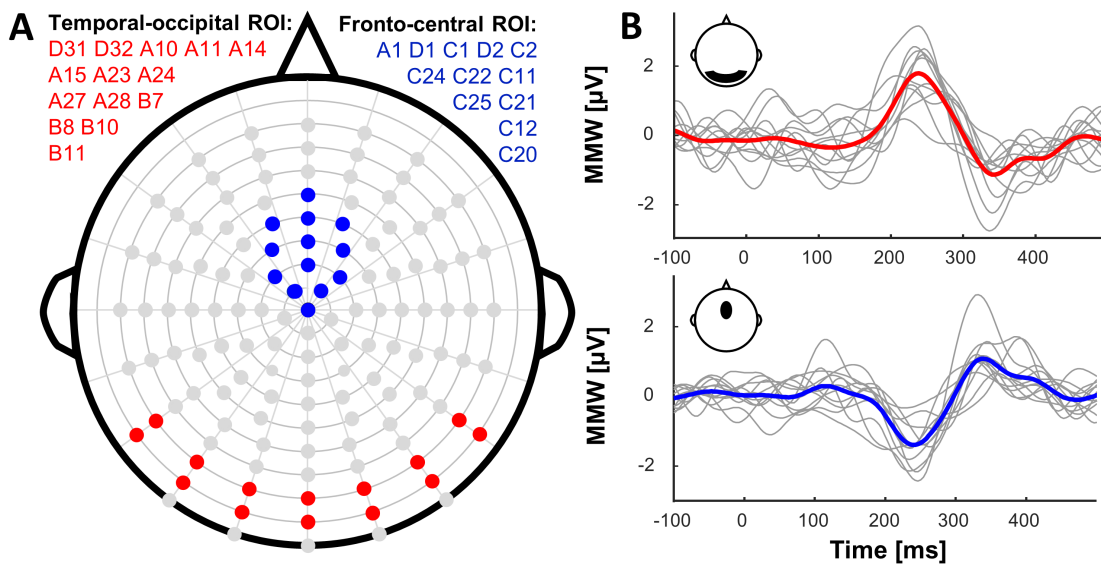


Figure 5.12: Overview of the electrode clusters in the regions of interest (ROI) and their mismatch waveforms (MMWs).

(A) Overview of the electrode clusters in the two ROIs. (B) Individual MMWs (grey) and group mean MMWs (bold) for the two ROIs for an amplitude modulation depth of 100%.

Group mean MMWs with subtraction-based processing

The subtraction-based artefact reduction was investigated as a potential time-efficient alternative to the common ICA-based processing pipeline for CI artefact reduction. Figure 5.13 shows the effect of introducing the AM-standard (MMW2) on artefact reduction for the subtraction-based artefact rejection procedure: The “classical” MMW1 showed remaining effects from differences in CI artefact between standard and deviant CAEPs as indicated by the arrows in Figure 5.13, whereas the MMW2 showed no visible signs of CI artefacts in comparison. In some individual data sets, the CI artefact was very pronounced in the MMW1, particularly before averaging across the electrode clusters, whereas in other participants it was not visible. Also depicted in Figure 5.13 are the MMW2s after secondary filtering. This more aggressively filtered data was quantified on an individual level, but due to comparatively poorer data quality (in comparison to data processed with ICA) neural threshold estimation was confounded by random fluctuations. It was decided to focus quantification and correlation analysis on the data with the highest quality, which was the data processed with ICA due to more extensive artefact rejection. The following section provides quantitative analysis based on this processed data.

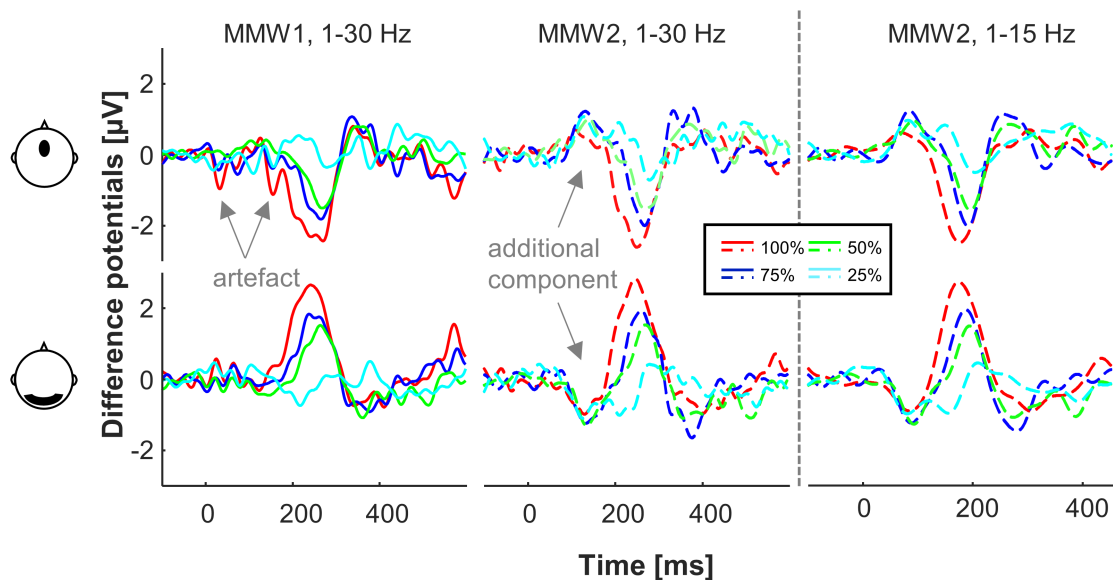


Figure 5.13: Group mean difference waveforms obtained with the subtraction-based processing pipeline.

Mismatch waveforms (MMWs) are shown for MMW1 (left) and MMW2 (right), for the fronto-central (top) and occipital-temporal (bottom) electrode clusters and for the four amplitude modulation depths. Arrows indicate the remaining artefact in the MMW1 and an unusual component preceding the MMN before 200 ms in the MMW2.

Group mean MMWs with ICA-based processing

No typical CI artefacts remained visible after artefact rejection with ICA. MMWs demonstrated clearly distinguishable MMN and P3a components for both ROIs and all AMD conditions except the 25% AMD (Figure 5.14). Visual comparison of MMW1s and MMW2s for each AMD, as depicted in Figure 5.14, illustrates their similarity in morphology with the exception of a time window preceding the MMN component around 150 ms. The MMW2 showed an additional positive deflection in fronto-central electrodes. This difference between MMW1 and MMW2 was also reflected in the topographical plots depicted in Figure 5.16 for the time stamp of 170 ms.

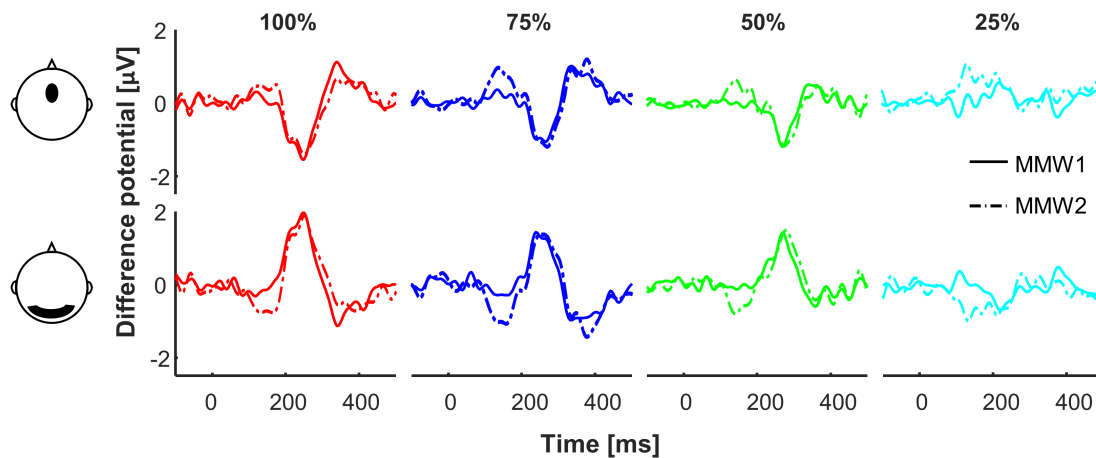


Figure 5.14: Comparison of mismatch waveforms (MMWs) for MMW1s and MMW2s for each amplitude modulation depth (AMD).

MMWs were averaged across all 12 cochlear implant users. Data was plotted together for MMW1s and MMW2s, showing a consistent difference across AMDs for the component preceding the MMN (≈ 150 ms). The composition of the electrode clusters is shown in Figure 5.12. Data was processed with the ICA-based processing pipeline and filtered from 1 – 30 Hz.

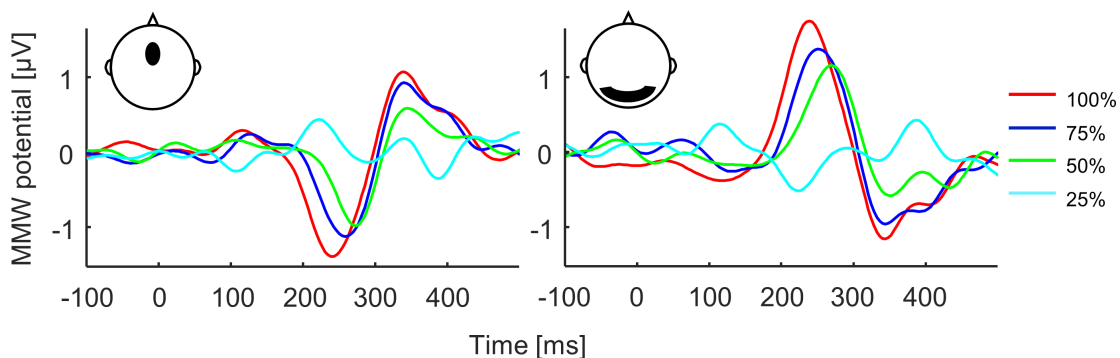


Figure 5.15: Comparison of mismatch waveforms (MMWs) across amplitude modulation depths (AMDs).

MMW1s are shown for the fronto-central (left) and occipital-temporal (right) electrode clusters for differing AMDs from 100% to 25%. Data was filtered from 1 – 15 Hz (secondary filtering) and averaged across all 12 cochlear implant users. The underlying individual data sets of this group mean data were used for quantification analysis for which results are reported in Section 5.2.3.

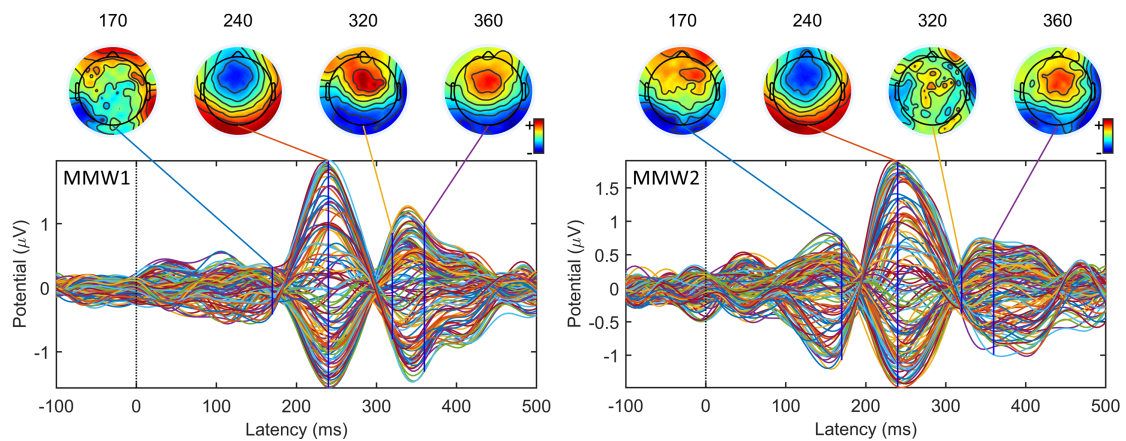


Figure 5.16: Butterfly plots and topographical plots of the mismatch waveforms (MMWs).

Plots show the MMW1 (left) and MMW2 (right) elicited in the 100% amplitude modulation depth condition. Pictured MMWs were calculated with the ICA-based processing pipeline and averaged over all 12 cochlear implant users. Data was filtered from between 1 – 15 Hz.

For quantification analysis of individual data sets, a secondary more aggressive bandpass filter was applied (1 – 15 Hz) to reduce the influence of higher-frequency noise. The influence of secondary filtering on group mean MMW1s can be seen by comparing Figure 5.14 to Figure 5.15. Figure 5.15 provides the direct comparison of MMW1s across AMDs for the two ROIs. Visual assessment of the MMW1s suggested that MMW amplitudes decreased and MMW latencies increased with decreasing AMDs (Figure 5.15), but no statistical analysis was carried out.

5.2.3 Quantification of individual EEG data from CI users

For quantification of MMW data, the individual MMW1s processed with the ICA-based pipeline and secondary filtering were chosen. This data had the highest data quality according to visual assessment, as a result of the more comprehensive artefact rejection combined with a higher number of available standard epochs in the MMW1 calculation compared to MMW2 calculation. Individual MMW1 data showed the expected morphology with the MMN and P3a components, which was crucial for meaningful objective MMW quantification. Figure 5.17 shows an example dataset from participant CI8, for whom the MMN and P3a components greatly exceeded the bootstrapped noise floor for the 100%, 75% and 50% AMD conditions. For the 25% AMD condition, the MMN and P3a components barely exceeded the noise floor in the time windows of interest, resulting in AUC values close to zero.

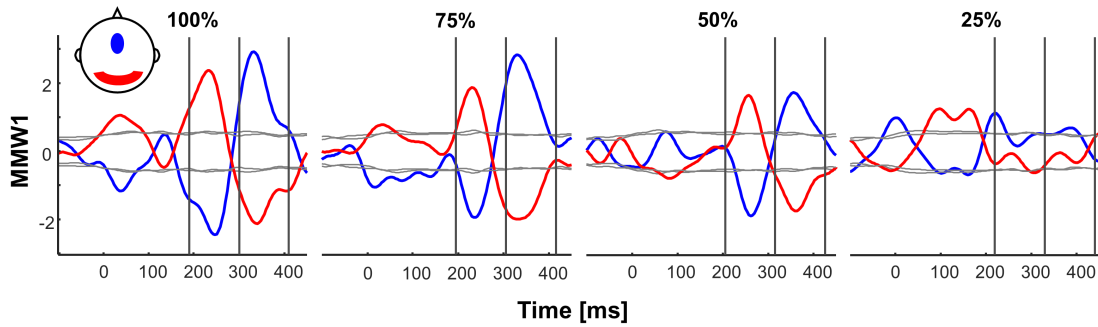


Figure 5.17: Example mismatch waveforms (MMWs) for individual participant CI8. Individual mismatch waveforms (MMWs) are shown for both regions of interest (ROI) for all four amplitude modulation depths (AMDs) from 100% to 25%. The individual bootstrapped noise floors are indicated by the horizontal grey lines. The shifting time windows of interest for the calculation of the area-under-the-curve (AUC) are indicated by the vertical grey lines.

Overall, participants' AUC values converged toward zero with decreasing AMD (Figure 5.18). Normalisation of AUCs resulted in more uniform AUC curves (with the exception of participant CI10), which benefited objective NT estimation. For participant CI10 the MMW for 100% AMD barely exceeded the noise floor, but the 75% MMW greatly exceeded the noise floor, resulting in an inflated normalised AUC score for the 75% AMD. However, this had only very limited influence on the final estimate of the NT.

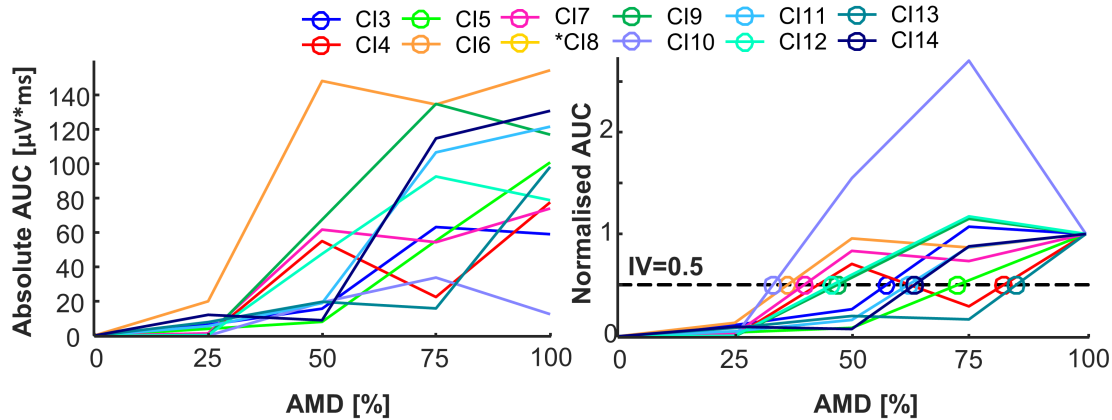


Figure 5.18: Neural threshold estimates from the individual area-under-the-curve (AUC) values. Absolute (left) and normalised (right) AUC values for individual participants at varying amplitude modulation depths (AMDs) between 25% and 100%. The right plot shows examples of neural threshold estimates for an example intersection value (IV) of 0.5. *Participant CI8 was removed due to non-performance in the behavioural AM detection task.

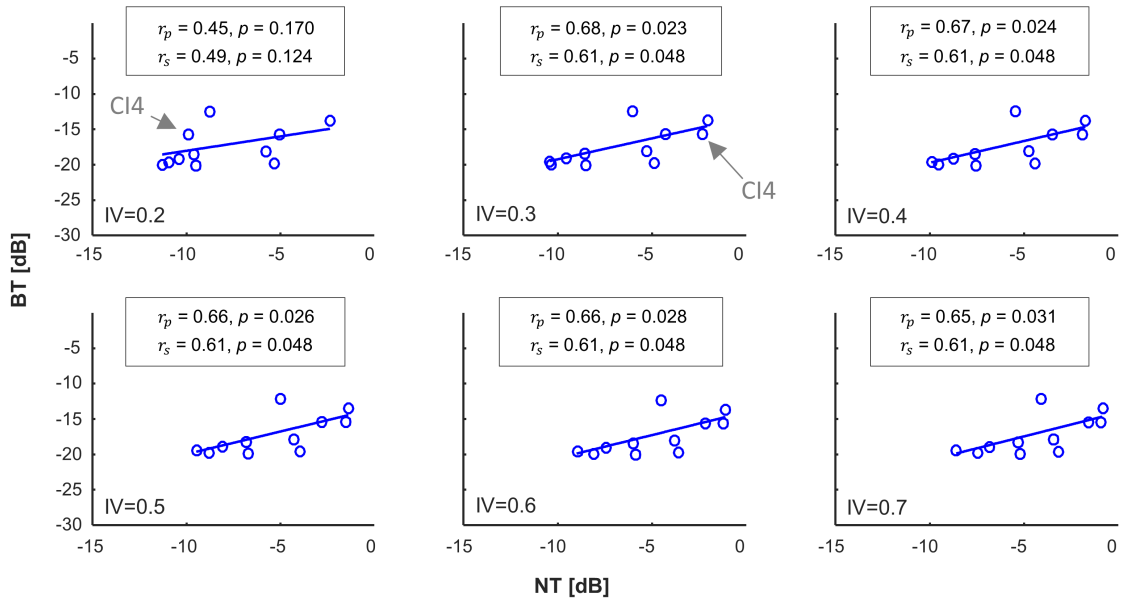


Figure 5.19: Overview of correlation results between behavioural thresholds (BTs) and neural thresholds (NTs) of amplitude modulation (AM) detection.

Correlation analysis was carried out for a range of intersection values (IVs) based on the normalised area-under-the-curve (AUC) values with Pearson's linear correlation coefficient r_p and Spearman's rank correlation coefficient r_s . AUCs were normalised to the individuals' AUC at 100% AM depth.

5.2.4 Correlations between BTs and NTs in CI users

Correlation analysis based on NTs obtained from normalised AUCs provided very uniform correlation coefficients r_p between 0.65 and 0.68 ($p \leq 0.031$) and r_s of 0.61 ($p = 0.048$), if the IV was set at 0.3 or above (Figure 5.19). The correlation coefficient for the IV of 0.2 was negatively impacted by the NT estimate of participant 'CI4'.

5.2.5 EEG acquired from NH cohort

In the original study design for the NH cohort, the 25% AMD condition was replaced by a subjectively loudness balanced 100% AMD condition, as it was believed that the MMW would disappear for an AMD of 50% according to findings from the study presented in **Chapter 3**. However, after having acquired data for participants NH3 and NH4, it was evident that based on the new experimental parameters and with the multi-channel EEG, MMWs were measurable for the 50% AMD. Under these circumstances it was decided to include a 25% AMD condition for further participants in place of the loudness balanced condition. Table 5.2 provides an overview of the data sets for each condition and individual.

Table 5.2: Overview of the employed paradigms in the individual normal-hearing participants.

The last column indicates how many participants' data sets n were available for each condition. Participants NH1 and NH2 only participated in a pilot study and were not included in the analysis of this study due to experimental changes. Abbreviations and acronyms: AMD – Amplitude modulation depth, NH – Normal-hearing, LB – Loudness balanced.

AMD	NH3	NH4	NH5	NH6	NH7	NH8	NH9	NH10	NH11	NH12	n
100%	X	X	X	X	X	X	X	X	X	X	12
75%	X	X	X	X	X	X	X	X	X	X	12
50%	X	X	X	X	X	X	X	X	X	X	12
25%	-	-	X	X	X	X	X	X	X	X	8
100% LB	X	X	-	-	-	-	-	X	X	-	6

EEG data from the NH cohort showed MMW amplitudes that decreased with decreasing AMDs (Figure 5.20). The MMN component was distinctly visible for AMDs as low as 50% (Figure 5.20). The P3a component was clearly distinguishable for the 100% and 75% AMD condition. For the 50% AMD, only a small and delayed P3a component was observed. For an AMD of 25% no MMN or P3a could be observed in either of the two ROIs (Figure 5.20).

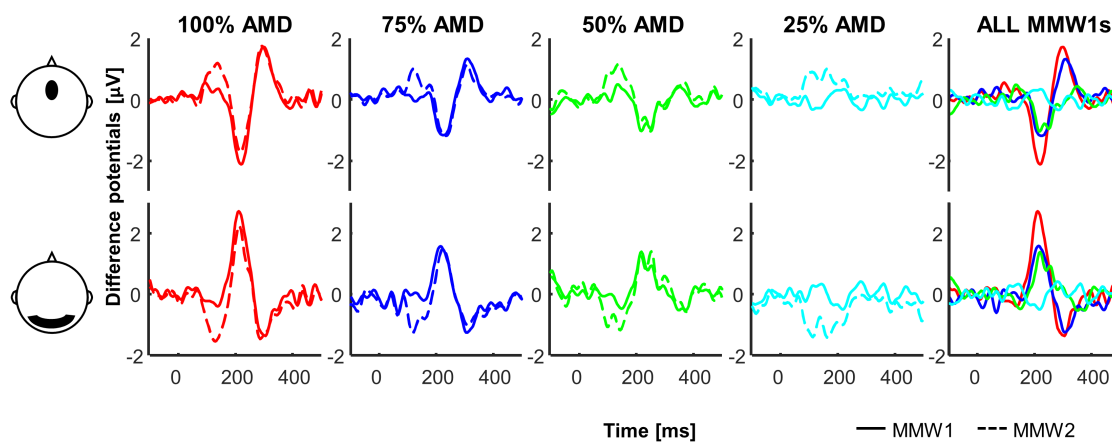


Figure 5.20: Overview of difference waves from the normal-hearing cohort across the four tested amplitude modulation depths.

Grand average data ($n = 8$, NH5 – NH12) is shown for the fronto-central and occipital-parietal region of interest. Difference waveforms show the mismatch waveforms (MMW) MMW1 and MMW2. Data was filtered from 1 – 30 Hz. Note: For participants NH3 & NH4 the 25% AMD condition was replaced with a loudness balanced condition, and therefore, data for these participants was excluded from the grand average in this figure.

The AUC values for MMW1s were calculated in line with the procedures outlined for the CI user cohort. The AUC values depicted in Figure 5.21 were of comparable magnitude to the CI user cohort (Figure 5.18). The exception was participant NH9, who showed very large MMW1s. Overall, AUCs decreased with the AMDs. In the study

outlined in **Chapter 3**, AUCs were found to increase for the 25% AMD for numerous participants due to random fluctuations. Thus, morphology weighting was implemented to reduce the influence of MMWs that did not resemble the expected waveform. In this study, random fluctuations posed less of an issue as reflected by the decreasing AUCs without morphology weighting. The increase of the number of deviant repetitions combined with the measurement of multi-channel EEG, and thus, the possibility to average across multiple channels in this study, had the benefit of decreasing the influence of random fluctuations on the AUC values.

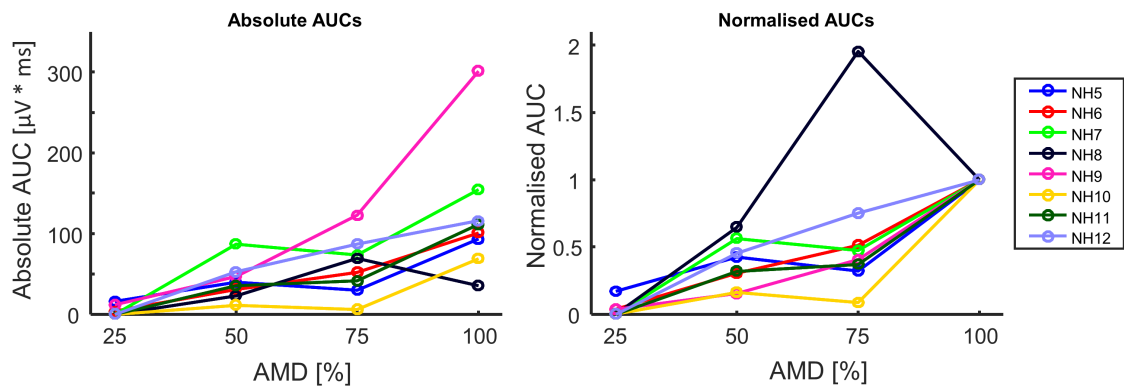


Figure 5.21: Individual absolute and normalised area-under-the-curve (AUC) values for the normal-hearing (NH) cohort.

AUC values are depicted for the four tested amplitude modulation depths (AMDs). AUCs were normalised to each individuals' AUC at 100% AMD. Participants NH3 and NH4 were excluded due to the missing data for the 25% AMD condition.

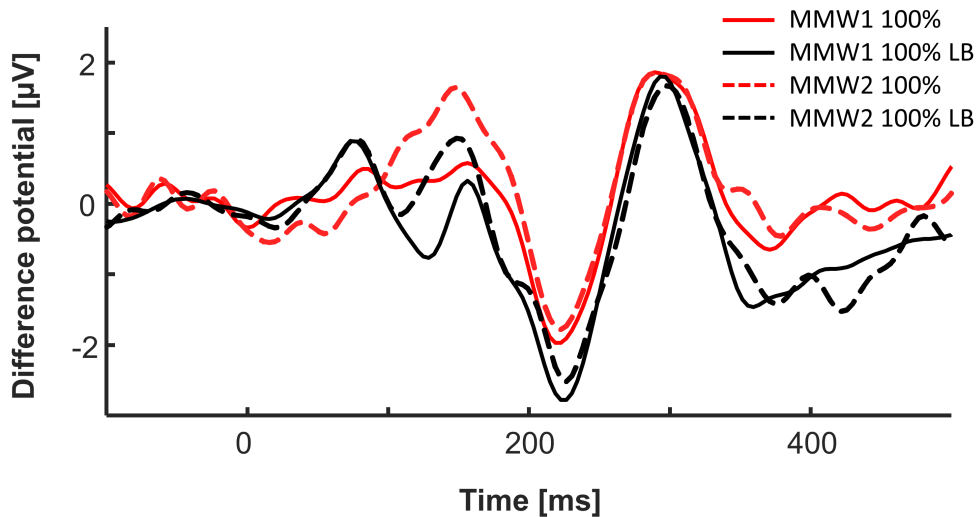


Figure 5.22: Overview of difference waves with and without subjective loudness balancing (LB).

Group mean data ($n = 4$) is shown for the fronto-central region of interest. Difference waveforms show the mismatch waveforms (MMWs) MMW1 and MMW2. Data was filtered from 1 – 30 Hz.

Figure 5.22 shows the MMW1s and MMW2s for the subjectively and objectively RMS-matched condition with an AMD of 100%. It was evident that subjective loudness

balancing did not eliminate the MMW, which provides evidence against the concern that MMWs may have been elicited as a result of loudness cues.

5.3 Discussion

5.3.1 Behavioural tests

In line with the literature, speech-in-noise recognition abilities varied greatly between cohorts, with all CI users demonstrating worse performance than all NH participants. Reported SRTs ranged between 4 dB and 22 dB for CI users and -4 dB to 0 dB for NH participants. In the commercially available BKB-SIN test, NH participants reportedly require an average SNR of -2.5 dB to perceive 50% of keywords correctly (Etymotic Research, 2005). This is in line with reported results. Wouters and Vanden Berghe (2001) reported SRTs between 3 dB and 15 dB for four CI users when measured at 60 dB SPL with the specially designed ICRA noise⁸ (ICRA, 1997). Poissant *et al.* (2014) reported SRTs between 10 dB and 22 dB for CI users measured with the Quick-SIN test (Etymotic Research, 2001) in four-talker babble noise, which is an alternative adaptive procedure to calculate SRTs. Overall, speech recognition abilities are known to vary greatly depending on the sound environment (Hazrati & Loizou, 2012; Gnansia *et al.*, 2014), individual parameters of the CI device (De Ceulaer *et al.*, 2015), hearing aetiology and history (Kraaijenga *et al.*, 2016), and daily fluctuations such as fatigue.

AM detection thresholds were higher on average for the CI user cohort, but numerous CI users presented thresholds in line with the NH participants demonstrating poor performance. AM detection thresholds lay between -11 dB to -20 dB (excluding the participant who showed non-performance) and -19 dB to -25 dB for CI users and NH participants, respectively. Gnansia *et al.* (2014) have reported thresholds ranging between -1 dB and -22 dB for AM detection in CI users with most experimental parameters being in line with the present study (500 ms stimulus duration, 8 Hz AM rate, level roving). The existence of poorer thresholds reported by Gnansia *et al.* (2014) may be due to the

⁸ The ICRA noise has been created by the Hearing Aid Clinical Test Environment standardisation work group for the International Collegium for Rehabilitative Audiology (ICRA) for application in hearing aid evaluation. The collection of noise signals has well defined spectral and temporal characteristics that are designed after real life speech and multi-talker speech signals.

recruitment criteria. For the present study only good to fair performers as indicated by BKB scores were included.

Loudness adjustments lay between -1.4 dB and 0.7 dB for CI users and -3.3 dB and 0.7 dB for NH participants. According to the literature, it is common that the AM sound is perceived as louder than the unmodulated equivalent at equal RMS-levels (Fraser & McKay, 2012). Despite this fact, an adjustment of ≈ -3 dB was considered to be extreme. It is possible that these two participants (see Figure 5.7) matched the peak level, rather than the overall loudness level.

5.3.2 Findings from CI users

CI artefact reduction

Subtraction-based artefact rejection was deemed successful for the grand average MMWs, however, individual data indicated remaining artefacts. This is in line with findings reported by Friesen and Picton (2010) who reported successful artefact reduction, although in some participants remaining artefact was visible. Friesen and Picton (2010) presented stimuli with direct input, stimulating only one electrode and bypassing the patient processor. Current pulses sent to the CI electrodes may vary from stimulus to stimulus when sounds are presented in sound field. Variation may arise from the automatic gain control, varying background noise levels, and the finite time window that the CI processing uses to sample sounds (Friesen & Picton, 2010). Relative timing differences between stimulus presentations will influence the information available in a sampled time window. In the present study, the influence of background noise and automatic gain control was limited given the advantages of controlling the sound-field with the Otocube. However, the influence of the sampling time window could not be controlled for. Ortmann *et al.* (2013) and Ortmann *et al.* (2017) presented stimuli with fluctuating envelopes (e.g. /bu/ vs. /ba/) in free-field and reported successful artefact reduction in the grand average CAEPs, although small influences of the artefact remained visible even in the grand average.

Another potential source for CI artefact variability may originate from the use of active electrodes. It is unknown how the pre-amplification of the active electrodes such as those from the Biosemi ActiveTwo system (BioSemi B. V., Amsterdam, Netherlands) employed in this study may affect the CI artefact. Overall, the data which had undergone ICA-based artefact rejection had greater SNRs on an individual level. This was most

likely due to the more comprehensive artefact reduction including biological artefacts and other discontinuities.

Correlation between NTs and BTs

The presented findings support the hypothesis that NTs estimated from MMW data provide a valuable alternative approach to assess CI users' low-rate AM sensitivity when behavioural AM detection thresholds are unreliable. Estimating NTs from normalised AUCs, rather than from absolute AUCs, eliminated the influence of naturally differing CAEP amplitudes across participants on NT estimates and focused on the intra-subject variability across AMDs. Numerous sets of NTs for varying IVs have been included in the correlation analysis to underscore that correlation results do not rely on the specific choice of the IV, and thus, no correction for multiple comparisons was applied. Overall, correlation coefficients between BTs and NTs were similar to findings from the NH cohort in the study reported in **Chapter 3**. That study showed correlation coefficients in the order of $r_p = 0.6$. In that study, morphology weighting of MMWs was employed, which weighted the AUCs depending on the similarity of the corresponding MMW to the individual participant's MMW at 100% AMD. This additional processing step was implemented to reduce the influence of random fluctuations on AUCs at low AMDs. However, in the present study an increased number of deviant repetitions and averaging across multiple recording channels reduced random fluctuations, and thus, no morphology weighting was required.

Speech recognition and low-rate AM sensitivity

The lack of correlations between BTs and speech-in-noise measures, as indicated by the SRTs, are at odds with the hypothesis. While it is widely believed that AM sensitivity plays an important role for speech recognition in electrical hearing (Cazals *et al.*, 1994; Fu, 2002; Luo *et al.*, 2008; Won *et al.*, 2011b; Gnansia *et al.*, 2014; De Ruiter *et al.*, 2015; Erb *et al.*, 2018), this is not the first time that a lack of correlation between AM detection thresholds and speech feature recognition in noise has been reported. Gnansia *et al.* (2014) also reported a lack of significant correlations between 8 Hz AM detection thresholds and vowel (in steady-state and fluctuating noise) as well as consonant (in fluctuating noise) recognition, despite significant correlations with vowel (in quiet and in steady-state noise) as well as consonant (in quiet) recognition abilities. These findings suggest that low-rate AM sensitivity may reflect CI users' abilities to extract cues from the slow envelope fluctuations of clear speech, but when the envelope cues are distorted

due to background noise, AM sensitivity does not provide a reliable predictor for speech recognition. Other features such as TFS processing abilities (Drennan *et al.*, 2007; Drennan *et al.*, 2008) and spectral resolution as assessed by spectral ripple discrimination abilities (Won *et al.*, 2007) may play a more defining role for speech-in-noise recognition. Additional support for the importance of low-rate AM sensitivity for speech recognition emerges from recently published findings by Erb *et al.* (2018), who reported that AM rate discrimination is a reliable predictor of sentence in quiet recognition. In contrast, Won *et al.* (2011b) showed significant correlations between average BTs across a range of AM rates and SRTs in noise as well as with CNC scores. This may point to the fact that AM detection at a fixed low rate (e.g. 8 Hz) may not provide sufficient information in relation to speech-in-noise recognition as opposed to a compound AM detection metric at a range of different modulation rates (as in Won *et al.* 2011). Overall, literature provides contradicting information regarding the relationship between AM sensitivity and speech recognition for varying parameter combinations and further research is required.

Clinical applications

The inclusion criteria for this study were limited to CI users with fair to good speech recognition outcomes. For potential future clinical applications, it should be investigated how the relationship between BTs and NTs evolves for CI users with limited rehabilitation success and also how neuronal maturation affects the MMWs and NTs. The present neurophysiological test procedure is very time consuming and may not be feasible for standardised clinical testing. Data acquisition time may be reduced by optimising the procedure, e.g. by reducing the number of recording channels, and thus, shortening the preparation time or by testing fewer AMDs such as 25%, 50% and 75%. The proposed method may offer an objective approach when subjective psychoacoustic tests are not feasible.

5.3.3 Findings from NH data

Although EEG data obtained from NH participants had a higher SNR on an individual level compared to data from CI users, MMWs were comparable in morphology as were AUC values as shown in Figure 5.18 and Figure 5.21. The additional positive component in the MMW2 preceding the MMN was observed in both cohorts. However, the underlying generator remains unknown. Given the fact that the MMW2 was calculated

by subtracting neural responses elicited by the same underlying physical stimulus, the existence of an additional early component prior to the MMN suggests that neural change detection may already take place prior to the MMN. To the author's knowledge, this additional component has not been reported in the literature.

Grand average MMWs were observed in both cohorts for AMDs of 50% and above. This finding lies in contrast to the obtained results in the single-channel NH study presented in **Chapter 3**. The single-channel data presented in **Chapter 3** showed no grand average MMW at the 50% AMD. The difference between the two studies was likely a result of the improved spatial distribution of recording channels. The possibility to average across multiple recording channels reduced the noise influence of individual channels, and also enabled biological artefact reduction based on ICA. The increased number of available deviant epochs from 56 deviant epochs to 68 deviant epochs also had a positive impact.

Findings from MMWs elicited by subjectively and objectively RMS-balanced stimuli eliminated the concern that the MMW may be based on potential loudness cues. Future work should determine if the MMW amplitude is significantly influenced by potential loudness cues as the current data-set for the loudness balanced condition is too small ($n = 4$) to make inferences on this research question.

5.3.4 Limitations

The subtraction-based processing pipeline currently has the limitation of lacking biological artefact reduction. Furthermore, this approach does not provide standard epochs free from CI artefacts to calculate the bootstrapped noise floor for quantification analysis. It may be feasible to employ the CI artefact reduction based on polynomial fitting reported by Mc Laughlin *et al.* (2013) to reduce the CI artefact for standard epochs, as neural standard responses were elicited by stimuli with approximately flat envelopes, which is required for this approach. This additional step may enable quantification analysis of MMW2s with the bootstrapped noise floor.

Employing a multi-channel system for EEG measurements has advantages and disadvantages. High-density EEG data enables artefact rejection based on ICA. Furthermore, it is possible to average across electrodes in a wider ROI, and thus, neural responses will not be missed due to the placement of electrodes. However, for future clinical applications time constraints may pose a greater challenge and would have to be

addressed by shortening the duration of data acquisition or by employing less EEG-channels to decrease set-up times.

Despite the small sample size of the clinical cohort in this study, which may have an influence on the reported effect size of the correlation analyses carried out for the CI user cohort, findings are encouraging, and justify further enquiry. Future study replications should increase the sample size to strengthen the statistical inferences drawn from the correlations, which will allow a more accurate assessment of the predictive value of NTs for BTs as well as speech recognition outcomes in CI rehabilitation.

Key Points

- The study presented in this chapter addressed the research questions Q2.1 – Q2.8.
- The MMW can be elicited in CI users with AM stimuli and the electrical artefact can be sufficiently reduced (Q2.1 – Q2.3).
- Findings support the hypothesis that NTs estimated from MMW data are correlated with behavioural thresholds of AM detection (Q2.4 – Q2.5).
- Speech-in-noise performance did not correlate with AM detection thresholds (Q2.6).
- MMWs were elicited for subjectively and objectively RMS-balanced stimulus pairs in the NH cohort (Q2.7).
- These findings were presented at the Speech in Noise Workshop, Oldenburg 2017; the IERASG symposium, Warsaw 2017; the AESOP symposium, Leuven 2018; and the 8th MMN conference, Helsinki 2018.
- Parts of the findings presented in this chapter were submitted to the international Journal *Trends in Hearing* (July 2018, TIH-18-0147) in the manuscript entitled “A neural correlate of low-rate amplitude modulation detection in cochlear implant users based on the mismatch waveform”.

Chapter 6 Objective measure of auditory temporal fine structure processing

As described in **Chapter 2**, TFS refers to the fast temporal variation in a sound in contrast to the slow amplitude variations which constitute the envelope. Monaural TFS sensitivity is important for pitch perception and sound segregation in noisy environments, whereas binaural TFS sensitivity plays an important role in sound localisation (Moore, 2016). Both monaural and binaural TFS processing are severely degraded in hearing impaired cohorts (Hopkins & Moore, 2011; Mathew *et al.*, 2016; Moore, 2016) and CI listeners (Drennan *et al.*, 2008; Heng *et al.*, 2011; Dincer D'Alessandro *et al.*, 2017). Füllgrabe *et al.* (2014) have shown that TFS processing is impaired in elderly listeners with normal audiometric thresholds. This indicates that TFS processing is affected by ageing beyond normal audiometric hearing loss, suggesting that neural function may be the determining factor in TFS processing rather than peripheral cochlear function. This is in line with findings reported by Harris and Dubno (2017) and Harris *et al.* (2014), who showed that neuronal phase locking abilities decrease with age even though audiometric thresholds are normal. Impaired TFS processing may contribute to the difficulties experienced with speech-in-noise perception by hearing impaired as well as elderly individuals. Therefore, it is of interest to develop psychoacoustic and neuroimaging tests to assess various aspects of TFS processing, as outcomes may provide non-redundant information about the function of the auditory system beyond audiometric thresholds.

Based on the observed adverse effects of ageing and hearing loss on TFS processing, there has been great research interest in determining psychoacoustic tests to assess TFS processing abilities. In contrast, literature on objective measures of TFS processing is lacking, as outlined in Section 2.5.2. Studies investigating CAEPs elicited by acoustic tone pairs with TFS differences were reported by Mathew *et al.* (2016), who investigated the ACC in response to TFS1 stimuli in a NH cohort, and by Leijssen *et al.*

(2015), who investigated the MMW as a potential objective measure of Schroeder-phase harmonic complex tone discrimination in CI users. Both studies had limitations and their results were inconclusive with regards to the applicability of CAEPs as an objective measure of TFS processing, as no consistent change responses were identifiable. Leijssen *et al.* (2015) employed a low number of deviant repetitions, which may have confounded the results. Furthermore, this study was carried out in a cohort of CI users and findings cannot address the question whether CAEPs can be elicited based on stimulus pairs that differ in their TFS in a NH cohort. Mathew *et al.* (2016) claimed that ACC responses were elicited in response to the TFS1 stimuli (i.e. a harmonic and frequency-shifted inharmonic stimulus pair), however, no statistical analysis was carried out, no clearly distinguishable ACCs were shown in included figures, and the alleged ACC response was also elicited in the control condition with a frequency shift of 0 Hz between the harmonic and inharmonic stimulus, and thus, findings have to be questioned.

The research study presented in this chapter aimed to more thoroughly investigate the applicability of CAEPs for objective auditory change detection based on TFS cues. Research studies presented in this chapter concentrated on monaural TFS processing, namely auditory discrimination between Schroeder-phase harmonic complex tone pairs and discrimination of HCU-ICU tone pairs adapted from the TFS1 test stimuli.

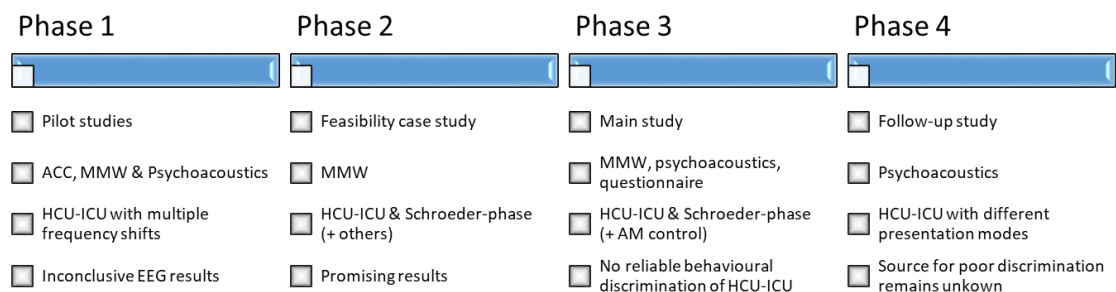


Figure 6.1: Schematic with a condensed overview of the four phases in Chapter 6.

Abbreviations and acronyms: ACC – Acoustic change complex, MMW – Mismatch waveform, HCU-ICU – refers to the experimental condition with a harmonic-inharmonic complex tone pair, AM – refers to the amplitude modulated tone pair introduced in Chapter 3.

This chapter is divided into four different phases (Figure 6.1), with the main study described in *Phase 3*. Each phase has investigated behavioural and/or neurophysiological measures of TFS change detection with differences in experimental paradigms, stimulus types and details of stimulus creation. All four phases contained a condition in which harmonic complex stimuli had to be discriminated from their frequency-shifted inharmonic counterparts. This condition is referred to as the HCU-ICU condition

throughout this chapter and its stimuli were designed to closely match the TFS1 stimuli by Moore and Sek (2009) with minor adjustments to suit the neurophysiological paradigm.

6.1 Phase 1 – Explorative pilot experiments

6.1.1 Methods

Pilot data was obtained with behavioural and neurophysiological paradigms, in which discrimination abilities of HCU-ICU tone pairs were assessed for varying frequency shifts. The objective was to assess the effect of change saliency on the neurophysiological responses, as it is known that discrimination abilities deteriorate with decreasing frequency shifts between HCU and ICU tones (Moore *et al.*, 2009). Neurophysiological data was obtained with an ACC and an MMW paradigm separately for different participants. Neurophysiological paradigms employed pre-determined frequency shifts Δf , whereas behavioural discrimination performance was assessed with an adaptive 1-up/2-down 3AFC procedure, which provided an estimate of the frequency shift Δf for which discrimination accuracy was approximately 70.7%.

It was hypothesized that the amplitude and latency of neurophysiological change responses (ACC and MMW) depend on the saliency of the acoustic change. Furthermore, it was hypothesized that participants with good behavioural thresholds show neurophysiological change detection responses for lower frequency shifts Δf than performers with poor behavioural thresholds.

Participants

Participants were young adults (mean = 23.2 years, standard deviation = 1.6 years) with no known hearing impairments. Prior to participation, participants signed their informed consent. The ACC paradigm was employed in four pilot participants, the MMW paradigm was employed in seven pilot participants, and behavioural thresholds were measured for all eleven pilot participants.

HCU-ICU stimulus design

HCU and ICU stimuli had a constant fundamental frequency $F0$ of 100 Hz. The HCU stimulus was created by adding harmonics of $F0$ from the second to the 20th

component. The summed signal was then bandpass-filtered with a 6th order infinite-impulse response (IIR) filter (roll-off of 30 dB/octave), which had a band-pass width of $5F0$, centred at the 12th component. As the filter was applied forwards and backwards with the function ‘filtfilt.m’, the effective filter roll-off was twice as sharp with 60 dB/octave. The ICU stimuli were generated by shifting all harmonics upwards by Δf , where Δf lies between 0 Hz and $0.5F0$. Moore and Sek (2009) employed TEN to mask potentially remaining excitation pattern cues from resolved components below the 8th component, and thus, components were believed to be unresolved (Moore *et al.*, 2006). In the present study, a broadband white Gaussian noise was added for masking purposes to yield an SNR of 15 dB. The overall presentation level was calibrated to 65 dBA. HCU and ICU stimuli were RMS-balanced and sounds were ramped on and off with 10 ms cosine ramps. All stimuli were presented monaurally to the left ear via headphones (Sennheiser HD 280 pro).

Neurophysiological paradigms

In the literature, stimuli in the TFS1 test and TFS2 test are presented as concatenated segments of HCU and ICU stimuli according to the pattern HHHH or HIHI, where H and I are HCU and ICU stimuli, respectively. The background TEN is presented before, throughout and after the presentation of the concatenated stimuli (Moore & Sek, 2009). Concatenation of stimuli with brief inter-stimulus intervals, where only TEN was audible, was not feasible for neurophysiological recordings, as each onset and offset of a sound may elicit an N1-P2 response. Therefore, the presentation mode had to be altered. Stimuli were presented individually (HCU or ICU) with background noise added for the duration of the complex tone. In the ACC paradigm, HCU and ICU tone segments were concatenated, each with a stimulus duration of 500 ms. Each concatenated sound was interleaved with a silent period of 1 s. In the MMW paradigm, standard tones (HCU) were presented with 90% occurrence probability and deviant tones (ICU) were presented with 10% occurrence probability. In total, 60 deviant stimuli were presented for each experimental condition. Stimuli presented in the oddball paradigm had a duration of 250 ms and the inter-stimulus interval was 1 s.

The ACC paradigm included five frequency shifts Δf (0 Hz, 5 Hz, 20 Hz, 35 Hz and 50 Hz) and due to time constraints, the MMW paradigm was reduced to four frequency shifts Δf (5 Hz, 20 Hz, 35 Hz and 50 Hz). A spectrally-rippled tone pair was included as a control condition, as it is known to elicit reliable neurophysiological change

responses (Lopez Valdes *et al.*, 2014). This provision enabled the assessment of the overall data quality in each data set. In the case of inconclusive neurophysiological data in the TFS conditions, data from the control condition would provide additional information on whether lacking responses were due to poor connectivity or if TFS cues were too subtle to reliably measure neural change detection.

6.1.2 Results and discussion

The measured behavioural discrimination thresholds (Figure 6.2A) were in line with those reported in the literature, e.g. thresholds reported by Moore and Sek (2009), which were reprinted in Figure 6.2B for visual comparison. In line with the literature, behavioural thresholds showed a wide spread in performance across the NH cohort.

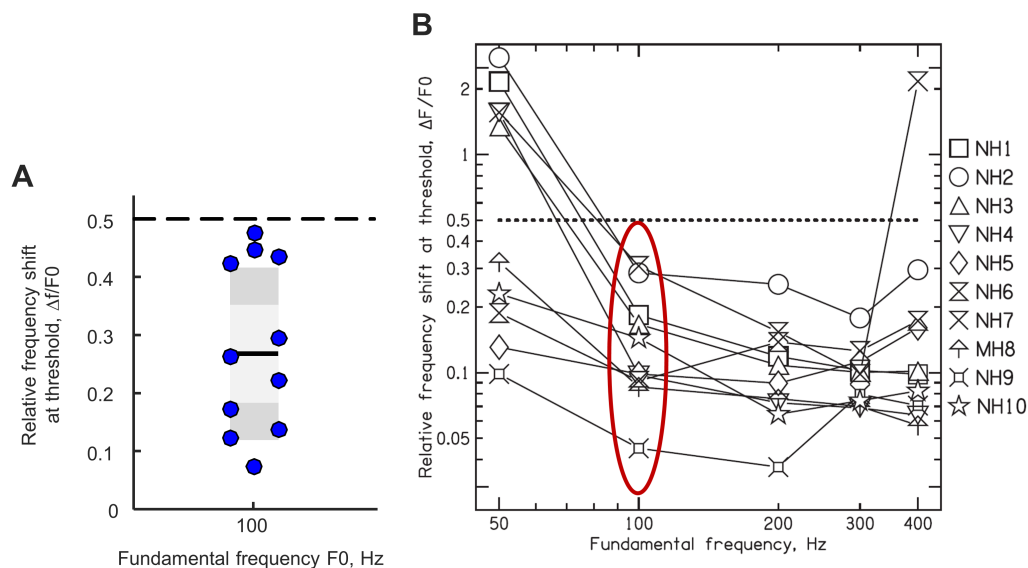


Figure 6.2: Behavioural thresholds of temporal fine structure (TFS) discrimination. (A) Thresholds were measured for eleven participants in the pilot experiments of Phase 1. (B) Behavioural discrimination thresholds measured with the TFS1 task which were reported by Moore and Sek (2009). Figure adapted from Moore and Sek (2009).

Neurophysiological pilot data showed clear MMW and ACC responses for the control condition (Figure 6.3 & Figure 6.4), which employed a spectral ripple tone pair. This validated the measurement set-up. Stimuli were created in line with (Lopez Valdes *et al.*, 2014) by summing 250 pure tones between 250 and 5000 Hz, where each pure tone's amplitude was determined by a full-wave rectified sinusoidal envelope. The generated spectral ripples were equally spaced on a logarithmic scale and for the control stimulus employed here, the ripple density was one ripple per octave (RPO). Stimuli were then filtered with an LTASS filter (Byrne *et al.*, 1994). To create stimulus pairs, the phase of the full-wave rectified sinusoidal spectral envelope was set to either zero or $\pi/2$ radians.

For the HCU-ICU tone pairs, neither ACCs (Figure 6.3) nor MMWs (Figure 6.4) were clearly distinguishable. The 50 Hz change condition may show a change detection response in both paradigms, however, it was not clearly identifiable.

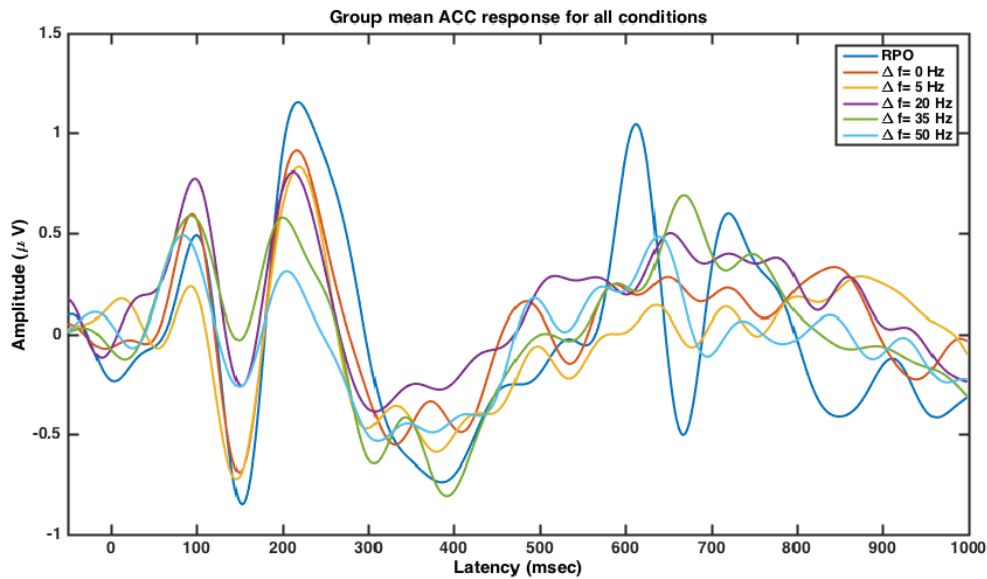


Figure 6.3: Cortical auditory evoked potentials (CAEPs) elicited by temporal fine structure stimuli.

Stimuli were elicited by concatenated harmonic (onset at 0 ms) and inharmonic stimuli (onset at 500 ms), where the inharmonic stimulus was created with varying frequency shifts between 0 Hz (control) and 50 Hz (max. shift). An additional control condition consisted of a spectral ripple sound pair with 1 ripple per octave (RPO, Lopez Valdes et al., 2014). CAEPs are shown for a central region of interest centred surrounding Cz with average reference. Adapted from Hablani (2017).

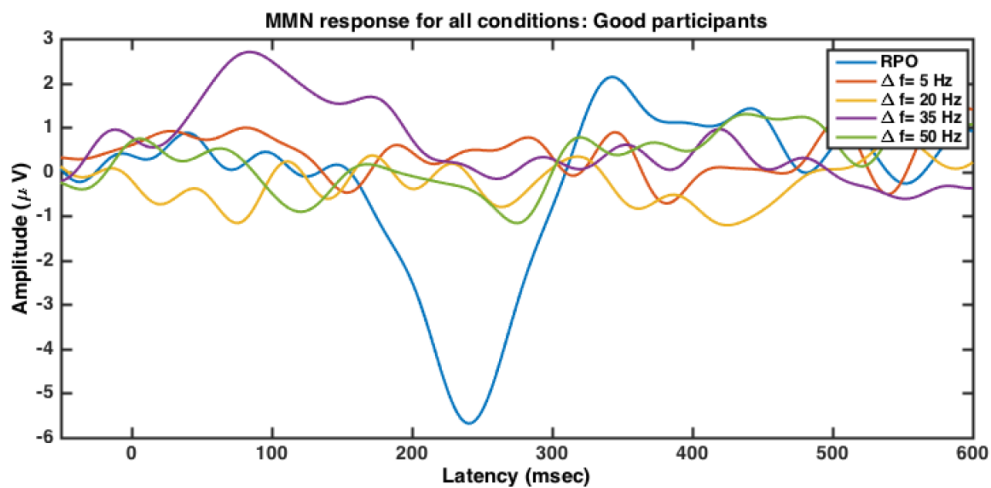


Figure 6.4: Difference waveforms elicited by temporal fine structure stimulus pairs.

Data is shown for good performers, defined as participants with clearly identifiable standard and deviant CAEPs. The difference waveform was calculated by subtracting the neural response to standard stimuli (harmonic) from the neural response to deviant stimuli (inharmonic) with varying frequency shifts between 5 Hz and 50 Hz (max. shift). An additional control condition consisted of a spectral ripple sound pair with 1 ripple per octave (RPO, Lopez Valdes et al., 2014). CAEPs are shown for a central region of interest centred surrounding Cz with average reference. Adapted from Hablani (2017).

Results were considered to be inconclusive. Therefore, *Phase 2* concentrated on the TFS1 stimulus pair with the maximum frequency shift ($\Delta f = 0.5F0$) with increased deviant repetitions to illuminate whether an MMW may be elicited and distinguished from background noise.

6.2 Phase 2 – Feasibility case study

Phase 2 presents findings from a feasibility case study. Instead of the multi-channel EEG set-up employed in *Phase 1*, *Phase 2* utilised the single-channel EEG set-up for the study introduced in **Chapter 3**, with the aim of reducing noise influence on CAEPs due to better electrode-skin interface preparation possibilities through the use of abrasive lotion. Furthermore, employing the single-channel set-up resulted in higher participant comfort, shorter set-up times and the potential for longer EEG data acquisition. Rather than testing multiple frequency shift conditions as in *Phase 1*, this pilot study concentrated on the maximum frequency shift between the HCU-ICU tone pair. Furthermore, the HCU-ICU stimulus design was adapted to match the original TFS1 stimulus design more closely (Moore & Sek, 2009). This was possible due to newly gained information from email correspondence with Professor Moore⁹, University of Cambridge.

In addition to the HCU-ICU condition, four other paradigms were employed. Tone discrimination based on TFS cues was also assessed with a Schroeder-phase harmonic complex stimulus pair to explore an alternative approach in the objective assessment of TFS discrimination abilities.

In an attempt to investigate underlying mechanisms of pitch extraction based on different acoustic cues, a pitch-change condition based on a difference in the fundamental frequency was added. A tone pair consisting of two harmonic stimuli was saliency-matched to the HCU-ICU tone pair as detailed in Section 6.2.1. This test condition was labelled HCU-F0 in the following. Given the poor data quality in *Phase 1*, the *Phase 2* study also incorporated control conditions, for which it was known that MMWs are elicited in most NH participants: The spectral ripple control condition introduced in *Phase 1* and an AM control condition with 100% AMD (for details see **Chapter 3**). These

⁹ Email correspondence on 17/10/2017, 25/10/2017, 27/10/2017, 9/3/2018, 14/3/2018 and 24/4/2018.

two control conditions both provide reliable MMWs, but with differing latencies, which added additional information for comparisons across conditions.

6.2.1 Methods

This case study concentrated on the neurophysiological MMW paradigm. Data was acquired for five deviant conditions as outlined above, which are consecutively labelled (1) HCU-ICU, (2) Schroeder-phase, (3) HCU-F0, (4) AM, and (5) RPO (representing the spectral ripple stimuli). In line with the MMW Study presented in **Chapter 5**, the deviant tone was also presented in a deviant-alone segment at the start of each block, enabling the calculation of the MMW based on neural responses elicited by the same physical stimulus. This ensured that potential deflections in the difference waveform were not a result of differential neural processing of the physical stimulus presented as a standard. The deviant probability was set to 0.15 in the oddball segment and deviant CAEPs were comprised of approximately 85 deviants for each condition. The deviant-alone CAEPs were comprised of approximately 125 epochs.

MMWs were calculated in line with the procedures for Study 1 reported in **Chapter 5**, meaning the MMW1 was calculated based on deviant and standard CAEPs and the MMW2 was calculated as the difference wave between deviant CAEPs and CAEPs from the deviant-alone segments. The bootstrap-procedure outlined in **Chapter 5** was employed to determine whether responses exceeded the noise floor.

Participant

The participant in this case study was a 28 year old female with no reported hearing impairment. Stimuli were presented monaurally to the left ear via headphones (Sennheiser HD 280 pro).

HCU-ICU tone pair

Harmonic complex tones were created by summing multiples of $F0 = 200$ Hz from the second to the 20th harmonic. Components were added in constant sine phase. Bandpass filtering of the summed signal removed undesired spectral cues from resolved harmonics and decreased the TFS complexity by decreasing the spectral range. The applied infinite impulse response (IIR) bandpass filter had a passband with a flat central region from the 10th to the 11th component (2 kHz to 2.2 kHz) and a flat roll-off of

30 dB/octave (Figure 6.5). This filter had a narrower passband compared to the filter designed in *Phase 1*. The filter was applied with MATLAB’s ‘filter.m’ function.

To minimize the influence of potentially remaining excitation pattern cues, a TEN was added (Moore *et al.*, 2000). The sound file was kindly made available by Professor Moore, University of Cambridge (October 2017). The level of the complex signal was 15 dB above the level of the TEN. The level of the TEN is commonly defined for the equivalent rectangular bandwidth¹⁰ (ERB) at 1 kHz, and can be calculated as the sum of the power of the spectral magnitudes across the spectral range specified by the ERB at 1 kHz (1000 Hz ± 0.5 * 132 Hz). In contrast, the level of the complex signal was calculated as the sum of the power of the spectral magnitudes across the full spectrum.

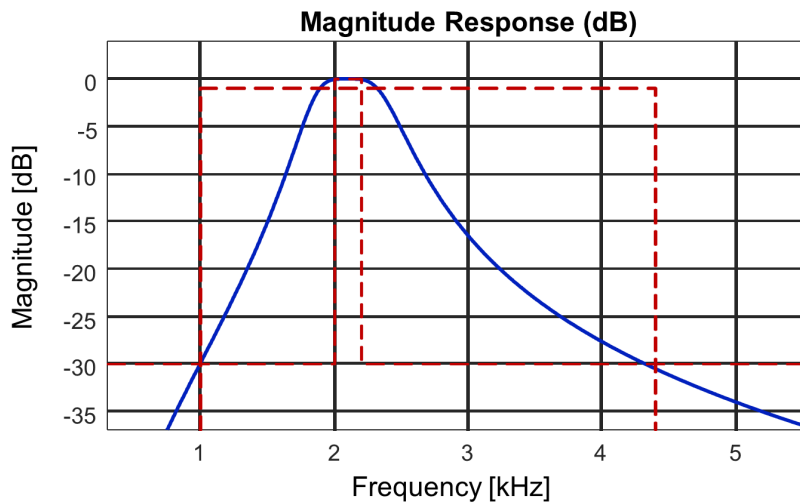


Figure 6.5: Bandpass filter to create HCU-ICU stimuli.
The IIR band pass filter had a central flat region from the 10th to the 11th component (2 kHz to 2.2 kHz) and a roll-off of 30 dB/octave.

Schroeder-phase harmonic complex tone pair

Schroeder-phase harmonic complex tones as illustrated in Figure 6.6 were generated by adding equal-amplitude harmonics of a specified $F0$:

$$S = \sum_1^N \sin(2 \cdot \pi \cdot n \cdot F0 \cdot t + \Theta_n),$$

Equation 6.1

where Θ_n was the phase of the n -th harmonic defined by Equation 6.2 with a positive or negative phase for the positive and negative Schroeder-phase harmonic complex, respectively:

¹⁰ ERB refers to the equivalent rectangular bandwidth of the auditory filter for listeners with normal hearing, as specified by Glasberg, B.R. & Moore, B.C.J. (1990) Derivation of auditory filter shapes from notched-noise data. *Hearing research*, **47**, 103-138.

$$\Theta_n = \pm \pi \cdot n \cdot \frac{n+1}{N}.$$

Equation 6.2

The time vector t was determined by the duration of the stimulus and its sampling rate, and N was the total number of harmonics contained within the stimulus calculated as the maximum frequency of 5000 Hz divided by $F0$. This study focused on a single $F0$ of 50 Hz, which has been shown to yield better discrimination accuracy between positive and negative stimuli compared to higher fundamental frequencies (Drennan *et al.*, 2008; Lauer *et al.*, 2009).

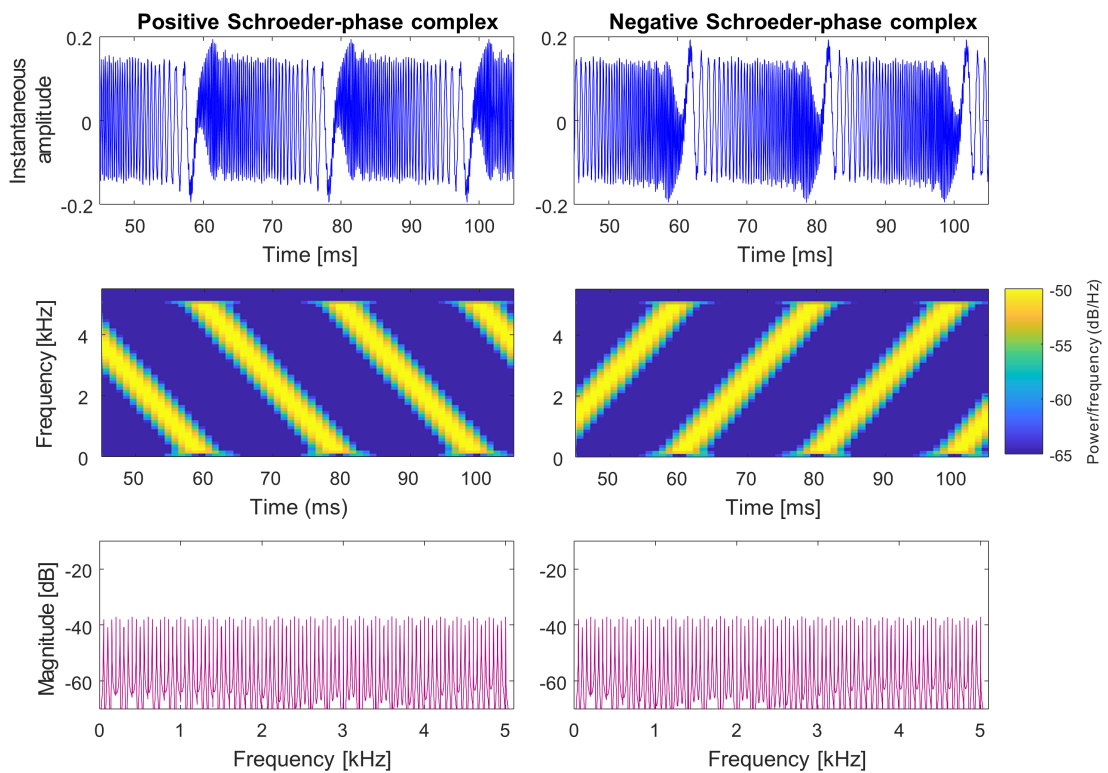


Figure 6.6: Positive and negative Schroeder-phase harmonic complex tones.

The top row shows the instantaneous amplitude and the middle row shows the spectrogram of the positive and negative Schroeder-phase harmonic complex tones zoomed in to a 50 ms wide time window. The bottom row shows the spectral magnitude calculated with the fast Fourier transform (FFT).

HCU-F0 test condition

The HCU-F0 test condition addressed an alternative idea on how to assess potential differences of pitch extraction for unresolved stimuli. Contrary to the HCU-ICU tone pair which shares the same $F0$, another tone pair was created which provides the same perceived pitch difference as the HCU-ICU pair, but based on an $F0$ -change. This was achieved by pitch matching the $F0$ of an HCU tone to the perceived pitch of the ICU

tone with a frequency shift of $0.5F_0$. This procedure resulted in two stimuli which share the same pitch, and thus, were saliency matched with regards to the HCU tone although they differed in the underlying acoustic cues.

Alternative experimental ideas

The harmonic-inharmonic change condition with unresolved components ($\geq 9^{\text{th}}$ component) relies on pitch change perception based on the successful use of TFS cues. An obvious control condition would be the same test with resolved harmonics, i.e. components below the 8^{th} harmonic, which would provide a combination of spectral and TFS cues. A comparison of the neural change response between the resolved and unresolved condition would aim to address whether neural processes underlying pitch extraction differ when using TFS cues rather than spectral cues. It would be of interest to see whether the MMN is more delayed when it relies on TFS cues compared to spectral cues. However, deviant saliency plays a large role in MMN amplitude and latency (Näätänen *et al.*, 1989; Tiitinen *et al.*, 1994), and pitch saliency is reported to be greater for stimuli with resolved components (Carlyon & Shackleton, 1994). Acoustic differences between resolved and unresolved stimuli can be behaviourally saliency matched by adding noise (Butler & Trainor, 2012), but this would add many more variables. Furthermore, shifting the harmonic stimulus by half of F_0 sometimes resulted in a perceived decrease in pitch for resolved stimuli, whereas for unresolved stimuli an increase in pitch was commonly perceived. This would introduce additional differences between resolved and unresolved tone pairs, and thus, this idea for an experimental design was abandoned.

6.2.2 Results and discussion

The participant in this pilot study had very good TFS and pitch discrimination abilities as confirmed by previous behavioural tests. The participant matched the ICU stimulus ($F_0 = 200$ Hz, $\Delta f = 100$ Hz) with an HCU tone containing an F_0 of 210 Hz for the HCU- F_0 condition.

MMW1s

The MMN component of the MMW1 only just exceeded the noise floor in the designated time window of interest between 90 ms and 230 ms (Figure 6.7, left) for the

HCU-ICU and the HCU-F0 conditions, although the participant could distinguish them without difficulty. The observed small MMN amplitude in the HCU-F0 condition suggests that the small MMN amplitudes in the HCU-ICU condition were not necessarily an effect of complex pitch extraction, but rather due to the subtlety of the acoustic change for the small perceived pitch difference. It should be noted that both conditions contained stimuli with unresolved components, which is associated with lesser pitch salience, which in turn relates to smaller MMW amplitudes. Despite its comparably low amplitude, the morphology of a typical MMN component was visible. The AM and the spectral ripple control conditions exhibited MMWs that greatly exceeded the noise floor (Figure 6.7) which was in line with observations from previous studies. For the Schroeder-phase condition, the MMN visibly exceeded the noise floor. However, it showed two negative peaks, rather than a single negative peak, for both the MMW1 and the MMW2.

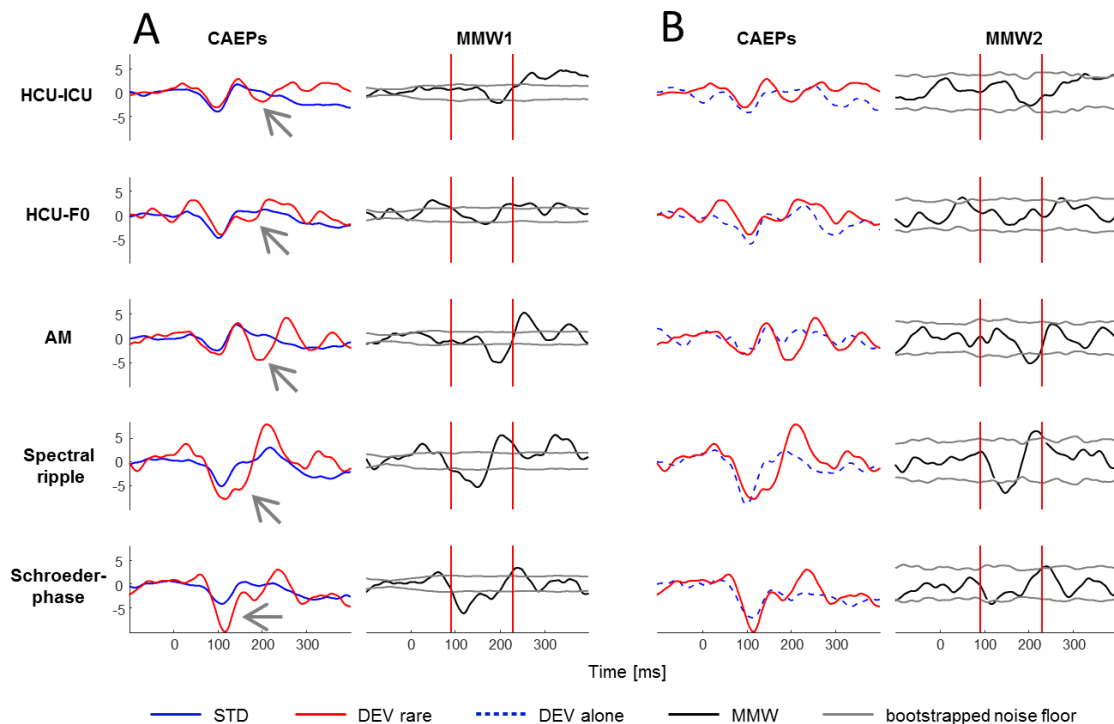


Figure 6.7: Cortical auditory evoked potentials (CAEPs) elicited by five different stimulus pairs for a pilot participant.

The acoustic tone pair differed for each row and is indicated on the left. (A) In the left column the standard (STD) and deviant (DEV) CAEPs are shown with arrows indicating the change related negativity in the DEV CAEPs. Their respective difference waves show the mismatch waveforms (MMWs). Grey lines indicate a bootstrapped noise floor and vertical red lines indicate the time range of interest for the mismatch negativity (MMN). (B) Here, the STD CAEP for the calculation of the difference wave was obtained by presenting the DEV stimulus in a DEV-alone condition. Abbreviations and acronyms: HCU – Harmonic complex with unresolved components, ICU – Inharmonic complex with unresolved components, AM – Amplitude modulation.

MMW2s

The deviant-alone CAEP only had 17.6% ($= \frac{15\%}{85\%}$) of the number of epochs available for the standard CAEPs, which resulted in a notably greater bootstrapped noise floor for the MMW2s (Figure 6.7, right) than for the MMW1s (Figure 6.7, left). For this reason, MMW2s exceeded the noise floor less than MMW1s. The lower number of deviant-alone epochs also affected the SNR of the MMW2s. For a fair comparison between MMW1s and MMW2s, the number of deviant-alone presentations should be equal to the number of standard presentations, which would significantly increase the data acquisition time. Overall, the morphology of MMW2s and MMW1s was similar, suggesting that deflections in the difference waveform were due to change detection mechanisms, rather than differential neural processing of the physical stimulus.

HCU-F0 condition

Pitch matching abilities are degraded for complex stimuli even in NH participants (Moore *et al.*, 1992) and a follow-up pilot study within the lab indicated that many people were unable to reliably match the pitch of the ICU stimulus to an HCU stimulus with a different F_0 . With inconsistent performance across as well as within participants, a pitch-matched paradigm would provide unreliable results in a neurophysiological paradigm. Therefore, this line of research was not further pursued.

In conclusion, the results from this case study provided support for the feasibility of investigating the MMW as a potential objective measure of TFS processing. MMWs were of small amplitude for the HCU-ICU condition, but were successfully measured. It should be noted that this case study looked at individual data, and results may be more distinguished on a group level.

6.3 Phase 3 – A study on the feasibility of neural change detection measures for TFS processing

The promising findings in *Phase 2* motivated the *third phase* of the TFS study, in which the MMW paradigm was employed to obtain neural change detection measures for three conditions: (1) the HCU-ICU stimulus pair with maximum frequency shift Δf , (2) the Schroeder-phase harmonic complex tone pair, and (3) the AM tone pair with 100%

AMD. The first two conditions probed discrimination abilities based on TFS cues, and the AM condition was added as a control condition. Additionally, behavioural discrimination abilities were measured to ascertain that participants could discriminate the stimuli. A questionnaire was administered to record participants' discrimination confidence.

The single-channel set-up employed in *Phase 2* was extended. A second recording channel was added by combining two amplifiers in the set-up (see Figure C.3 in Appendix C). Having two recording sites reduced the risk of missing a neural response in the measurement, especially when the expected response had small amplitudes. The two recording electrodes were placed at Cz and Fz. These two electrode positions are the most widely reported for MMN recordings and commonly provide the largest MMN amplitudes. Referencing to the contralateral (with respect to the side of stimulus presentation) mastoid was expected to provide good signal-to-noise ratios as the MMN has opposite polarities between central and mastoid electrode locations. The new dual-channel measurement set-up was validated and results are presented in Appendix A.

6.3.1 Methods

Participants

Eleven healthy, young participants with no reported hearing impairments participated in this study. Informed written consent was obtained from all participants prior to participation and all experimental procedures were approved by the Ethics (Medical Research) Committee at Beaumont Hospital, Beaumont, Dublin and the Research Ethics Committee at Trinity College Dublin.

Participants were seated in a quiet room and auditory stimuli were presented monaurally to the left ear via headphones (SONY MDR-XD200) for all tests. The presentation level of 70 dB SPL was verified with a pure tone (1 kHz) which was RMS-balanced with the experimental stimuli. Loudness measurements were carried out with a KEMAR mannequin (45 BC) with pinna simulator (KB 0091), pre-amplifier (26CS) and pre-polarized pressure microphone (40A0) (all from G.R.A.S. Sound & Vibration). All stimuli were energy matched by adjusting the RMS amplitude.

Stimuli

HCU-ICU stimuli and Schroeder-phase stimuli were created according to the descriptions in *Phase 2* in Section 6.2.1. The stimulus pair for the AM control condition was designed as outlined in Section 3.1.2. All stimuli were RMS-balanced and contained 10 ms on/off-ramps. Schroeder-phase harmonic complex tones had a fundamental frequency of 50 Hz. HCU-ICU tones had a fundamental frequency of 200 Hz, with a constant frequency shift of 100 Hz ($0.5F0$). All stimuli had a duration of 375 ms with an ISI of 200 ms.

Behavioural paradigm

Behavioural TFS discrimination abilities were assessed with a non-adaptive 3AFC paradigm for two conditions: Participants had to discriminate between HCU and ICU tones or between positive and negative Schroeder-phase harmonic complex tones. For each condition, data was acquired for two blocks with 30 responses each. Discrimination scores were calculated as the percentage of correct discriminations. Performance was considered to be significantly above chance level if the discrimination score was above 43.3%. This value was calculated using the binomial distribution to determine the probability of scoring n out of 60 trials correct by chance, with a probability $p = 0.33$ to score an individual trial correct by chance. The probability of scoring 26 or more trials correct by chance was less than 0.05, and thus, scores equal to or greater than 26 correct responses out of 60 (43.3%) were considered as significantly above chance level. A questionnaire containing four questions was administered for the two TFS conditions to gauge discrimination ability, confidence, effort, and concentration levels (Figure 6.9).

Neurophysiological paradigm

EEG data was acquired with a custom-designed dual-channel system (for details see Figure C.3 in Appendix C). Recording electrodes were placed at Cz and Fz, both referenced to the right mastoid while the ground electrode was placed on the right collarbone. One of the amplifiers developed a fault after data acquisition for the eighth participant. Data for the following three participants was acquired with only one recording channel placed at Fz. Data analysis showed near identical results for data from Cz and Fz in the participants where both channels were available, and thus, analysis was reduced to the data recorded from Fz in the following.

Data was acquired divided into four blocks for each of the three conditions. Within each block, 18 deviant stimuli were presented at the start in a deviant-alone segment, followed by ten standard stimuli to “prime” the brain for the oddball segment. In the oddball segment, stimuli were pseudo-randomized. Deviant stimuli had an occurrence probability of 12% and standards were presented in the remaining 88% of cases. Each oddball segment contained 18 deviants, resulting in 72 deviant presentation in total per condition. Stimuli had a duration of 375 ms equal to the behavioural discrimination test, with an ISI of 800 ms. Table 6.1 provides an overview of the stimulus assignment to standard and deviant stimulus in each condition.

Table 6.1: Overview of stimulus assignment in the neurophysiological paradigm.
Abbreviations and acronyms: AM – amplitude modulation, AMD – Amplitude modulation depth, HCU – Harmonic complex with unresolved components, ICU – Inharmonic complex with unresolved components.

	Standard (n = 568)	Deviant (n = 72)	Deviant-alone (n = 72)
HCU-ICU	HCU	ICU	ICU
Schroeder-phase	Positive complex	Negative complex	Negative complex
AM	Unmodulated noise	AM noise, 100% AMD	AM noise, 100% AMD

EEG post-processing

Continuous EEG data was filtered between 1 Hz and 15 Hz with a 4th order Butterworth bandpass filter. Data was epoched from -300 ms pre-stimulus until 600 ms post-stimulus according to the trigger type. Baseline correction was applied to standard, deviant and deviant-alone CAEPs for a baseline window of -100 ms – 0 ms. MMW1s and MMW2s were calculated in line with the procedures in *Phase 2* (Section 6.1.1).

Statistical analysis: In this study, it was of interest to determine whether a significant MMW was elicited for each of the tested deviant conditions. Non-parametric Wilcoxon signed rank tests were employed for each sample in time across participants’ mean difference waveforms to test the hypothesis that each sample distribution had a median of zero. If p-values fell below 0.05, this hypothesis could be rejected and one assumes that the difference waveform is significantly different from zero. However, due to multiple comparisons when testing the individual sample distributions in time, it was necessary to minimise the number of computed tests. Based on the *a priori* knowledge of the time window for the MMW, a time window for the analysis was chosen as 150 ms until 350 ms. Furthermore, data was down-sampled to provide one sample every 10 ms. This approach reduced the number of required tests for each condition to 21 comparisons.

The significance level was adjusted according to the false discovery rate (FDR) adjustment by Benjamini and Yekutieli (2001).

6.3.2 Results and Discussion

Behavioural results were unexpected, as most participants were unable to reliably discriminate the HCU-ICU tone pair (Figure 6.8). Responses from the questionnaire suggested that participants were very concentrated on the task, but despite such focusing many participants were unable to differentiate HCU and ICU stimuli. This was reflected in participants' reported high level of uncertainty about task performance. For the Schroeder-phase condition, participants showed robust discrimination abilities resulting in ceiling effects. All participants were confident about their discrimination abilities and the task load was low, as indicated by the responses gathered with the questionnaire (Figure 6.9).

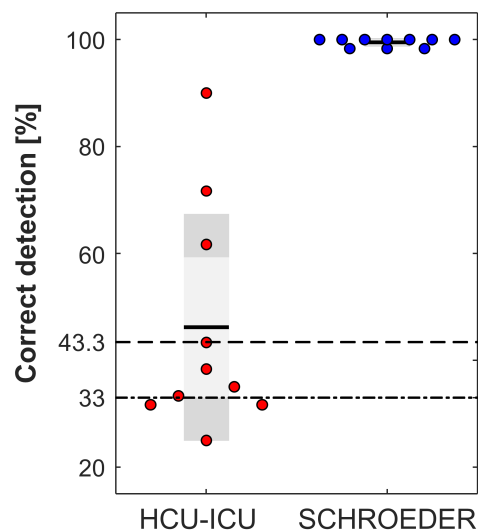


Figure 6.8: Behavioural tone discrimination results.

Results show ceiling effects for the Schroeder-phase harmonic complex tone pairs for all participants. For the harmonic-inharmonic complex tone pair, many participants showed performance around chance level ($\approx 33\%$). Only four participants showed performance that was considered to be significantly above chance level ($\geq 43.3\%$). Descriptive statistics include the arithmetic means (black line) and standard deviations (shaded grey boxes).

The lacking discrimination abilities for the HCU-ICU condition were reflected in the neurophysiological responses. Figure 6.10 compares the CAEPs elicited by standard, deviant and deviant-alone stimuli, and shows their respective difference waveforms MMW1 and MMW2. Figure 6.11 shows a direct comparison of the MMW1s across conditions. For the HCU-ICU condition, the CAEPs were virtually identical, which resulted in an almost flat line for the difference waveform, which would be expected

based on the lacking behavioural discrimination. For the Schroeder-phase condition, the difference waveform showed two negative deflections, which is in line with observations from *Phase 2*, and no positive component associated with the P3a component. It is assumed that the second negative component is associated with the MMN, as its latency coincides with the latency of the MMN elicited by the AM control condition. However, the grand average MMN amplitude in the Schroeder-phase condition was measured as $\approx 1 \mu\text{V}$, whereas the MMN amplitude of the AM control condition was measured as almost $4 \mu\text{V}$.

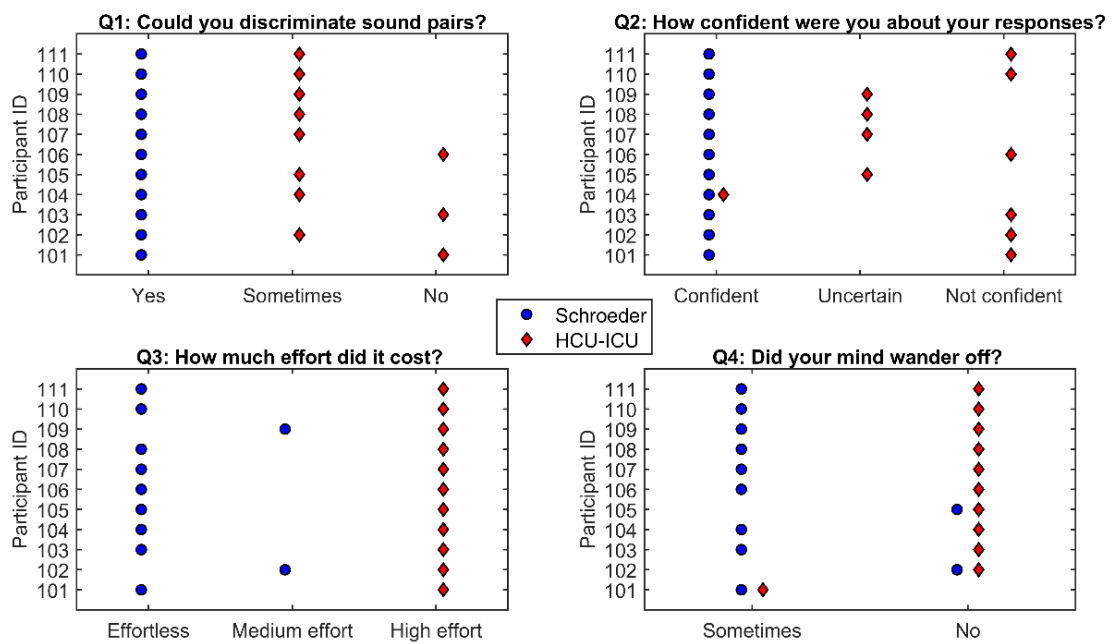


Figure 6.9: Questionnaire responses on temporal fine structure tone discrimination.

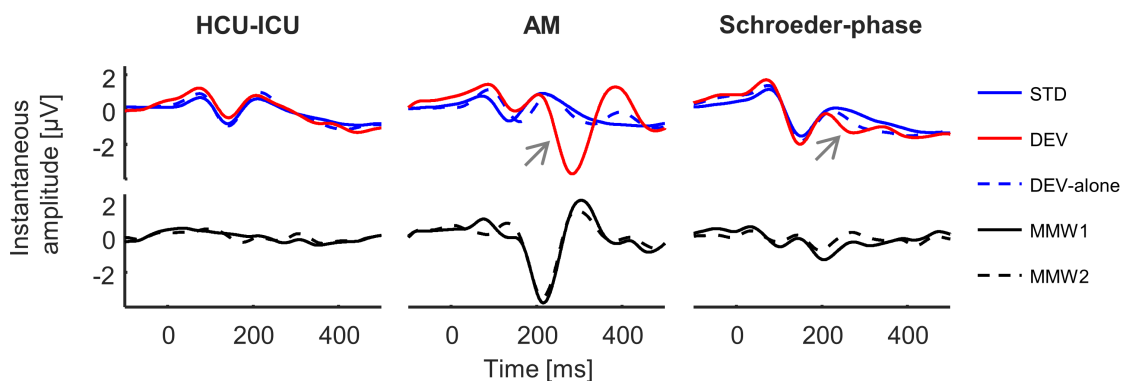


Figure 6.10: Comparison of grand average cortical auditory evoked potentials (CAEPs) and their respective difference waveforms.

CAEPs were elicited by standard (STD), deviant (DEV) and deviant-alone (DEV-alone) stimuli. The mismatch waveform (MMW) labelled MMW1 was calculated as the difference wave between STD and DEV CAEPs and the MMW2 was calculated as the difference between the DEV and the DEV-alone CAEPs. The change-related negativity in DEV CAEPs is indicated by the grey arrows.

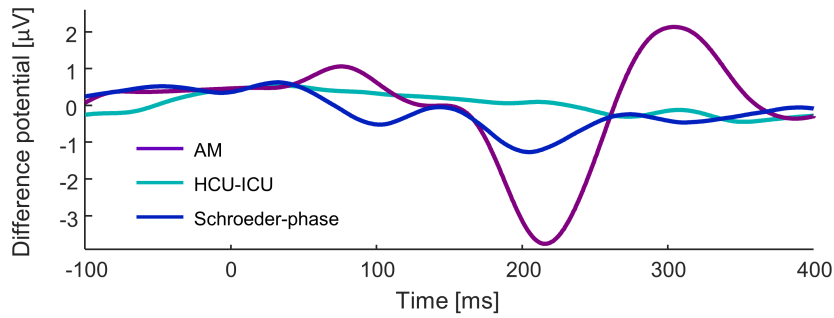


Figure 6.11: Overview of grand average mismatch waveforms (MMWs).
Comparison of the MMWs for the three tested deviant conditions.

The clear MMW in the AM condition as well as the non-existent MMW for the HCU-ICU condition (Figure 6.11) lent support to the data quality of the measurements. If excessive noise was remaining after averaging across epochs, the MMW of the HCU-ICU condition would show random fluctuations. This supports the existence of an MMW in the Schroeder-phase condition, given that the difference waveform should show no deflections if tones were not discriminable.

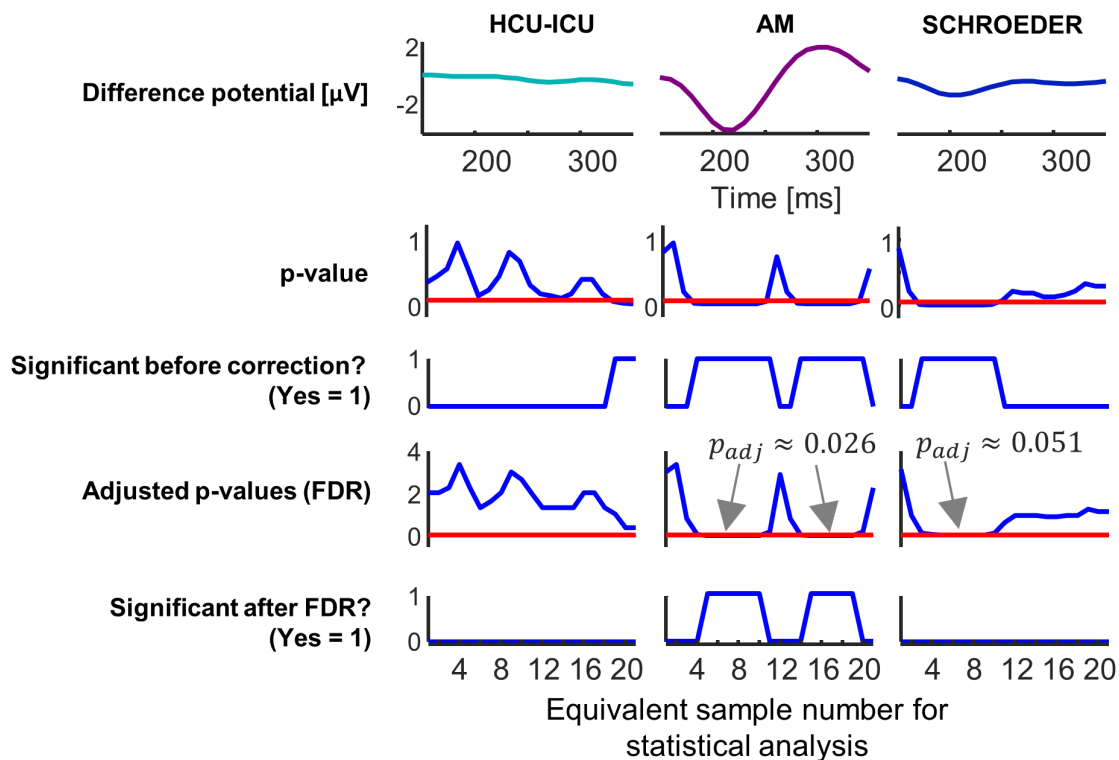


Figure 6.12: Detailed processing steps of the statistical analysis of the difference waveform with false discovery rate (FDR) adjustment.

The difference potentials of the three assessed conditions are shown in the top row for the time window of interest for the existence of the mismatch waveform (MMW) between 150 ms and 350 ms. The four rows below show outcomes of statistical testing for each sample along the x-axis. The p-values (2nd row) are the results of Wilcoxon's non-parametric two tailed signed-rank tests examining whether the difference waveform is significantly different from zero for each sample, with one sample per 10 ms. It is necessary to adjust for multiple comparisons across samples, which is achieved with the false discovery rate (FDR) adjustment by Benjamini and Yekutieli (2001).

Statistical analysis with Wilcoxon signed-rank tests before adjustment for multiple comparisons (Figure 6.12) showed that the AM condition had significant responses in the latency range of the MMN and the P3a, the Schroeder-phase condition had significant responses at the latency of the MMN and the HCU-ICU condition showed significant difference potentials beyond the P3a component (significance $p < 0.05$). It is crucial to adjust for multiple comparisons before interpreting the data. Results were adjusted with the FDR-procedure by Benjamini and Yekutieli (2001). Findings showed significant difference potentials only for the AM control condition, for both the MMN and P3a latency. It should be noted, that the Schroeder-phase condition had a corrected p-value of 0.051. An increased sample size may address whether this effect is significant.

6.4 Phase 4 – Addressing limitations of Phase 3 with psychoacoustic experiments

The lack of behavioural discrimination abilities in the HCU-ICU condition in *Phase 3* gave rise to *Phase 4*, in which potential influencing factors in stimulus design and stimulus presentation were assessed in psychoacoustic experiments.

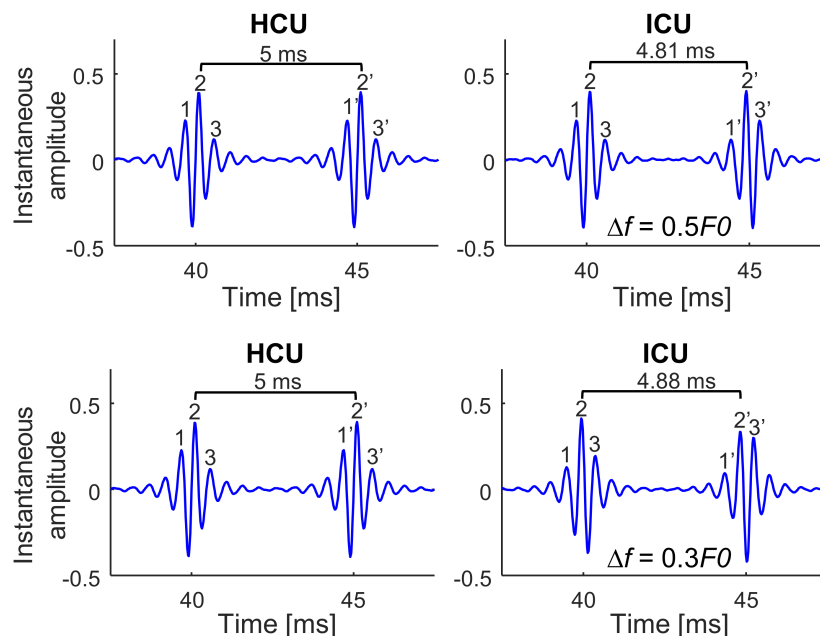


Figure 6.13: Peak timing of harmonic and inharmonic complex stimuli with a fundamental frequency F_0 of 200 Hz.

Instantaneous amplitudes of the harmonic complex tone with unresolved harmonics (HCU) and the frequency-shifted inharmonic complex tone with unresolved harmonics (ICU) prior to adding threshold-equalizing noise. Depicted ICU tones were created with upwards frequency shifts of 100 Hz (top) and 60 Hz (bottom). The latency between the major peaks was consistent at 5 ms for the HCU tone, whereas for frequency-shifted ICU stimuli the peak timing varies, resulting in perceived pitch variations.

One of the potential reasons for the lacking discrimination abilities in *Phase 3* may have been related to the presentation mode of the stimuli. The perceived pitch of the HCU and ICU stimuli as shown in Figure 6.15 may be ambiguous. The brain may determine the pitch based on the timing difference between differing peaks. As illustrated in Figure 6.13, it is possible that the brain uses different peak timing cues with each stimulus presentation, e.g. peak 2 and 2' and the next time between 2 and 3' or 3 and 2' (Moore, 1993). The resulting pitch ambiguity may negatively impact on discrimination performance. If this is the case, discrimination performance should be significantly improved when stimuli are presented in a concatenated fashion (HHHH vs. HIHI) as is the case for the TFS1 studies by Moore and colleagues. The objective of this follow-up study was to determine whether discrimination performance differs significantly between individual and concatenated stimulus presentation.

6.4.1 Methods

Thirteen young adults without known hearing impairment participated in this behavioural study. Each participant spent approximately 20 minutes with the researcher. Behavioural discrimination thresholds were estimated for two presentation modes of the HCU-ICU tone pair: for individual tone presentation of HCU and ICU tones (H or I) and concatenated tone presentation (HHHH or HIHI).

Improving the HCU-ICU stimulus design

Based on participants' unexpected difficulties in discriminating the harmonic complex tones from their frequency-shifted counterparts in *Phase 3*, an in-depth analysis of stimulus creation was carried out. It was discovered that non-linear phase effects during filtering of the stimuli with 'filter.m' introduced signal distortions (Figure 6.14), which may have negatively impacted discrimination performance.

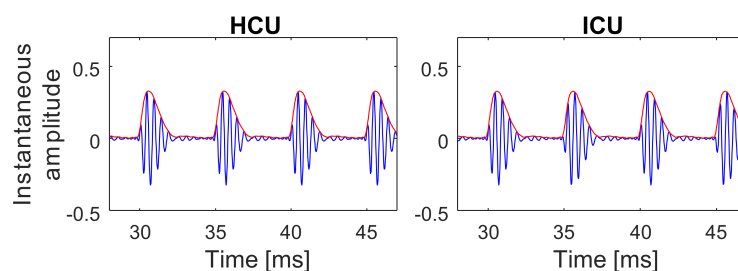


Figure 6.14: Example of signal distortions due to non-linear phase effects. Stimuli are depicted prior to adding background noise. The asymmetric envelopes are evidence of non-linear phase effects due to filtering of the summed components with MATLAB's function 'filter.m'.

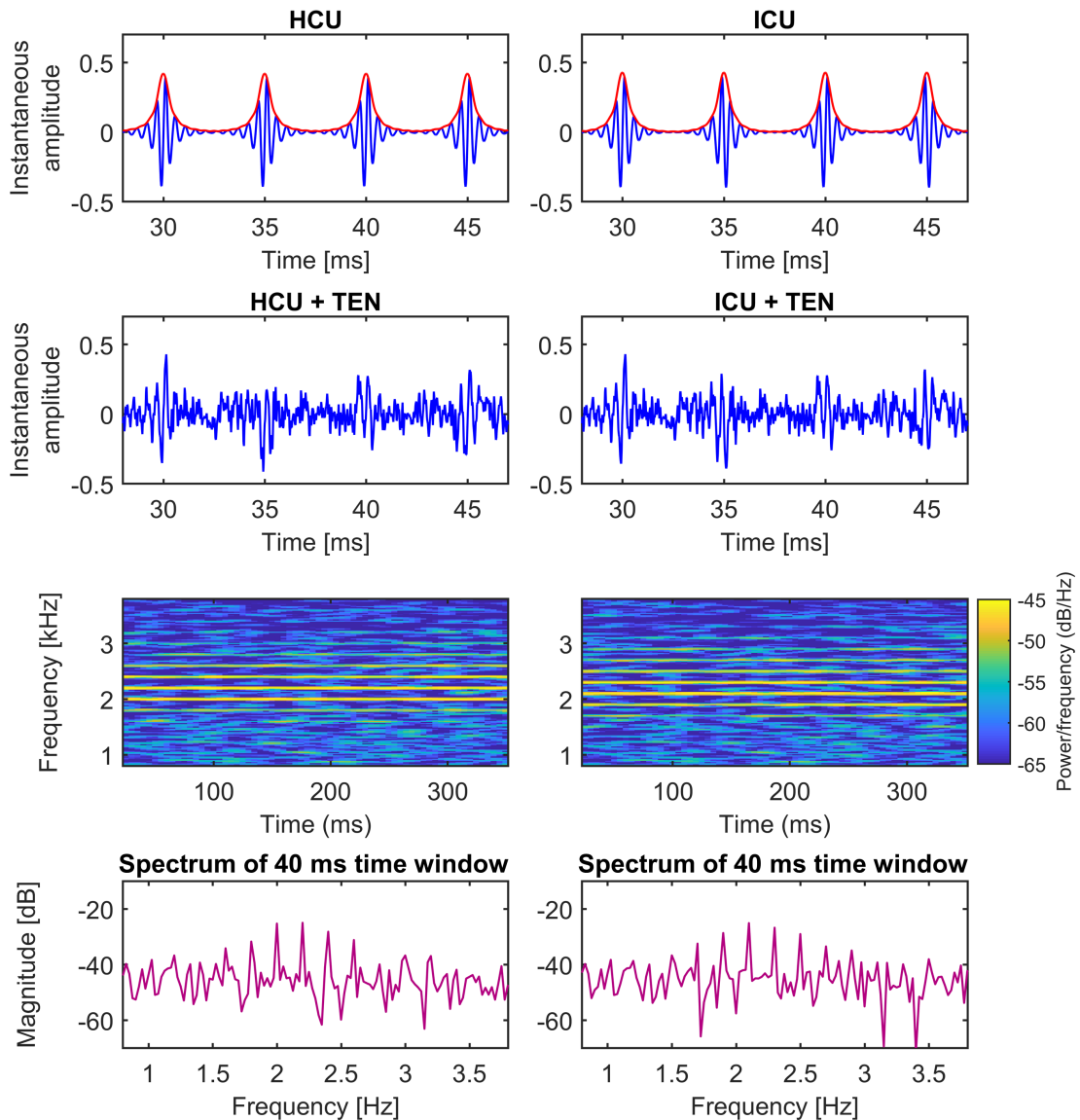


Figure 6.15: Harmonic and inharmonic stimuli with threshold-equalizing noise (TEN). Pictured are differing time windows of the harmonic complex tone with unresolved harmonics (HCU) and the frequency-shifted inharmonic complex tone with unresolved harmonics (ICU) with and without added TEN. Their fundamental frequencies F_0 are 200 Hz and the components of the ICU are shifted upwards by 100 Hz. The first row shows the instantaneous amplitudes of the complex tones without TEN and their symmetric envelopes (red). The second row shows the influence of the TEN on the instantaneous amplitude of the complex tones. The third row shows the spectrogram of the overall stimulus. The fourth row depicts the Fast-Fourier-Transform (FFT) of a 40 ms time window¹¹ of the stimuli. The FFT was calculated for a time window rather than the full stimulus duration of 375 ms, as calculating the spectrum for the whole stimulus duration of 375 ms would widely overestimate the “perceived” signal-to-noise ratio between the TEN and the complex tone.

¹¹ A window duration of 40 ms was chosen as a crude estimate for the human auditory temporal integration window. The choice of length for the temporal integration window is widely debated and the temporal integration window fluctuates with stimulus and task. (Balaguer-Ballester, E., Clark, N.R., Coath, M., Krumbholz, K. & Denham, S.L. (2010) Understanding Pitch Perception as a Hierarchical Process with Top-Down Modulation. In Lopez-Poveda, E.A., Palmer, A.R., Meddis, R. (eds) *The Neurophysiological Bases of Auditory Perception*. Springer Science + Business Media, pp. 201-210.).

To avoid non-linear phase effects, zero-phase filtering was implemented with MATLAB's 'filtfilt.m'-function. However, 'filtfilt.m' applies the created filter twice, forwards and backwards, effectively doubling its order. In order to maintain an effective roll-off of 30 dB/octave, the filter's roll-off was reduced to 15 dB/octave. The created stimuli no longer presented undesired signs of distortion¹² (Figure 6.15). However, the specified flat bandpass with a width of $F0$ around the centre frequency could no longer be obtained with this approach.

Continued email correspondence with Professor Moore¹³, University of Cambridge, revealed that stimuli were not in fact filtered with the described filter settings (flat pass-band around the centre frequency, 30 dB/octave roll-off), but individual harmonic components were adjusted in a manner that *simulates* these filter settings. This may explain the persistent discrepancies in the stimuli's spectra when generated stimuli were compared to recorded stimuli from the TFS1 software¹⁴ (Moore & Sek, 2009). For this *fourth phase* of the study, stimuli were no longer filtered to limit spectral content, but rather, harmonic components were scaled by a weighting matrix prior to summation, and thus, simulating the described filter properties.

Psychoacoustic paradigms

Behavioural discrimination abilities of HCU and ICU tones were assessed with a 3AFC test. In the individual condition, two HCU tones and one ICU tone were presented in randomised order. In the concatenated condition, two segments of the pattern HHHH and one segment of the pattern HIHI were presented, where H corresponds to the HCU tone and I corresponds to the ICU tone. Individual tones were presented with a duration of 375 ms and an ISI of 300 ms. In the concatenated condition, the individual segments of H or I tones were of 200 ms duration, with a 100 ms gap in between each segment. The ISI between two consecutive concatenated segments was 300 ms.

Adaptive procedure: The starting frequency shift between HCU and ICU stimuli was 100 Hz (which equals $0.5F0$). The frequency shift was adapted according to the 2-down/1-up procedure. The frequency shift was changed in line with Füllgrabe *et al.*

¹² Behavioural data obtained from lab members suggested that performance was not influenced by the distortion due to non-linear phase effects, as participants did not show improved performance for stimuli without distortions.

¹³ Email correspondence from March and April 2018.

¹⁴ The software to carry out the original TFS1 test can be obtained from the following source: <http://hearing.psychol.cam.ac.uk/>.

(2014) by a factor of $(1.25)^3$ until the first reversal, by a factor of $(1.25)^2$ until the second reversal and by a factor of 1.25 from the third reversal onward. The block was terminated after the eighth reversal and the threshold was calculated as the geometric mean of the frequency shifts at the last six reversals.

Non-adaptive procedure: If participants' discrimination abilities were poor and the adaptive procedure returned to the maximum frequency shift of $0.5F0$ after the first reversal, the procedure was changed from adaptive to non-adaptive. In this case, the frequency shift was kept constant at $0.5F0$. Performance was assessed as the percentage of correct discriminations across 25 repetitions per block.

Statistical analysis

Data was obtained with either the adaptive or non-adaptive procedure as outlined in the previous section, depending on the participants' discrimination abilities. To allow comparison of the data, results were converted to d' values (Green & Swets, 1974) in line with procedures described by Hopkins and Moore (2007). The conversion followed the table by Hacker and Ratcliff (1979). The adaptive procedure tracked the 70.7% correct point on the psychometric function, which corresponds to an interpolated value of 1.268 for d' in a 3AFC, 2-down/1-up procedure. Estimates of the value which would be measured for a frequency shift of $0.5F0$, as measured in the non-adaptive procedure, were calculated by dividing 1.268 by the measured threshold in the adaptive procedure and by multiplying this value by $0.5F0$ (Hopkins & Moore, 2007). A value of d' below 0.36 was considered as chance performance in line with procedures described by Hopkins and Moore (2011). This value was calculated using the binomial distribution to determine the probability of scoring n out of 50 trials correct by chance, with a probability $p = 0.33$ to score an individual trial correct by chance. The probability of scoring 22 or more trials correct by chance was less than 0.05, and thus, scores equal to or greater than 22 correct responses out of 50 (which corresponded to $d' \geq 0.36$) were considered to be significantly better than chance.

6.4.2 Results and discussion

Figure 6.16 illustrates discrimination results prior to conversion to d' values for a better understanding of the data. The left plot shows results for participants that were unable to reliably discriminate harmonic from inharmonic tones, and who were therefore

assessed on their discrimination performance for the maximum frequency shift. The right plot presents results of participants who were able to reliably discriminate harmonic and inharmonic tones for frequency shifts below the maximum frequency shift of $0.5F_0$. Results are presented as the estimate of the frequency shift at which participants achieve 70.7% correct discrimination.

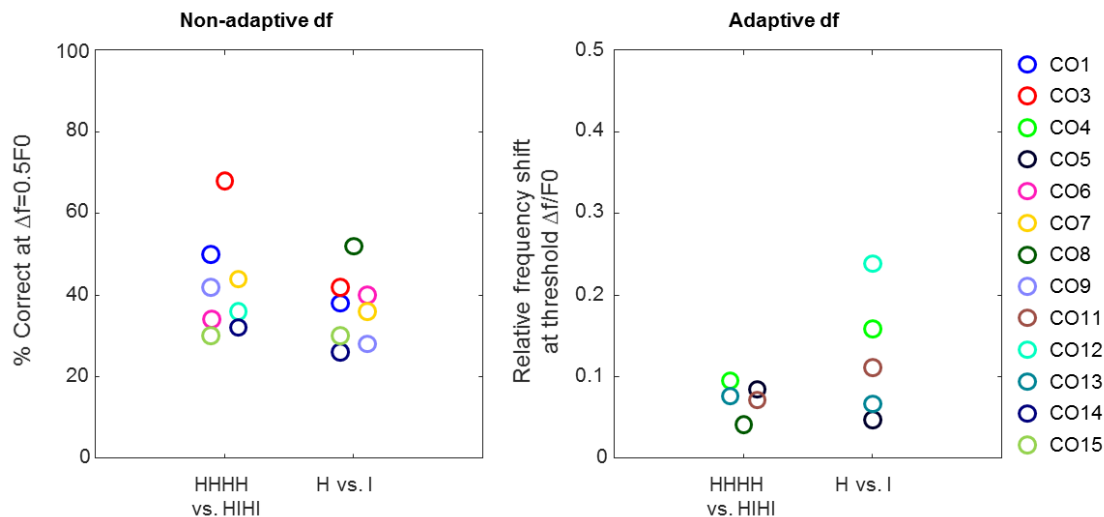


Figure 6.16: Psychoacoustic results for discrimination performance between harmonic (H) and inharmonic (I) stimuli.

Stimuli were presented individually (H vs. I) or in concatenated segments (HHHH vs. HIHI). When participants were able to reliably discriminate the ‘odd one out’ in the three-alternative forced choice paradigm, performance is indicated as a threshold based on the adaptive tracking procedure (right). In the case of poor discrimination abilities, performance was measured as percentage correct discrimination at the maximum frequency shift of $0.5F_0$ (left).

The d' values depicted in Figure 6.17 show that performance of six (concatenated presentation mode) and seven participants (individual presentation mode) was not significantly different from chance performance. No prominent bias towards better performance in one of the two presentation modes was observed (Figure 6.17, right plot). Most participants demonstrated no large performance differences with two exceptions: As indicated in Figure 6.17, participant ‘CO12’ was unable to detect the difference when tones were presented in concatenated segments ($d' = 0.09$), but achieved a threshold of 47.7 Hz frequency shift when tones were presented individually. In contrast, participant ‘CO8’ was able to achieve a very low (good) threshold of 8.2 Hz frequency shift when tones were presented in concatenated segments, but showed very poor performance when tones were presented individually with 52% correct detections ($d' = 0.62$), which was only marginally above chance performance ($d' < 0.36$). The reason for such a stark

performance difference in two participants with the effect in opposite directions remains elusive.

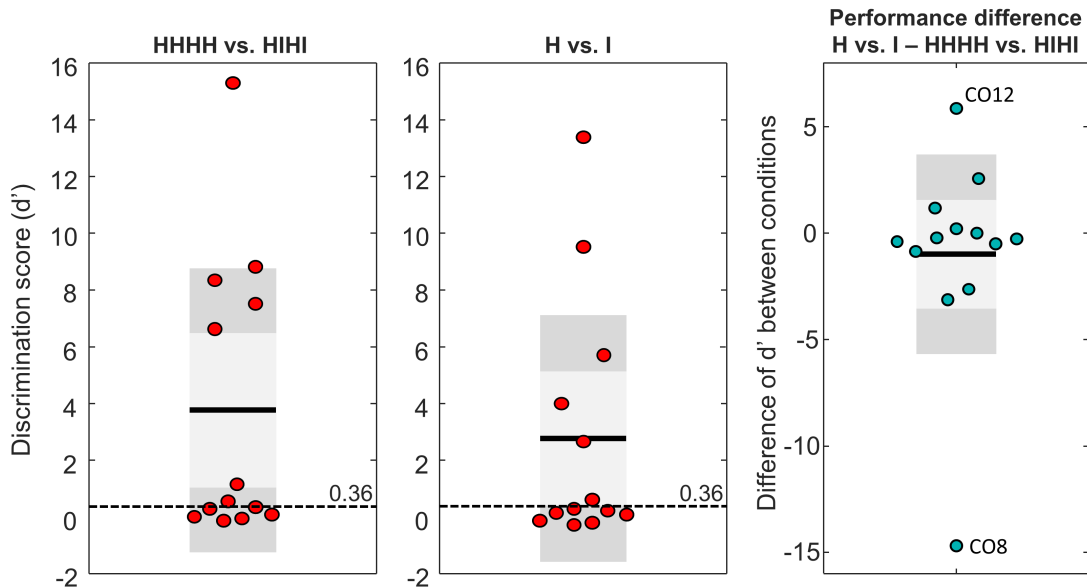


Figure 6.17: Comparison of discrimination performance between harmonic and inharmonic tones for two presentation modes.

Individual mean d' values for discrimination of harmonic (H) and frequency-shifted inharmonic (I) tones for the 'concatenated' presentation mode ($HHHH$ vs. $HIHI$, left) and the 'individual' presentation mode (H vs. I , middle). A value of $d' \leq 0.36$ indicates chance performance. The performance difference between the two presentation modes is visualized in the right plot. Descriptive statistics include the arithmetic means (black lines) and standard deviations (shaded grey boxes) of the group data.

Statistical analysis with a two-tailed non-parametric Wilcoxon signed rank test confirmed that the median difference- d' values (Figure 6.17, right) was not significantly different from zero ($W = 27$, $p = 0.367$). This supports the statement that performance was not significantly different between the two presentation modes, and thus, the presentation of individual tones rather than concatenated tones was not the source for the observed lack in discrimination performance in many NH participants during *Phase 3*.

6.5 Summary

In conclusion, findings from the different phases of this study illustrated the great difficulties with stimulus replication of the TFS1 stimuli due to lacking information in the literature. In *Phase 1*, psychoacoustic testing employing custom-designed harmonic-inharmonic tone pairs provided behavioural discrimination thresholds in line with those reported in the literature for the TFS1 test. However, neurophysiological measures of change detection were inconclusive. In *Phase 2*, stimuli were created more closely in line

with TFS1 stimuli and the neurophysiological paradigm concentrated on the maximum frequency shift between the HCU-ICU tone pair. MMWs were successfully measured for the pilot participant. In *Phase 3*, the same HCU-ICU tone pair as in *Phase 2* was employed for a cohort of eleven NH participants. Only three participants were able to discriminate the ICU tone from HCU tones with performance better than chance. Flat difference waves indicated no significant differences in neural processing of the ICU tones among HCU tones. *Phase 4* was concerned with the investigation of potential sources of the discrimination difficulties. Non-linear filter effects which had arisen during stimulus creation were avoided by modelling the desired filter effects and performance was assessed for individual stimulus presentation (in line with *Phases 1 – 3*) and concatenated stimulus presentation (in line with the TFS1 test by Moore and Sek (2009)). No significant difference in performance was observed for the two presentation modes, but overall more participants were able to discriminate HCU and ICU tones with approximately half of the participants performing above chance level.

To date, it is unknown what aspect of the stimulus design resulted in the difficulties in discrimination performance. The author believes that the only potentially remaining difference lies in the SNR between background TEN and the complex tone. In future work, stimuli should be created in collaboration with Moore and colleagues with the original code to avoid any potential discrepancies in stimulus design. However, it is very interesting how greatly discrimination performance varied within the NH cohort for HCU-ICU tone discrimination.

Further findings from *Phase 2* and *Phase 3* provided evidence for the elicitation of MMWs in response to a Schroeder-phase harmonic complex tone pair, supporting the feasibility of employing the MMW paradigm to objectively assess TFS processing abilities. However, MMW amplitudes were low and future work has to address whether the MMW can be successfully employed to assess Schroeder-phase discrimination for varying fundamental frequencies and in hearing impaired cohorts.

At this stage it should be noted that the Schroeder-phase harmonic complex tone offers a more promising assessment tool for TFS processing in hearing impaired cohorts than the HCU-ICU tone pair: Previous studies have shown that CI users can successfully discriminate Schroeder-phase tone pairs (Drennan *et al.*, 2008; Leijssen *et al.*, 2015). However, no studies have been reported in the literature that have investigated whether CI users are able to perform the TFS1 test. Based on difficulties of hearing impaired cohorts with the TFS1 test (Hopkins & Moore, 2007; 2011) it is unlikely that CI users

can successfully perform this test. It is essential to determine psychoacoustic tests that can be employed in participants with a wide range of hearing abilities, in order for the tests to be clinically applicable. Following this step, further research may establish the feasibility of employing the chosen TFS stimuli in neurophysiological tests to obtain objective measures of discrimination abilities.

Key Points

- The studies presented in this chapter addressed the research question Q3.1. MMWs could be observed for the Schroeder-phase harmonic complex tone pair, although statistical analysis provided adjusted p-values of 0.051 for the existence of a significant difference waveform.
- No MMWs were observed for the HCU-ICU tone pair, which is in line with lacking behavioural discrimination abilities.
- Aspects of stimulus design and presentation mode were investigated to explore the underlying source for discrimination difficulties, but no combination of parameters was found that successfully replicated TFS1-stimuli and matched discrimination performance reported in the literature.
- These findings, or parts thereof, were presented at the IERASG symposium, Warsaw 2017, and the 8th MMN conference, Helsinki 2018.

Chapter 7 General discussion

7.1 Thesis summary

The presented studies investigated the feasibility and clinical applicability of CAEP-based neurophysiological change detection measures as objective metrics of temporal auditory processing abilities.

In the first study presented in **Chapter 3**, MMWs were successfully measured in a NH cohort in response to AM cues (Q1.1). MMWs differed across AMD conditions according to the change saliency (Q1.2). Objective neural thresholds were successfully obtained (Q1.3) and showed significant correlations with behavioural AM detection thresholds (Q1.4). No significant correlations (after adjustment for multiple comparisons) were observed between speech-in-noise recognition and behavioural AM detection thresholds (Q1.5).

In the case study presented in **Chapter 4**, ACCs were successfully measured from a pilot participant with a CI in response to AM changes and also for a spectral control condition (Q-CS.1). The spectral control condition elicited ACCs of much greater amplitude and SNR compared to the AM change condition, highlighting one of the difficulties of assessing temporal features compared to spectral features. Neural responses showed strong electrical artefacts from CI stimulation prior to artefact reduction procedures. Continuous presentation of stimuli resulted in reduced pedestal artefacts from electrical stimulation compared to individual stimulus presentation due to the power-up and power-down of the device (Q-CS.2). CI artefacts were successfully reduced with the proposed automated ICA-based algorithm (Q-CS.2).

Findings from Study 2, which were outlined in **Chapter 5**, showed that MMWs could be successfully obtained from individuals with CIs in response to AM stimulus sound pairs (Q2.1). The CI artefact was successfully reduced with ICA despite differing

stimulus envelopes between standard and deviant stimuli (Q2.2). The introduction of the deviant-alone stimulus segment was beneficial for artefact reduction based on subtraction (without ICA) to calculate MMW2s, but data quality was inferior to MMW1s calculated with ICA-based artefact reduction (Q2.3). Individual neural thresholds could be estimated (Q2.4) and were significantly correlated with behavioural thresholds of AM detection (Q2.5). However, no significant correlations were observed between speech recognition in noise and behavioural AM detection thresholds (Q2.6). Data obtained from NH control participants showed similar morphology to the data from CI users. The additional subjectively loudness balanced condition confirmed that MMWs were not elicited based on remaining loudness cues (Q2.7).

Pilot studies presented in **Chapter 6** showed the feasibility of measuring behavioural (Phase 1) and neurophysiological (Phase 2) discrimination of tone pairs based on TFS cues (Q3.1). However, Study 3 showed that most NH participants were unable to discriminate the tone pair. This demonstrates the large variability in discrimination performance within a NH cohort. It also indicates stimulus replication issues of the TFS1 test stimuli.

7.2 Discussion of the main findings

The EEG-based metric provided the required temporal resolution to assess rapid temporal changes. EEG is non-invasive, cost-efficient and readily available, and therefore, it provides the optimal tool for research and clinical settings. The proposed methodologies such as neural threshold estimation based on CAEPs offer useful tools for clinical settings to aid rehabilitation procedures and diagnostics, as well as in basic auditory research which attempts to increase our understanding of how the brain processes complex tones.

Having a CAEP-based neurophysiological measure allows the use of complex acoustic stimuli, which has advantages over other peripheral neurophysiological measures such as ECAPs and EABRs, which are commonly elicited by simplistic stimuli such as click trains. As CAEPs can be elicited by complex acoustic stimuli and are measured at the cortical level, higher-order auditory processing may be assessed. Studies reported in the literature have shown that metrics assessing higher-order (central) processing show better links to speech perception outcomes in CI rehabilitation (Groenen

et al., 1996; Firszt *et al.*, 2002; Kelly *et al.*, 2005; Groenen *et al.*, 2009; Zhang *et al.*, 2011) than peripheral measures such as ECAPs and EABRs (Miller *et al.*, 2008). The CAEP-based metric has advantages over previously investigated continuous measures of temporal auditory processing such as the (E)ASSR with regards to its applicability in a clinical CI user cohort: Measurements can be obtained with the patients' clinical speech processors without the need for proprietary research equipment for each CI manufacturer, as is the case for EASSR measurements (Gransier *et al.*, 2016). However, continuous measures such as the (E)ASSR provide advantages with respect to the assessment of temporally evolving stimuli. In theory, continuous measures may provide a more accurate measure of temporal processing than their time-locked counterparts due to continuous integration of the perceived information over longer periods of time. In the case of time-locked change detection in CAEPs (MMW & ACC), the integration time window of sensory information is limited, as responses are typically observed between 100 ms and 400 ms after the acoustic change onset. For a 4-Hz AM stimulus this constitutes less than 2 AM cycles. The limited integration time window may reduce the sensitivity of CAEP-based change detection measures, as difficult to discriminate stimuli may require prolonged integration of information as indicated by increasing reaction times with task difficulty. It is possible that the exact time point of neural change detection ($\hat{=}$ decision making) exhibits an increasing temporal jitter with increasing task demand, which in turn leads to diminished change detection responses due to averaging. Despite these caveats, the results of the studies presented in **Chapters 3-6** show that it is possible to elicit meaningful change detection responses based on CAEPs.

Study 1 defined the novel framework of neural threshold estimation from MMW data incorporating morphology weighting of the obtained neural data. Findings demonstrated that the morphology weighting reduced the influence of random fluctuations in neural data, and thus, has a positive influence on objective neural threshold estimation from noise-affected data. Numerous studies reported in the literature have relied on visual assessment of neural data for neural threshold estimation (Harris *et al.*, 2007; Martin, 2007; Brown *et al.*, 2008; He *et al.*, 2014). The proposed methodology in Study 1 provides an objective alternative to such subjective neural threshold estimation. Other studies have investigated relationships between behavioural measures and MMN/ACC amplitudes and latencies (Hoppe *et al.*, 2010; Rahne *et al.*, 2010; Turgeon *et al.*, 2014; Brown *et al.*, 2015). However, the amplitude and latency are susceptible to the influence of random noise. It is preferable to employ amplitude averages over a time range

of interest (Rahne *et al.*, 2014) or to calculate the AUC (Lopez Valdes *et al.*, 2014; Waechter *et al.*, 2018), as the influence of noise would be reduced (assuming noise has a temporal average of zero).

It was demonstrated that the proposed ACC and MMW metrics are sensitive to the cortical processing underlying AM detection. Pilot studies described in **Chapter 4** and Appendix B investigated the ACC as a potential neural metric of AM detection. However, when presenting sounds to CI users under free-field conditions, it was not possible to control for unwanted cues in the ACC paradigm. Free-field presentation of stimuli in CI users could result in electrode changes at the acoustic change, which in itself can elicit a neural change response. Furthermore, in the ACC paradigm the ACC may be elicited by the sudden change in amplitude at the acoustic change from unmodulated to modulated noise sound, rather than the detection of AM. For this reason and also due to more robust¹⁵ measurements of the neural change response in MMW paradigms (Lopez Valdes *et al.*, 2015), Study 2 and Study 3 focused on the feasibility of employing the MMW paradigm to obtain objective neural indications of discrimination performance.

One of the great challenges addressed in the presented research studies was the desire to employ EEG methodologies on an individual level. A vast majority of EEG research investigates group level differences. Group level analysis is very useful in increasing the understanding of the auditory system by comparing neural activity between conditions or cohorts. However, for clinical applications it is necessary to acquire individual information that may help in diagnosis or expectation management of individual rehabilitation outcomes. The neural threshold approach proposed in Study 1 and Study 2 takes a step towards individual assessment of auditory discrimination abilities. With continuous advancements in technology, data quality is bound to improve and with it the scope for new and improved methodologies.

The mind map in Figure 7.1 highlights the inter-dependencies of the presented research. Assessment methods and their applications are manifold, but each application brings its own requirements and challenges, e.g. psychoacoustics require participants who are able to provide reliable feedback. In the case of assessing the applicability of CAEPs in CI rehabilitation, challenges included the electrical artefact as well as the vast variability in the cohort demographics. CI users have complex histories with a range of

¹⁵ Note that data acquisition times differed between ACC and MMW paradigm. Data acquisition was planned independently to optimise each paradigm.

influencing factors such as cause of deafness, duration of deafness pre-implantation, implanted device type, stimulation rates among many other influencing parameters. A great challenge lies in the implementation of a research study with a tightly controlled CI cohort that is matched with regards to the previously mentioned parameters. Such an undertaking would require a collaboration of multiple research centres and clinics to gather data for a sufficiently large sample size. This and other challenges are outlined in the next Section.

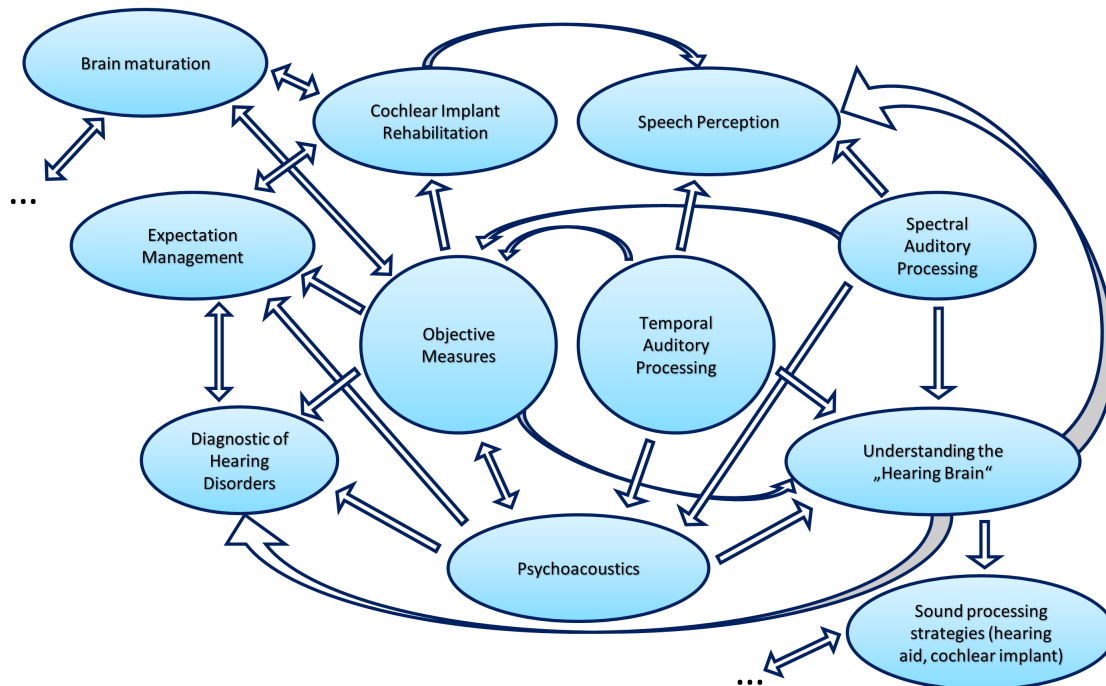


Figure 7.1: Mindmap illustrating the complexity of auditory research.

The mind-map focuses on the research topics of interest relating to the research questions posed in Chapter 2, namely the investigation of objective measures, temporal auditory processing and their importance for cochlear implant (CI) rehabilitation. This schematic does not claim to provide a complete account of auditory research.

7.3 Challenges of the research

Restrictions in the data acquisition time pose the greatest challenge in designing research studies based on EEG. As discussed previously, increasing the number of stimulus repetitions per condition improves outcome SNRs. Additionally, it would be beneficial to assess neurophysiological change detection for additional AMDs to improve the accuracy of NT estimation. Furthermore, complementing the experimental paradigm with additional AM rates (e.g. 40 Hz and 100 Hz) would be of interest to provide a more complete overview of AM detection abilities in line with a temporal modulation transfer

function. The trade-off between the informational value of the gathered data and the data acquisition time is a great challenge in the experimental design and requires thorough deliberation in the study design phase, especially when acquiring data in clinical settings and from paediatric cohorts.

Research studies with CI users present their own range of challenges from stimulus presentation to low cohort sizes. Stimuli may be presented in realistic, everyday free-field conditions with the patients' own speech processors, which limits the control over internal processes of the speech processor such as automatic gain control settings. Alternatively, stimuli can be presented via research speech processors with direct stimulation, which allows full control over the conveyed stimulation. In the presented CI study, it was of interest to assess the relationship between individual behavioural and neural thresholds of AM detection, and thus, any effects of stimulus presentation mode are reflected in both measures.

The challenge of low cohort sizes in studies with CI cohorts has been addressed. Collaborations across multiple CI centres would increase the potential cohort size. Ireland has one centralised National Cochlear Implant Programme, and thus, collaborations would have to be created internationally. CI programmes in the UK would be best suited to collaborate with due to the geographical and linguistic proximity. On the one hand, the employed speech tests already employed a British sentence corpus (BKB test), allowing data acquisition with the existing experimental paradigm from a UK cohort. On the other hand, employing British speech tests in an Irish cohort may negatively impact outcome scores if CI users struggle with the different accent.

7.4 Clinical impact of the research

7.4.1 Cochlear implant rehabilitation

CIs have restored functional hearing for many individuals, but there is great variability in rehabilitation outcomes. The reasons for this variability are poorly understood. CAEPs and the proposed methodologies in the presented studies may offer a useful tool to increase our understanding of the neural mechanisms underlying electrical hearing. Advancements in speech processing strategies with regards to TFS cues will give rise to a demand for objective assessment tools of TFS processing abilities in CI users.

Further research is necessary to develop a reliable neurophysiological measure of TFS processing abilities to complement existing psychoacoustic tests.

Speech perception in CI users commonly improves throughout the first year after switch-on. Psychoacoustic discrimination abilities based on non-linguistic, but speech-relevant stimulus pairs provide a good indicator of speech perception outcomes later in the rehabilitation process (Drennan *et al.*, 2015). Therefore, neural discrimination responses obtained from such stimulus pairs at switch-on may provide a good predictor of future rehabilitation success, which may be validated with a longitudinal study.

Fitting procedures may be aided by assessing basic auditory discrimination abilities (e.g. AM detection) with the proposed objective measures. Should the obtained objective data suggest lacking discrimination abilities, the clinical team can initiate intervention procedures. Such procedures could address whether the chosen speech processing strategy is adequate or whether the stimulation rate is suitable for the patient. For example, if a patient's speech processor uses a sophisticated new strategy that aims to increase the conveyed TFS information, but very basic AM sensitivity is lacking, it should be considered to change the strategy.

Overall, the presented research takes a step towards an objective measure of central auditory processing which may assist in expectation management and fitting procedures during CI rehabilitation. The proposed CAEP-based objective measures may not inform the clinician of the exact parameter values, but they can provide a more general insight into whether basic auditory information can be processed appropriately, enabling timely intervention opportunities.

7.4.2 Auditory neuropathy spectrum disorder

Auditory neuropathy spectrum disorder (ANSD) is a hearing disorder associated with temporal processing deficits. The affected population shows great variability across and within patients, which makes its diagnosis very challenging (Sharma & Cardon, 2015). In general, ANSD is associated with fluctuating hearing abilities, poor speech perception and particular difficulty with understanding speech in noisy conditions (Kraus *et al.*, 2000). Pure tone thresholds can vary across the full audiometric spectrum and commonly do not match hearing abilities (Starr *et al.*, 1996; Berlin *et al.*, 2005). Spectral processing is largely unaffected in ANSD and speech perception difficulties are rooted in temporal processing deficits caused by dysynchronous neuronal firing (Zeng *et al.*, 1999;

Michalewski *et al.*, 2005; Zeng *et al.*, 2005; Berlin *et al.*, 2010). The cochlea function is commonly normal (or near normal) as indicated by normal otoacoustic emissions, but ABRs are often absent or highly abnormal (Starr *et al.*, 1996). This indicates a disruption of the healthy auditory pathway between the cochlea and the brainstem. The lack of measurable ABRs supports the hypothesis of potential causes based on diminished neuronal firing or impaired neural synchrony. However, at the level of the cortex, CAEPs have been successfully measured (Michalewski *et al.*, 2005; Dimitrijevic *et al.*, 2011; He *et al.*, 2013; He *et al.*, 2015) albeit delayed and with decreased amplitudes compared to NH cohorts. Given the successful elicitation and measurement of CAEPs in ANSD cohorts, the proposed CAEP-based objective measure of temporal auditory processing may be applicable in the complex diagnosis of this hearing disorder. For a detailed review on ANSD the reader is referred to Sharma and Cardon (2015).

7.5 Future research directions

A goal for future research is to integrate the findings from this research with previous research by our group. This would yield a combined test battery for the objective assessment of spectro-temporal auditory processing, which tests the full spectrum of acoustic cues important for successful speech perception. The proposed objective metric may be employed in longitudinal research studies to objectively assess brain plasticity after implantation and to monitor brain maturation in implanted infants, children and teenagers. Tremendous advancements in stem cell research suggest that in the near future it may be possible to restore cochlea function with stem cell treatment (Chen *et al.*, 2012; Hu & Ulfendahl, 2013; Park, 2015; Mittal *et al.*, 2017). Such successful restoration of cochlea function would further increase the demand for objective metrics of auditory processing to assess treatment outcomes and to monitor the neural adaptation after prolonged hearing loss.

The promising findings from studies presented in **Chapter 3** and **Chapter 5** encourage further research into the MMW as an objective metric of AM discrimination. A recent study by (Erb *et al.*, 2018) has demonstrated that temporal sensitivity, as measured with a behavioural AM rate discrimination paradigm after CI switch-on, is a reliable predictor for speech recognition outcomes at 6 months post-implantation in CI users. This evidence encourages the inclusion of AM rate discrimination conditions in

future research studies to complement the presented research with regards to the influence of the AMD on discrimination abilities.

As stated in Section 2.4.1, the MMW/MMN can be observed across all age groups from new-borns to adults. Nonetheless, future research studies should validate the proposed paradigms which assess AM detection for varying AMDs across age groups to evaluate the influence of brain maturation on the obtained neural thresholds. The MMW morphology may vary across age groups, which would affect the objective assessment and quantification of data. It has to be validated whether the TOIs and ROIs are consistent across age groups to successfully employ the proposed objective neural threshold estimation procedures. It should also be noted that feasible data acquisition times vary between adult and paediatric cohorts and increased influence of movement artefact should be expected in paediatric data.

Studies in **Chapter 4** and **Chapter 5** employed a multi-channel EEG set-up to enable CI artefact rejection based on ICA. However, the multi-channel approach is not clinically friendly due to its lengthy set-up time. Thus, it is of interest to determine whether the proposed subtraction-based artefact reduction introduced in **Chapter 5** may provide an alternative to achieve adequate artefact reduction in the high-sampling rate single-channel set-up which was employed in the study presented in **Chapter 3**.

Findings from studies presented in **Chapter 6** did not fully demonstrate the MMW as a potential objective metric of TFS processing. Although TFS processing may be encoded in the neural processes underlying MMW elicitation, amplitudes were very low and many stimulus repetitions would be required to reach a satisfactory SNR. Given the importance of TFS processing for functional hearing and the increasing interest in improving the conveyed TFS cues in CI speech processing strategies (Wilson, 2000; Hochmair *et al.*, 2006; Arnoldner *et al.*, 2007; Krenmayr *et al.*, 2011; Müller *et al.*, 2012; Qi *et al.*, 2012; Li *et al.*, 2013; Churchill *et al.*, 2014; Apoux *et al.*, 2015), objective metrics remain a very active area of scientific research.

7.6 Final conclusions

The body of research from the studies presented provides a novel methodology to assess cortical processes involved in temporal auditory processing. The non-invasive EEG-based metric offers a promising tool to assess changes in the rapid temporal

dynamics of sound. Although its applicability may be limited with regards to the assessment of TFS processing abilities due to the subtlety of the acoustic cues, it was shown that the proposed methodologies provide a promising tool to assess AM detection abilities in both, NH and clinical CI user cohorts. The research questions posed in **Chapter 2** were addressed during the course of multiple studies. In conclusion, the main findings indicate that the developed objective metric may provide a promising tool to assess temporal aspects of auditory processing in clinical hearing rehabilitation.

References

- Abbas, P.J. & Brown, C.J. (2006) Utility of electrically evoked potentials in cochlear implant users. In Cooper, H.R., Craddock, L.C. (eds) *Cochlear implants- A practical guide*. Whurr Publishers, pp. 245-273.
- Abbas, P.J. & Miller, C.A. (2004) Biophysics and Physiology. In Zeng, F.G., Popper, A.N., Fay, R.R. (eds) *Cochlear Implants- Auditory Protheses and Electric Hearing*. Springer Science+Business Media, LLC, pp. 149-212.
- Alexandrov, A.A., Boricheva, D.O., Pulvermuller, F. & Shtyrov, Y. (2011) Strength of word-specific neural memory traces assessed electrophysiologically. *PloS one*, **6**, e22999.
- Alho, K. (1995) Cerebral generators of mismatch negativity (MMN) and its magnetic counterpart (MMNm) elicited by sound changes. *Ear and hearing*, **16**, 38-51.
- Allen, J., Kraus, N. & Bradlow, A. (2000) Neural representation of consciously imperceptible speech sound differences. *Perception & psychophysics*, **62**, 1383-1393.
- ANSI (1994) ANSI S1.1-1994. American National Standard Acoustical Terminology. American National Standards Institute, New York.
- Apoux, F., Youngdahl, C.L., Yoho, S.E. & Healy, E.W. (2015) Dual-carrier processing to convey temporal fine structure cues: Implications for cochlear implants. *The Journal of the Acoustical Society of America*, **138**, 1469-1480.
- Arnoldner, C., Riss, D., Brunner, M., Durisin, M., Baumgartner, W.D. & Hamzavi, J.S. (2007) Speech and music perception with the new fine structure speech coding strategy: preliminary results. *Acta oto-laryngologica*, **127**, 1298-1303.
- Axon, P.R., Temple, R.H., Saeed, S.R. & Ramsden, R.T. (1998) Cochlear ossification after meningitis. *The American journal of otology*, **19**, 724-729.
- Bacon, S.P. & Gleitman, R.M. (1992) Modulation detection in subjects with relatively flat hearing losses. *Journal of speech and hearing research*, **35**, 642-653.

- Bacon, S.P. & Viemeister, N.F. (1985) Temporal modulation transfer functions in normal-hearing and hearing-impaired listeners. *International journal of audiology*, **24**, 117-134.
- Balaguer-Ballester, E., Clark, N.R., Coath, M., Krumbholz, K. & Denham, S.L. (2010) Understanding Pitch Perception as a Hierarchical Process with Top-Down Modulation. In Lopez-Poveda, E.A., Palmer, A.R., Meddis, R. (eds) *The Neurophysiological Bases of Auditory Perception*. Springer Science + Business Media, pp. 201-210.
- Baldeweg, T., Klugman, A., Gruzelier, J. & Hirsch, S.R. (2004) Mismatch negativity potentials and cognitive impairment in schizophrenia. *Schizophrenia Research*, **69**, 203-217.
- Bartha-Doering, L., Deuster, D., Giordano, V., am Zehnhoff-Dinnesen, A. & Dobel, C. (2015) A systematic review of the mismatch negativity as an index for auditory sensory memory: From basic research to clinical and developmental perspectives. *Psychophysiology*, **52**, 1115-1130.
- Bench, J., Kowal, A. & Bamford, J. (1979) The BKB (Bamford-Kowal-Bench) sentence lists for partially-hearing children. *British journal of audiology*, **13**, 108-112.
- Benjamini, Y. & Yekutieli, D. (2001) The control of the false discovery rate in multiple testing under dependency. *Annals of statistics*, 1165-1188.
- Berlin, C.I., Hood, L.J., Morlet, T., Wilensky, D., John, P.S., Montgomery, E. & Thibodaux, M. (2005) Absent or Elevated Middle Ear Muscle Reflexes in the Presence of Normal Otoacoustic Emissions: A Universal Finding in 136 Cases of Auditory Neuropathy/Dys-synchrony. *Journal of the American Academy of Audiology*, **16**, 546-553.
- Berlin, C.I., Hood, L.J., Morlet, T., Wilensky, D., Li, L., Mattingly, K.R., Taylor-Jeanfreau, J., Keats, B.J.B., John, P.S., Montgomery, E., Shallop, J.K., Russell, B.A. & Frisch, S.A. (2010) Multi-site diagnosis and management of 260 patients with Auditory Neuropathy/Dys-synchrony (Auditory Neuropathy Spectrum Disorder*). *International journal of audiology*, **49**, 30-43.
- Bertoli, S., Heimberg, S., Smurzynski, J. & Probst, R. (2001) Mismatch negativity and psychoacoustic measures of gap detection in normally hearing subjects. *Psychophysiology*, **38**, 334-342.
- Botros, A. & Psarros, C. (2010) Neural response telemetry reconsidered: I. The relevance of ECAP threshold profiles and scaled profiles to cochlear implant fitting. *Ear and hearing*, **31**, 367-379.
- Brannon, E.M., Libertus, M.E., Meck, W.H. & Woldorff, M.G. (2008) Electrophysiological Measures of Time Processing in Infant and Adult Brains: Weber's Law Holds. *Journal of cognitive neuroscience*, **20**, 193-203.

- Brown, C.J., Etler C Fau - He, S., He S Fau - O'Brien, S., O'Brien S Fau - Erenberg, S., Erenberg S Fau - Kim, J.-R., Kim Jr Fau - Dhuldhoya, A.N., Dhuldhoya An Fau - Abbas, P.J. & Abbas, P.J. (2008) The electrically evoked auditory change complex: preliminary results from nucleus cochlear implant users.
- Brown, C.J., Hughes, M.L., Luk, B., Abbas, P.J., Wolaver, A. & Gervais, J. (2000) The relationship between EAP and EABR thresholds and levels used to program the nucleus 24 speech processor: data from adults. *Ear and hearing*, **21**, 151-163.
- Brown, C.J., Jeon, E.K., Chiou, L.K., Kirby, B., Karsten, S.A., Turner, C.W. & Abbas, P.J. (2015) Cortical Auditory Evoked Potentials Recorded From Nucleus Hybrid Cochlear Implant Users. *Ear and hearing*, **36**, 723-732.
- Brown, C.J., Jeon, E.K., Driscoll, V., Mussoi, B., Deshpande, S.B., Gfeller, K. & Abbas, P.J. (2017) Effects of Long-Term Musical Training on Cortical Auditory Evoked Potentials. *Ear and hearing*, **38**, e74-e84.
- Burkard, R.F., Eggermont, J.J. & Don, M. (2007) *Auditory Evoked Potentials: Basic Principles and Clinical Application*. Lippincott Williams & Wilkins.
- Butler, B.E. & Trainor, L.J. (2012) Sequencing the Cortical Processing of Pitch-Evoking Stimuli using EEG Analysis and Source Estimation. *Frontiers in Psychology*, **3**, 180.
- Byrne, D., Dillon, H., Tran, K., Arlinger, S., Wilbraham, K., Cox, R., Hagerman, B., Hetu, R., Kei, J., Lui, C., Kiessling, J., Kotby, M.N., Nasser, N.H.A., El Kholy, W.A.H., Nakanishi, Y., Oyer, H., Powell, R., Stephens, D., Meredith, R., Sirimanna, T., Tavartkiladze, G., Frolenkov, G.I., Westerman, S. & Ludvigsen, C. (1994) An international comparison of long-term average speech spectra. *The Journal of the Acoustical Society of America*, **96**, 2108-2120.
- Carlyon, R.P. & Shackleton, T.M. (1994) Comparing the fundamental frequencies of resolved and unresolved harmonics: Evidence for two pitch mechanisms? *The Journal of the Acoustical Society of America*, **95**, 3541-3554.
- Cazals, Y., Pelizzone, M., Saudan, O. & Boex, C. (1994) Low-pass filtering in amplitude modulation detection associated with vowel and consonant identification in subjects with cochlear implants. *The Journal of the Acoustical Society of America*, **96**, 2048-2054.
- Chatterjee, M. & Oberzut, C. (2011) Detection and rate discrimination of amplitude modulation in electrical hearing. *The Journal of the Acoustical Society of America*, **130**, 1567-1580.
- Chen, W., Jongkamonwiwat, N., Abbas, L., Eshtan, S.J., Johnson, S.L., Kuhn, S., Milo, M., Thurlow, J.K., Andrews, P.W., Marcotti, W., Moore, H.D. & Rivolta, M.N. (2012) Restoration of auditory evoked responses by human ES-cell-derived otic progenitors. *Nature*, **490**, 278-282.

- Cheng, Y.Y., Wu, H.C., Tzeng, Y.L., Yang, M.T., Zhao, L.L. & Lee, C.Y. (2015) Feature-specific transition from positive mismatch response to mismatch negativity in early infancy: mismatch responses to vowels and initial consonants. *International journal of psychophysiology : official journal of the International Organization of Psychophysiology*, **96**, 84-94.
- Cheour, M., Alho, K., Ceponiene, R., Reinikainen, K., Sainio, K., Pohjavuori, M., Aaltonen, O. & Naatanen, R. (1998) Maturation of mismatch negativity in infants. *International journal of psychophysiology : official journal of the International Organization of Psychophysiology*, **29**, 217-226.
- Churchill, T.H., Kan, A., Goupell, M.J. & Litovsky, R.Y. (2014) Spatial hearing benefits demonstrated with presentation of acoustic temporal fine structure cues in bilateral cochlear implant listeners. *The Journal of the Acoustical Society of America*, **136**, 1246.
- Ciorba, A., Bianchini, C., Pelucchi, S. & Pastore, A. (2012) The impact of hearing loss on the quality of life of elderly adults. *Clinical Interventions in Aging*, **7**, 159-163.
- Clark, G. (2003) *Cochlear Implants-Fundamentals and Applications*. Springer, New York.
- Cooper, H.R. (2006) Selection criteria and prediction of outcomes. In Cooper, H.R., Craddock, L.C. (eds) *Cochlear Implants- A Practical Guide*. Whurr Publishers, pp. 132-150.
- Crosse, M.J., Di Liberto, G.M., Bednar, A. & Lalor, E.C. (2016) The Multivariate Temporal Response Function (mTRF) Toolbox: A MATLAB Toolbox for Relating Neural Signals to Continuous Stimuli. *Frontiers in human neuroscience*, **10**.
- Davis, A., McMahon, C.M., Pichora-Fuller, K.M., Russ, S., Lin, F., Olusanya, B.O., Chadha, S. & Tremblay, K.L. (2016) Aging and Hearing Health: The Life-course Approach. *The Gerontologist*, **56 Suppl 2**, S256-267.
- De Ceulaer, G., Swinnen, F., Pascoal, D., Philips, B., Killian, M., James, C., Govaerts, P.J. & Dhooge, I. (2015) Conversion of adult Nucleus(R) 5 cochlear implant users to the Nucleus(R) 6 system. *Cochlear implants international*, **16**, 222-232.
- de Cheveigne, A. (2005) Pitch Perception Models. In Plack, C.J., Oxenham, A.J., Fay, R.R., Popper, A.N. (eds) *Pitch*. Springer New York, pp. 169-233.
- De Ruiter, A.M., Debruyne, J.A., Chenault, M.N., Francart, T. & Brokx, J.P. (2015) Amplitude Modulation Detection and Speech Recognition in Late-Implanted Prelingually and Postlingually Deafened Cochlear Implant Users. *Ear and hearing*, **36**, 557-566.
- de Winter, J.C., Gosling, S.D. & Potter, J. (2016) Comparing the Pearson and Spearman correlation coefficients across distributions and sample sizes: A tutorial using simulations and empirical data. *Psychological methods*, **21**, 273-290.

- Delorme, A. & Makeig, S. (2004) EEGLAB: an open source toolbox for analysis of single-trial EEG dynamics including independent component analysis. *Journal of neuroscience methods*, **134**, 9-21.
- Deouell, L.Y., Parnes, A., Pickard, N. & Knight, R.T. (2006) Spatial location is accurately tracked by human auditory sensory memory: evidence from the mismatch negativity. *The European journal of neuroscience*, **24**, 1488-1494.
- Deprez, H., Hofmann, M., van Wieringen, A., Wouters, J. & Moonen, M. (2014) Cochlear Implant Artifact Rejection in Electrically Evoked Auditory Steady State Responses *22nd European Signal Processing Conference (EUSIPCO)*, Lisbon.
- Desjardins, R.N., Trainor, L.J., Hevenor, S.J. & Polak, C.P. (1999) Using mismatch negativity to measure auditory temporal resolution thresholds. *Neuroreport*, **10**, 2079-2082.
- Dimitrijevic, A., Alsamri, J., John, M.S., Purcell, D., George, S. & Zeng, F.G. (2016) Human Envelope Following Responses to Amplitude Modulation: Effects of Aging and Modulation Depth. *Ear and hearing*, **37**, e322-335.
- Dimitrijevic, A., Lolli, B., Michalewski, H.J., Pratt, H., Zeng, F.G. & Starr, A. (2009) Intensity changes in a continuous tone: auditory cortical potentials comparison with frequency changes. *Clinical neurophysiology : official journal of the International Federation of Clinical Neurophysiology*, **120**, 374-383.
- Dimitrijevic, A., Michalewski, H.J., Zeng, F.G., Pratt, H. & Starr, A. (2008) Frequency changes in a continuous tone: auditory cortical potentials. *Clinical neurophysiology : official journal of the International Federation of Clinical Neurophysiology*, **119**, 2111-2124.
- Dimitrijevic, A. & Ross, B. (2008) Neural generators of the auditory steady-state response. In Rance, G. (ed) *Auditory Steady-State Response: Generation, Recording, and Clinical Application*. Plural Publishing, San Diego, pp. 83-108.
- Dimitrijevic, A., Starr, A., Bhatt, S., Michalewski, H.J., Zeng, F.-G. & Pratt, H. (2011) Auditory cortical N100 in pre- and post-synaptic auditory neuropathy to frequency or intensity changes of continuous tones. *Clinical neurophysiology : official journal of the International Federation of Clinical Neurophysiology*, **122**, 594-604.
- Dincer D'Alessandro, H., Ballantyne, D., Boyle, P.J., De Seta, E., DeVincentiis, M. & Mancini, P. (2017) Temporal Fine Structure Processing, Pitch, and Speech Perception in Adult Cochlear Implant Recipients. *Ear and hearing*.
- Dinces, E., Chobot-Rhodd, J. & Sussman, E. (2009) Behavioral and electrophysiological measures of auditory change detection in children following late cochlear implantation: a preliminary study. *International journal of pediatric otorhinolaryngology*, **73**, 843-851.

- Drennan, W.R., Longnion, J.K., Ruffin, C. & Rubinstein, J.T. (2008) Discrimination of Schroeder-phase harmonic complexes by normal-hearing and cochlear-implant listeners. *Journal of the Association for Research in Otolaryngology : JARO*, **9**, 138-149.
- Drennan, W.R., Won, J.H., Dasika, V.K. & Rubinstein, J.T. (2007) Effects of temporal fine structure on the lateralization of speech and on speech understanding in noise. *Journal of the Association for Research in Otolaryngology : JARO*, **8**, 373-383.
- Drennan, W.R., Won, J.H., Timme, A.O. & Rubinstein, J.T. (2015) Nonlinguistic Outcome Measures in Adult Cochlear Implant Users Over the First Year of Implantation. *Ear and hearing*.
- Dreschler, W.A. & Plomp, R. (1980) Relation between psychophysical data and speech perception for hearing-impaired subjects. I. *The Journal of the Acoustical Society of America*, **68**, 1608-1615.
- Dreschler, W.A. & Plomp, R. (1985) Relations between psychophysical data and speech perception for hearing-impaired subjects. II. *The Journal of the Acoustical Society of America*, **78**, 1261-1270.
- Drullman, R. (1995) Temporal envelope and fine structure cues for speech intelligibility. *The Journal of the Acoustical Society of America*, **97**, 585-592.
- Drullman, R., Festen, J.M. & Plomp, R. (1994) Effect of reducing slow temporal modulations on speech reception. *The Journal of the Acoustical Society of America*, **95**, 2670-2680.
- Edwards, E. & Chang, E.F. (2013) Syllabic (approximately 2-5 Hz) and fluctuation (approximately 1-10 Hz) ranges in speech and auditory processing. *Hearing research*, **305**, 113-134.
- Eggermont, J.J., Ponton, C.W., Don, M., Waring, M.D. & Kwong, B. (1997) Maturational delays in cortical evoked potentials in cochlear implant users. *Acta otolaryngologica*, **117**, 161-163.
- Erb, J., Ludwig, A.A., Kunke, D., Fuchs, M. & Obleser, J. (2018) Temporal Sensitivity Measured Shortly After Cochlear Implantation Predicts 6-Month Speech Recognition Outcome. *Ear and hearing*.
- Ernst, S.M.A. & Moore, B.C.J. (2013) Frequency difference limens at high frequencies for normal-hearing and hearing-impaired subjects. *Conf Proc 39th German Annual Conference on Acoustics (DAGA)*, pp. 1330-1331.
- Etymotic Research (2001) QuickSIN Speech in Noise Test, Elk Grove Village.
- Etymotic Research (2005) Bamford-Kowal-Bench Speech-in-Noise Test (Version 1.03) [Audio CD]. Elk Grove Village.
- Fastl, H. & Zwicker, E. (2007) *Psychoacoustics - Facts and Models*. Springer, Berlin.

- Festen, J.M. & Plomp, R. (1983) Relations between auditory functions in impaired hearing. *The Journal of the Acoustical Society of America*, **73**, 652-662.
- Files, B., Auer, E. & Bernstein, L. (2013) The visual mismatch negativity elicited with visual speech stimuli. *Frontiers in human neuroscience*, **7**.
- Firszt, J.B., Chambers, R.D. & Kraus, N. (2002) Neurophysiology of cochlear implant users II: comparison among speech perception, dynamic range, and physiological measures. *Ear and hearing*, **23**, 516-531.
- Fisher, D.J., Grant, B., Smith, D.M. & Knott, V.J. (2011) Effects of deviant probability on the 'optimal' multi-feature mismatch negativity (MMN) paradigm. *International journal of psychophysiology : official journal of the International Organization of Psychophysiology*, **79**, 311-315.
- Fishman, Y.I. (2014) The mechanisms and meaning of the mismatch negativity. *Brain topography*, **27**, 500-526.
- Fraser, M. & McKay, C.M. (2012) Temporal modulation transfer functions in cochlear implantees using a method that limits overall loudness cues. *Hearing research*, **283**, 59-69.
- Friesen, L.M. & Picton, T.W. (2010) A method for removing cochlear implant artifact. *Hearing research*, **259**, 95-106.
- Friesen, L.M. & Tremblay, K.L. (2006) Acoustic change complexes recorded in adult cochlear implant listeners. *Ear and hearing*, **27**, 678-685.
- Fu, Q.J. (2002) Temporal processing and speech recognition in cochlear implant users. *Neuroreport*, **13**, 1635-1639.
- Füllgrabe, C., Harland, A.J., Sek, A.P. & Moore, B.C.J. (2017) Development of a method for determining binaural sensitivity to temporal fine structure. *International journal of audiology*, **56**, 926-935.
- Füllgrabe, C., Moore, B.C.J. & Stone, M.A. (2014) Age-group differences in speech identification despite matched audiometrically normal hearing: contributions from auditory temporal processing and cognition. *Frontiers in aging neuroscience*, **6**, 347.
- Garrido, M.I., Kilner, J.M., Kiebel, S.J. & Friston, K.J. (2009a) Dynamic causal modeling of the response to frequency deviants. *Journal of neurophysiology*, **101**, 2620-2631.
- Garrido, M.I., Kilner, J.M., Stephan, K.E. & Friston, K.J. (2009b) The mismatch negativity: a review of underlying mechanisms. *Clinical neurophysiology : official journal of the International Federation of Clinical Neurophysiology*, **120**, 453-463.

- Geier, L., Barker, M., Fisher, L. & Opie, J. (1999) The effect of long-term deafness on speech recognition in postlingually deafened adult CLARION cochlear implant users. *The Annals of otology, rhinology & laryngology. Supplement*, **177**, 80-83.
- Gilley, P.M., Sharma, A., Dorman, M., Finley, C.C., Panch, A.S. & Martin, K. (2006) Minimization of cochlear implant stimulus artifact in cortical auditory evoked potentials. *Clinical neurophysiology : official journal of the International Federation of Clinical Neurophysiology*, **117**, 1772-1782.
- Giraud, A.L., Lorenzi, C., Ashburner, J., Wable, J., Johnsrude, I., Frackowiak, R. & Kleinschmidt, A. (2000) Representation of the temporal envelope of sounds in the human brain. *Journal of neurophysiology*, **84**, 1588-1598.
- Glasberg, B.R. & Moore, B.C.J. (1989) Psychoacoustic abilities of subjects with unilateral and bilateral cochlear hearing impairments and their relationship to the ability to understand speech. *Scandinavian audiology. Supplementum*, **32**, 1-25.
- Glasberg, B.R. & Moore, B.C.J. (1990) Derivation of auditory filter shapes from notched-noise data. *Hearing research*, **47**, 103-138.
- Glick, H. & Sharma, A. (2017) Cross-modal plasticity in developmental and age-related hearing loss: Clinical implications. *Hearing research*, **343**, 191-201.
- Gnansia, D., Lazard, D.S., Leger, A.C., Fugain, C., Lancelin, D., Meyer, B. & Lorenzi, C. (2014) Role of slow temporal modulations in speech identification for cochlear implant users. *International journal of audiology*, **53**, 48-54.
- Goldstein, J.L. (1973) An optimum processor theory for the central formation of the pitch of complex tones. *The Journal of the Acoustical Society of America*, **54**, 1496-1516.
- Goldsworthy, R.L., Delhorne, L.A., Braida, L.D. & Reed, C.M. (2013) Psychoacoustic and phoneme identification measures in cochlear-implant and normal-hearing listeners. *Trends Amplif*, **17**, 27-44.
- Goossens, T., Vercammen, C., Wouters, J. & van Wieringen, A. (2016) Aging Affects Neural Synchronization to Speech-Related Acoustic Modulations. *Frontiers in aging neuroscience*, **8**, 133.
- Graham, J.M. (2006) Medical and surgical considerations. In Cooper, H.R., Craddock, L.C. (eds) *Cochlear Implants- A Practical Guide*. Whurr Publishers, pp. 179-198.
- Gransier, R., Deprez, H., Hofmann, M., Moonen, M., van Wieringen, A. & Wouters, J. (2016) Auditory steady-state responses in cochlear implant users: Effect of modulation frequency and stimulation artifacts. *Hearing research*, **335**, 149-160.
- Green, D.M. & Swets, J.A. (1974) *Signal detection theory and psychophysics*. Krieger, New York.

- Groenen, P., Snik, A. & van den Broek, P. (1996) On the clinical relevance of mismatch negativity: results from subjects with normal hearing and cochlear implant users. *Audiology & neuro-otology*, **1**, 112-124.
- Groenen, P.A.P., Beynon, A.J., Snik, A.F.M. & Broek, P.v.d. (2009) Speech-evoked cortical potentials recognition in cochlear implant users and speech. *Scandinavian audiology*, **30**, 31-40.
- Groves, A.K. (2010) The challenge of hair cell regeneration. *Experimental biology and medicine (Maywood, N.J.)*, **235**, 434-446.
- Hablani, S. (2017) Towards Objective Measures of Assessing Temporal Fine Structure Processing in Normal Hearing. *Trinity Centre for Bioengineering*. Trinity College Dublin, The University of Dublin.
- Hacker, M.J. & Ratcliff, R. (1979) A revised table of d' for M-alternative forced choice. *Perception & psychophysics*, **26**, 168-170.
- Haigh Sarah, M., Matteis Mario, D., Coffman Brian, A., Murphy Timothy, K., Butera Christiana, D., Ward Kayla, L., Leiter-McBeth Justin, R. & Salisbury Dean, F. (2017) Mismatch negativity to pitch pattern deviants in schizophrenia. *European Journal of Neuroscience*, **46**, 2229-2239.
- Hall, J.W. & Swanepoel, D.W. (2010) Rationale for Objective Hearing Assessment. *Objective Assessment of Hearing*. Plural Pub Inc, pp. 1-5.
- Han, J.H. & Dimitrijevic, A. (2015) Acoustic change responses to amplitude modulation: a method to quantify cortical temporal processing and hemispheric asymmetry. *Front Neurosci*, **9**, 38.
- Harris, K.C. & Dubno, J.R. (2017) Age-related deficits in auditory temporal processing: Unique contributions of neural dyssynchrony and slowed neuronal processing. *Neurobiology of aging*, **53**, 150-158.
- Harris, K.C., Mills, J.H. & Dubno, J.R. (2007) Electrophysiologic correlates of intensity discrimination in cortical evoked potentials of younger and older adults. *Hearing research*, **228**, 58-68.
- Harris, K.C., Vaden, K.I., Jr. & Dubno, J.R. (2014) Auditory-evoked cortical activity: contribution of brain noise, phase locking, and spectral power. *Journal of basic and clinical physiology and pharmacology*, **25**, 277-284.
- Hay, R.A., Roach, B.J., Srihari, V.H., Woods, S.W., Ford, J.M. & Mathalon, D.H. (2015) Equivalent mismatch negativity deficits across deviant types in early illness schizophrenia-spectrum patients. *Biological psychology*, **105**, 130-137.
- Hazrati, O. & Loizou, P.C. (2012) The combined effects of reverberation and noise on speech intelligibility by cochlear implant listeners. *International journal of audiology*, **51**, 437-443.

- He, C., Hotson, L. & Trainor, L.J. (2007) Mismatch responses to pitch changes in early infancy. *Journal of cognitive neuroscience*, **19**, 878-892.
- He, C., Hotson, L. & Trainor, L.J. (2009) Maturation of cortical mismatch responses to occasional pitch change in early infancy: effects of presentation rate and magnitude of change. *Neuropsychologia*, **47**, 218-229.
- He, S., Grose, J.H., Teagle, H.F. & Buchman, C.A. (2014) Objective measures of electrode discrimination with electrically evoked auditory change complex and speech-perception abilities in children with auditory neuropathy spectrum disorder. *Ear and hearing*, **35**, e63-74.
- He, S., Grose, J.H., Teagle, H.F., Woodard, J., Park, L.R., Hatch, D.R. & Buchman, C.A. (2013) Gap detection measured with electrically evoked auditory event-related potentials and speech-perception abilities in children with auditory neuropathy spectrum disorder. *Ear and hearing*, **34**, 733-744.
- He, S., Grose, J.H., Teagle, H.F., Woodard, J., Park, L.R., Hatch, D.R., Roush, P. & Buchman, C.A. (2015) Acoustically evoked auditory change complex in children with auditory neuropathy spectrum disorder: a potential objective tool for identifying cochlear implant candidates. *Ear and hearing*, **36**, 289-301.
- Heng, J., Cantarero, G., Elhilali, M. & Limb, C.J. (2011) Impaired perception of temporal fine structure and musical timbre in cochlear implant users. *Hearing research*, **280**, 192-200.
- Hochmair, I., Nopp, P., Jolly, C., Schmidt, M., Schöber, H., Garnham, C. & Anderson, I. (2006) MED-EL Cochlear Implants: State of the Art and a Glimpse Into the Future. *Trends in Amplification*, **10**, 201-219.
- Hofmann, M. & Wouters, J. (2010) Electrically evoked auditory steady state responses in cochlear implant users. *Journal of the Association for Research in Otolaryngology : JARO*, **11**, 267-282.
- Hofmann, M. & Wouters, J. (2012) Improved electrically evoked auditory steady-state response thresholds in humans. *Journal of the Association for Research in Otolaryngology : JARO*, **13**, 573-589.
- Hopkins, K. & Moore, B.C.J. (2007) Moderate cochlear hearing loss leads to a reduced ability to use temporal fine structure information. *The Journal of the Acoustical Society of America*, **122**, 1055-1068.
- Hopkins, K. & Moore, B.C.J. (2009) The contribution of temporal fine structure to the intelligibility of speech in steady and modulated noise. *The Journal of the Acoustical Society of America*, **125**, 442-446.
- Hopkins, K. & Moore, B.C.J. (2010a) Development of a fast method for measuring sensitivity to temporal fine structure information at low frequencies. *International journal of audiology*, **49**, 940-946.

- Hopkins, K. & Moore, B.C.J. (2010b) The importance of temporal fine structure information in speech at different spectral regions for normal-hearing and hearing-impaired subjects. *The Journal of the Acoustical Society of America*, **127**, 1595-1608.
- Hopkins, K. & Moore, B.C.J. (2011) The effects of age and cochlear hearing loss on temporal fine structure sensitivity, frequency selectivity, and speech reception in noise. *The Journal of the Acoustical Society of America*, **130**, 334-349.
- Hopkins, K., Moore, B.C.J. & Stone, M.A. (2008) Effects of moderate cochlear hearing loss on the ability to benefit from temporal fine structure information in speech. *The Journal of the Acoustical Society of America*, **123**, 1140-1153.
- Hoppe, U., Liebscher, T. & Hornung, J. (2016) Anpassung von Cochleaimplantatsystemen. *HNO*.
- Hoppe, U., Wohlberedt, T., Danilkina, G. & Hessel, H. (2010) Acoustic change complex in cochlear implant subjects in comparison with psychoacoustic measures. *Cochlear implants international*, **11 Suppl 1**, 426-430.
- Houston, D.M. & Miyamoto, R.T. (2010) Effects of early auditory experience on word learning and speech perception in deaf children with cochlear implants: Implications for sensitive periods of language development. *Otology & neurotology : official publication of the American Otological Society, American Neurotology Society [and] European Academy of Otology and Neurotology*, **31**, 1248-1253.
- HSE (2011) HSE National audiology review, Health Service Executive.
- HSE (2013) Newborn Hearing Screening Programme.
- Hu, Z. & Ulfendahl, M. (2013) The potential of stem cells for the restoration of auditory function in humans. *Regenerative medicine*, **8**, 309-318.
- Hughes, M. (2012) *Objective Measures in Cochlear Implants*. Plural Publishing Inc.
- ICRA (1997) CD ICRA Noise Signals Version 0.3. In International Collegium of Rehabilitative Audiology, H.A.C.T.E.S.W.G. (ed).
- Innes-Brown, H., Tsongas, R., Marozeau, J. & McKay, C. (2016) Towards Objective Measures of Functional Hearing Abilities. *Advances in experimental medicine and biology*, **894**, 315-325.
- Jackson, H.M. & Moore, B.C.J. (2014) The role of excitation-pattern, temporal-fine-structure, and envelope cues in the discrimination of complex tones. *The Journal of the Acoustical Society of America*, **135**, 1356-1370.
- Jin, S.H., Liu, C. & Sladen, D.P. (2014) The effects of aging on speech perception in noise: comparison between normal-hearing and cochlear-implant listeners. *Journal of the American Academy of Audiology*, **25**, 656-665.

- Johnson, B.W., Tesan, G., Meng, D. & Crain, S. (2013) A custom-engineered MEG system for use with cochlear implant recipients. *Front. Hum. Neurosci. Conference Abstract: ACNS-2013 Australasian Cognitive Neuroscience Society Conference*.
- Katayama, J. & Polich, J. (1998) Stimulus context determines P3a and P3b. *Psychophysiology*, **35**, 23-33.
- Kelly, A.S., Purdy, S.C. & Thorne, P.R. (2005) Electrophysiological and speech perception measures of auditory processing in experienced adult cochlear implant users. *Clinical neurophysiology : official journal of the International Federation of Clinical Neurophysiology*, **116**, 1235-1246.
- Kim, J.R. (2015) Acoustic Change Complex: Clinical Implications. *Journal of audiology & otology*, **19**, 120-124.
- Kim, J.R., Brown, C.J., Abbas, P.J., Etler, C.P. & O'Brien, S. (2009) The effect of changes in stimulus level on electrically evoked cortical auditory potentials. *Ear and hearing*, **30**, 320-329.
- Kimura, M. & Takeda, Y. (2013) Task difficulty affects the predictive process indexed by visual mismatch negativity. *Frontiers in human neuroscience*, **7**, 267.
- Kirby, B.J. & Brown, C.J. (2015) Effects of Nonlinear Frequency Compression on ACC Amplitude and Listener Performance. *Ear and hearing*.
- Kraaijenga, V.J., Smit, A.L., Stegeman, I., Smilde, J.J., van Zanten, G.A. & Grolman, W. (2016) Factors that influence outcomes in cochlear implantation in adults, based on patient-related characteristics - a retrospective study. *Clinical otolaryngology : official journal of ENT-UK ; official journal of Netherlands Society for Oto-Rhino-Laryngology & Cervico-Facial Surgery*, **41**, 585-592.
- Kral, A. & O'Donoghue, G.M. (2010) Profound deafness in childhood. *The New England journal of medicine*, **363**, 1438-1450.
- Kraus, N., Bradlow, A.R., Cheatham, M.A., Cunningham, J., King, C.D., Koch, D.B., Nicol, T.G., McGee, T.J., Stein, L.K. & Wright, B.A. (2000) Consequences of neural asynchrony: A case of auditory neuropathy. *Journal of the Association for Research in Otolaryngology*, **1**, 33-45.
- Kraus, N., McGee, T., Micco, A., Sharma, A., Carrell, T. & Nicol, T. (1993a) Mismatch negativity in school-age children to speech stimuli that are just perceptibly different. *Electroencephalography and Clinical Neurophysiology/Evoked Potentials Section*, **88**, 123-130.
- Kraus, N., Micco, A.G., Koch, D.B., McGee, T., Carrell, T., Sharma, A., Wiet, R.J. & Weingarten, C.Z. (1993b) The mismatch negativity cortical evoked potential elicited by speech in cochlear-implant users. *Hearing research*, **65**, 118-124.

- Krenmayr, A., Visser, D., Schatzer, R. & Zierhofer, C. (2011) The effects of fine structure stimulation on pitch perception with cochlear implants. *Cochlear implants international*, **12 Suppl 1**, S70-72.
- Kujala, T., Kallio, J., Tervaniemi, M. & Näätänen, R. (2001) The mismatch negativity as an index of temporal processing in audition. *Clinical Neurophysiology*, **112**, 1712-1719.
- Kushnerenko, E., Ceponiene, R., Balan, P., Fellman, V. & Naatanen, R. (2002) Maturation of the auditory change detection response in infants: a longitudinal ERP study. *Neuroreport*, **13**, 1843-1848.
- Lalor, E.C., Power, A.J., Reilly, R.B. & Foxe, J.J. (2009) Resolving precise temporal processing properties of the auditory system using continuous stimuli. *Journal of neurophysiology*, **102**, 349-359.
- Lappe, C., Steinsträter, O. & Pantev, C. (2013) A Beamformer Analysis of MEG Data Reveals Frontal Generators of the Musically Elicited Mismatch Negativity. *PloS one*, **8**, e61296.
- Lauer, A.M., Molis, M. & Leek, M.R. (2009) Discrimination of time-reversed harmonic complexes by normal-hearing and hearing-impaired listeners. *Journal of the Association for Research in Otolaryngology : JARO*, **10**, 609-619.
- Leake, P.A. & Rebscher, S.J. (2013) Anatomical Considerations and Long-Term Effects of Electrical Stimulation. In Zeng, F.-G., Fay, R.R. (eds) *Cochlear implants: Auditory prostheses and electric hearing*. Springer Science & Business Media, pp. 101-148.
- Leijssen, A.M., Valdes, A.L., Laughlin, M.M., Smith, J., Viani, L., Walshe, P. & Reilly, R.B. (2015) An approach to develop an objective measure of temporal processing in cochlear implant users based on Schroeder-phase harmonic complexes. *IEEE Eng Med Biol Soc*, pp. 699-702.
- Levitt, H. (1971) Transformed up-down methods in psychoacoustics. *The Journal of the Acoustical Society of America*, **49**, 467-477.
- Li, X., Nie, K., Imennov, N.S., Rubinstein, J.T. & Atlas, L.E. (2013) Improved perception of music with a harmonic based algorithm for cochlear implants. *IEEE transactions on neural systems and rehabilitation engineering : a publication of the IEEE Engineering in Medicine and Biology Society*, **21**, 684-694.
- Li, X., Nie, K., Karp, F., Tremblay, K.L. & Rubinstein, J.T. (2010) Characteristics of stimulus artifacts in EEG recordings induced by electrical stimulation of cochlear implants. *3rd International Conference on Biomedical Engineering and Informatics*, pp. 799-803.
- Liang, M., Zhang, X., Chen, T., Zheng, Y., Zhao, F., Yang, H., Zhong, Z., Zhang, Z., Chen, S. & Chen, L. (2014) Evaluation of auditory cortical development in the early stages of post cochlear implantation using mismatch negativity

measurement. *Otology & neurotology : official publication of the American Otological Society, American Neurotology Society [and] European Academy of Otology and Neurotology*, **35**, e7-14.

Licklider, J. (1956) *Auditory frequency analysis*. Academic Press, New York.

Lonka, E., Kujala, T., Lehtokoski, A., Johansson, R., Rimmanen, S., Alho, K. & Näätänen, R. (2004) Mismatch negativity brain response as an index of speech perception recovery in cochlear-implant recipients. *Audiology & neuro-otology*, **9**, 160-162.

Lonka, E., Relander-Syrjanen, K., Johansson, R., Näätänen, R., Alho, K. & Kujala, T. (2013) The mismatch negativity (MMN) brain response to sound frequency changes in adult cochlear implant recipients: a follow-up study. *Acta otolaryngologica*, **133**, 853-857.

Lopez Valdes, A., Mc Laughlin, M., Viani, L., Walshe, P., Smith, J., Zeng, F.G. & Reilly, R.B. (2014) Objective assessment of spectral ripple discrimination in cochlear implant listeners using cortical evoked responses to an oddball paradigm. *PLoS one*, **9**, e90044.

Lopez Valdes, A., Mc Laughlin, M., Viani, L., Walshe, P., Smith, J., Zeng, F.G. & Reilly, R.B. (2015) Electrophysiological Correlates of Spectral Discrimination for Cochlear Implant Users. *IEEE Eng Med Biol Soc*.

Lorenzi, C., Gilbert, G., Carn, H., Garnier, S. & Moore, B.C.J. (2006) Speech perception problems of the hearing impaired reflect inability to use temporal fine structure. *Proc Natl Acad Sci U S A*, **103**, 18866-18869.

Luke, R., De Vos, A. & Wouters, J. (2016) Source Analysis Of Auditory Steady-State Responses In Acoustic And Electric Hearing. *NeuroImage*.

Luke, R., Van Deun, L., Hofmann, M., van Wieringen, A. & Wouters, J. (2015) Assessing temporal modulation sensitivity using electrically evoked auditory steady state responses. *Hearing research*, **324**, 37-45.

Luo, X., Fu, Q.J., Wei, C.G. & Cao, K.L. (2008) Speech recognition and temporal amplitude modulation processing by Mandarin-speaking cochlear implant users. *Ear and hearing*, **29**, 957-970.

Macmillan, N.A. & Kaplan, H.L. (1985) Detection theory analysis of group data: estimating sensitivity from average hit and false-alarm rates. *Psychological bulletin*, **98**, 185-199.

Manju, V., Gopika, K.K. & Arivudai Nambi, P.M. (2014) Association of auditory steady state responses with perception of temporal modulations and speech in noise. *ISRN otolaryngology*, **2014**, 374035.

- Manrique, M., Cervera-Paz, F.J., Huarte, A. & Molina, M. (2004) Advantages of cochlear implantation in prelingual deaf children before 2 years of age when compared with later implantation. *The Laryngoscope*, **114**, 1462-1469.
- Marmel, F., Plack, C.J., Hopkins, K., Carlyon, R.P., Gockel, H.E. & Moore, B.C.J. (2015) The role of excitation-pattern cues in the detection of frequency shifts in bandpass-filtered complex tones. *The Journal of the Acoustical Society of America*, **137**, 2687-2697.
- Marschark, M., Shaver, D.M., Nagle, K.M. & Newman, L.A. (2015) Predicting the Academic Achievement of Deaf and Hard-of-Hearing Students From Individual, Household, Communication, and Educational Factors. *Exceptional children*, **81**, 350-369.
- Martin, B.A. (2007) Can the acoustic change complex be recorded in an individual with a cochlear implant? Separating neural responses from cochlear implant artifact. *Journal of the American Academy of Audiology*, **18**, 126-140.
- Martin, B.A. & Boothroyd, A. (1999) Cortical, auditory, event-related potentials in response to periodic and aperiodic stimuli with the same spectral envelope. *Ear and hearing*, **20**, 33-44.
- Martin, B.A. & Boothroyd, A. (2000) Cortical, auditory, evoked potentials in response to changes of spectrum and amplitude. *The Journal of the Acoustical Society of America*, **107**, 2155-2161.
- Mathew, A.K., Purdy, S.C., Welch, D., Pontoppidan, N.H. & Ronne, F.M. (2016) Electrophysiological and behavioural processing of complex acoustic cues. *Clinical neurophysiology : official journal of the International Federation of Clinical Neurophysiology*, **127**, 779-789.
- Mathew, R., Undurraga, J., Li, G., Meerton, L., Boyle, P., Shaida, A., Selvadurai, D., Jiang, D. & Vickers, D. (2017) Objective assessment of electrode discrimination with the auditory change complex in adult cochlear implant users. *Hearing research*.
- Mc Laughlin, M., Lopez Valdes, A., Reilly, R.B. & Zeng, F.G. (2013) Cochlear implant artifact attenuation in late auditory evoked potentials: a single channel approach. *Hearing research*, **302**, 84-95.
- McAlpine, D., Haywood, N., Undurraga, J. & Marquardt, T. (2016) Objective Measures of Neural Processing of Interaural Time Differences. *Advances in experimental medicine and biology*, **894**, 197-205.
- McConkey Robbins, A., Koch, D.B., Osberger, M.J., Zimmerman-Phillips, S. & Kishon-Rabin, L. (2004) Effect of age at cochlear implantation on auditory skill development in infants and toddlers. *Archives of otolaryngology--head & neck surgery*, **130**, 570-574.

- Michalewski, H.J., Starr, A., Nguyen, T.T., Kong, Y.Y. & Zeng, F.G. (2005) Auditory temporal processes in normal-hearing individuals and in patients with auditory neuropathy. *Clinical neurophysiology : official journal of the International Federation of Clinical Neurophysiology*, **116**, 669-680.
- Miller, C.A., Brown, C.J., Abbas, P.J. & Chi, S.L. (2008) The clinical application of potentials evoked from the peripheral auditory system. *Hearing research*, **242**, 184-197.
- Miller, S. & Zhang, Y. (2014) Validation of the cochlear implant artifact correction tool for auditory electrophysiology. *Neurosci Lett*, **577**, 51-55.
- Mittal, R., Nguyen, D., Patel, A.P., Debs, L.H., Mittal, J., Yan, D., Eshraghi, A.A., Van De Water, T.R. & Liu, X.Z. (2017) Recent Advancements in the Regeneration of Auditory Hair Cells and Hearing Restoration. *Frontiers in Molecular Neuroscience*, **10**, 236.
- Moberly, A.C., Bhat, J. & Shahin, A.J. (2015) Acoustic Cue Weighting by Adults with Cochlear Implants: A Mismatch Negativity Study. *Ear and hearing*.
- Mognon, A., Jovicich, J., Bruzzone, L. & Buiatti, M. (2011) ADJUST: An automatic EEG artifact detector based on the joint use of spatial and temporal features. *Psychophysiology*, **48**, 229-240.
- Moore, B.C.J. (1993) Frequency Analysis and Pitch Perception. In Yost, W.A., Popper, A.N., Fay, R.R. (eds) *Human Psychophysics*. Springer, pp. 56 - 115.
- Moore, B.C.J. (2008) The role of temporal fine structure processing in pitch perception, masking, and speech perception for normal-hearing and hearing-impaired people. *Journal of the Association for Research in Otolaryngology : JARO*, **9**, 399-406.
- Moore, B.C.J. (2014) *Auditory processing of temporal fine structure: Effects of age and hearing loss*. World Scientific.
- Moore, B.C.J. (2016) Effects of Age and Hearing Loss on the Processing of Auditory Temporal Fine Structure. *Advances in experimental medicine and biology*, **894**, 1-8.
- Moore, B.C.J., Glasberg, B.R. & Hopkins, K. (2006) Frequency discrimination of complex tones by hearing-impaired subjects: Evidence for loss of ability to use temporal fine structure. *Hearing research*, **222**, 16-27.
- Moore, B.C.J., Glasberg, B.R. & Proctor, G.M. (1992) Accuracy of pitch matching for pure tones and for complex tones with overlapping or nonoverlapping harmonics. *The Journal of the Acoustical Society of America*, **91**, 3443-3450.
- Moore, B.C.J., Hopkins, K. & Cuthbertson, S. (2009) Discrimination of complex tones with unresolved components using temporal fine structure information. *The Journal of the Acoustical Society of America*, **125**, 3214-3222.

- Moore, B.C.J., Huss, M., Vickers, D.A., Glasberg, B.R. & Alcantara, J.I. (2000) A test for the diagnosis of dead regions in the cochlea. *British journal of audiology*, **34**, 205-224.
- Moore, B.C.J. & Sek, A. (2009) Development of a fast method for determining sensitivity to temporal fine structure. *International journal of audiology*, **48**, 161-171.
- Moore, B.C.J. & Sek, A. (2011) Effect of level on the discrimination of harmonic and frequency-shifted complex tones at high frequencies. *The Journal of the Acoustical Society of America*, **129**, 3206-3212.
- Moore, B.C.J., Vickers, D.A., Baer, T. & Launer, S. (1999) Factors affecting the loudness of modulated sounds. *The Journal of the Acoustical Society of America*, **105**, 2757-2772.
- Moore, B.C.J., Vickers, D.A. & Mehta, A. (2012) The effects of age on temporal fine structure sensitivity in monaural and binaural conditions. *International journal of audiology*, **51**, 715-721.
- Moore, G.A. & Moore, B.C.J. (2003) Perception of the low pitch of frequency-shifted complexes. *The Journal of the Acoustical Society of America*, **113**, 977-985.
- Moore, J.K., Niparko, J.K., Miller, M.R. & Linthicum, F.H. (1994) Effect of profound hearing loss on a central auditory nucleus. *The American journal of otology*, **15**, 588-595.
- Moore, J.K., Niparko, J.K., Perazzo, L.M., Miller, M.R. & Linthicum, F.H. (1997) Effect of adult-onset deafness on the human central auditory system. *The Annals of otology, rhinology, and laryngology*, **106**, 385-390.
- Morr, M.L., Shafer, V.L., Kreuzer, J.A. & Kurtzberg, D. (2002) Maturation of mismatch negativity in typically developing infants and preschool children. *Ear and hearing*, **23**, 118-136.
- Müller, J., Brill, S., Hagen, R., Moeltner, A., Brockmeier, S.J., Stark, T., Helbig, S., Maurer, J., Zahnert, T., Zierhofer, C., Nopp, P. & Anderson, I. (2012) Clinical trial results with the MED-EL fine structure processing coding strategy in experienced cochlear implant users. *ORL J Otorhinolaryngol Relat Spec*, **74**, 185-198.
- Näätänen, R. (1990) The role of attention in auditory information processing as revealed by event-related potentials and other brain measures of cognitive function. *Behavioral and Brain Sciences*, **13**, 201-233.
- Näätänen, R., Gaillard, A.W.K. & Mäntysalo, S. (1978) Early selective-attention effect on evoked potential reinterpreted. *Acta Psychologica*, **42**, 313-329.
- Näätänen, R., Kujala, T. & Winkler, I. (2011) Auditory processing that leads to conscious perception: a unique window to central auditory processing opened by the mismatch negativity and related responses. *Psychophysiology*, **48**, 4-22.

- Näätänen, R., Paavilainen, P. & Reinikainen, K. (1989) Do event-related potentials to infrequent decrements in duration of auditory stimuli demonstrate a memory trace in man? *Neurosci Lett*, **107**, 347-352.
- Näätänen, R., Paavilainen, P., Rinne, T. & Alho, K. (2007) The mismatch negativity (MMN) in basic research of central auditory processing: a review. *Clinical neurophysiology : official journal of the International Federation of Clinical Neurophysiology*, **118**, 2544-2590.
- Näätänen, R., Pakarinen, S., Rinne, T. & Takegata, R. (2004) The mismatch negativity (MMN): towards the optimal paradigm. *Clinical Neurophysiology*, **115**, 140-144.
- Nicholas, J.G. & Geers, A.E. (2007) Will they catch up? The role of age at cochlear implantation in the spoken language development of children with severe to profound hearing loss. *Journal of speech, language, and hearing research : JSLHR*, **50**, 1048-1062.
- Niquette, P., Arcaroli, J., Revit, L., Parkinson, A., Staller S., Skinner, M. & Killion, M. (Year) Development of the BKB-SIN Test. . Annual Meeting of the American Auditory Society. City.
- O'Sullivan, J.A., Power, A.J., Mesgarani, N., Rajaram, S., Foxe, J.J., Shinn-Cunningham, B.G., Slaney, M., Shamma, S.A. & Lalor, E.C. (2015) Attentional Selection in a Cocktail Party Environment Can Be Decoded from Single-Trial EEG. *Cerebral cortex (New York, N.Y. : 1991)*, **25**, 1697-1706.
- Oh, S.H., Kim, C.S., Kang, E.J., Lee, D.S., Lee, H.J., Chang, S.O., Ahn, S.H., Hwang, C.H., Park, H.J. & Koo, J.W. (2003) Speech perception after cochlear implantation over a 4-year time period. *Acta oto-laryngologica*, **123**, 148-153.
- Ortmann, M., Knief, A., Deuster, D., Brinkheetker, S., Zwitserlood, P., am Zehnhoff-Dinnesen, A. & Dobel, C. (2013) Neural correlates of speech processing in prelingually deafened children and adolescents with cochlear implants. *PloS one*, **8**, e67696.
- Ortmann, M., Zwitserlood, P., Knief, A., Baare, J., Brinkheetker, S., Am Zehnhoff-Dinnesen, A. & Dobel, C. (2017) When Hearing Is Tricky: Speech Processing Strategies in Prelingually Deafened Children and Adolescents with Cochlear Implants Having Good and Poor Speech Performance. *PloS one*, **12**, e0168655.
- Oxenham, A.J. (2012) Pitch perception. *The Journal of neuroscience : the official journal of the Society for Neuroscience*, **32**, 13335-13338.
- Oxenham, A.J. & Kreft, H.A. (2014) Speech perception in tones and noise via cochlear implants reveals influence of spectral resolution on temporal processing. *Trends Hear*, **18**, 1-14.

- Oxenham, A.J. & Simonson, A.M. (2006) Level dependence of auditory filters in nonsimultaneous masking as a function of frequency. *The Journal of the Acoustical Society of America*, **119**, 444-453.
- Paavilainen, P. (2013) The mismatch-negativity (MMN) component of the auditory event-related potential to violations of abstract regularities: A review. *International Journal of Psychophysiology*, **88**, 109-123.
- Paavilainen, P., Karlsson, M.L., Reinikainen, K. & Naatanen, R. (1989) Mismatch negativity to change in spatial location of an auditory stimulus. *Electroencephalography and clinical neurophysiology*, **73**, 129-141.
- Park, Y.-H. (2015) Stem Cell Therapy for Sensorineural Hearing Loss, Still Alive? *Journal of audiology & otology*, **19**, 63-67.
- Patrick, J.F., Seligman, P.M. & Clark, G.M. (1997) Engineering. Singular Publishing, pp. 125-145.
- Peelle, J.E., Troiani, V., Grossman, M. & Wingfield, A. (2011) Hearing loss in older adults affects neural systems supporting speech comprehension. *The Journal of neuroscience : the official journal of the Society for Neuroscience*, **31**, 12638-12643.
- Petermann, M., Kummer, P., Burger, M., Lohscheller, J., Eysholdt, U. & Döllinger, M. (2009) Statistical detection and analysis of mismatch negativity derived by a multi-deviant design from normal hearing children. *Hearing research*, **247**, 128-136.
- Petersen, B., Weed, E., Sandmann, P., Brattico, E., Hansen, M., Sorensen, S.D. & Vuust, P. (2015) Brain responses to musical feature changes in adolescent cochlear implant users. *Frontiers in human neuroscience*, **9**, 7.
- Picton, T.W. (2011) *Human Auditory Evoked Potentials*. Plural Pub.
- Picton, T.W. (2013) Hearing in time: evoked potential studies of temporal processing. *Ear and hearing*, **34**, 385-401.
- Picton, T.W., Bentin, S., Berg, P., Donchin, E., Hillyard, S.A., Johnson, R., Jr., Miller, G.A., Ritter, W., Ruchkin, D.S., Rugg, M.D. & Taylor, M.J. (2000) Guidelines for using human event-related potentials to study cognition: recording standards and publication criteria. *Psychophysiology*, **37**, 127-152.
- Picton, T.W., John, M.S., Dimitrijevic, A. & Purcell, D. (2003) Human auditory steady-state responses. *International journal of audiology*, **42**, 177-219.
- Plack, C.J. & Oxenham, A.J. (2005) The Psychophysics of Pitch. In Plack, C.J., Oxenham, A.J., Fay, R.R., Popper, A.N. (eds) *Pitch*. Springer New York, pp. 7-55.

- Poissant, S.F., Bero, E.M., Busekroos, L. & Shao, W. (2014) Determining cochlear implant users' true noise tolerance: use of speech reception threshold in noise testing. *Otology & neurotology : official publication of the American Otological Society, American Neurotology Society [and] European Academy of Otology and Neurotology*, **35**, 414-420.
- Polich, J. (2007) Updating P300: An integrative theory of P3a and P3b. *Clinical Neurophysiology*, **118**, 2128-2148.
- Ponton, C.W. & Don, M. (1995) The mismatch negativity in cochlear implant users. *Ear and hearing*, **16**, 131-146.
- Ponton, C.W., Don, M., Eggermont, J.J., Waring, M.D., Kwong, B. & Masuda, A. (1996a) Auditory system plasticity in children after long periods of complete deafness. *Neuroreport*, **8**, 61-65.
- Ponton, C.W., Don, M., Eggermont, J.J., Waring, M.D. & Masuda, A. (1996b) Maturation of human cortical auditory function: differences between normal-hearing children and children with cochlear implants. *Ear and hearing*, **17**, 430-437.
- Ponton, C.W., Eggermont, J.J., Don, M., Waring, M.D., Kwong, B., Cunningham, J. & Trautwein, P. (2000) Maturation of the mismatch negativity: effects of profound deafness and cochlear implant use. *Audiology & neuro-otology*, **5**, 167-185.
- Potts, L.G., Skinner, M.W., Gotter, B.D., Strube, M.J. & Brenner, C.A. (2007) Relation between neural response telemetry thresholds, T- and C-levels, and loudness judgments in 12 adult nucleus 24 cochlear implant recipients. *Ear and hearing*, **28**, 495-511.
- Presacco, A., Innes-Brown, H., Goupell, M.J. & Anderson, S. (2017) Effects of Stimulus Duration on Event-Related Potentials Recorded From Cochlear-Implant Users. *Ear and hearing*.
- Pryse-Phillips, W. (2009) *Companion to Clinical Neurology*. Oxford University Press, USA.
- Purcell, D.W., John, S.M., Schneider, B.A. & Picton, T.W. (2004) Human temporal auditory acuity as assessed by envelope following responses. *The Journal of the Acoustical Society of America*, **116**, 3581-3593.
- Purves, D., Augustine, G.J., Fitzpatrick, D., Hall, W.C., LaMantia, A.-S., McNamara, J.O. & Williams, M.W. (2004) *Neuroscience*. Sinauer Associates, Sunderland, Massachusetts.
- Qi, B., Krenmayr, A., Zhang, N., Dong, R., Chen, X., Schatzer, R., Zierhofer, C., Liu, B. & Han, D. (2012) Effects of temporal fine structure stimulation on Mandarin speech recognition in cochlear implant users. *Acta oto-laryngologica*, **132**, 1183-1191.

- Rahne, T., Bohme, L. & Gotze, G. (2011) Timbre discrimination in cochlear implant users and normal hearing subjects using cross-faded synthetic tones. *Journal of neuroscience methods*, **199**, 290-295.
- Rahne, T., Plontke, S.K. & Wagner, L. (2014) Mismatch negativity (MMN) objectively reflects timbre discrimination thresholds in normal-hearing listeners and cochlear implant users. *Brain research*, **1586**, 143-151.
- Rahne, T., Ziese, M., Rostalski, D. & Muhler, R. (2010) Logatome discrimination in cochlear implant users: subjective tests compared to the mismatch negativity. *TheScientificWorldJournal*, **10**, 329-339.
- Rajan, G., Tavora-Vieira, D., Baumgartner, W.D., Godey, B., Muller, J., O'Driscoll, M., Skarzynski, H., Skarzynski, P., Usami, S.I., Adunka, O., Agrawal, S., Bruce, I., De Bodt, M., Caversaccio, M., Pilsbury, H., Gavilan, J., Hagen, R., Hagr, A., Kameswaran, M., Karltorp, E., Kompis, M., Kuzovkov, V., Lassaletta, L., Yongxin, L., Lorens, A., Manoj, M., Martin, J., Mertens, G., Mlynski, R., Parnes, L., Pulibalathingal, S., Radeloff, A., Raine, C.H., Rajeswaran, R., Schmutzhard, J., Sprinzel, G., Staecker, H., Stephan, K., Sugarova, S., Zernotti, M., Zorowka, P. & Van de Heyning, P. (2017) Hearing preservation cochlear implantation in children: The HEARRING Group consensus and practice guide. *Cochlear implants international*, 1-13.
- Robson, H., Cloutman, L., Keidel, J.L., Sage, K., Drakesmith, M. & Welbourne, S. (2014) Mismatch negativity (MMN) reveals inefficient auditory ventral stream function in chronic auditory comprehension impairments. *Cortex*, **59**, 113-125.
- Rose, J.E., Brugge, J.F., Anderson, D.J. & Hind, J.E. (1967) Phase-locked response to low-frequency tones in single auditory nerve fibers of the squirrel monkey. *Journal of neurophysiology*, **30**, 769-793.
- Ruffin, C.V., Tyler, R.S., Witt, S.A., Dunn, C.C., Gantz, B.J. & Rubinstein, J.T. (2007) Long-term performance of Clarion 1.0 cochlear implant users. *The Laryngoscope*, **117**, 1183-1190.
- Saarinen, J., Paavilainen, P., Schoger, E., Tervaniemi, M. & Naatanen, R. (1992) Representation of abstract attributes of auditory stimuli in the human brain. *Neuroreport*, **3**, 1149-1151.
- Salisbury, D.F. (2012) Finding the missing stimulus mismatch negativity (MMN): Emitted MMN to violations of an auditory gestalt. *Psychophysiology*, **49**, 544-548.
- Sams, M., Paavilainen, P., Alho, K. & Näätänen, R. (1985) Auditory frequency discrimination and event-related potentials. *Electroencephalography and clinical neurophysiology*, **62**, 437-448.
- Sandmann, P., Eichele, T., Buechler, M., Debener, S., Jancke, L., Dillier, N., Hugdahl, K. & Meyer, M. (2009) Evaluation of evoked potentials to dyadic tones after cochlear implantation. *Brain : a journal of neurology*, **132**, 1967-1979.

- Sandmann, P., Kegel, A., Eichele, T., Dillier, N., Lai, W., Bendixen, A., Debener, S., Jancke, L. & Meyer, M. (2010) Neurophysiological evidence of impaired musical sound perception in cochlear-implant users. *Clinical neurophysiology : official journal of the International Federation of Clinical Neurophysiology*, **121**, 2070-2082.
- Sandmann, P., Plotz, K., Hauthal, N., de Vos, M., Schonfeld, R. & Debener, S. (2014) Rapid bilateral improvement in auditory cortex activity in postlingually deafened adults following cochlear implantation. *Clinical neurophysiology : official journal of the International Federation of Clinical Neurophysiology*.
- Schierholz, I., Finke, M., Kral, A., Büchner, A., Rach, S., Lenarz, T., Dengler, R. & Sandmann, P. (2017) Auditory and audio–visual processing in patients with cochlear, auditory brainstem, and auditory midbrain implants: An EEG study. *Human brain mapping*, **38**, 2206-2225.
- Schnupp, J., Nelken, I. & King, A. (2011) *Auditory Neuroscience: Making Sense of Sound*. MIT Press.
- Schoof, T., Green, T., Faulkner, A. & Rosen, S. (2013) Advantages from bilateral hearing in speech perception in noise with simulated cochlear implants and residual acoustic hearing. *The Journal of the Acoustical Society of America*, **133**, 1017-1030.
- Schoof, T. & Rosen, S. (2015) High sentence predictability increases the fluctuating masker benefit. *The Journal of the Acoustical Society of America*, **138**, EL181-186.
- Schouten, J. (1938) The perception of subjective tones. *Proc Kon Akad Wetenschap* **41**, 1086-1093.
- Schouten, J. (1940) The residue and the mechanism of hearing. *Proc Kon Akad Wetenschap* **43**, 991-999.
- Schroeder, L., Petrou, S., Kennedy, C., McCann, D., Law, C., Watkin, P.M., Worsfold, S. & Yuen, H.M. (2006) The economic costs of congenital bilateral permanent childhood hearing impairment. *Pediatrics*, **117**, 1101-1112.
- Schroeder, M. (1970) Synthesis of low-peak-factor signals and binary sequences with low autocorrelation (Corresp.). *IEEE Transactions on Information Theory*, **16**, 85-89.
- Scott, S.K., Rosen, S., Lang, H. & Wise, R.J. (2006) Neural correlates of intelligibility in speech investigated with noise vocoded speech--a positron emission tomography study. *The Journal of the Acoustical Society of America*, **120**, 1075-1083.
- Sek, A. & Moore, B.C.J. (2012) Implementation of two tests for measuring sensitivity to temporal fine structure. *International journal of audiology*, **51**, 58-63.

- Shackleton, T.M. & Carlyon, R.P. (1994) The role of resolved and unresolved harmonics in pitch perception and frequency modulation discrimination. *The Journal of the Acoustical Society of America*, **95**, 3529-3540.
- Shamma, S. & Lorenzi, C. (2013) On the balance of envelope and temporal fine structure in the encoding of speech in the early auditory system. *The Journal of the Acoustical Society of America*, **133**, 2818-2833.
- Shannon, R.V., Zeng, F.G., Kamath, V., Wygonski, J. & Ekelid, M. (1995) Speech recognition with primarily temporal cues. *Science (New York, N.Y.)*, **270**, 303-304.
- Sharma, A. & Cardon, G. (2015) Cortical Development and Neuroplasticity in Auditory Neuropathy Spectrum Disorder. *Hearing research*, **330**, 221-232.
- Sharma, A., Dorman, M.F. & Kral, A. (2005) The influence of a sensitive period on central auditory development in children with unilateral and bilateral cochlear implants. *Hearing research*, **203**, 134-143.
- Sharma, A., Gilley, P.M., Dorman, M.F. & Baldwin, R. (2007) Deprivation-induced cortical reorganization in children with cochlear implants. *International journal of audiology*, **46**, 494-499.
- Sharma, A. & Glick, H. (2016) Cross-Modal Re-Organization in Clinical Populations with Hearing Loss. *Brain sciences*, **6**.
- Sharma, M., Purdy, S.C., Newall, P., Wheldall, K., Beaman, R. & Dillon, H. (2004) Effects of identification technique, extraction method, and stimulus type on mismatch negativity in adults and children. *Journal of the American Academy of Audiology*, **15**, 616-632.
- Sheft, S. & Yost, W.A. (1990) Temporal integration in amplitude modulation detection. *The Journal of the Acoustical Society of America*, **88**, 796-805.
- Shen, Y. (2014) Gap detection and temporal modulation transfer function as behavioral estimates of auditory temporal acuity using band-limited stimuli in young and older adults. *Journal of speech, language, and hearing research : JSLHR*, **57**, 2280-2292.
- Shen, Y. & Richards, V.M. (2013) Temporal modulation transfer function for efficient assessment of auditory temporal resolution. *The Journal of the Acoustical Society of America*, **133**, 1031-1042.
- Small, S.A., Sharma, M., Bradford, M. & Mandikal Vasuki, P.R. (2017) The Effect of Signal to Noise Ratio on Cortical Auditory-Evoked Potentials Elicited to Speech Stimuli in Infants and Adults With Normal Hearing. *Ear and hearing*.
- Spahr, A.J., Dorman, M.F., Litvak, L.M., Van Wie, S., Gifford, R.H., Loizou, P.C., Loiselle, L.M., Oakes, T. & Cook, S. (2012) Development and validation of the AzBio sentence lists. *Ear and hearing*, **33**, 112-117.

- Starr, A., Picton, T.W., Sininger, Y., Hood, L.J. & Berlin, C.I. (1996) Auditory neuropathy. *Brain : a journal of neurology*, **119 (Pt 3)**, 741-753.
- Stoody, T.M., Saoji, A.A. & Atcherson, S.R. (2011) Auditory mismatch negativity: detecting spectral contrasts in a modulated noise. *Perceptual and motor skills*, **113**, 268-276.
- Stothart, G. & Kazanina, N. (2013) Oscillatory characteristics of the visual mismatch negativity: what evoked potentials aren't telling us. *Frontiers in human neuroscience*, **7**, 426.
- Strickland, E.A. & Viemeister, N.F. (1997) The effects of frequency region and bandwidth on the temporal modulation transfer function. *The Journal of the Acoustical Society of America*, **102**, 1799-1810.
- Strouse, A., Ashmead, D.H., Ohde, R.N. & Grantham, D.W. (1998) Temporal processing in the aging auditory system. *The Journal of the Acoustical Society of America*, **104**, 2385-2399.
- Takahashi, G.A. & Bacon, S.P. (1992) Modulation detection, modulation masking, and speech understanding in noise in the elderly. *Journal of speech and hearing research*, **35**, 1410-1421.
- Tervaniemi, M., Maury, S. & Näätänen, R. (1994) Neural representations of abstract stimulus features in the human brain as reflected by the mismatch negativity. *Neuroreport*, **5**, 844-846.
- Tiitinen, H., May, P., Reinikainen, K. & Näätänen, R. (1994) Attentive novelty detection in humans is governed by pre-attentive sensory memory. *Nature*, **372**, 90-92.
- Timm, L., Vuust, P., Brattico, E., Agrawal, D., Debener, S., Buchner, A., Dengler, R. & Wittfoth, M. (2014) Residual neural processing of musical sound features in adult cochlear implant users. *Frontiers in human neuroscience*, **8**, 181.
- Todd, J., Finch, B., Smith, E., Budd, T.W. & Schall, U. (2011) Temporal processing ability is related to ear-asymmetry for detecting time cues in sound: a mismatch negativity (MMN) study. *Neuropsychologia*, **49**, 69-82.
- Trainor, L.J., Marie, C., Bruce, I.C. & Bidelman, G.M. (2014) Explaining the high voice superiority effect in polyphonic music: evidence from cortical evoked potentials and peripheral auditory models. *Hearing research*, **308**, 60-70.
- Trainor, L.J., Samuel, S.S., Desjardins, R.N. & Sonnadora, R.R. (2001) Measuring temporal resolution in infants using mismatch negativity. *Neuroreport*, **12**, 2443-2448.
- Tseng, C.C., Hu, L.Y., Liu, M.E., Yang, A.C., Shen, C.C. & Tsai, S.J. (2016) Risk of depressive disorders following sudden sensorineural hearing loss: A nationwide

- population-based retrospective cohort study. *Journal of affective disorders*, **197**, 94-99.
- Turgeon, C., Lazzouni, L., Lepore, F. & Ellemberg, D. (2014) An objective auditory measure to assess speech recognition in adult cochlear implant users. *Clinical neurophysiology : official journal of the International Federation of Clinical Neurophysiology*, **125**, 827-835.
- Uther, M., Jansen, D.H., Huotilainen, M., Ilmoniemi, R.J. & Näätänen, R. (2003) Mismatch negativity indexes auditory temporal resolution: evidence from event-related potential (ERP) and event-related field (ERF) recordings. *Cogn Brain Res*, **17**, 685-691.
- Viemeister, N.F. (1979) Temporal modulation transfer functions based upon modulation thresholds. *The Journal of the Acoustical Society of America*, **66**, 1364-1380.
- Viola, F.C., De Vos, M., Hine, J., Sandmann, P., Bleack, S., Eyles, J. & Debener, S. (2012) Semi-automatic attenuation of cochlear implant artifacts for the evaluation of late auditory evoked potentials. *Hearing research*, **284**, 6-15.
- Visram, A.S., Innes-Brown, H., El-Deredy, W. & McKay, C.M. (2015) Cortical auditory evoked potentials as an objective measure of behavioral thresholds in cochlear implant users. *Hearing research*, **327**, 35-42.
- Von Helmholtz, H.L.F. (1895) *On the Sensations of Tone as a Physiological Basis for the Theory of Music*. Longmans, Green and Co.
- von Wedel, H. (1982) Cortical evoked potentials in response to brief modulation of signal amplitude. Experiments on auditory temporal resolution. *Archives of oto-rhino-laryngology*, **234**, 235-243.
- Vuust, P., Pallesen, K.J., Bailey, C., van Zuijen, T.L., Gjedde, A., Roepstorff, A. & Ostergaard, L. (2005) To musicians, the message is in the meter pre-attentive neuronal responses to incongruent rhythm are left-lateralized in musicians. *NeuroImage*, **24**, 560-564.
- Wable, J., van den Abbeele, T., Gallego, S. & Frachet, B. (2000) Mismatch negativity: a tool for the assessment of stimuli discrimination in cochlear implant subjects. *Clinical neurophysiology : official journal of the International Federation of Clinical Neurophysiology*, **111**, 743-751.
- Waechter, S.M., Lopez Valdes, A., Simoes-Franklin, C., Viani, L. & Reilly, R.B. (2018) Depth matters – Towards finding an objective neurophysiological measure of behavioral amplitude modulation detection based on neural threshold determination. *Hearing research*, **359**, 13-22.
- Wagner, L., Maurits, N., Maat, B., Başkent, D. & Wagner, A.E. (2018) The Cochlear Implant EEG Artifact Recorded From an Artificial Brain for Complex Acoustic Stimuli. *IEEE Transactions on Neural Systems and Rehabilitation Engineering*, **26**, 392-399.

- Wagner, L., Plontke, S.K. & Rahne, T. (2017) Perception of Iterated Rippled Noise Periodicity in Cochlear Implant Users. *Audiology and Neurotology*, **22**, 104-115.
- Walker, K.M., Bizley, J.K., King, A.J. & Schnupp, J.W. (2011) Cortical encoding of pitch: recent results and open questions. *Hearing research*, **271**, 74-87.
- Watson, C.S. & Kidd, G.R. (2002) On the Lack of Association between Basic Auditory Abilities, Speech Processing, and other Cognitive Skills. *Semin Hear*, **23**, 83-94.
- Wilson, B. (2000) Strategies for representing speech information with cochlear implants. In Niparko, J.K., Kirk, K.I., Mellon, N.K., Robbins, A.M., Tucci, D.L., Wilson, B. (eds) *Cochlear implants: principles and practices*. Lippincott Williams & Wilkins, Philadelphia, pp. 129-170.
- Wilson, B.S. (2004) Engineering Design of Cochlear Implants. In Zeng, F.G., Popper, A.N., Fay, R.R. (eds) *Cochlear Implants- Auditory Protheses and Electric Hearing*. Springer Science+Business Media, LLC.
- Wilson, B.S. & Dorman, M.F. (2009) The Design of Cochlear Implants. In Niparko, J.K. (ed) *Cochlear Implants- Principles & Practices*. Lippincott Williams & Wilkins, Philadelphia, pp. 95-136.
- Wilson, B.S., Tucci, D.L., Merson, M.H. & O'Donoghue, G.M. (2017) Global hearing health care: new findings and perspectives. *The Lancet*, **390**, 2503-2515.
- Winkler, I. (2007) Interpreting the Mismatch Negativity. *Journal of Psychophysiology*, **21**, 147-163.
- Won, J.H., Clinard, C.G., Kwon, S., Dasika, V.K., Nie, K., Drennan, W.R., Tremblay, K.L. & Rubinstein, J.T. (2011a) Relationship between behavioral and physiological spectral-ripple discrimination. *Journal of the Association for Research in Otolaryngology : JARO*, **12**, 375-393.
- Won, J.H., Drennan, W.R., Nie, K., Jameyson, E.M. & Rubinstein, J.T. (2011b) Acoustic temporal modulation detection and speech perception in cochlear implant listeners. *The Journal of the Acoustical Society of America*, **130**, 376-388.
- Won, J.H., Drennan, W.R. & Rubinstein, J.T. (2007) Spectral-Ripple Resolution Correlates with Speech Reception in Noise in Cochlear Implant Users. *JARO: Journal of the Association for Research in Otolaryngology*, **8**, 384-392.
- Wong, D.D. & Gordon, K.A. (2009) Beamformer suppression of cochlear implant artifacts in an electroencephalography dataset. *IEEE transactions on bio-medical engineering*, **56**, 2851-2857.
- Wong, D.D.E., Fuglsang, S.A., Hjortkjær, J., Ceolini, E., Slaney, M. & de Cheveigné, A. (2018) A Comparison of Temporal Response Function Estimation Methods for Auditory Attention Decoding. *bioRxiv*.

- Wouters, J. & Vanden Berghe, J. (2001) Speech recognition in noise for cochlear implantees with a two-microphone monaural adaptive noise reduction system. *Ear and hearing*, **22**, 420-430.
- Xu, L., Thompson, C.S. & Pfingst, B.E. (2005) Relative contributions of spectral and temporal cues for phoneme recognition. *The Journal of the Acoustical Society of America*, **117**, 3255-3267.
- Xu, Y., Chen, M., LaFaire, P., Tan, X. & Richter, C.P. (2017) Distorting temporal fine structure by phase shifting and its effects on speech intelligibility and neural phase locking. *Scientific reports*, **7**, 13387.
- Zeng, F.-G., Popper, A.N. & Fay, R.R. (2013) *Cochlear implants: Auditory prostheses and electric hearing*. Springer Science+Business Media, New York.
- Zeng, F.G., Kong, Y.Y., Michalewski, H.J. & Starr, A. (2005) Perceptual consequences of disrupted auditory nerve activity. *Journal of neurophysiology*, **93**, 3050-3063.
- Zeng, F.G., Oba, S., Garde, S., Sininger, Y. & Starr, A. (1999) Temporal and speech processing deficits in auditory neuropathy. *Neuroreport*, **10**, 3429-3435.
- Zhang, C. & Zeng, F.G. (1997) Loudness of dynamic stimuli in acoustic and electric hearing. *The Journal of the Acoustical Society of America*, **102**, 2925-2934.
- Zhang, F., Benson, C. & Cahn, S.J. (2013a) Cortical encoding of timbre changes in cochlear implant users. *Journal of the American Academy of Audiology*, **24**, 46-58.
- Zhang, F., Benson, C. & Fu, Q.J. (2013b) Cortical encoding of pitch contour changes in cochlear implant users: a mismatch negativity study. *Audiology & neuro-otology*, **18**, 275-288.
- Zhang, F., Hammer, T., Banks, H.L., Benson, C., Xiang, J. & Fu, Q.J. (2011) Mismatch negativity and adaptation measures of the late auditory evoked potential in cochlear implant users. *Hearing research*, **275**, 17-29.
- Ziat, M. & Bensmaia, S. (2015) Neuroprosthetics. In Wright, J.D. (ed) *International Encyclopedia of the Social & Behavioral Sciences*. Elsevier, Oxford, pp. 714-721.
- Zirn, S., Arndt, S., Aschendorff, A., Laszig, R. & Wesarg, T. (2016) Perception of Interaural Phase Differences With Envelope and Fine Structure Coding Strategies in Bilateral Cochlear Implant Users. *Trends in Hearing*, **20**, 2331216516665608.

Appendices

Appendix A: Supplementary Material for Chapter 6

A.1 Validation of recording equipment

To create two recording channels, the acquisition system outlined in **Chapter 3** was duplicated and combined. The signals from the reference and ground electrodes were split with a Y-connector¹⁶ which fed the electrode signals into two individual Stanford Research amplifiers (SR560). The recording electrodes were positioned at the vertex (Cz) and the left mastoid.

To validate the measurement set-up, any potential bridging effects of recorded signals due to the common ground and reference electrodes had to be evaluated. In a validation experiment, CAEPs were recorded for three conditions, all of which were referenced to the right mastoid and the ground electrode was placed on the collarbone. (1) Amplifier-1 recording from Cz and Amplifier-2 recording from the left mastoid, (2) amplifiers swapped, and (3) both amplifiers receiving the input signal from Cz, which was split with a third Y-connector.

The recorded data showed that both channels measured independent signals as indicated by Figure A.1. Both plots in Figure A.1 show the N1-P2 complex for the channel located at Cz, and a near flat line for the channel measuring from the contralateral mastoid (with respect to the reference electrode). When both channels were measured from the same electrode via a third Y-connector cable, the measured signals were nearly identical (Figure A.2) as expected.

¹⁶ 1M2F Y-Connector (SA9315) purchased from www.nexgenergo.com/ergonomics/thought-EEG.html

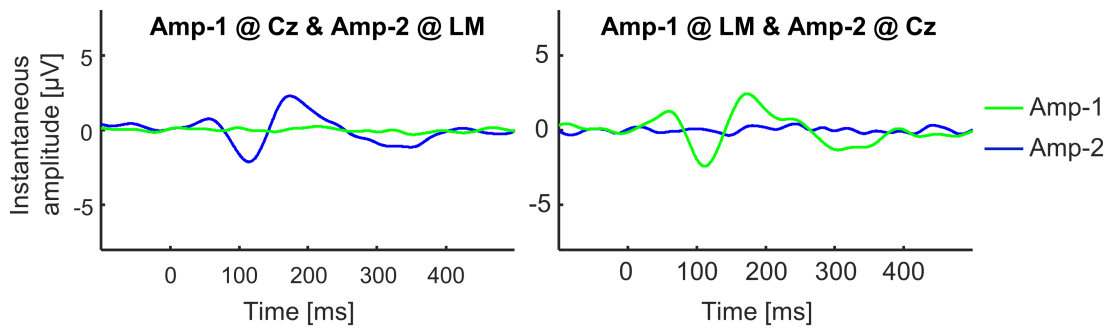


Figure A.1: Validation results of the dual-channel electroencephalography acquisition system with recordings from different electrodes.

Plots show cortical auditory evoked potentials (CAEPs) acquired with a 500 ms pure tone (500 Hz). Both amplifiers were connected and were measuring from Cz and the left mastoid (LM). CAEPs show robust N1-P2-complexes when recorded from Cz and a near flat line when recorded from the LM. Abbreviations and acronyms: Amp. – Amplifier, LM – Left mastoid.

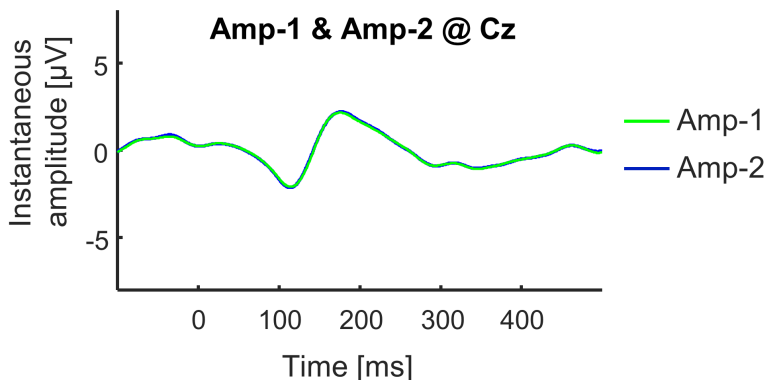


Figure A.2: Validation results of the dual-channel electroencephalography acquisition system with recordings from the same electrode.

Plots show cortical auditory evoked potentials (CAEPs) acquired with a 500 ms pure tone (500 Hz). Both amplifiers were measuring from the electrode located at Cz. CAEPs show virtually identical N1-P2-complexes. Abbreviations and acronyms: Amp. – Amplifier.

Appendix B: The influence of experimental parameters on the neural response – Insights from NH pilot studies

This section aims to give an overview of numerous pilot studies that were conducted in the attempt to find parameters that greatly influence neural measures in the hope of increasing the amplitude of neural change detection measures. None of the pilot studies mentioned in this chapter had the statistical power to draw meaningful general conclusions from the findings, however, the process of thoroughly debating the influence of each parameter on the neural measure deepened the understanding of the topic and improved study designs of final studies. Hence, a small overview of these various pilot studies is given in the following with tentative interpretations of the results.

Findings from **Chapter 3** have provided evidence for the feasibility of measuring CAEPs to represent AM detection among unmodulated noise sounds. However, new questions arose from the observed discrepancy (offset) between behavioural and neural thresholds of AM detection. To investigate the influence of various stimulus and methodological parameters on neurophysiological responses, a set of pilot experiments were conducted. The aim was to illuminate the influence of the differing parameters on the elicited neural response as well as to find the optimum parameters for robust responses with time-efficient data acquisition for future studies. Pilot experiments have explored the ACC as a measure of neural change detection with particular focus on the following experimental parameters:

- A. Stimulus duration
- B. AM phase onset
- C. AM change vs. amplitude decrease
- D. AM rate
- E. Other
 - a. Carrier signal
 - b. Attention
 - c. Binaural vs. monaural
 - d. AM rate discrimination and change direction
- F. General observations

For the various stimulus parameters under investigation, pilot data was obtained for one to five participants. Due to low participant numbers, no conclusions of statistical significance can be drawn, but the pilot studies were merely a tool to increase the

understanding of neural change responses towards AM stimuli prior to designing a new study. The maximum AMD was set to 80% in the pilot experiments to avoid gap effects, which may result from 100% AMD.

B.1 Observations ACC experiments

Influence of stimulus duration

Neurophysiological data was acquired for a short and long stimulus duration paradigm from five and four participants, respectively. For the long paradigm, the stimulus was created with 500 ms unmodulated noise immediately followed by 500 ms modulated noise with an inter-stimulus interval of 1s silence. For the short paradigm, the stimulus consisted of 250 ms unmodulated noise and 300 ms modulated noise without a gap and the inter-stimulus interval was set to 1000 ms. The AM rate was set to 8 Hz. The AMD was varied to assess the ACC for decreasing AMDs (80%, 50%, 20%, 12.5% and 5% AMD). Robust primary N1-P2 responses were elicited for all conditions in both, the short and long stimulus paradigm (examples in Figure B.1).

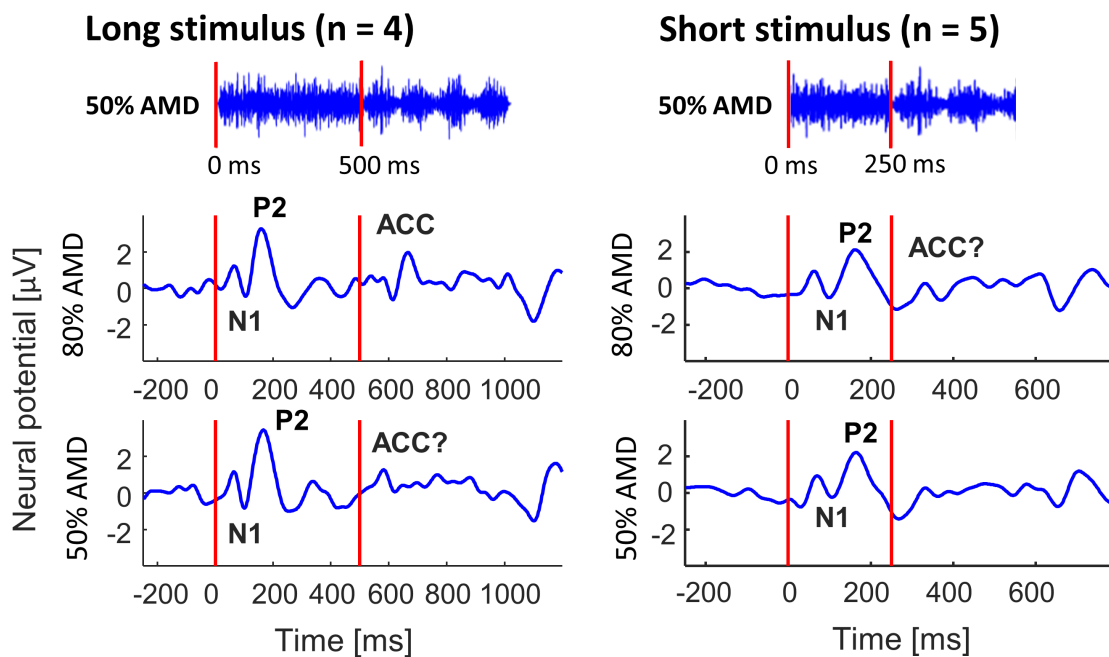


Figure B.1: The influence of stimulus duration on the cortical auditory evoked potentials (CAEPs).

Group mean CAEPs show primary N1-P2 complexes following sound onset (time = 0 ms) and secondary N1-P2 complexes (acoustic change complex, ACC). The acoustic change represents the change from unmodulated to modulated noise as indicated by the second vertical red line. CAEPs were calculated for an average of electrodes surrounding the vertex (Cz). CAEPs are presented for the long stimulus condition (left) and the short stimulus condition (right) for example amplitude modulation depths (AMDs) of 80% (top) and 50% (bottom). Examples of the acoustic stimuli are shown in the top row for an example AMD of 50%.

In the short stimulus duration condition, neural activity had not returned to baseline at the time point of the acoustic change (250 ms), which interfered with the secondary N1-P2 complex (ACC). For the long stimulus duration, a clear ACC was observed for the 80% AMD condition, but not for lower AMDs (Figure B.1). Results for AMDs below 50% are not displayed, but did not show any ACCs. Shortening the stimulus duration to decrease the data acquisition time is not recommendable to the extent that was tested in the short stimulus duration condition, as neural activity had not returned to baseline after 250 ms post-stimulus onset.

For data quality control purposes, an additional paradigm was added for the group with long stimuli, which consisted of a spectral ripple sound and its inverted version for one ripple per octave. For detailed information on this stimulus the reader is referred to Lopez Valdes *et al.* (2014). Very clear primary and secondary (ACC) N1-P2 complexes were elicited (see Figure B.2), providing evidence for an adequate measurement set-up.

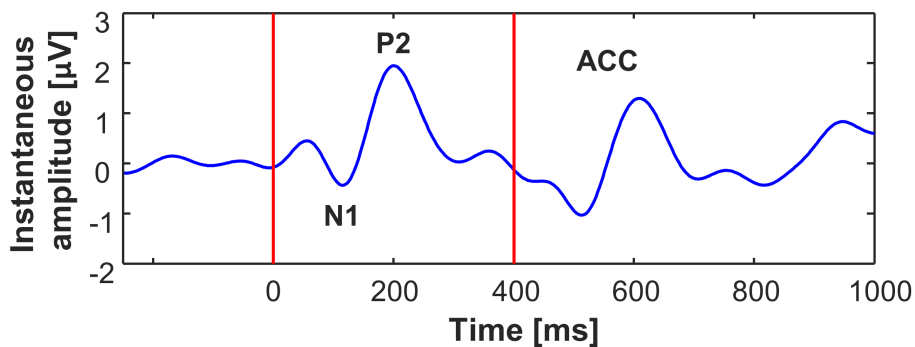


Figure B.2: Cortical auditory evoked potentials (CAEPs) for the spectral ripple control condition.

Group mean CAEPs (#participants $n = 4$) show the primary and the secondary N1-P2 complex (ACC) elicited by a spectrally-rippled sound with a ripple density of one ripple per octave (RPO) (Lopez Valdes *et al.*, 2014); Sound onset (0 ms) and spectral ripple inversion (400 ms) are indicated by the red vertical lines. Depicted data was averaged for a central region of interest around the vertex.

Influence of AM phase onset

The influence of the AM's phase onset was investigated for a pilot participant with a continuous ACC paradigm, meaning no silent inter-stimulus interval was present. A continuous sound was presented consisting of unmodulated noise interspersed with 1 s segments of AM noise. The onset of the AM noise was randomized. The phase onset of the modulated sound varied between four values (2π , 1.5π , 1π and 0.5π , see Figure B.3 for examples). The AM rate was chosen as 4 Hz and the AMD was constant with 80%.

Neural change detection as indicated by the ACC response showed increasing ACC latencies with increasing AM trough latency in the AM stimulus (see Figure B.3).

A phase onset of 1.5π in the AM stimulus represents a sudden change from unmodulated noise to the decreased amplitude in the AM trough, and resulted in the shortest ACC latency and highest ACC amplitude. This finding suggests that the change response may be mainly due to the amplitude change between peak and trough amplitude.

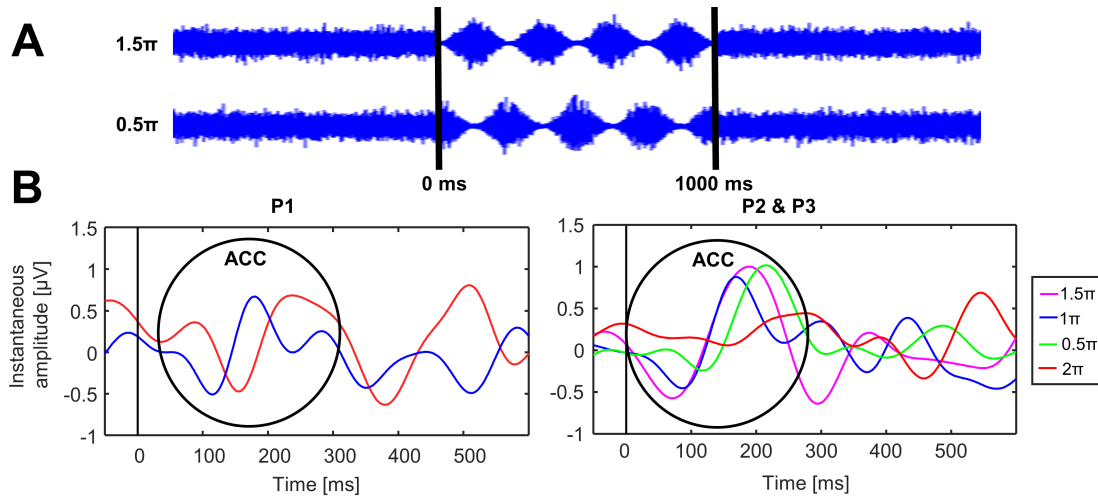


Figure B.3: (A) Acoustic change stimuli and (B) cortical auditory evoked potentials (CAEPs) for varying AM phase onsets.

(A) Time extracts of the continuous stimuli are shown for two phase onsets (1.5π and 0.5π). The time point of 0 ms represents the acoustic change from unmodulated to modulated stimulus with an amplitude modulation depth of 80%. CAEPs are shown for one pilot participant (P1, left) for which two phase onset conditions were tested and for two participants (averaged, P2 and P3, right) for which four AM phase onset conditions were tested. The phase onsets in the legend are ordered by observed latency of the acoustic change complex (ACC). CAEPs were averaged for a central region of interest around the vertex and electrodes were re-reference to average reference.

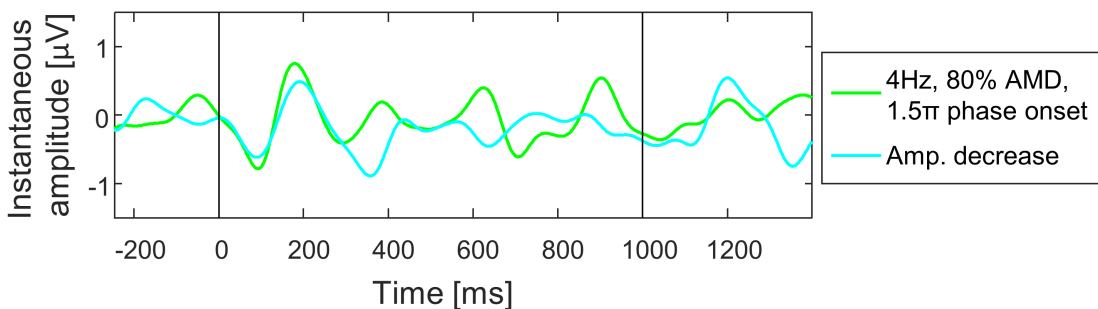


Figure B.4: Comparison of cortical auditory evoked potentials (CAEPs) for the amplitude modulation (AM) change condition and the amplitude change condition.

AM stimuli had an AM rate of 4 Hz with an amplitude modulation depth (AMD) of 80% and phase onset of 1.5π (green). Amplitude change stimuli were either RMS matched with the AM stimulus (high amplitude segment) or the amplitude was equal to the trough amplitude of the AM stimulus (lower amplitude segment); CAEPs were averaged for a central region of interest around the vertex.

Comparison of AM change vs. sudden amplitude drop

CAEPs were recorded with a continuous change paradigm and were compared between two conditions within one participant (Figure B.4): (1) acoustic change between

unmodulated noise and AM noise and (2) change between unmodulated noise stimuli of differing amplitudes, where the higher amplitude corresponded to the amplitude of the unmodulated noise in the AM change condition and the lower amplitude corresponded to the trough amplitude of the AM stimulus in the AM change condition. Neural responses showed clear ACCs with virtually identical latencies. The identical latencies lend support to the idea that the elicited change response in the AM change condition relies on the sudden change in amplitude due to the choice of AM onset, rather than the AM itself. If the AM elicited the ACC, the ACC latency should be increased compared to the amplitude change condition, as a latency increase would reflect longer integration of stimulus information following the acoustic change.

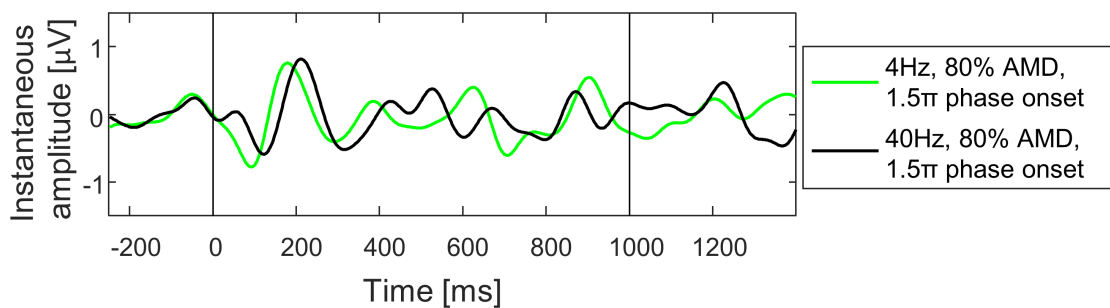


Figure B.5: Comparison of cortical auditory evoked potentials (CAEPs) for amplitude modulation (AM) change conditions for two different AM rates.

CAEPs from two continuous stimulus paradigms with different AM rates; Acoustic change from unmodulated to modulated (0 ms) or reversed (1000 ms); The AM depth was set to 80% and the phase onset to 1.5π ; Neural responses are averaged for a central region of interest around the vertex and average referenced.

Influence of the AM rate

CAEPs were assessed for two different AM rate conditions with a continuous ACC paradigm in which stimuli altered between unmodulated and modulated noise stimuli with AM rates of 4 Hz and 40 Hz. The phase onset was set to 1.5π (e.g. trough at AM onset). Data was acquired from one participant with known robust CAEPs. Obtained ACCs look very similar, although the 40 Hz response is slightly delayed compared to the 4 Hz response and shows a small decrease in peak-to-peak amplitude (Figure B.5). The differences were very minor, but align with reported observations in literature (Han & Dimitrijevic, 2015). It is interesting to note that the change from modulated to unmodulated stimulus (1000 ms) did not result in clear ACCs. A study looking at the combined effects of AM rate and AM phase onset may illuminate further, which feature of AM elicits the neural change response.

Influence of other parameters

Many parameters were assessed in pilot experiments with one or two participants. It was of interest to see if any one parameter results in a clearly visible improvement of the SNR of the CAEPs. Observations from further pilot experiments can be summarised as follows:

Carrier signal: Changing the carrier signal from a broadband carrier to a pure tone carrier of 500 Hz did not improve the CAEP SNRs at lower AMDs.

Attention: Changing the experimental paradigm from an ‘unattended’ to an ‘attended’ condition did not show a clearly visible benefit in neural responses. Besides not being an objective measure, changing to an attended experiment would also greatly impact on participant comfort during the experiment.

Binaural sound presentation: Presenting the stimulus binaurally did not result in a clear improvement of ACC amplitudes. Due to the planned experiment replication in a CI cohort, stimuli should be presented monaurally as the Irish adult CI cohort is unilaterally implanted.

AM rate discrimination and change direction (modulated vs. modulated or unmodulated vs modulated): Previously, change detection was considered for the change from unmodulated to modulated sounds. In another pilot experiment, the change type was altered to an AM rate discrimination paradigm where both stimuli were modulated. Changing the AM rate from slow to fast (e.g. 6 Hz to 15 Hz) resulted in very clear ACCs even for an AMD of 50%, whereas a change from fast to slow AM did not show such clear ACC responses. Higher AM rates are associated with faster rise times of the AM, which may lead to improvement in the time-locking of neural responses, and thus, in sharper neural change detection. However, an acoustic change in terms of AM rate assesses a different aspect of AM detection to the change from unmodulated noise, which is equivalent to 0% AMD, and modulated noise. This thesis focused on the influence of AMD on AM detection abilities, rather than the ability to discriminate between differing AM rates.

General observations

Some participants did not show an ACC response even for 100% AMD for any of the tested paradigms, whereas other participants exhibited an ACC response for AMDs as low as 50% AMD. It is difficult to draw a conclusion on the sensitivity and efficiency of the MMW and ACC paradigms without direct comparisons in the same cohort. The

ACC is certainly more time-efficient in the data acquisition and more epochs can be acquired. However, the lack of clearly distinguishable ACC responses in some participants is concerning.

Conclusions

Pilot studies were carried out with the ACC paradigm due to its time efficiency and with the hope of running a continuous ACC study with CI users to avoid onset artefacts from stimulation. Following the experience with the pilot studies, the main concern with the ACC paradigm was that the neural response may be mostly a result of the sudden change in the envelope at the time point of the acoustic change (see Figure B.3), rather than perception of AM over time. The MMW is not as susceptible to this issue because stimuli are presented individually and no sudden change is present. Stimulus onsets of AM sounds and unmodulated sounds are quite similar due to the onset ramps and in itself would not elicit the MMN. Based on MMN findings relating to temporal pattern violation in segments of tones (Saarinen *et al.*, 1992; Tervaniemi *et al.*, 1994; Vuust *et al.*, 2005; Haigh Sarah *et al.*, 2017), I believe that the MMN provides the better “temporal” measure of change detection with a longer window of information integration, and thus, Studies 2 and 3 (**Chapter 5** and **Chapter 6**) employed MMW paradigms.

Appendix C: Measurement set-ups

C.1 Single-channel set-ups

C.1.1 Normal-hearing participants

- Software: MATLAB Release 2014a or prior, The MathWorks, Inc., Natick, Massachusetts, United States ('analogoutput.m' not supported in later versions)
- Hardware:
 - SR560 Stanford Research Systems amplifier
 - Headphones
 - National Instruments DAQ

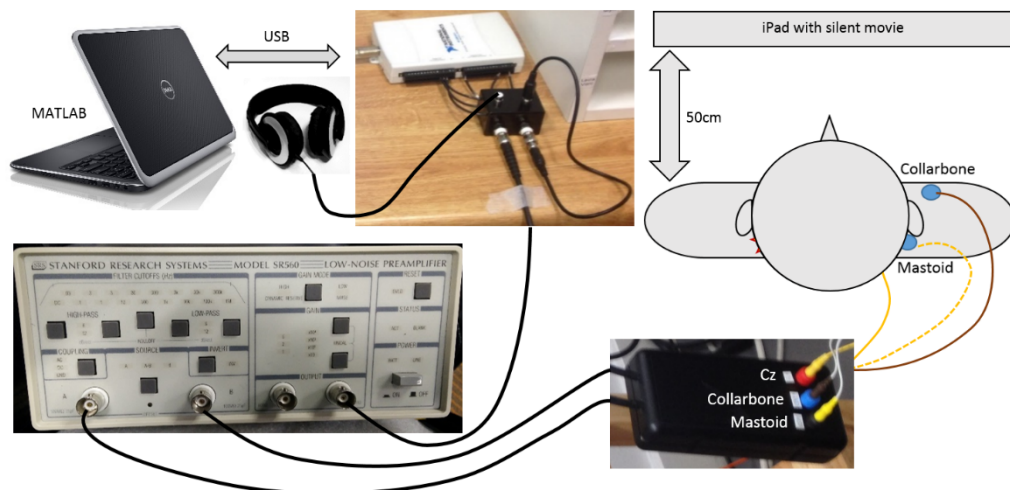


Figure C.1: Custom-designed single-channel data acquisition set-up for normal-hearing participants.

C.1.2 CI users

- Software: MATLAB Release 2014a or prior, The MathWorks, Inc., Natick, Massachusetts, United States ('analogoutput.m' not supported in later versions)
- Hardware:
 - SR560 Stanford Research Systems amplifier
 - Otocube ®
 - National Instruments DAQ

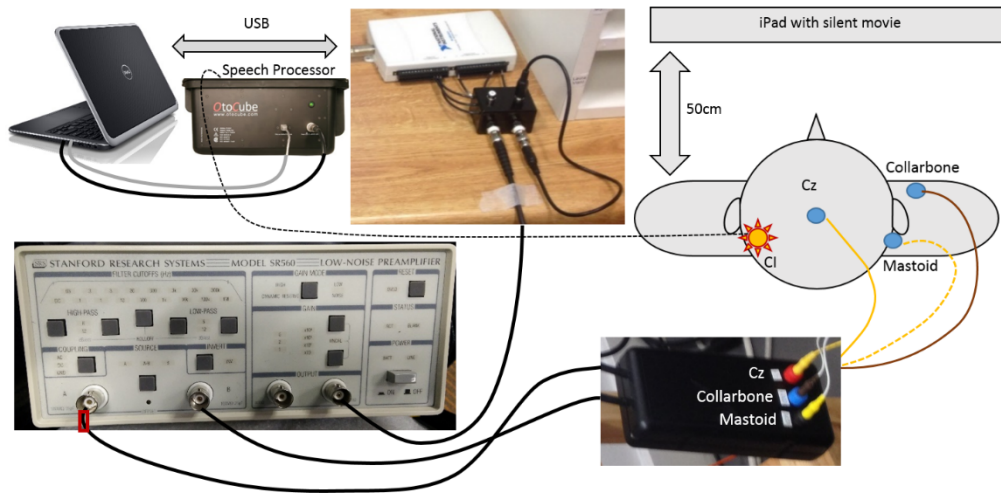


Figure C.2: Custom-designed single-channel data acquisition set-up for users.

C.2 Dual-channel set-up for normal-hearing participants

- Software: MATLAB Release 2014a or prior, The MathWorks, Inc., Natick, Massachusetts, United States ('analogoutput.m' not supported in later versions)
- Hardware:
 - 2 x SR560 Stanford Research Systems amplifier
 - Otocube[®]
 - National Instruments DAQ

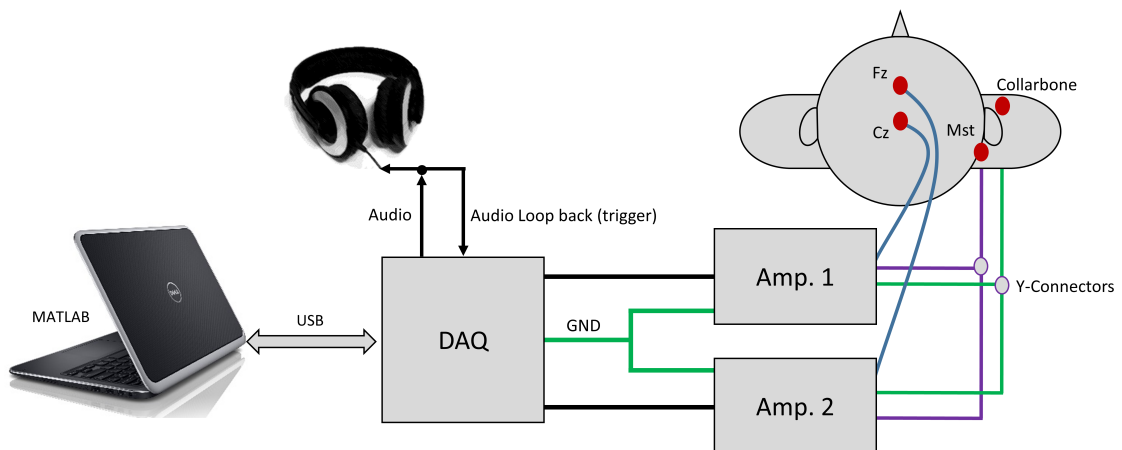


Figure C.3: Schematic of the dual-channel set-up.

Amp. – Amplifier, *Cz* – Electrode at vertex, *DAQ* – Data acquisition device, *Fz* – Electrode frontal from vertex, *Mst.* – Mastoid electrode

C.3 Multi-channel set-ups

C.3.1 Normal hearing participants

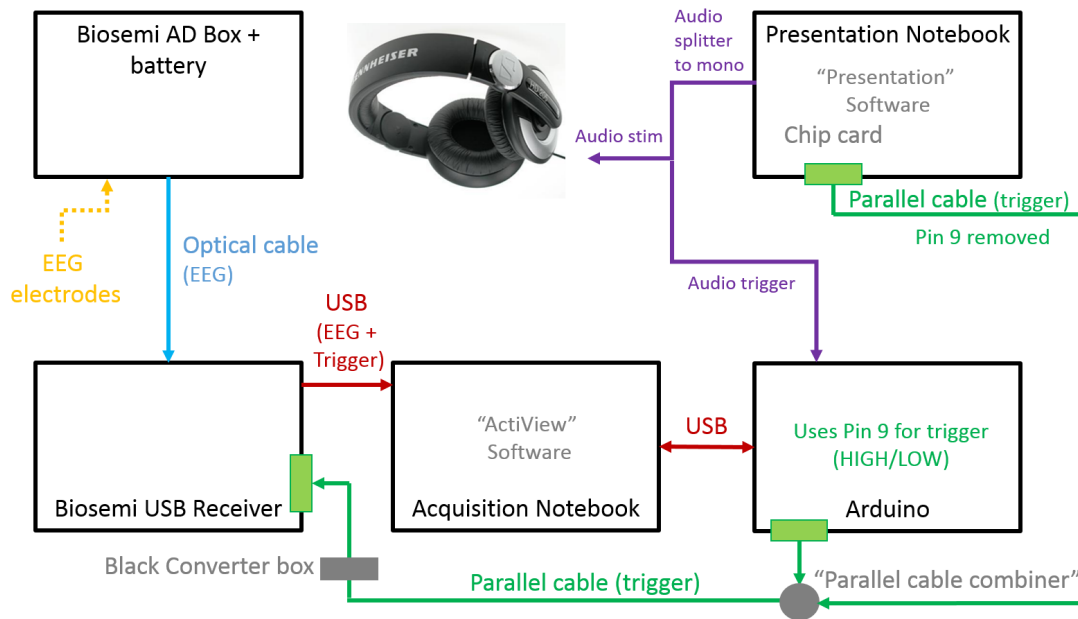


Figure C.4: Schematic of the data acquisition set-up for continuous sound presentation.

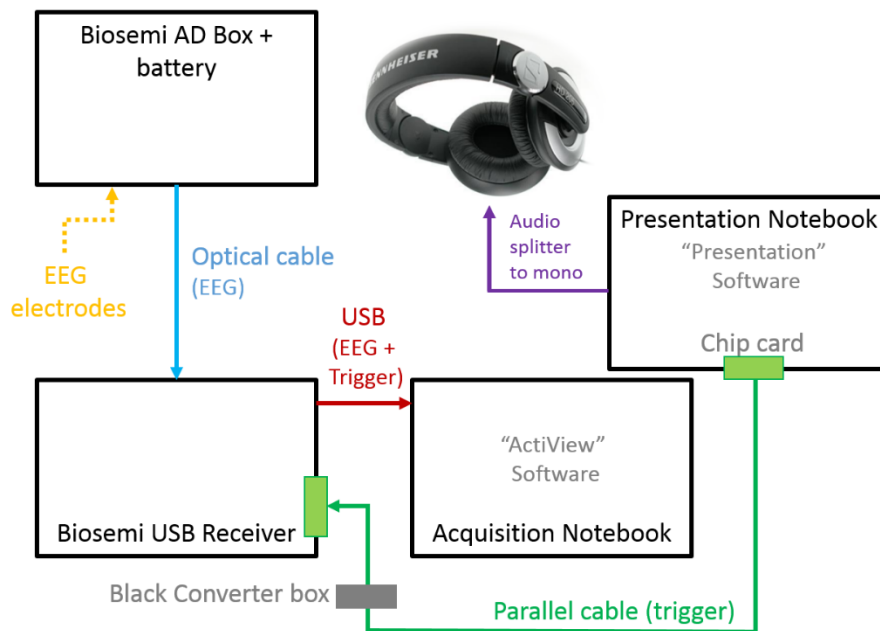


Figure C.5: Schematic of the data acquisition set-up for intermittent sound presentation.

C.3.2 CI users

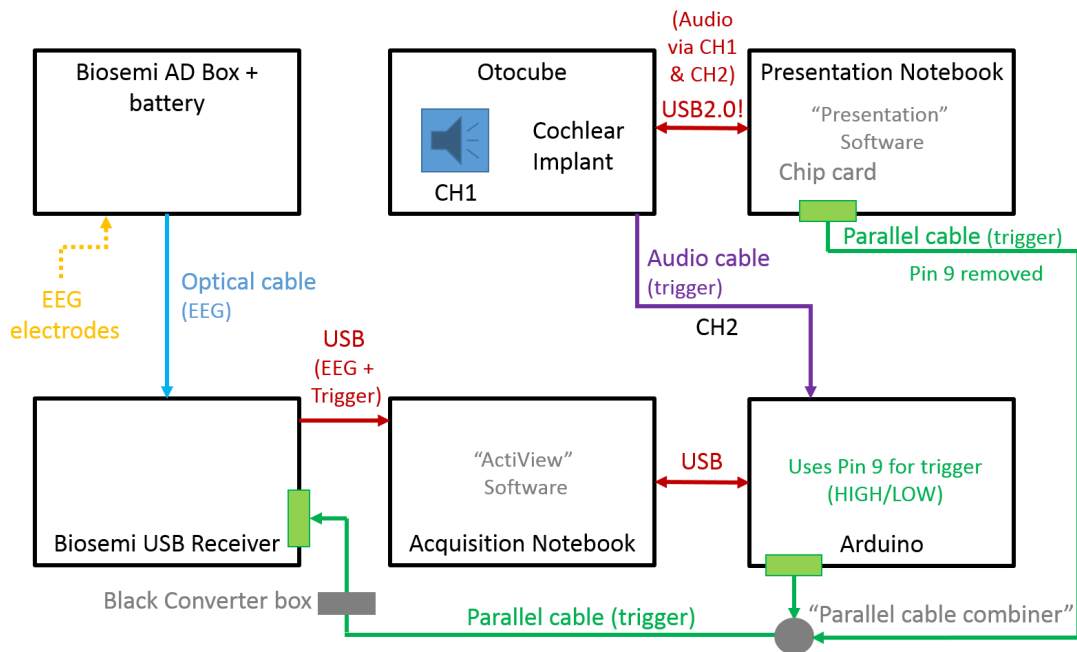


Figure C.6: Schematic of the data acquisition set-up for continuous sound presentation.

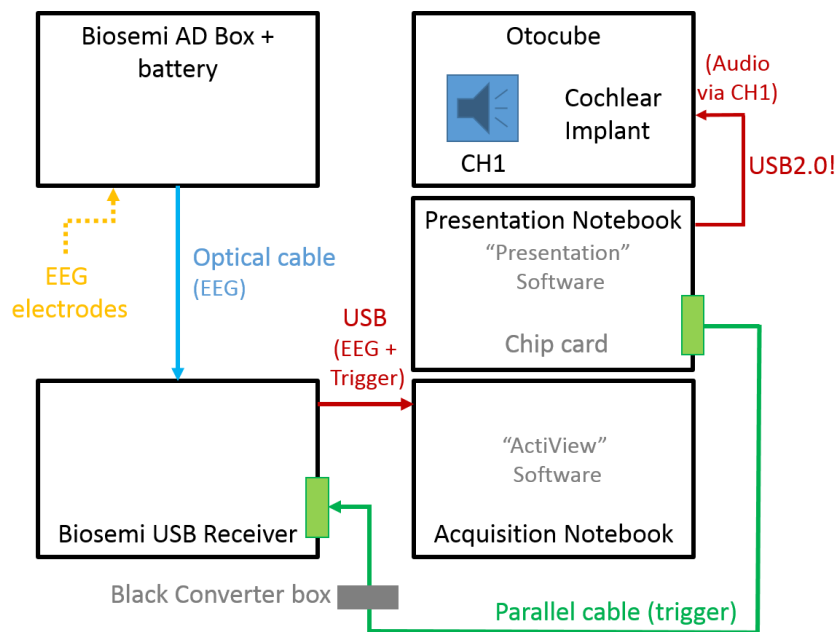


Figure C.7: Schematic of the data acquisition set-up for intermittent sound presentation.